



HAL
open science

Functional study of the role played by nucleolar proteins in the control of neural progenitor homeostasis using zebrafish as a model

Alessandro Brombin

► **To cite this version:**

Alessandro Brombin. Functional study of the role played by nucleolar proteins in the control of neural progenitor homeostasis using zebrafish as a model. Molecular biology. Université Paris Sud - Paris XI, 2015. English. NNT : 2015PA112237 . tel-01599238

HAL Id: tel-01599238

<https://theses.hal.science/tel-01599238>

Submitted on 2 Oct 2017

HAL is a multi-disciplinary open access archive for the deposit and dissemination of scientific research documents, whether they are published or not. The documents may come from teaching and research institutions in France or abroad, or from public or private research centers.

L'archive ouverte pluridisciplinaire **HAL**, est destinée au dépôt et à la diffusion de documents scientifiques de niveau recherche, publiés ou non, émanant des établissements d'enseignement et de recherche français ou étrangers, des laboratoires publics ou privés.

UNIVERSITÉ PARIS-SUD

ÉCOLE DOCTORALE 426 : GÈNES GÉNOMES CELLULES

Laboratoire : CNRS, UMR 9197, Institut des Neurosciences Paris-Saclay

THÈSE DE DOCTORAT

SCIENCES DE LA VIE ET DE LA SANTÉ

par

Alessandro BROMBIN

Functional study of the role played by nucleolar proteins in
the control of neural progenitor homeostasis using zebrafish
as a model

Date de soutenance : 29/09/2015

Composition du jury :

Directeur de thèse :	Jean-Stéphane JOLY	DR1 (INRA)
Rapporteurs :	Francesco ARGENTON Pierre-Emmanuel GLEIZES	Professeur (Università degli Studi di Padova) Professeur (Université de Toulouse - Paul Sabatier)
Examineurs :	Pierre CAPY Frédéric CATEZ Morgane LOCKER	Professeur (Université de Paris Sud) CR1 (CNRS) MCF (Université de Paris Sud)
Membres invités :	Françoise JAMEN	MCF (Université de Paris Sud)

Acknowledgements

Because so many people helped me so much during these years, I think I will never be able to express all my gratitude well enough towards everybody and I apologize in advance to people I may have forgotten to mention.

To begin, I would like to especially thank Dr. Jean-Stéphane Joly and Dr. Françoise Jamen without whom I would have never settled down in France and I would have possibly never started a thesis after all. Six years ago, you took the decision to bet on a non-French-speaker Italian student and you brought me until here. Thank you for all the support during all these years: for all the meetings, discussions, advice, preparations for presentations, searching for the best strategy to make experiments work and helping me with my written works. Thanks to both of you for never letting go.

I must express my special thanks to all the members of my examination committee who readily agreed to participate in the evaluation and defense of my thesis: Prof. Francesco Argenton, Prof. Pierre Capy, Dr. Frédéric Catez, Prof. Pierre-Emmanuel Gleizes, Dr. Morgane Locker. Thank you very much to Francesco Argenton and Pierre-Emmanuel Gleizes who accepted the heavy task of being a “rapporteur” without hesitation.

During these years all my colleagues turned into friends and I wish to thank all of them for this. First of all I wish to thank my past and present bureau: we shared so much all together and I consider you as my family. Aurélie, Emilie, Mathilde, Matthieu, Rosaria, Stéphanie and Tibi (in strict alphabetical order) we had never ending discussion about science, thesis, postdoc, fashion, films, series, food and everything. It was a joy to come every day at work. Emilie, thanks because you have been “ma postdoc” and my Timon. Aurélie, thanks for all the things that we shared in the lab and outside (I will miss our gossip dance with the chairs). Matthieu, thanks for being our conscience. Thanks also to my “pote” Joshua. Thanks Rosaria and Stéphanie because you went through my writing period without punching me. Stéphanie and Aurélie, you are my “padawans”: hold on, girls! Thanks to all of you because you forced me to stop being “sentimentalement coincé” (you know that I would have used another term) and made me write these acknowledgements.

How to forget the members of the “extended bureau”? I wish to thank Jean-Michel for his precious support, long discussions amazing dinners and wine. Thanks also to Franck for all the scientific discussions.

Thanks to Johanna for being always so positive and for laughing as much loud as me (I am still in debt with you), to Pierre for the amazing breaks and for making me feel like a professional chef.

Thanks Lucie for making me feel like a genius, to Barbara for our car discussions and to Maryline for her advices both on my experiments and recipes. Thanks to all the members of the “couloir des fous” (Arnim, Elodie, Laurie, Sylvie, Stéphane, Victor, Adeline, ...): I always found help, support and friendship.

Thanks to the past and present members of the Amagen unit for technical help, but also for being what you are. I wish to thank Sosthène for being exactly like me, Joanne for our “good morning meetings” before 8 a.m., Naïma for her smile, Sylvia for always remembering that Italy is an amazing place, Zlatko for being my example (I think about you) and Noémie for the many advices and for our beers. Thanks to Fred, Laurent, Ben and Céline.

Thanks to all the past and present members of DEPSN/NED/NeuroPSI (yes, I have been part of the three units): Yan and Hélène (my zombie friends), Julia (always helping me), Alex, Olivier, Hélène, Karine, Karen, Raphaël, Jean-Baptiste, Yannick, Ingrid, Audrey, Gaëlle, Yvette. All of you made me feel like home.

Now, I must also express my special gratitude to Ludo who welcomed me in his apartment. We fought and we laughed, we cooked and we discussed. For this I thank you! (you know that I will be always ready to start the “coloc 2.0”).

Thanks to all my “Parisian” friends: Vale and Andi (always caring about me, even if I disappeared), Marco and Clèm (for having brought a little bit of “Colli” here), Micol, Simone, Elisa, Ale and Anna. Thanks as well to the “non-Parisians” who are in Italy (I always think about you).

Finally, I wish to thank my family with a “grazie” : mi avete sempre supportato dall’Italia e non sapete quanto sia stato importante sapervi sempre vicini (finalmente riuscirete anche voi a godervi Parigi come ho fatto io in questi anni).

ABSTRACT

In neural stem cells (NSCs) and neural progenitors (NPs), as in other cell types, cell identity is characterized by specific molecular signatures that depend on the environment provided by neighboring cells. Thus, it is important to study progenitor cells *in vivo*.

The zebrafish optic tectum (OT) is a suitable model for that purpose. Indeed, this large structure of the dorsal midbrain displays life-long oriented growth supported by neuroepithelial cells present at its periphery (in the peripheral midbrain layer, PML). Moreover, neuroepithelial progenitors, fast-amplifying progenitors and post-mitotic cells are found in adjacent domains of the OT, as a consequence of its oriented growth. Each cell population is marked by concentric gene expression patterns. Interestingly, a datamining of the ZFIN gene expression database allowed us to identify around 50 genes displaying biased expression in PML cells (neuroepithelial progenitors). Interestingly, many “PML genes” code for ribosome biogenesis factors.

The accumulation of transcripts for such ubiquitously expressed genes in SAPs was very surprising so during my thesis I examined whether ribosome biogenesis may have specific roles in these neuroepithelial cells, while improving our knowledge. Indeed, although it is generally admitted that ribosome biogenesis is essential in all cells, it has been shown quite recently that several components of the ribosome biogenesis have tissue restricted roles. For example, *Notchless* is required for the survival of the inner cell mass in the preimplantation mouse embryo. More recently, conditional knock-out experiments in mice showed that *Notchless* is necessary for the maintenance of hematopoietic stem cells and intestinal stem cells, but not for committed progenitors and differentiated cells. Indeed in the absence of *Notchless* in stem cells, the immature 60S subunit cannot be exported from the nucleus and accumulates. This does not happen in differentiated cells where *Notchless* is dispensable. I started a functional study based on the conditional overexpression of a dominant-negative form of the gene *notchless homolog 1* (*nle1*, the zebrafish homolog of the mammalian gene *Notchless*). My hypothesis was that the PML slow-amplifying progenitors (SAPs) may require *Notchless* for the maturation of the 60S subunit, but not the differentiated cells which could survive also after the deletion of this gene. Experiments are still underway. So far we could demonstrate that *nle1* has a crucial role in SAPs.

I studied zebrafish mutants for genes coding for the components of the box C/D small nucleolar ribonucleoprotein (snoRNP) complex (Fibrillarin, Nop56, Nop58). Mutants displayed a similar phenotype with massive apoptosis and a deregulation of the cell cycle in the whole tectum at 48hpf. Our data suggest a cell cycle arrest at the G2/M transition, highlighting novel possible mechanisms of cell cycle arrest upon impaired ribosome biogenesis.

All together, these data highlight how ribosome biogenesis factors and the whole ribosome biogenesis contribute to the fine regulation of cell homeostasis thereby contributing to the determination of progenitor cell identity.

RESUME

L'identité des cellules souches et des progéniteurs neuraux, comme celle de tout type cellulaire, est caractérisée par des signatures moléculaires spécifiques qui dépendent de l'environnement dans lesquelles les cellules se trouvent. Ainsi, il est primordial d'étudier ces cellules dans un contexte *in vivo*.

Le toit optique du poisson zèbre est un modèle idéal pour ce type d'étude. En effet, c'est une large partie du cerveau moyen localisée en position dorsale et qui présente la particularité de croître de manière orientée tout au long de la vie de l'animal grâce aux cellules neuroépithéliales présentes à sa périphérie (dans la « peripheral midbrain layer », PML). De plus, les progéniteurs neuroépithéliaux, les progéniteurs lents et les cellules post-mitotiques sont localisées dans des domaines adjacents du toit, conséquence de sa croissance orientée. Chaque population cellulaire est marquée par des profils d'expression particuliers. Ainsi, une recherche dans la base de données ZFIN nous a permis d'identifier environ 50 gènes ayant une forte expression dans les cellules de la PML (progéniteurs neuroépithéliaux). De façon intéressante, beaucoup de « gènes PML » codent pour des facteurs de la biogenèse des ribosomes.

L'accumulation de ce type de transcrits dans les progéniteurs lents était surprenante. Ainsi, au cours de mon doctorat, j'ai étudié le rôle spécifique des facteurs de la biogenèse des ribosomes dans le maintien des cellules neuroépithéliales de la PML. En effet, bien qu'il soit généralement admis que la biogenèse des ribosomes est un processus essentiel dans toutes les cellules, il a été récemment démontré que plusieurs facteurs nécessaires à la synthèse des ribosomes ont un rôle tissu-spécifique. Par exemple, *Notchless* est requis pour la survie de la masse cellulaire interne de l'embryon préimplantatoire de souris. Récemment, des expériences de knock-out conditionnel chez la souris ont montré que *Notchless* était nécessaire au maintien des cellules souches hématopoïétiques et intestinales, mais pas à celui des cellules différenciées. En effet, en absence de *Notchless* dans les cellules souches, la grosse sous-unité ribosomique (60S) ne peut pas être exportée hors du noyau et s'accumule. Au contraire, dans les cellules différenciées, où *Notchless* n'est pas indispensable, cette accumulation n'est pas observée. J'ai commencé une étude fonctionnelle basée sur la surexpression conditionnelle de la forme dominante-négative du gène *notchless homolog 1* (*nle1*, homologue poisson zèbre du gène *Notchless* mammifère). Selon mon hypothèse, les progéniteurs lents de la PML (Slow amplifying progenitors, SAPs) pourraient avoir besoin de *Notchless* pour la maturation de la sous-unité 60S, contrairement aux cellules différenciées qui pourraient survivre après la délétion de ce gène. Des expériences sont encore en cours, mais nous avons déjà pu démontrer que *nle1* joue un rôle crucial dans la survie des progéniteurs neuroépithéliaux de la PML.

En parallèle, j'ai étudié des lignées de poisson-zèbre mutantes pour des gènes codants pour des composants du complexe de snoRNP (box C/D small nucleolar ribonucleoprotein : Fibrillarine, Nop56, Nop58). Les trois mutants présentent des phénotypes similaires, en particulier une apoptose massive et une dérégulation du cycle cellulaire dans l'ensemble du toit optique à 48 heures de développement. Etonnamment, ces résultats sont en faveur d'un arrêt du cycle cellulaire à la transition G2/M. Ainsi, cette étude pourrait permettre de mettre en évidence de nouveaux mécanismes d'arrêt du cycle cellulaire lors de défauts de biogenèse des ribosomes.

L'ensemble de ces résultats montrent comment les facteurs de la biogenèse des ribosomes (tout comme le processus) contribue à la régulation fine de l'homéostasie cellulaire, et donc à la détermination de l'identité des cellules progénitrices.

TABLE OF CONTENTS

Acknowledgements	I
Abstract	II
Résumé	III
Table of contents	IV
List of figures	VII
List of tables	VIII
List of abbreviations	IX

Functional study of the role played by nucleolar proteins in the control of neural progenitor homeostasis using zebrafish as a model

CHAPTER 1 GENERAL INTRODUCTION

PART I NEUROEPITHELIAL CELLS OF THE OPTIC TECTUM

1 NEUROEPITHELIAL CELLS: SPECIFICATION, COMPARATIVE DEFINITION AND IMPORTANCE	1
1.1 Neural stem cells and neural progenitors: definitions	1
1.1.1 Stem/progenitor cell glossary	1
1.1.2 Neural stem cells and neural progenitors	2
1.2 The cell biology of neurogenesis	4
1.2.1 Embryonic origin and maintenance/recruitment of the neural progenitors	4
1.2.1.1 <i>Neural induction and early patterning</i>	4
1.2.1.2 <i>Notch is a master regulator during neurogenesis</i>	8
1.2.1.3 <i>Proneural clusters vs. progenitor pools</i>	11
1.2.2 Neural progenitors	13
1.2.2.1 <i>Neuroepithelial cells</i>	14
1.2.2.2 <i>Radial Glia</i>	16
1.2.2.3 <i>Astrocytes</i>	16
1.3 The undervalued importance of neuroepithelial cells	17
2. THE OPTIC TECTUM AND ITS “NEUROEPITHELIAL ORIGIN”	21
2.1 The optic tectum is an evolutionary conserved part of the midbrain	21
2.2 Embryonic origin of the optic tectum	23
2.2.1 Induction of the isthmic organizer	23
2.2.2 Induction of the <i>zona limitans intrathalamica</i>	23
2.2.3 The midbrain/hindbrain domain of neurogenesis	24
2.3 The teleost ot displays life-long growth supported by neuroepithelial cells	26
2.3.1 The optic tectum grows radially	26
2.3.2 Neuroepithelial cells support growth at adulthood	27
2.4 The OT is a cellular conveyor belt that can be used as a predictive model to study gene function	30

PART II RIBOSOME BIOGENESIS IS IMPORTANT FOR CELL HOMEOSTASIS 33

1 RIBOSOME BIOGENESIS AND CELL CYCLE PROGRESSION	35
1.1 Mutual regulation of the rDNA transcription and cell cycle progression	35
1.2 Nucleolar stress and cell cycle progression	36
1.2.1 p53-dependent mechanisms coupling ribosome biogenesis and cell cycle	36

progression	
1.2.2 p53-independent mechanisms coupling ribosome biogenesis and cell cycle progression	40
1.2.3 Can the cell cycle be arrested besides the G1/S transition upon nucleolar stress?	42
2 DOES RIBOSOME BIOGENESIS PARTICIPATE TO CELL IDENTITY SPECIFICATION?	44
2.1 Shifting ribosome specificity to change the cellular proteome	44
2.2 Different cells possess different ribosomes	46
2.2.1 Different paralogs of the same RP are differently expressed and play different roles	46
2.2.2 Different RPs contribute to the translation of specific genes	47
2.2.3 Mutations of RP and RBF-coding genes lead to tissue-specific phenotypes	49
2.2.4 Does ribosome biogenesis contribute to stem/progenitor cells homeostasis?	51
Publication 1: “New tricks for an old dog: ribosome biogenesis contributes to stem cell homeostasis”	53
PART III AIM OF THE PhD	63

CHAPTER 2 RESULTS

PART I ZEBRAFISH MIDBRAIN SLOW-AMPLIFYING PROGENITORS EXHIBIT HIGH LEVELS OF TRANSCRIPTS FOR NUCLEOTIDE AND RIBOSOME BIOGENESIS 67

Publication 2: “Zebrafish midbrain slow-amplifying progenitors exhibit high levels of transcripts for nucleotide and ribosome biogenesis” 69

PART II FUNCTIONAL STUDY OF THE ROLE PLAYED BY NUCLEOLAR PROTEINS IN THE CONTROL OF NEURAL PROGENITOR HOMEOSTASIS USING ZEBRAFISH AS A MODEL 79

1 Lack of snoRNP coding genes leads to p53-dependent apoptosis at the G2/M transition in zebrafish. 81

1.1 Introduction 83

1.2 Results 83

 1.2.1 Box C/D snoRNP coding genes are strongly expressed in PML cells 83

 1.2.2 Box C/D snoRNP mutants display common phenotypes 84

 1.2.3 Midbrain structures seem to be most affected in box C/D snoRNP mutants 86

 1.2.4 Cells in mutants undergo massive apoptosis 87

 1.2.5 Cell cycle is affected in snoRNP mutants 89

1.3 Discussion 89

 1.3.1 Do box C/D snoRNP mutants display specific phenotypes? 89

 1.3.2 At which point of the cell cycle do mutant cells undergo apoptosis? 92

2 Functional study of *nle1* 95

2.1 Introduction 95

2.2 Results 97

 2.2.1 *nle1* transcripts are accumulated in PML cells 97

 2.2.2 Reverse genetics approaches to study *nle1* function 99

 2.2.3 *nle1 DN* overexpression leads to developmental delays and embryonic death 100

 2.2.4 60S subunit export is not modified upon *nle1DN* overexpression 104

 2.2.5 PML-specific *nle1DN* overexpression triggers cell death in the tectum 106

2.3 Discussion 107

2.3.1	Finding the good way to assess ribosome biogenesis in zebrafish	109
2.3.2	Is the DN mutation active in zebrafish?	110
2.3.3	Does <i>nle1</i> play a specific role in progenitor cells?	110
CHAPTER 3 FINAL REMARKS		
1	THE TELEOST PML AS MODEL TO STUDY NEUROEPITHELIAL CELLS	115
2	THE TELEOST PML IS CHARACTERIZED BY A SPECIFIC MOLECULAR SIGNATURE	116
3	APOPTOSIS AT THE G2/M TRANSITION	116
4	FUNCTIONAL STUDY OF <i>nle1</i>	117
CHAPTER 4 EXPERIMENTAL PROTOCOLS AND REAGENTS		
1	GENERAL METHODS	123
1.1	Fish lines and husbandry	123
1.2	Microinjection of zebrafish embryos	123
1.3	Histology	123
1.4	Imaging	124
2.	GENOTYPING	124
2.1	Lysis of embryos and fin clips	124
2.2	Genotyping of the <i>fb1</i> ^{hi2581} , <i>nop56</i> ^{hi3101} , <i>nop58</i> ^{hi2581} lines	124
2.3	Genotyping of the <i>nle1</i> mutants	124
3.	GENE/PROTEIN EXPRESSION ANALYSES	125
3.1	Whole-mount <i>in situ</i> hybridization	125
3.2	RT-PCR	125
3.3	Immunohistochemistry (IHC)	125
4.	CELL PROLIFERATION AND CELL DEATH ANALYSES	126
4.1	EdU incorporation and revelation	126
4.2	TUNEL staining	126
5.	OVEREXPRESSION OF THE <i>nle1</i> CDS	126
5.1	<i>nle1</i> CDS subcloning and site-directed mutagenesis	126
5.2	<i>In vitro</i> transcription and injection	127
5.3	Constructions for transient transgenesis	127
6.	CELL CULTURE METHODS	128
6.1	ZFTU line	128
6.2	Transfection plasmids	128
6.3	Transfection	128
6.4	Cell dissociation after mRNA injection	128
6.5	Assessment of the exportation of the 60S ribosomal subunit	128
6.5.1	RP-IF	128
6.5.2	RNA-FISH	129
REFERENCES		133
ANNEX		151
Publication 3: “Genome-wide analysis of the POU genes in medaka, focusing on expression in the optic tectum”		

List of figures

Figure 1. Neural progenitor cells form “developmental continuum” in mammals.	3
Figure 2. Neural induction and early patterning.	6
Figure 3. Schematic representation of Notch signaling pathway core elements.	8
Figure 4. A model for regulated self-renewal and differentiation in asymmetrically dividing radial glial progenitors.	9
Figure 5. The dynamics of <i>Hes1</i> in neocortical progenitors.	11
Figure 6. Different expression dynamics of <i>Hes1</i> in the developing mammalian nervous system.	13
Figure 7. Apico-basal polarity in neuroepithelial and radial glial cells.	15
Figure 8. Overview of the stem cell/progenitor niches in the zebrafish adult brain.	18
Figure 9. The ability of a vertebrate to regenerate brain damage correlates with its phylogenetic position.	19
Figure 10. Localization of the optic tectum within the adult teleost brain.	21
Figure 11. Retinotopic map in the OT.	22
Figure 12. Specification of the secondary neuroepithelial organizers.	24
Figure 13. <i>her5</i> is the earliest marker of the MHB and <i>her5+</i> cells contribute to the formation of the midbrain until the end of the somitogenesis.	25
Figure 14. The teleost optic tectum grows radially.	26
Figure 15. Proliferating cells are present at the tectal margins in adult zebrafish brains.	27
Figure 16. <i>her5</i> -positive cells do not contribute to OT formation at adulthood.	29
Figure 17. Schematic representations of three examples of cellular conveyor belts.	31
Figure 18. Ribosome biogenesis occurs mainly in the nucleolus.	34
Figure 19. rRNA transcription is regulated during cell cycle progression in a cyclin-CDK-dependent mechanism.	36
Figure 20. p53 activation upon nucleolar stress.	37
Figure 21. NPM and ARF couple ribosome biogenesis with cell cycle progression.	39
Figure 22. Examples of p53-independent apoptosis and cell cycle arrest mechanisms in metazoans.	41
Figure 23. Two different checkpoints can be activated upon ribosome biogenesis impairment.	42
Figure 24. Fbl and p53 levels are mutually and inversely controlled.	45
Figure 25. Different paralogs of the same RP are differently expressed.	47
Figure 26. RPL38 is rate-limiting for the translation of HOX mRNAs.	48
Figure 27. Schematic representation of the box C/D snoRNP complex in eukaryotes.	81
Figure 28. PML cells and retinal stem cells express the same genes.	82
Figure 29. Box C/D snoRNP coding genes are strongly expressed in the PML.	83
Figure 30. The insertional mutants for the SnoRNP coding genes are null and generate similar phenotypes.	85
Figure 31. Differentiation markers are affected in SnoRNP mutants.	87
Figure 32. SnoRNP mutants display p53-mediated apoptosis.	88
Figure 33. Lack of the snoRNP coding genes leads to cell cycle arrest at both G1/S and G2/M transitions.	90
Figure 34. Targeted expression of a DN form of <i>Nle1</i> .	96
Figure 35. <i>nle1</i> transcript is over-represented in PML cells and proliferative tissues, but <i>Nle1</i> protein does not show biased expression.	98
Figure 36. TALEN mediated mutagenesis of the <i>nle1</i> locus in zebrafish.	100
Figure 37. The E114 residue in <i>Rsa4</i> yeast protein is ultraconserved.	102
Figure 38. <i>nle1</i> DN overexpression leads to developmental delays and embryonic death.	103
Figure 39. Assessment of the ribosome biogenesis at the cellular level.	104
Figure 40. 60S subunit export is not modified upon <i>nle1DN</i> overexpression.	105
Figure 41. Transgenesis strategy.	107
Figure 42. PML-specific <i>nle1DN</i> overexpression triggers cell death in the tectum.	108

List of tables

Table 1. Similarities and differences between the different kinds of neural progenitors in terms of some molecular markers.	14
Table 2. Similarities and differences between the different kinds of neural progenitors in terms of cellular behavior.	14
Table 3. Mutations on RBF-coding genes lead to tissue-specific phenotypes.	49
Table 4. Primers used for genotyping.	129
Table 5. Riboprobes used for WMISH.	130
Table 6. Primers and RT-PCR conditions.	131
Table 7. Primers used for <i>nle1WT</i> and <i>nle1DN</i> overexpression.	131

LIST OF ABBREVIATIONS

aPKC: atypical Protein Kinase C	CZ: central zone	HSC: hematopoietic stem cells
ADE: anterior definitive endoderm	DAB: 3,3'-diaminobenzidine	Hyp: Hypothalamus
AF: anterior forebrain	DKC1: X-Linked Dyskeratosis Congenita-1	IGF: Insulin like Growth Factors
AH: adenohipophysis	DKK1: Dickkopf-1	INL: inner nuclear layer
AM: axial mesendoderm	Dll: Delta-like ligand	INM: Interkinetic Nuclear Migration
AP: alar plate	DN: Dominant-Negative	IPC: intermediate progenitor cell
AVE: anterior visceral endoderm	DV: dorso-ventral	IPL: inner plexiform layer
BA: branchial arches	DTN, dorsal thalamic nucleus	<i>Iro/irx: Iroquois</i>
bHLH: basic Helix-Loop-Helix	eGFP: enhanced green fluorescent protein	IsO: isthmus organizer
BLBP: Brain lipid-binding protein	FAP: fast-amplifying progenitors	IZ: intervening zone
BM: basement membrane	FBL: Fibrillarin	KO: knock-out
BMP: Bone Morphogenetic Protein	FGF: Fibroblast Growth Factors	MA: mantle
BP: basal plate	FISH: Fluorescent <i>In Situ</i> Hybridization	MB: midbrain
BrdU: Bromo-deoxyuridine	FITC: Fluorescein	MHB: midbrain/hindbrain boundary
Brn3a : brain-specific homeobox/POU domain protein 3A	FP: floor plate	mpz: marginal proliferation zone
Cb: cerebellum	Frzb1: Frizzled b1	MZ: marginal zone
cb: ciliary body	GCL: ganglion cell layer	NE: neuroepithelium
CCe: <i>Corpus cerebelli</i>	GFP: Green Fluorescent Protein	NeCs: neuroepithelial cells
CCB: cellular conveyor belt	GFAP: Glial fibrillary acidic protein	nIPC: neuronal progenitor cell
CDK: cyclin-dependent kinase	GLAST: Glutamate Astroglial Transporter	NICD: Notch intracellular domain
CNS: central nervous system	Hb: hindbrain	Nle: Notchless
Cntn1b: contactin 1b	H/E(Spl): Hairy/Enhancer of Split	NLV: <i>nucleus lateralis valvulae</i>
CMZ: ciliary marginal zone	Hpf: hours post-fertilization	NSC: Neural Stem Cell
Ctec: tectal commissure		Nucleophosmin: Npm1
		Nucleostemin: NS

oIPC: oligodendrocytic progenitor cell	RP: ribosomal protein	Teg: tegmentum
OB: olfactory bulb	RPC: retinal progenitor cell	Tel: telencephalon
OPL: outer plexiform layer	RP-IF: ribosomal protein immunofluorescence	TeO: optic tectum
OT: optic tectum	rRNA: ribosomal RNA	TL: <i>torus longitudinalis</i>
Pal: pallium	RSC: retinal stem cell	TPZ: tectal proliferation zone
<i>Pax: Paired box</i>	SAC: <i>stratum album centrale</i>	TS/TSc: <i>torus semicircularis</i>
PCNA: Proliferative Cell Nuclear Antigen	SAP: Slow-amplifying progenitor	Ts: tail-short
PF: posterior forebrain	SC: spinal cord	UBF: upstream binding factor
PGZ: periventricular grey zone	SFGS: <i>stratum fibrosum et griseum superficiale</i>	Val: <i>valvula cerebelli lateralis</i>
PhRL: photoreceptor layer	SGC: <i>stratum griseum centrale</i>	Vam: <i>valvula cerebelli medialis</i>
PML: posterior mesencephalic lamina (Grandel et al., 2006)	Shh: Sonic hedgehog	VL: ventricle lumen
PML: peripheral midbrain layer (Recher et al., 2013)	SM: <i>stratum marginale</i>	VZ: ventricular zone
pp: prechordal plate	snoRNA: small nucleolar RNA	WMISH: whole mount in situ hybridization
pRb: protein Retinoblastoma	snoRNP: Small nucleolar ribonucleoproteins	XIAP: X-linked inhibitor of apoptosis protein
Ps: Presenilin proteases	SO: <i>stratum opticum</i>	<i>Xiro: Xenopus iroquois</i>
PVN: periventricular neuron	Sox: SRY-related HMG box	<i>Zic: Zinc finger of the cerebellum</i>
RBF: ribosome biogenesis factors	SP: subpallium	Zli: <i>zona limitans intrathalamica</i>
RG/RGC: radial glia/radial glia cell	SPV: <i>stratum periventriculare</i>	ZO-1 : Zona Occludens-1
RP: roof plate	SVZ: subventricular zone	
	SZ: superficial zone	

Functional study of the role played
by nucleolar proteins in the control
of neural progenitor homeostasis
using zebrafish as a model

CHAPTER 1

GENERAL INTRODUCTION

PART I NEUROEPITHELIAL CELLS OF THE OPTIC TECTUM

1. NEUROEPITHELIAL CELLS: SPECIFICATION, COMPARATIVE DEFINITION AND IMPORTANCE.

1.1 NEURAL STEM CELLS AND NEURAL PROGENITORS: DEFINITIONS

1.1.1 Stem/progenitor cell glossary

A stem cell is defined by its capacity for indefinite self-renewal (capacity to generate new stem cells upon division) and by its multipotency (capacity to generate different cell types).

Stem cells are classified on the basis of their source and on the basis of their capacity to generate different cell types. Thus, the term “embryonic stem cells” is generally used for cells derived from the inner cell mass of mammalian blastocysts. These cells are capable of producing all the cells of the embryo. Adult stem cells, as suggested by the name, can be found in completely matured organs. These cells are indeed usually involved in repairing tissues of that particular organ and they can form only a subset of cell types.

The ability of a stem cell to generate numerous different cell types is its potency and it decreases during development. Cells which are able to generate cells of the three embryonic layers (namely endoderm, mesoderm, ectoderm) are pluripotent and cells which are able to generate cells of only one embryonic layer are multipotent (**Gilbert S., Developmental Biology, 9th ed.**). Therefore, stem cells are heterogeneous and their definition and categorization is more complicated than what is described in textbooks. For example, embryonic stem cells can indefinitely self-renew *in vitro*, while their potential *in vivo* is limited since they divide only a few times before acquiring lineage-restricted phenotypes.

Related to stem cells, progenitor cells are not unambiguously defined either. In its textbook, Scott Gilbert (**Gilbert S., Developmental Biology, 9th ed.**) defines them as cells with limited self-renewal capacities that only divide a few times before differentiating. This definition had been recently used in a similar way (**Hartenstein and Stollewerk, 2015**). Interestingly, the authors point out the fact that the term “progenitor” is also used to generally define undifferentiated and mitotically active cells in a developing organism. In this case, the proliferative fate of a cell (unlimited or not) is usually not known and the term “precursor” could be used as an alternative.

In this manuscript, I will use the term “progenitor cell” to refer to all classes of undifferentiated proliferating cells. Since the whole manuscript is written in a “developmental perspective”, the term “stem cell” will be used as a synonym of “adult stem cells”.

1.1.2 Neural stem cells and neural progenitors

Neural progenitors and neural stem cells are defined by their capacity of generating neurons and glia. Cell types that fulfill this definition are diverse and they change between species and between developmental stages.

Mammalian neurogenesis and, more specifically, murine neurogenesis are considered as the “standard” in the field (**Than-Trong and Bally-Cuif, 2015**). Hence, terminology related to neural stem cells and neural progenitors in vertebrates is used accordingly. In mammals there are three main types of neural progenitors. They form a “developmental continuum” and they differ in terms of *in vivo* localization, *in vitro* behavior, multipotency, division mode and genetic markers. The first neural progenitors to appear (neuroepithelial cells) arise from the specified ectoderm. Early neuroepithelial cells are columnar, touching both the ventricle (apical side) and pial surfaces (basal side) during the cell cycle. These cells divide first symmetrically and later asymmetrically to generate differentiated progeny. At mid-gestation, in mouse, neurogenesis becomes spatially restricted and supported by radial glial cells. This second kind of neural progenitors contributes to the expansion of the central nervous system until birth. By postnatal ages, radial glia turns into astrocyte-like stem cell which can be considered as the adult neural stem cells (NSCs) since they contribute to adult neurogenesis (**Figure 1; Temple, 2001; Götz and Huttner, 2005; Kriegstein and Alvarez-Buylla, 2009; Götz et al., 2015**).

Astrocytes that retain stem cell features seem to be a mammalian-specific feature and adult neurogenesis is supported mainly by radial glial cells in other vertebrates, or by neuroepithelial cells in amphibians and fish (**Grandel and Brand, 2013**; see *Ch1.1 section 1.3*). Nevertheless, it is important to understand how neural progenitor cells change their identity during mammalian development. Neural progenitors in other vertebrate classes are often described from a mammalian point of view (e.g. “non-glial progenitors” is used to identify neuroepithelial cells). Moreover, there is no specific marker to univocally identify neuroepithelial cells and they are often recognized by the lack of astroglial markers.

In order to understand the commonalities and the differences between the different neural progenitors, I will review in the next section the numerous developmental cues and signaling pathways which specify and modify their identity. At the end of the section, the main features of the different neural progenitors will be summarized.

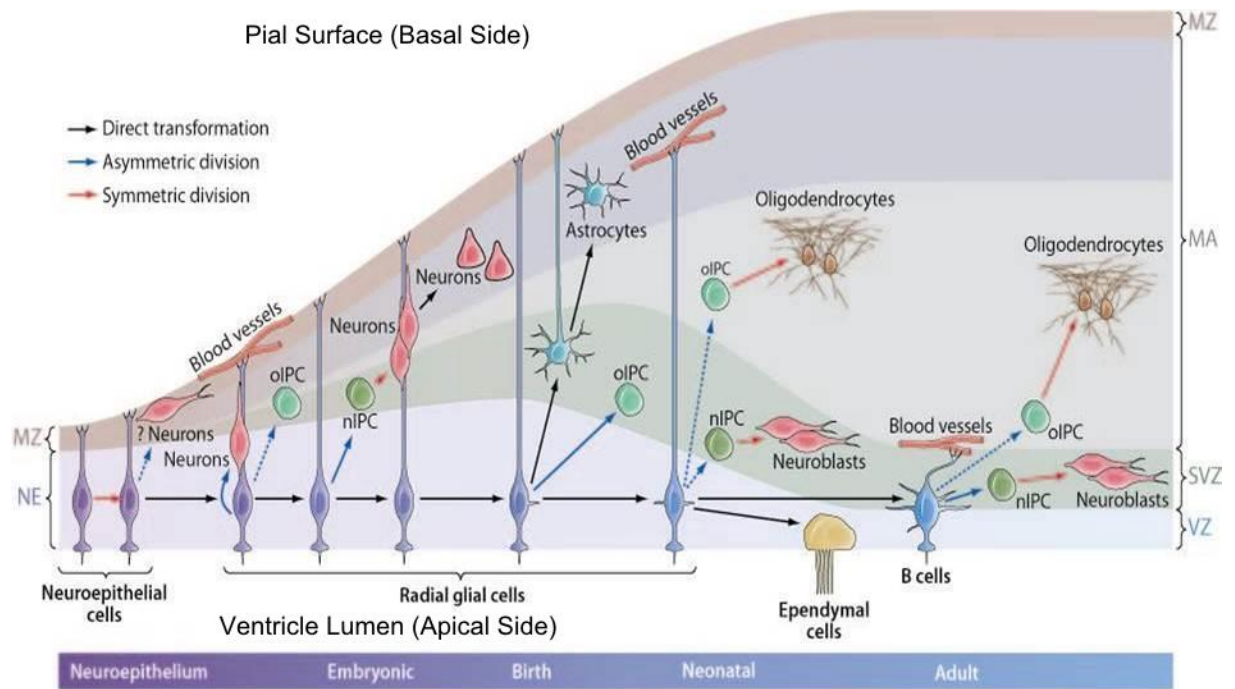


Figure 1. Neural progenitor cells form “developmental continuum” in mammals.

Neuroepithelial cells are the first neural progenitors that arise from the unstructured neuroectoderm. They contact both the ventricular and pial surfaces and they divide symmetrically to expand the neuroepithelium. At the onset of neurogenesis, they upregulate astroglial markers (such as GFAP and BLBP) thereby becoming radial glial cells (RGCs) which contribute to neurogenesis until birth. These cells divide asymmetrically to generate a new RGC and a neuron or a neuronal intermediate progenitor cell (nIPC) or oligodendrocytic intermediate progenitor cell (oIPC). Newly generated neurons migrate along the radial fibers to the outer layers, while radial glial cells remain in the ventricular zone. After birth these cells either give rise to neurons or convert into ependymal cells, or convert into adult SVZ astrocyte-like NSC (type B cells) that continue to function as neural stem cells in the adult. B cells maintain an epithelial organization with apical contact at the ventricle and basal endings in blood vessels. B cells continue to generate neurons and oligodendrocytes through intermediate progenitors.

Solid arrows are supported by experimental evidence; dashed arrows are hypothetical. Colors depict symmetric, asymmetric, or direct transformation. From **Kriegstein and Alvarez-Buylla, 2009**.

IPC: intermediate progenitor cell; MA: mantle; MZ: marginal zone; NE: neuroepithelium; nIPC: neuronal progenitor cell; oIPC: oligodendrocytic progenitor cell; RG: radial glia; SVZ: subventricular zone; VZ: ventricular zone.

1.2 THE CELL BIOLOGY OF NEUROGENESIS

Without exception, neural progenitors arise from the ectoderm which is specified towards a neural fate. The specification of the neuroectoderm is remarkably similar across animal phyla (**O'Connell, 2013; Hartenstein and Stollewerk, 2015**).

In vertebrates, the neuroectoderm constitutes the neural plate that, after gastrulation, starts to thicken and folds (in mammals and birds) thereby forming the neural tube. Both structures are made of neuroepithelial cells. Within the neural tube, neurogenesis does not occur simultaneously but it is restricted to some regions (proneural clusters) in which radial glial cells appear. These latter retain epithelial characteristics (apico-basal polarity) and divide asymmetrically. Between proneural clusters, cells retain neuroepithelial identity and constitute the secondary neuroepithelial organizers. Within these regions neurogenesis is delayed. They act as secondary signaling centers that contribute to the regionalization of the developing nervous system. The neural tube is then subdivided in three main compartments along the antero-posterior axis: prosencephalon (forebrain), mesencephalon (midbrain) and rhombencephalon (hindbrain). Once the embryonic development is achieved, neurogenesis will continue only in defined areas of the central nervous system supported by adult neural stem cells. Radial glia represent the most common type of adult stem cells (among vertebrates), but in mammals they appear to be transient developmental progenitors. As previously mentioned, astrocyte-like cells contribute to adult neurogenesis in mammals (**Gilbert S., Developmental Biology, 9th ed.; Götz and Huttner, 2005; Grandel and Brand, 2013; Götz et al., 2015**).

Once neuroepithelial plate is formed, several developmental mechanisms contribute to the final specification of the different cell types and regions in the brain. The fate of a progenitor cell is determined according to its position in the neural plate. Indeed, each cell will respond to different concentrations of morphogens. Gene expression will change accordingly and this will ultimately determine cell identity. Nevertheless, other basic cellular processes, some with stochastic elements, also influence progenitor fate (**Willardsen and Link, 2011**).

1.2.1 Embryonic origin and maintenance/recruitment of the neural progenitors

1.2.1.1 Neural induction and early patterning in vertebrates

In vertebrates, the development of the nervous system is triggered by signals emanating from the organizers of the early embryo during gastrulation. It occurs according to the so-called "default model" of neural induction developed in amphibians (**Ozair et al., 2013**). In short,

ectodermal cells differentiate into neural tissue unless exposed to Bone Morphogenetic Proteins (BMPs) secreted from the ventral side of the gastrula. BMP signaling antagonists such as Noggin, Chordin and Follistatin are secreted dorsally and trigger neural plate formation from the dorsal ectoderm (**Pera et al., 2014**). Moreover, ectoderm will follow an anterior neural fate unless instructed otherwise. This is realized by virtue of a Wnt/ β -catenin gradient which is perpendicular to the BMP gradient along the antero-caudal axis. The organizer secretes Wnt antagonists Frzb1, Cerberus, and Dkk1 (**Figure 2A**), which during gastrulation translocate to the anterior pole of the embryo and establish a Wnt/ β -catenin gradient that determines the antero-posterior polarity of the neural plate (**Figure 2B; Niehrs, 2010**). Perpendicular activity gradients of BMP and Wnt signals are not restricted to *Xenopus*. Chordin and BMP have universal functions in bilateria for patterning the DV axis during gastrulation. Key roles for anterior Wnt inhibition by Dkk and posterior Wnt signals have been validated in most animals (**Niehrs, 2010; Ozair et al., 2013**).

The Fibroblast Growth Factors (FGF8) and Insulin like Growth Factors (IGFs) pathways are required for neural induction before gastrulation and act in favor of a caudalization of the tissue (**Pera et al., 2014**). These signals together are integrated at the level of the BMP signaling transducer Smad1, which is thus differentially phosphorylated (**Eivers et al., 2009**) and inhibition of its phosphorylation leads to the neural fate induction.

Neural plate induction is followed by the commitment of embryonic neural progenitors to a neural fate and, as previously mentioned, this does not occur homogenously and simultaneously throughout the neural plate. The so-called proneural domains arise following the coordinated activity of “prepattern” genes (**Lee et al., 2014; Figure 2C**) that defines competent fields of neurogenesis and activates proneural factors. Among the most important and conserved “prepattern genes” are the SoxB factors that are expressed at the end of the gastrulation in many bilaterians. *SRY-related HMG box B (SoxB)* genes provide neurogenic potential but, at the same time, inhibit neural differentiation, maintaining the neuroectoderm in a proliferative state (**Hartenstein and Stollewerk, 2015**). *SoxD* and *Sox2*, and *Zinc finger of the cerebellum 1 (Zic1)*, are directly induced by the BMP inhibitor Chordin (**Mizuseki et al., 1998a, 1998b**). Other prepattern genes belong to the *Iroquois (iro/irx)* gene family such as *Xiro1* in *Xenopus* (**Gómez-Skarmeta and Modolell, 2002**) and *iro3* in zebrafish (**Kudoh and Dawid, 2001**).

Another example of master regulator at this stage appears to be *Paired box 6 (Pax6)* that is expressed in several brain regions, such as forebrain, retina and hindbrain (**Osumi et al., 2008**). Together these genes activate the proneural genes which specify the different neuronal identities. These genes constitute a heterogenous group encoding basic helix-loop-helix (bHLH)

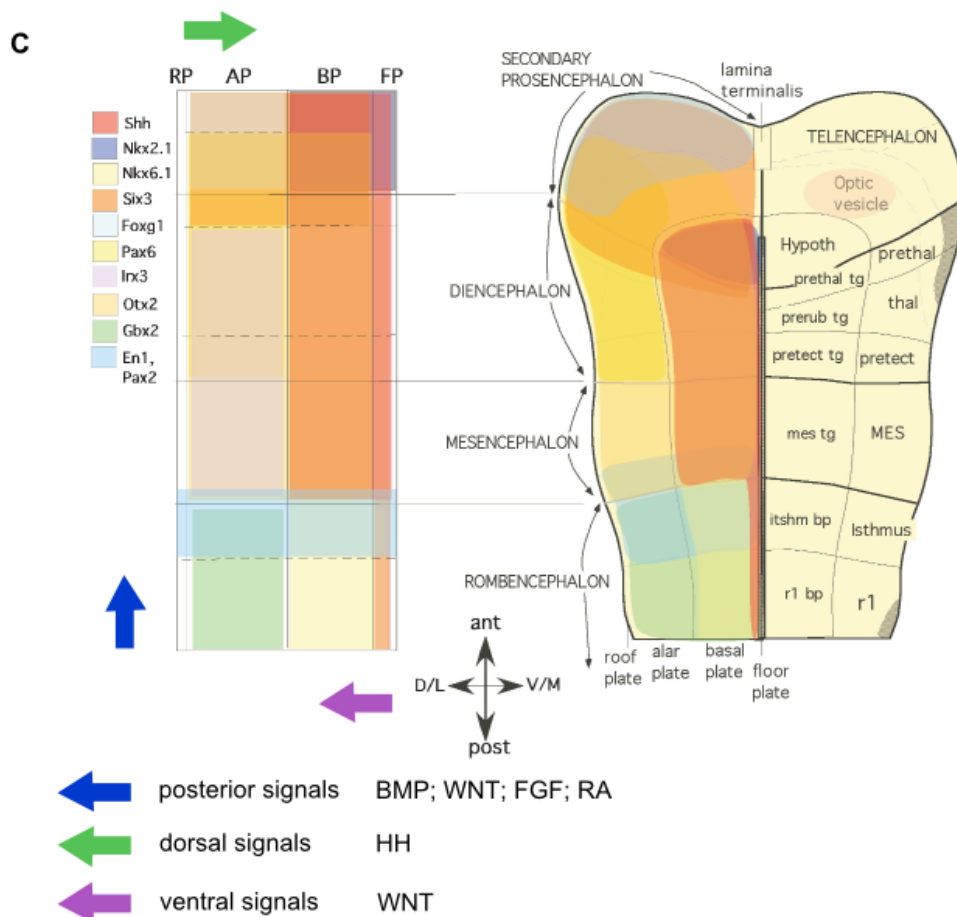
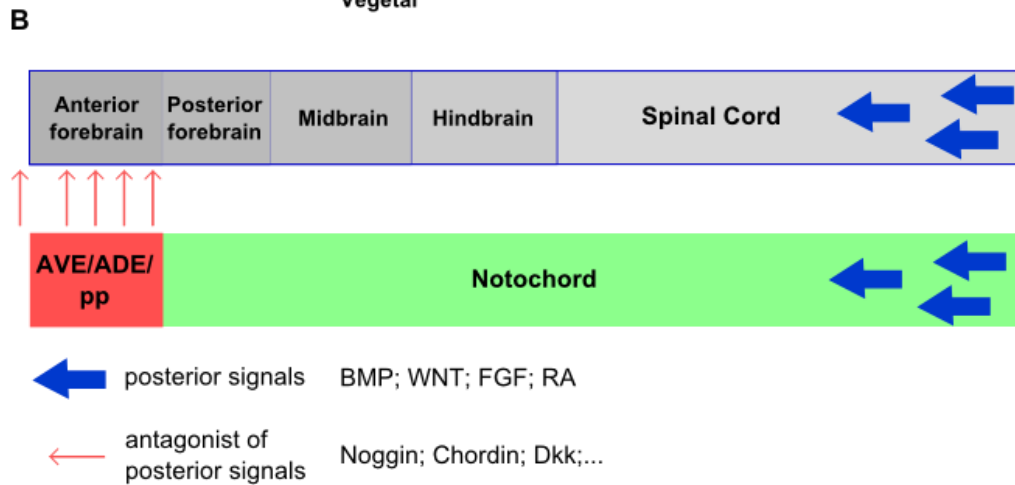
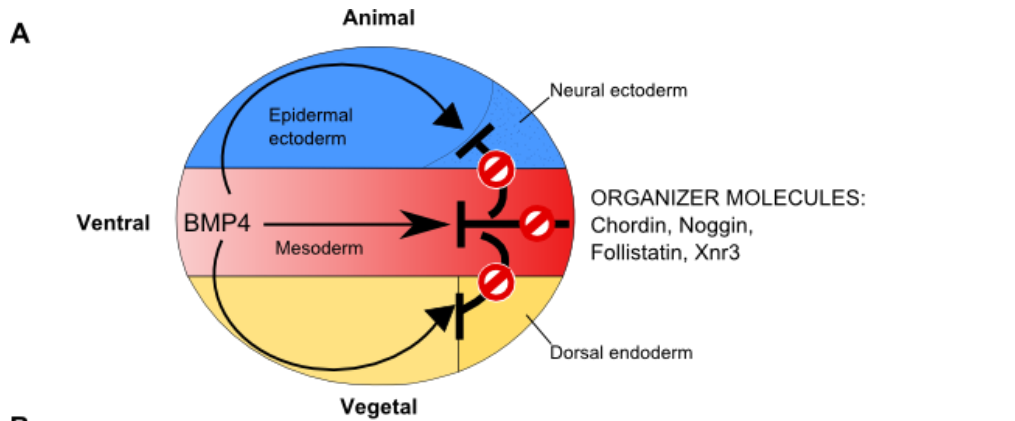


Figure 2. Neural induction and early patterning. (A) In amphibians, BMP4 (along with certain other molecules) is a powerful ventralizing factor. Organizer proteins such as Chordin, Noggin and the block the action of BMP4; their inhibitory effects can be seen in all the three germ layers. Drawing depicts the classical model for organizer signaling developed in amphibians. This model applies to all vertebrates. From **Gilbert S., Developmental Biology, 9th ed. (B)** Signals exert a posteriorizing action on the neural plate (blue arrows). Antagonists of the respective pathways in the anterior forebrain, such as secreted Cerberus, Lefty1, Dkk1, Noggin, and Chordin (red arrows) are released by the underlying AVE, ADE, and prechordal plate. Those are the molecules of the organizer that translocates anteriorly during gastrulation. Thus, the neuroectoderm is roughly regionalized along the antero-posterior axis at the end of the gastrulation. A series of vesicles develop at the anterior end of this tube, indicating neural patterning along the anteroposterior axis: the prosencephalon or forebrain, the mesencephalon or midbrain, and the rombencephalon or hindbrain. (Adapted from **Andoniadou and Martinez-Barbera, 2013**). **(C)** Simultaneously, the neural tube is partitioned along the dorsoventral axis under the influence of the underlying meso-endodermal tissue, as well as by the effect of adjacent non-neural ectodermal structures. Thus the floor plate, the basal plate, the alar plate and the roof plate develop within the neural tube from ventral to dorsal. As a result of these patterning events, a rough three-dimensional grid is established by the expression of numerous prepattern genes, setting the foundation for its overall regional specialization. In other words, diverse neurons of specific identity will later be produced within these different territories. (Adapted from **Vieira et al., 2010**).

AP: alar plate; ADE: anterior definitive endoderm; AVE: anterior visceral endoderm; BP: basal plate; FP: floor plate; pp: prechordal plate; RP: roof plate.

transcription factors. They control neurogenesis by regulating Notch-mediated lateral inhibition (see next section) and initiating the expression of downstream differentiation genes. Proneural genes had been initially identified in *Drosophila* based on their ability to confer a neural (rather than epidermal) identity onto naïve ectodermal cells. The original proneural genes identified included members of the *achaete-scute* complex (AS-C), which comprises the four genes *achaete* (*ac*), *scute* (*sc*), *lethal of scute* (*lsc*), and *asense* (*as*) (all but *as* have proneural activity). Additional proneural genes were subsequently identified in *Drosophila*, including *atonal* (*ato*), *amos*, and *cato*. Not only have proneural genes been conserved throughout evolution, but also this gene family has greatly expanded in vertebrates. Mouse *ato* orthologs fall into three distinct gene families: *Neurogenin* genes (*Neurog1*, *Neurog2*, *Neurog3*), *Neurogenic differentiation* genes (*NeuroD1*, *NeuroD2*, *Neurod4/Math3/Atoh3*, *Neurod6/Math2/Atoh2*, *Atoh1/Math1*, *Atoh7/Math5*), and *Olig* genes (*Olig1*, *Olig2*, *Olig3*). Members of this family are even more numerous in zebrafish. In contrast, there are only two AS-C-related genes in mouse: *Ascl1/Mash1*, which is expressed in the nervous system, and *Ascl2/Mash2*, which is not. Vertebrate proneural genes are primarily expressed in neuroepithelial cells and not in

unspecified ectodermal cells like in *Drosophila*. Besides this difference they act exactly in the same way and their expression patterns define different proneural domains along the antero-posterior axis of the developing embryo (Huang *et al.*, 2014).

1.2.1.2 Notch: a master regulator of neural progenitor maintenance, differentiation and survival

Notch signaling pathway (Figure 3) is a master regulator of neurogenesis and more precisely of cell fate. It plays different roles depending on the targeted cell. Nevertheless, in general once the Notch signal is active in a cell, this cell will not acquire neuronal fate (Pierfelice *et al.*, 2011).

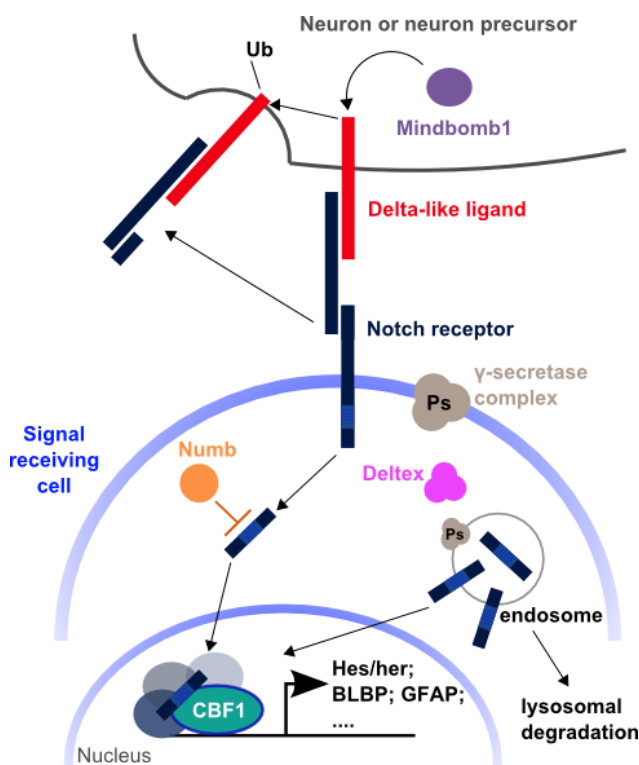


Figure 3. Schematic representation of Notch signaling pathway core elements.

Notch signaling is regulated by cell-cell interactions, with Notch receptors on one cell activated by ligands, the Delta-like and Jagged proteins, expressed on neighboring cells. Receptor stimulation involves dynamin-mediated endocytosis on the signal-sending and signal receiving cells, with ubiquitination of the ligands (by the E3 ligase Mindbomb1, for example) and receptors (by the E3 ligase Deltex, for example) employed to drive internalization. Upon receptor activation, the Notch intracellular domain (NICD) is ultimately cleaved at site by the Presenilin proteases (Ps) of the γ -

secretase complex, and translocates to the nucleus to associate with CBF1 (also called RBP-J or CSL) and Mastermind-like proteins to activate transcription of target genes. Among the target genes are the *Hes/her* genes and astroglial markers including BLBP and GFAP. Thus, the receiving cell does not acquire neuronal fate. Neuroepithelial cells are Notch-independent. From Pierfelice *et al.*, 2011.

Highly polarized and symmetrically dividing neuroepithelial cells constitute the neural plate and the neural tube. After the ventricular lumen formation neuroepithelial cells turn into radial glial cells which are still highly polarized along the apico-basal axis, but divide asymmetrically. Each

asymmetric cell division generates one new radial glial cell and one neuron or neuronal precursor (**Figure 1**). Neurons migrate along the radial fibers to the outer layers in the mammalian cerebral cortex, while radial glial cells remain in the ventricular zone (**Kageyama et al., 2008**). The asymmetric inheritance of a subcellular membrane domain of the dividing progenitors is strongly correlated with the asymmetric fate of the daughter cells in zebrafish neural tube (**Alexandre et al., 2010**). Thus, the more apically derived daughter cell becomes a neuron, whereas the basally derived cell retains a glial identity and contributes to the progenitor pool maintenance. Notch signaling is important for fate decision: basal self-renewing daughter cells display high Notch activity and apical neuronal daughter cells show a low Notch activity (**Dong et al., 2012**). The orientation of Notch signaling involves Pard3-dependent (see *Ch1.1 section 1.2.1.2*) asymmetric localization of Mindbomb1 to the apical daughter. This latter is a RING ubiquitin ligase and interacts with the intracellular domain of Delta to promote its ubiquitylation and internalization. This facilitates intramembranous cleavage of the remaining Notch receptor, release of the Notch intracellular fragment, and activation of target genes in neighboring cells (radial glial cells; **Itoh et al., 2003; Figure 4**).

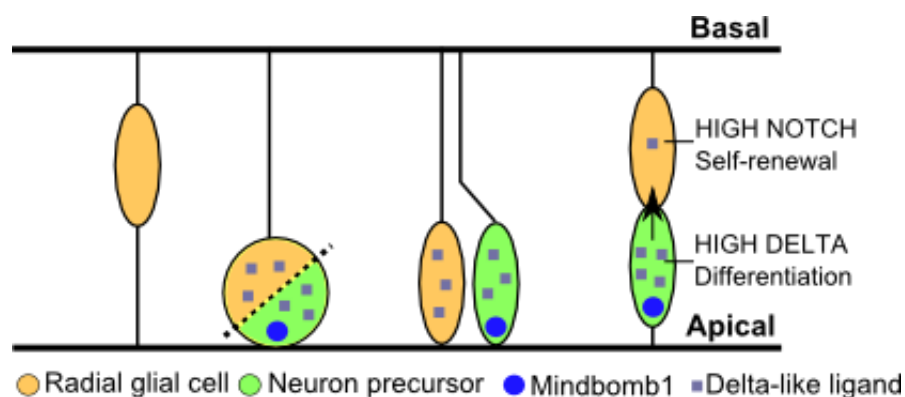


Figure 4. A model for regulated self-renewal and differentiation in asymmetrically dividing radial glial progenitors. Notch signaling is important for fate decision: basal self-renewing daughter cells display high Notch activity and apical neuronal daughter cells show a low Notch activity. Adapted from **Dong et al., 2012**.

Work in the zebrafish retina has provided insights into the function of the Notch pathway with regards to the geometry of signaling between newly generated ligand-expressing neurons and the receptor expressing retinal progenitors which are inhibited from differentiating (**Del Bene et al., 2008**). Del Bene and colleagues found that apico-basal gradients exist in the expression of both Notch receptors and ligands and, interestingly, those gradients are opposed *i.e.* the concentration of the receptor is -higher apically (ventricular side) and the one of the ligand is higher basally. Furthermore the expression patterns of Notch ligands, receptors and indicators of

Notch activation were consistent with higher levels of Notch signaling on the apical side of the retina neuroepithelium than on the basal side. Moreover a recent work, also in zebrafish, has suggested that Notch signaling is not only correlated with the apico-basal polarity of the neuroepithelium, but that it plays a causal role in the generation of that polarity (**Ohata et al., 2011**).

Interestingly, Notch signaling plays an “instructive” role for radial glial specification, as reviewed by Pierfelice and colleagues. For example, Notch receptor activation can drive the expression of specific astroglial markers including Brain lipid-binding protein (BLBP) and Glial fibrillary acidic protein (GFAP) (**Pierfelice et al., 2011**).

Among the main targets of Notch signaling are the *Hes* genes (*her* in zebrafish), which are the homologs of *Drosophila hairy* and *Enhancer of split* (**Kageyama et al., 2008**). These genes encode basic helix-loop-helix (bHLH) transcriptional receptors which repress the function of bHLH proneural proteins (**Pierfelice et al., 2011**). Both *Hes/her* and proneural genes are expressed in a salt-and-pepper pattern (**Shimojo et al., 2011**) within proneural clusters (see previous section). This relies on the “lateral inhibition” phenomenon linked to the activation of Notch pathway and is due to the mutual repression of ligands and Notch targets in juxtaposed cells. Thus, cells contacting each other cannot activate Notch simultaneously, thereby starting a “snowball effect” that leads to an increase in Notch signaling in one cell compared to the other. One cell thus become Notch ON and expresses *H/E(Spl)* transcription factors, and the adjacent one is Notch OFF and expresses proneural genes (**Shimojo et al., 2011**), the latter becoming competent to differentiate into a neuron. In mouse, *Delta-like ligand 1 (Dll1)* and *Notch1* are induced in the neurogenic progenitors that signal to one another, generating the expression of *Hes1* in the Notch-positive progenitor. It is worth noting that among *Hes1* targets is the *Hes1* gene itself. Thus, an auto-regulation of *Hes1* by its own expression would generate an oscillatory expression pattern of *Hes1* in the neural progenitors (**Figure 5; Kageyama et al., 2008; Kageyama et al., 2015**). Due to this particular type of expression, proneural genes, inhibited by *Hes1*, are periodically inhibited and thus oscillate as well with a reverse period (**Kageyama et al., 2008**). Finally, Delta ligands expression oscillates due to the oscillations of proneural genes responsible for its transcriptional activation. Thus, in the neural sheet at time *t*, some cells highly express *Hes/her* genes and a low level of proneural genes. Some additional cues must be involved in stabilizing proneural expression and thus trigger neuronal commitment from these “neurogenic competent” progenitors. The situation is similar in zebrafish where, within a proneural cluster, cells expressing higher levels of proneural genes are selected to become neurons whereas cells expressing high levels of *Her4* (that responds to Notch activation) are selected to keep radial

glial fate. (Schmidt *et al.*, 2013). It is noteworthy that there are many Notch-independent *Hes/her* genes which contribute to the specification of boundaries between two different proneural clusters.

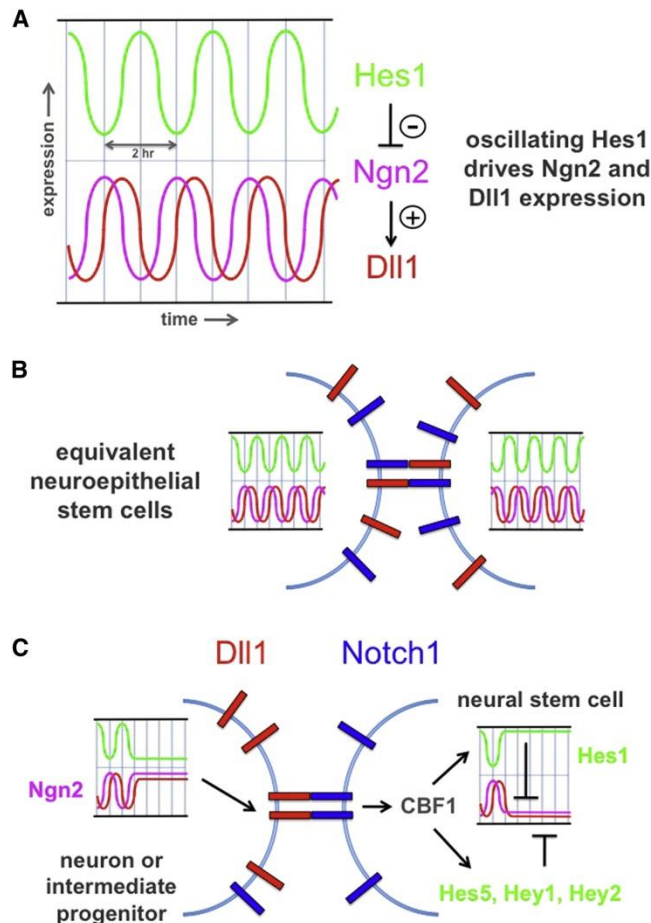


Figure 5. The dynamics of *Hes1* in neocortical progenitors.

(A) Oscillations in *Hes1* expression are driven by a negative autoregulatory feedback loop. The periodicity of these cycles leads to the cyclical expression of Neurogenin2 (*Neurog2*) and Delta-like 1 (*Dll1*). **(B)** Early in neocortical development, many adjacent cells are equivalent, and have cycling *Hes1*, *Neurog2*, and *Dll1*. **(C)** Interactions between adjacent cells will fix the gene expression status of those cells, such that some will become intermediate progenitors and neurons, while other will remain as RGCs. Thus, this kind of interaction is responsible of the maintenance of the RGC pool within the proneural clusters. Outside proneural clusters (boundary regions) neuroepithelial cells are maintained in a Notch-independent manner and there is *Hes/her* oscillation within these

1.2.1.3 Proneural clusters vs progenitor pools

At the neural plate stage, large domains that do not express proneural genes separate proneural clusters. These domains are the so called progenitor pools and correspond to the boundary regions in the developing brain. They are induced by the secondary neuroepithelial organizers such as the *zona limitans intrathalamica* (ZLI) and the isthmus organizer (IsO) (Vieira *et al.*, 2010; Cavodeassi and Houart, 2012; *Ch1.1 section 2.2*). They exhibit delayed differentiation and cell tracing indicates that they will be progressively recruited in early neurogenesis and/or will participate in later neurogenesis events (Stigloher *et al.*, 2008).

The work of Laure Bally-Cuif group in zebrafish highlighted that progenitor pools are specified and maintained at the undifferentiated state through the activity of a subfamily of Notch-independent Hes/Her factors such as Her3 (ortholog to mouse Hes3), Her9 (orthologous to human HES4), Her5 and Her11 (both ortholog to mouse Hes7). They do not require Notch signaling for their activation (**Geling *et al.*, 2004; Hans *et al.*, 2004; Bae *et al.*, 2005**), and their expression in the neural plate is regulated by positional cues such as FGF, Wnt, or BMP signaling (**Stigloher *et al.*, 2008**). These “non-canonical” *her* genes are necessary to maintain the progenitors pools as their inhibition leads to up-regulation of proneural genes or “canonical” *her* genes, thus to their transition towards a proneural cluster (**Geling *et al.*, 2004**). This transition from progenitor pool to proneural cluster-like cells likely occurs normally during development, as neurogenesis is gradually turned on in these territories over time (see following sections). It has been hypothesized that part of the neurogenic cascade involved in progenitor pools is maintained, or re-used, to regulate the stem cell during adulthood (**Stigloher *et al.*, 2008**).

The specification of the progenitor pools of the boundaries seems to occur similarly in mammals. In these regions, Hes1 protein is persistently expressed at high levels. *Hes3* is mainly expressed in the isthmus, whereas *Hes5* is not expressed in boundaries. However, ectopic *Hes5* expression occurs in boundary regions of *Hes1* KO mice, compensating for their maintenance. Thus, all three *Hes* genes are expressed in boundary cells, where proneural genes are not expressed. It is noteworthy that *Hes1* is expressed in both neurogenic and non-neurogenic domains displaying a differential regulation depending on the progenitor subtypes (see *Ch1.1 section 1.2.1.2*). Contrary to neurogenic regions, where there is a Notch-dependent oscillatory expression, in the non-neurogenic domains, *Hes1* is expressed at a high and sustained level inhibiting neurogenesis in the domain (**Kageyama *et al.*, 2008; Kageyama *et al.*, 2015**). Interestingly, sustained expression of *Hes1* in embryonic pools (such as the isthmus at the boundary between midbrain and hindbrain) cannot be correlated with the formation of the adult neural stem cell pools in mammals which are limited to the telencephalic regions (**Figure 6**).

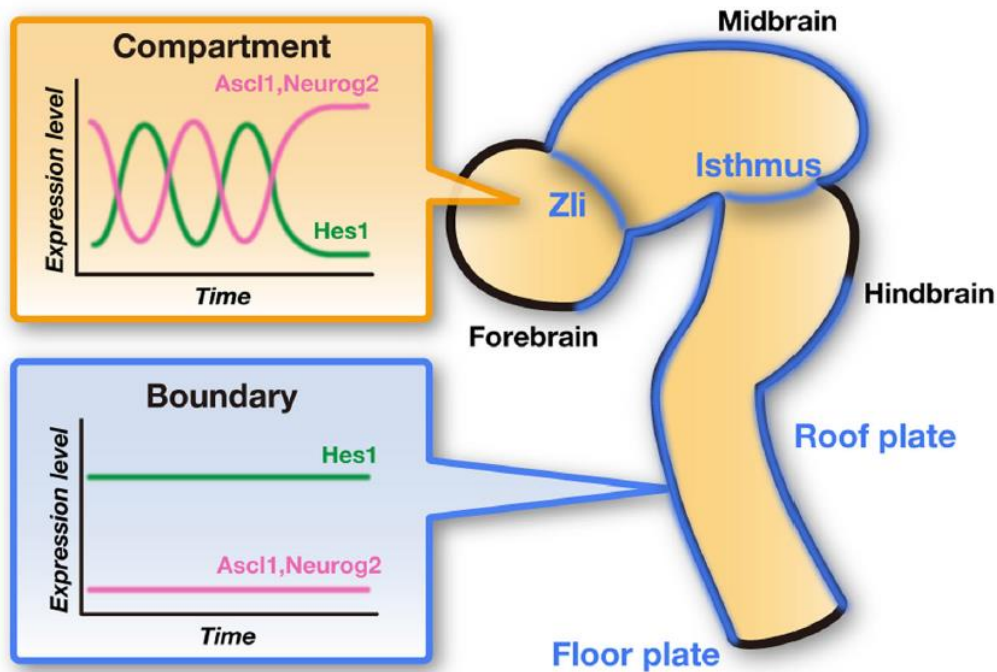


Figure 6. Different expression dynamics of Hes1 in the developing mammalian nervous system.

The developing nervous system is partitioned into many compartments by boundaries such as the isthmus and the zona limitans intrathalamica (Zli). Boundary regions contain cells that retain neuroepithelial features (progenitor pools or secondary neuroepithelial organizers), in contrast to the neural progenitor cells which are present in compartments. In mammals, boundary cells express Hes1 in a sustained manner, whereas compartmental neural progenitor cells present in compartments express Hes1 in an oscillatory manner. This is similar to what happens in teleosts where progenitor pools express Notch-independent *her* genes like *her5* in isthmus. These Notch-independent *her* genes are not expressed in an oscillatory manner. From **Kageyama *et al.*, 2015**.

1.2.2 Neural progenitors

In this section I will summarize the characteristics of the different kinds of neural progenitors (see **Table 1** and **Table 2**). Both neuroepithelial cells and radial glial cells (RGCs) can be found in all vertebrates.

	Neuroepithelial cells	Radial Glia (early)	Radial Glia (late)	Mammalian aNSCs (Astrocyte-like stem cells)
GFAP	-	-/+	+	+++
GLAST	-	++	++	++
Glutamine synthetase	-	-	+	++
S100- β	-	-	+	+
Nestin	+++	+++	+++	+++
Vimentin	-	+	++	+++
BLBP	++	+++	+++	++
Sox2	+++	+++	+++	++
ZO-1	+	-	-	-
aPKC	+	+	+	ND

Table 1. Similarities and differences between the different kinds of neural progenitors in terms of some molecular markers. Adapted from Götz *et al.*, 2015.

	Neuroepithelial cells	Radial Glia (early)	Radial Glia (late)	Mammalian aNSCs (Astrocyte-like stem cells)
Glutamate uptake	-	+	++	+++
K-conductance at rest	-	-	++	++
Glycogen storage	-	+	++	++
Blood vessel contact	-	+	++	+++
Interkinetic Nuclear Migration	+++	++	++	-
Cell division	+++	+++	++	++
Multipotency	+++	+++	++	+++
Self-renewal	++	++	+++	++

Table 2. Similarities and differences between the different kinds of neural progenitors in terms of cellular behavior. Adapted from Götz *et al.*, 2015.

1.2.2.1 Neuroepithelial cells

Once gastrulation is achieved, the neural tube starts to form in a process called neurulation. Both the neural plate and the neural tube are made of neuroepithelial cells. These cells are relatively homogenous during the earliest phases of the central nervous system (CNS) development and they go through a massive proliferation phase, greatly expanding their population prior to cell fate specification.

Neuroepithelial cells are polarized along their apico-basal axis. They are connected to each other at the apical surface (ventricular surface) by adherens junctions. Tight junction markers (like zonula occludens-1, ZO-1) can also be found at their apical (ventricular) domain. As a consequence of the presence of the junctional components, as well as of directed intracellular trafficking, the apical domain contains proteins and lipids that are distinct from those in the

basolateral membrane. The apical domain is really important for fate decision upon division. Both the overexpression and the depletion of proteins of the PAR complex (Par3, Par6 and aPKC) promote symmetric proliferative divisions to the detriment of the asymmetric neurogenic divisions in different cell types and model organisms (Willardsen and Link, 2011). A salient feature of the apical domain is the primary cilium. This microtubule-based protrusion is now well known to localize signaling components. It is a dynamic structure maintained by intraflagellar transport and is disassembled before the mitosis.

The neuroepithelium looks layered (“pseudo-stratified”) due to interkinetic nuclear migration (INM; Figure 7A). This process is linked with cell cycle progression (Götz and Huttner, 2005; Willardsen and Link, 2011). M-phase nuclei are positioned at the apical-most region. G1/S phase nuclei move to more basal locations. During G2 phase nuclei rapidly move back to the apical surface to enter the M-phase (Figure 7A). Recently it has been proposed an instrumental role of INM in determining cell fate of neural progenitors, by moving their nuclei through signaling gradients along the apico-basal axis of the epithelium. (Del Bene, 2011).

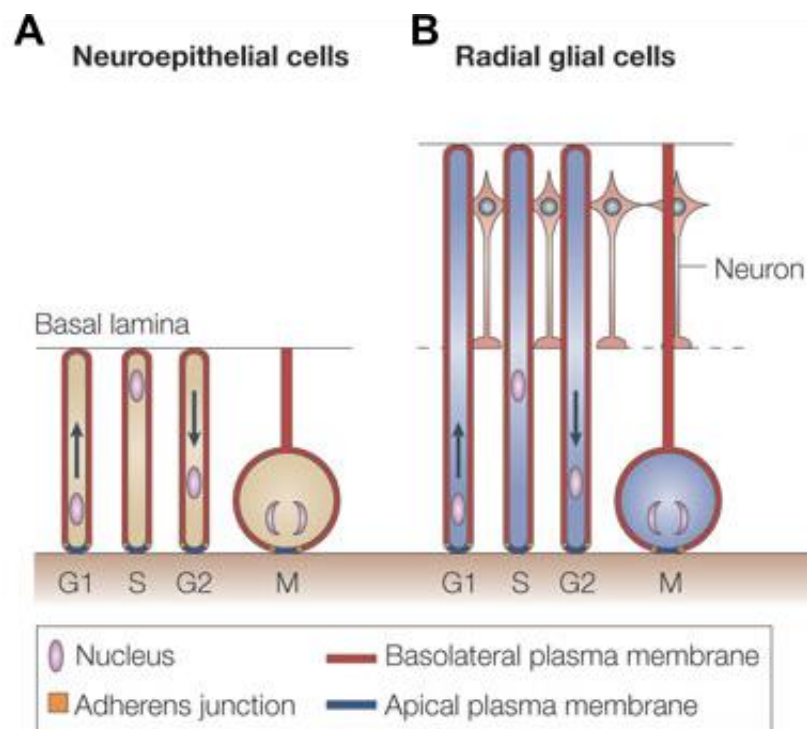


Figure 7. Apico-basal polarity in neuroepithelial and radial glial cells. (A) In neuroepithelial cells, interkinetic nuclear migration spans the entire apico–basal axis of the cell, with the nucleus migrating to the basal side during G1 phase, being at the basal side during S phase, migrating back to the apical side during G2 phase, and mitosis occurring at the apical surface. **(B)** In radial glial cells, the basally directed interkinetic nuclear migration does not extend all the way to the

basal side (that is, through the neuronal layer to their pial end-feet), but is confined to the portion of the cell between the apical surface and the basal boundary of the ventricular zone or the subventricular zone (not shown).

1.2.2.2 Radial glial cells

As embryonic neurogenesis progresses, neuroepithelial cells mature into regionally-specified progenitors (**Guérout *et al.*, 2014**) and radial glial cells appear. They derive from neuroepithelial cells and acquire a radial morphology, with their cell bodies located along the ventricular zone (VZ). In addition to Nestin expression, already present in neuroepithelial cells, RGCs express glial markers such as GLAST, BLBP, GFAP and Vimentin (**Table 1**). RGCs keep several features of neuroepithelial cells such as apico-basal polarity, adherens junctions, primary cilium at the apical surface and interkinetic nuclear migration (**Kriegstein and Alvarez-Buylla, 2009**). Moreover, they contain glycogen granules (an ultrastructural characteristic of astroglial cells; **Gadisseux and Evrard, 1985**). The transition from neuroepithelial cells to RGCs is also correlated with the expression of Pax6 and the concomitant down-regulation of the SoxB genes (Sox 1-3). Pax 6 promotes neurogenesis in several CNS regions, such as the forebrain, the retina and the hindbrain through the induction of bHLH proneural genes such as Neurogenins (**Paridaen and Huttner, 2014**).

INM is also different between neuroepithelial cells and RGCs. In these latter nuclei do not move along the whole apico-basal axis, but movements are confined to the portion of the cell between the apical surface and the basal boundary of the ventricular zone or subventricular zone (**Götz and Huttner, 2005; Figure 7B**).

Finally, the transition from neuroepithelial cells and RGCs is also characterized by the switch between symmetric, proliferative division to asymmetric neurogenic division.

1.2.2.3 Mammalian adult neural stem cells

Although the vast majority of CNS neurons are generated during embryogenesis, new neurons are also formed throughout adulthood. Adult neurogenesis occurs in two regions of the mammalian telencephalon: the subventricular zone (SVZ) of the lateral ventricles and the subgranular zone of the dentate gyrus of the hippocampus. These two neurogenic niches contain slowly dividing, astrocyte-like adult neural stem cells (aNSCs; see **Table 1** and **Table 2** for summary), which give rise to transient amplifying progenitors that in turn produce committed neuroblasts that migrate and differentiate into olfactory bulb or hippocampal neurons,

respectively (**Götz *et al.*, 2015**). Recent literature points out the fact that neurogenesis might be more widespread in the mammalian brain. Indeed, stem cell niches are present along the entire ventricular system of the rat brain (**Lin and Iacovitti, 2015**). Also in these cases neurogenesis seems to be supported by adult neural stem cells with astroglial characteristics.

Adult stem cells seem to support only normal renewal in mammals since regeneration relies on the activation of differentiated cell types. Thus, Nestin-negative non-proliferative and terminally differentiated cells (such as astrocytes and ependymal cells) are activated to supply cell loss upon injury (**Meletis *et al.*, 2008; Göritz *et al.*, 2011; Götz *et al.*, 2015**).

1.3. THE UNDEREVALUATED IMPORTANCE OF NEUROEPITHELIAL CELLS

As described above, neural progenitors have different morphology and can express different markers, but they also share common characteristics such as the single cilium or the expression of Nestin. Their identities are specified in a temporal ordered manner and the functional consequences of this change are poorly understood.

What is considered the “standard” in bio-medical sciences must be reconsidered in an evolutionary context. Astroglial adult stem cells appear to be a mammalian-specific feature (**Grandel and Brand, 2013**). Indeed, outside this group astrocytes do not contribute to adult neurogenesis which is mainly supported by radial glial cells. At present, these cells appear to be the only adult neural stem cells in the telencephalon in sauropsids. Radial glial cells contribute to adult neurogenesis in anamniotes as well (**Grandel and Brand, 2013**). Nonetheless, both in amphibians and fish, neuroepithelial cells are maintained until adulthood (**Figure 8A**). Neuroepithelial cells have been found in the cerebellum of zebrafish (**Kaslin *et al.*, 2009; Figure 8A₁ and 8D**) and in the visual system of both amphibians and fish where they contribute to the life-long neurogenesis in the optic tectum (**Figure 8A₁ and 8C**) and in the retina; (**Grandel and Brand, 2013; Schmidt *et al.*, 2013; Than-Trong and Bally-Cuif, 2015**). Interestingly, proliferative Notch-independent non-glial cells have been found both in the subpallium (**Figure 8A₁ and 8B₂**) and the hypothalamus of zebrafish (**Lindsey *et al.*, 2012, de Oliveira-Carlos *et al.*, 2013; Figure 8A₁**) and recently Dirian and colleagues demonstrated that “a minute population of neuroepithelial progenitors persist throughout life ant the posterolateral edge of the pallial ventricular zone” (**Dirian *et al.*, 2014; Figure 8B₃**).

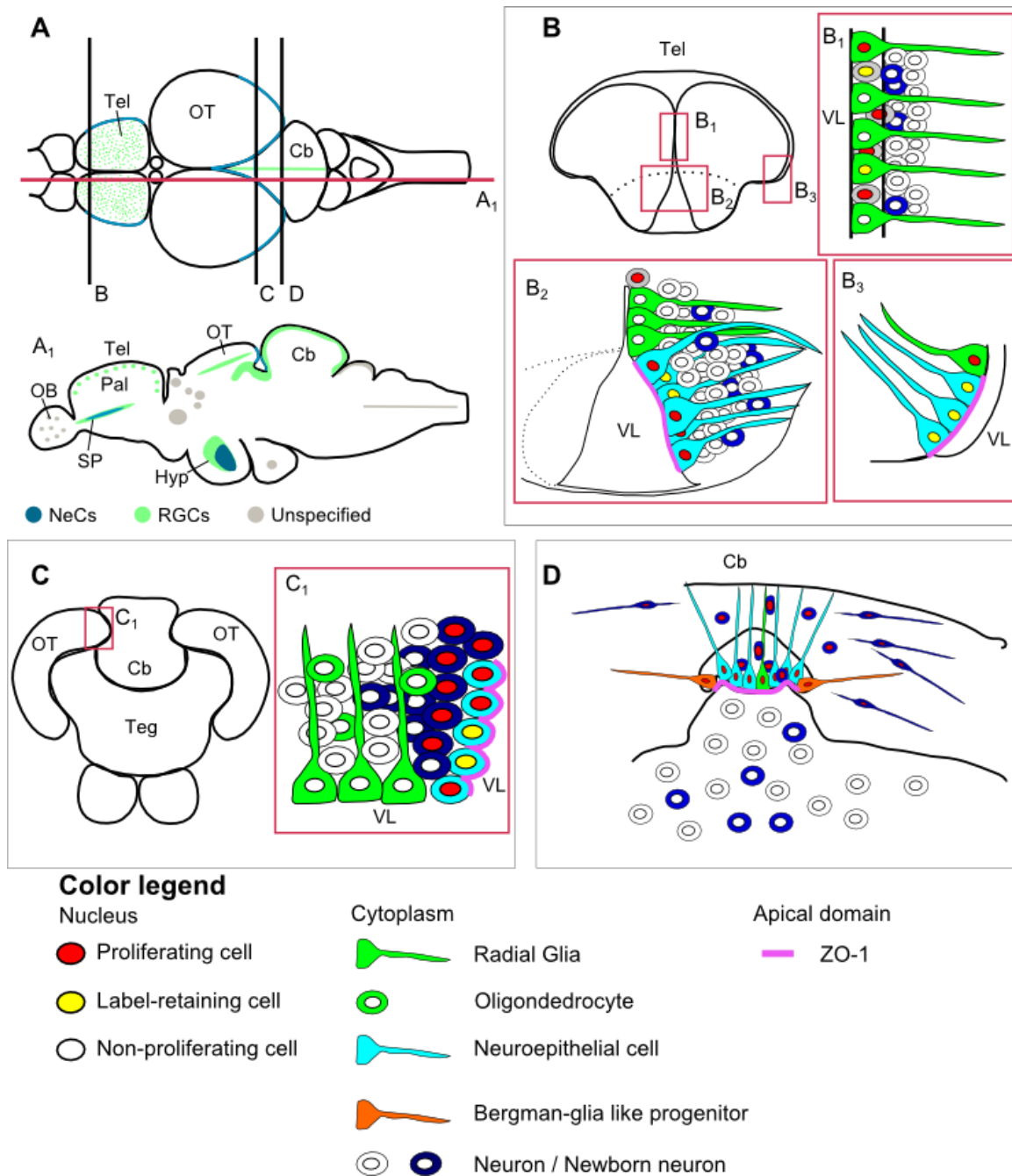


Figure 8. Overview of the stem cell/progenitor niches in the zebrafish adult brain. The zebrafish adult brain contains at least fifteen neurogenic niches. Both radial glial cells (RGCs) and neuroepithelial cells contribute to neurogenesis at adulthood. **(A)** Dorsal view of the zebrafish brain. **(A₁)** Red line indicates sagittal section. Black lines indicate section levels through **(B)** telencephalon, **(C)** optic tectum and **(D)** cerebellum. **(B)** Telencephalic cross section indicating neurogenic niches in the pallium/dorsal telencephalon **(B₁)**, subpallium/ventral telencephalon **(B₂)** and lateral pallium **(B₃)** that are magnified in the same panel. RGC cells support neurogenesis in the pallium (GFAP+, vimentin+, S100β+), whereas neuroepithelial cells support neurogenesis in the subpallium and in the lateral pallium (nestin+; ZO1+ in apical membrane). **(C)** Neurogenic niche in the tectum around the margin of the periventricular grey zone facing the tectal ventricle. Boxed area depicts location of the tectal neurogenic niche in **C₁**: non-glia (GFAP-, BLBP-, S100β-) polarized (ZO-1+, γ-tubulin+, aPKC+ at apical membrane) progenitor

cells give rise to neurons and periventricular radial glia. **(D)** The cerebellar neurogenic niche gives rise to granule cells and some Bergmann glia. Cerebellar stem/progenitor cells are non-glia (GFAP⁻, vimentin⁻, BLBP⁻, S100 β ⁻) but neuroepithelial-like polarized cells (nestin⁺; ZO-1⁺, β -catenin⁺, γ -tubulin⁺, aPKC⁺ at the apical membrane). VL indicates the position of the ventricle lumen in every structure. Adapted from **Grandel and Brand, 2013**.

Cb: cerebellum; Hyp: Hypothalamus; NeCs: neuroepithelial cells; OB: olfactory bulb; OT: optic tectum; Pal: pallium; RGCs: radial glial cells; SP: subpallium; Teg: tegmentum; Tel: telencephalon; VL: ventricle lumen.

It is noteworthy that, in vertebrates, the ability to regenerate brain damage correlates with the phylogenetic position and it appears to be related to the prevalence of constitutive adult neurogenesis in that particular species examined (**Grandel and Brand, 2013; Figure 9**).

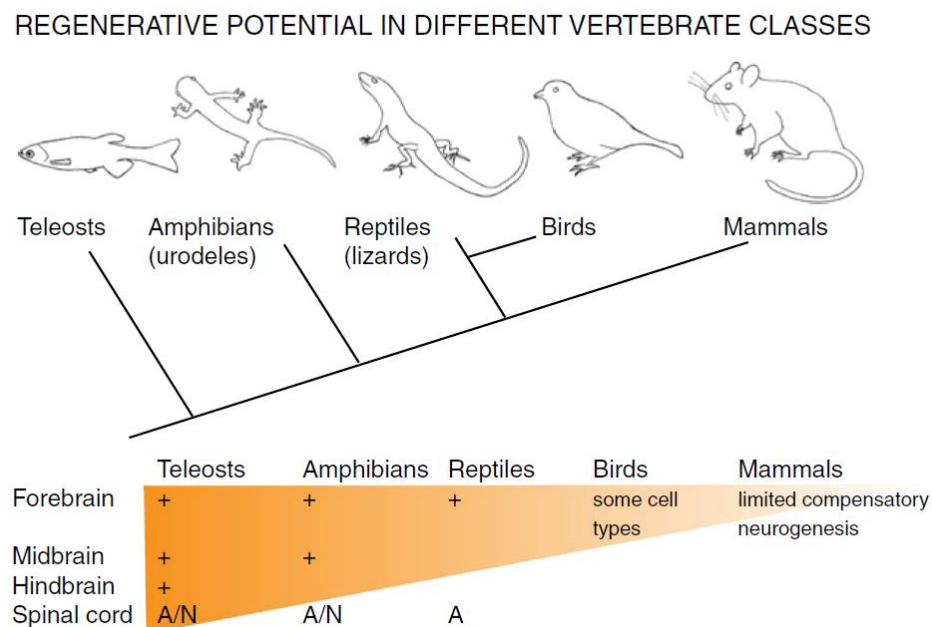


Figure 9. The ability of a vertebrate to regenerate brain damage correlates with its phylogenetic position. Phylogenetic interrelations of vertebrate classes (upper panel) and the regenerative potential of the brain (lower panel). The “wedge” represents the distribution of regenerative activity in different parts of the brain which is most widespread in teleosts, while in amphibians and amniotes, it becomes successively restricted to fewer and more anterior brain regions. Only limited compensatory neurogenesis has been observed in the mammalian telencephalon. The gradient symbolizes profound (dark colour) or limited (light colour) regenerative potential in different classes.

Plus signs refer to the brain parts that were reported to regenerate. The spinal cord shows (A) axonogenesis and (N) neurogenesis during regeneration. From **Grandel and Brand, 2013**.

Mammalian regeneration in the CNS appears to rely mostly on the reactivation of parenchymal astrocytes (**Kizil *et al.*, 2012; Sabelström *et al.*, 2013; Götz *et al.*, 2015; Ch1.1 section 1.2.2.3**). In non-mammalian vertebrates, regeneration is driven by RGCs activation and, to date, there are no examples of neuroepithelial-driven regeneration (even in anamniotes). Particularly interesting in this context are the cells contained in the ciliary marginal zone (CMZ) of the neural retina. The CMZ is a ring of cells at the periphery of the retina that contains retinal stem cells and retinal progenitor cells (RSCs and RPCs, respectively) which are neuroepithelial cells. Retinal neurons are added to the periphery of the retina by differentiation of these CMZ RSCs and RPCs. In fish and amphibians, a significant portion of the retina is formed from the CMZ after the initial differentiation of the neuroepithelium. Birds have a CMZ and the mammalian retina contains cells in the ciliary epithelium that can be induced to behave like stem cells in culture (**Perron and Harris, 2000; Fisher *et al.*, 2013**) and that express genes characteristic of retinal progenitor cells *in vivo* (**Janssen *et al.*, 2012**). Despite this, retinal neuroepithelial cells do not seem to participate to regeneration and biomedical research is thus focused on the reactivation of the Müller glia cells (RGCs of the retina; **Lenkowski and Raymond, 2014**). Nonetheless, after the discovery of the life-long lasting presence of neuroepithelial cells in the lateral pallium of zebrafish, it has been postulated that these cells could contribute to constitutive neurogenesis and regeneration when Notch-dependent progenitors are depleted (**Ninkovic and Götz, 2014**).

Neuroepithelial cells are transiently present and active during mammalian development and their proliferation is responsible of the size of the neural tube. Studying neuroepithelial cells could give insight on the etiology of human microcephalies (**Passemard *et al.*, 2011**).

It is clear that all neurons derive directly or indirectly from neuroepithelial cells which are hardly accessible (due to the *in utero* development) and poorly understood in mammals. These cells have an underestimated developmental importance. Thus, studies on zebrafish neuroepithelial cells are important for elucidating basic principles of neurogenesis from development to adulthood.

2. THE OPTIC TECTUM AND ITS “NEUROEPITHELIAL ORIGIN”

During my PhD, I have studied a small population of neuroepithelial progenitors located at the periphery of the zebrafish optic tectum.

In this section I will provide a detailed description of the tectum, of its anatomy, embryonic origin and growth mode.

2.1 THE OPTIC TECTUM IS PART OF THE MIDBRAIN

The optic tectum (OT) is a paired and dorsal structure of the vertebrate midbrain. In mammals its corresponding structure is the superior colliculus (even if the adjective “tectal” is used).

The OT is an evolutionary conserved layered structure known to control eye movements and it is involved in spatial orientation. Moreover, it controls visual spatial attention (**Krauzlis *et al.*, 2013; Zénon and Krauzlis, 2014**) and it receives some auditory afferents as well (**Celesia, 2015**).

In some teleosts, it represents the biggest part of the midbrain (**Figure 10**). It mainly receives axons from the retina ganglion cells, but also from the pretectum, the dorsal thalamus, the tegmentum, the nucleus isthmi and in some cases from the tegmentum (**Cervený *et al.*, 2012**). It is noteworthy that the size of the tecta and their complexity change between fish species, depending on their behavior and ecological niches. Thus, species that process more visual information have larger tecta (**Ito *et al.*, 2007**). Particularly interesting in this context are the intraspecific variations that can be found in subpopulations adapted to live in constant darkness compared with river-adapted subpopulation (**Eifert *et al.*, 2015**).

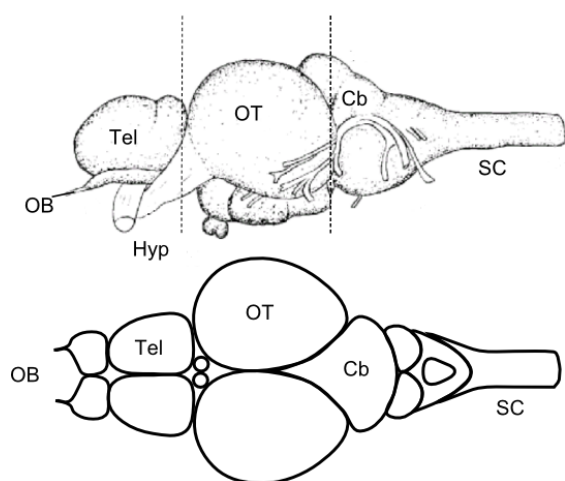


Figure 10. Localization of the optic tectum within the adult teleost brain. Upper panel: drawing of the lateral view of an adult medaka brain from **Nguyen *et al.*, 1999**. Dotted lines delimit, from left, rostral to right, caudal the telencephalon (forebrain), the mesencephalon (midBrain) and the rhombencephalon (hindbrain). Names of the structures are reported on a sketch of a dorsal view representing a teleost brain in dorsal view (lower panel). The optic tectum is a large, dorsal and pair structure of the midbrain.

Cb: cerebellum; Hyp: Hypothalamus; OB: olfactory bulb; OT: optic tectum; SC: spinal cord; Tel: telencephalon.

In teleosts, different layers can be histologically distinguished. The *stratum periventriculare* (SPV, also known as periventricular grey zone, PGZ) contains the cell bodies of most tectal neurons (periventricular neurons, PVNs). This is the deepest layer of the tectum and it is covered by a synaptic neuropil. This latter contains the PVNs' dendrites and axons as well as the axons of retinal ganglion cells. In medaka, two other layers of cell bodies, the central zone and the superficial zone, can be found within the tectal neuropil (Nguyen *et al.*, 1999). Dendrites and axons are organized in layers, thus the neuropil has a gross laminated structure (Figure 11A).

One of the main features of the teleost visual system, which is conserved among vertebrates, is the topography of the retinotectal projections. Thus, the tectal termini of retinal afferents reflect their cell body position in the retina (Baier, 2013; Figure 11A). Axons of retinal ganglion cells project to the contralateral (and, in some species, also to the ipsilateral) part of the tectum. In teleosts the projection is only contralateral. Thus the Cartesian coordinates of the image on the eye are projected onto the optic tectum (or superior colliculus) thereby creating a retinotopic map in the tectum (Cervený *et al.*, 2012; Figure 11B).

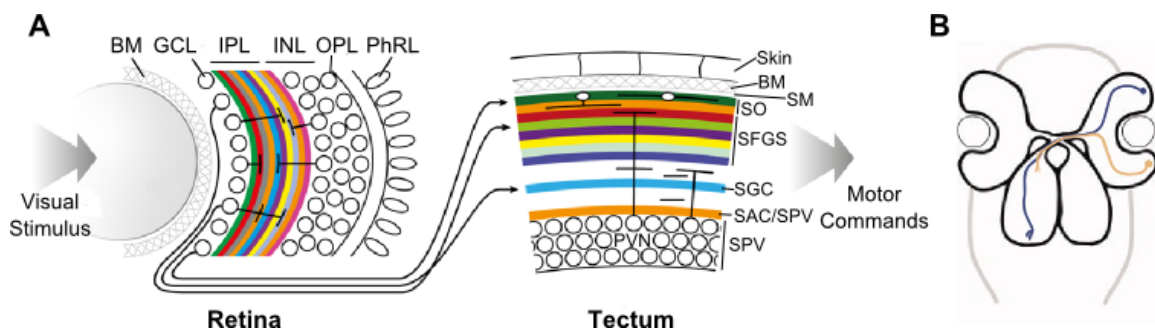


Figure 11. Retinotopic map in the OT. (A) The tectal afferent projections from the retina map the position of their origin. In the retina, the neurites of ganglion cells and amacrine cells join up together to form a ten-layered network (colored bands on the left, IPL). The axons of ganglion cells leave the eye via the optic nerve and project to the optic tectum. Here they each terminate in one of ten layers in the tectal neuropil (colored bands on the right). The position of one synapses in the tectum correspond to a position of a visual stimulus in the retina (B). Thus the visual space has a retinotopic projection in the tectum that corresponds to a space representation in the tectum. The life-long growth of the visual system in anamniotes leads to the continuous remodeling of the retinotectal connections. Thus, the retinotectal connections change over time but maintain the appropriate representation of visual space. Both sketches represent the topography and orientation of retinotectal connections in a zebrafish larva. (A) is from Baier, 2013 and (B) is from Cervený *et al.*, 2012.

BM: basement membrane; GCL: ganglion cell layer; INL: inner nuclear layer; IPL: inner plexiform layer; OPL: outer plexiform layer; PhRL: photoreceptor layer; PVN: periventricular neurons; SAC: *stratum album centrale*; SAC/SPV, boundary between SAC and SPV; SFGS: *stratum fibrosum et griseum superficiale*; SGC: *stratum griseum centrale*; SM: *stratum marginale*; SO: *stratum opticum*; SPV: *stratum periventriculare* (also called periventricular grey zone, PGZ); PVN: Periventricular neurons.

2.2 THE EMBRYONIC ORIGIN OF THE OPTIC TECTUM

The optic tectum originates from the alar plate (dorsal part of the forming neural tube) in the territory specified towards midbrain fate. This region is molecularly delimited by the activity of two neuroepithelial secondary organizers: the *zona limitans intrathalamica* anteriorly and the isthmic organizer posteriorly. This latter induces the formation of the midbrain/hindbrain boundary (MHB) that anatomically separates the midbrain from the hindbrain (cerebellum; **Cavodeassi and Houart, 2012**).

2.2.1 Induction of the isthmic organizer

With no exception in vertebrate development, at the end of the gastrulation, the anterior neural plate is broadly divided in two segments by the complementary expression of two pre-pattern genes: *Otx2* (anteriorly) and *Gbx2* (posteriorly; **Wurst and Bally-Cuif 2001**). The position of the *Otx2/Gbx2* interphase is defined by the extrinsic action of the of the Wnt molecules secreted by the lateral mesoderm. Wnt signaling, indeed, directly represses *Otx2* induce *Gbx2* expression in the posterior neuroectoderm. The *Otx2/Gbx2* expression interphase ultimately defines the position of the IsO and of the MHB lately. Both this structures are signaling centers by their own. In zebrafish, they express *fgf8* and *wnt1* contributing in defining hindbrain vs. midbrain identity. Indeed, *Fgf8* at the MHB is required to repress *Otx* in the presumptive anterior hindbrain. In the absence of *Fgf8* cerebellar identity is lost, but if both *Otx* and *Fgf* activity are absent, hindbrain fate is recovered (**Cavodeassi and Houart, 2012; Figure 12A**).

2.2.2 Induction of the zona limitans intrathalamica

The ZLI (**Figure 12B**) is a neuroepithelial secondary organizer that arises later during development. It is localized between the prospective prethalamus and thalamus. It is characterized by ventral presence of Sonic hedgehog (Shh) and the dorsal presence of the Wnt signaling (**Cavodeassi and Houart, 2012**).

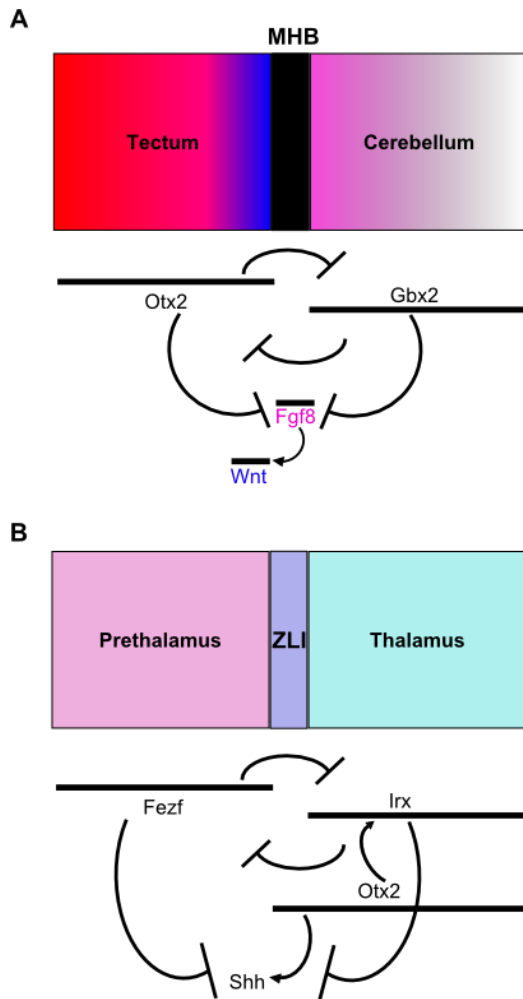


Figure 12. Specification of the secondary neuroepithelial organizers. Morphogenetic signals from the anterior ventral endoderm (AVE) and axial mesendoderm (AM) determine the early establishment of anterior and posterior properties in the neuroepithelium (*Ch1.1 section 1.2.1* and **Figure 2**).

Molecular interactions at the limits between these domains specify the development of morphogenetic organizers that generate a secondary wave of inductive signals to regulate the development of structural properties in the surrounding neural tube regions. **(A)** The first organizer to be induced is the isthmus organizer thanks to the mutual repression between *Otx2* and *Gbx2* that defines and refines the position of the MHB. **(B)** Then, the induction of the *zona limitans intrathalamica* limits the midbrain domain anteriorly. This secondary neuroepithelial organizer is induced via the mutual repression between *Fezf* and *Irxd*. Cells in this area express *Otx2* and secrete Sonic hedgehog (Shh) proteins ventrally. Adapted from **Cavodeassi and Houart, 2012**.

MHB: midbrain/hindbrain boundary; ZLI: *zona limitans intrathalamica*.

2.2.3 The midbrain/hindbrain domain of neurogenesis

The expression of *Fgf8* is induced, between the caudal limit of *Otx2* and the rostral limit of *Gbx2* in MHB. *Fgf8* expression domain corresponds to a neuron-free neuroepithelial zone in which neurogenesis is delayed. This feature is conserved across evolution (**Vieira et al., 2010**).

In zebrafish, this neuroepithelial zone had been named the intervening zone (IZ) and it has been demonstrated that, in this region, neurogenesis is inhibited by virtue of Her5 protein action (**Geling et al., 2003**). Moreover, it has been shown that *her5+* cells could contribute both to the midbrain and to the hindbrain formation until the end of the somitogenesis thereby highlighting that *her5* is the earliest marker of the MHB (**Figure 13; Tallafuss and Bally-Cuif, 2003**). *her5* expression characterizes some cells that will contribute to the midbrain growth until adulthood (**Chapouton et al., 2006; Ch1.1 section 2.3**).

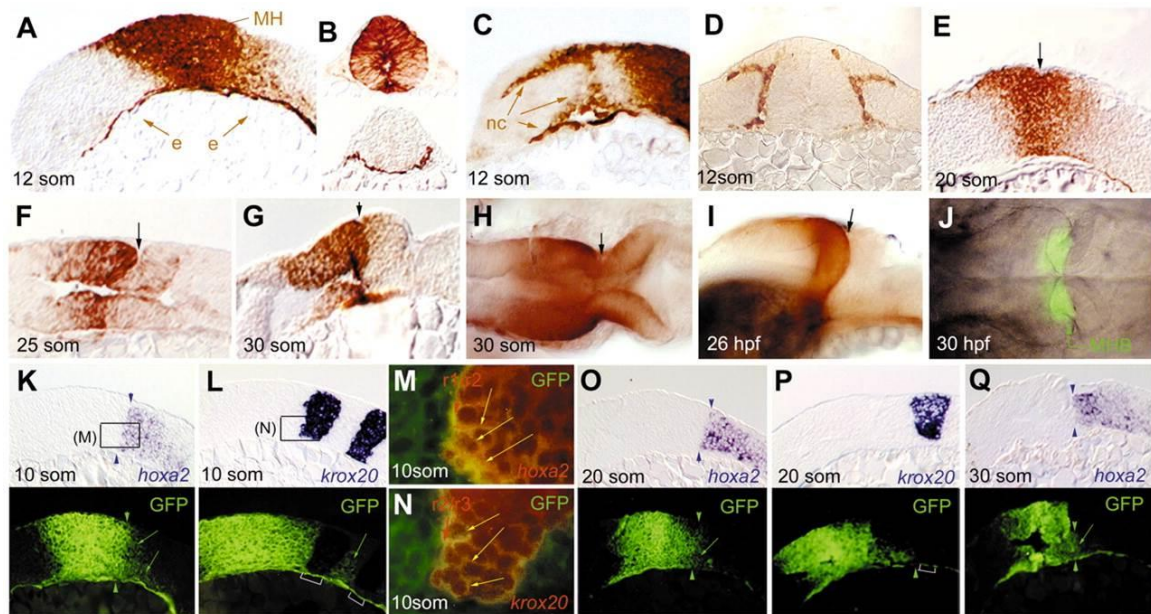


Figure 13. *her5* is the earliest marker of the MHB and *her5*⁺ cells contribute to the formation of the midbrain until the end of the somitogenesis. In order to study *her5* contribution to the formation of the midbrain Tallafuss and colleagues generated a GFP-reporter line (*her5PAC:egfp*). The distribution of GFP protein in *her5PAC:egfp* embryos revealed the fate of endodermal and neuroectodermal cells expressing *her5* at gastrulation. The GFP protein in *her5PAC:egfp* embryos was observed on live specimen (**J**) or revealed by immunocytochemistry (**A-I**, brown DAB staining; and **K-Q**, green FITC staining) at the stages indicated. (**H-J**) Whole-mount views: (**H, J**) dorsal views, anterior leftwards; (**I**) lateral view, anterior leftwards. (**K-Q**) Sagittal sections, anterior leftwards. In **K, L, O-Q**, the top and bottom panels are bright-field and fluorescent views, respectively, of the same sections that were each processed for *in situ* hybridization and immunocytochemistry against GFP protein. (**M, N**) High magnifications of equivalent levels to those boxed in **K** and **L**, respectively. Overlay pictures of the *in situ* hybridization staining (revealed using Fast Red, red fluorescence) and GFP immunocytochemistry (FITC staining). The cytoplasm of cells doubly positive for GFP protein and for the *in situ* hybridization marker (*hoxa2* or *krox20*, respectively) appears yellow. At 12 somites, the descendants of neural *her5*-expressing cells distribute over a broad domain around the midbrain-hindbrain boundary. In **E-J**, arrows indicate the midbrain-hindbrain boundary; note that GFP protein distributes posterior to this level (i.e. to hindbrain derivatives) until 24 hpf. Thus, *her5*⁺ cells appear to contribute both to the midbrain and to the hindbrain. The contribution to the hindbrain is limited to the anterior-most rhombomers during somitogenesis. *her5*-derived cells can be found all over the midbrain and the optic tectum during somitogenesis. Interestingly, at the end of the somitogenesis, GFP expression is restricted to the MHB (**J**, dorsal view). Thus, it does not encompass the whole tectal proliferation area. Moreover, *her5* expression becomes restricted to a small medial ventral domain at later stages thereby highlighting the possibility that *her5*⁺ positive cells do not contribute anymore to tectal and cerebellar growth later during development (see *Ch1.1 section 2.3.2*). From Tallafuss and Bally-Cuif, 2003. Part of the legend had been taken from Tallafuss and Bally-Cuif, 2003.

long radial growth of the tectum. The development of the tectum in other teleosts occurs according to an equivalent timeline. Medaka stages from left to right: stage 22 (9 somite stage), stage 28 (30 somite stage), stage 32 (Somite completion stage), stage 39 (Hatching stage). Adapted from **Nguyen *et al.*, 2009**. **(B)** The growth of the OT will then continue throughout lifespan via the addition of columns of cells at the periphery of the structure (blue area). The OT grows thereby radially increasing its size from the periphery (green arrows indicate the growth direction) Cells will differentiate in the central-most part of the OT. Thus, a gradient of differentiation is created from the periphery towards the center of each tectal hemisphere (red arrows).

Cb: Cerebellum; CZ: central zone; mpz: marginal proliferation zone; OT: optic tectum; SZ: superficial zone; PGZ: periventricular grey zone; Tel: telencephalon.

2.3.2 Neuroepithelial cells support growth at adulthood

Several studies demonstrated that, in the adult zebrafish OT, PCNA-positive (*i.e.* proliferating) cells exist within the dorsal, caudal, and ventral margins of the periventricular gray zone (PGZ; **Grandel *et al.*, 2006; Marcus *et al.*, 1999, Zupanc *et al.*, 2005**). Interestingly, Grandel and colleagues (**Grandel *et al.*, 2006**) using simple pulse BrdU experiments labeled a region that has been named PML (posterior mesencephalic lamina; **Figure 15A and 15B**). This thin layer of cells starts dorsally at the proliferative tectal margin, continues as non-proliferative lamina and becomes proliferative again as it touches the cerebellar surface. Cells in the PML contribute to the formation of the OT at adulthood. Moreover, they contribute to the formation of the *torus semicircularis* (the mesencephalic structure underlying the OT; **Figure 15C**).

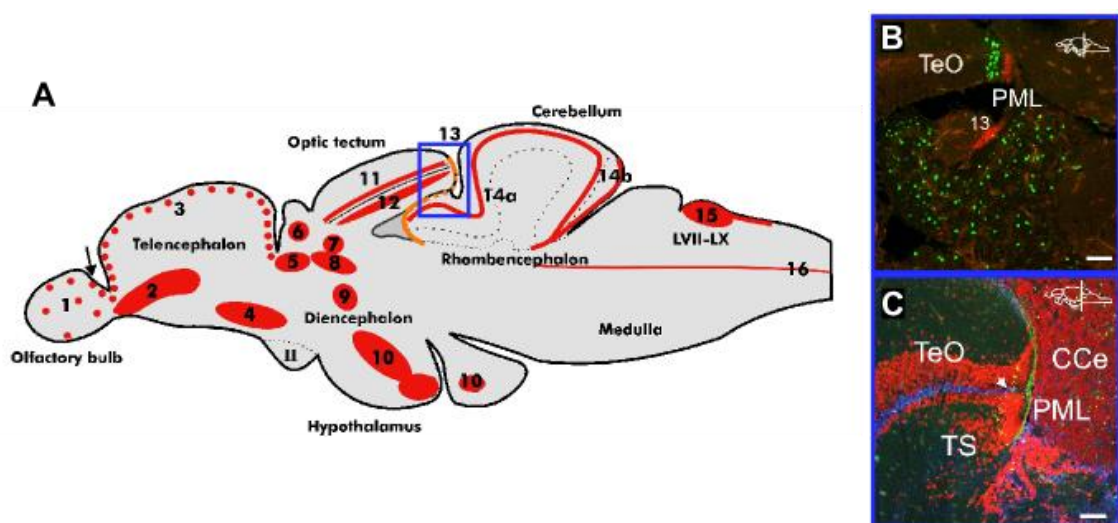


Figure 15. Proliferating cells are present at the tectal margins in adult zebrafish brains. Grandel and colleagues highlighted the presence of sixteen proliferation zones within the zebrafish adult

brain which are depicted on the schematic drawing of a parasagittal section and indicated by numbers **(A)**. Particularly interesting, it is the midbrain proliferation zone (zone 13, blue box). Using simple pulse BrdU experiments labelled the PML (posterior mesencephalic lamina). The PML thin layer of cells connects the dorsally the proliferative tectal margin, continues as non-proliferative lamina and becomes proliferative again as it touches the cerebellar surface. PML cells are actively proliferating as it can be seen in **B** on fourteen-micrometer cross-sections of a brain of a 7-month-old adult zebrafish double stained for BrdU (green), 46 days after an initial 48 hours pulse, and PCNA (red) to visualize actively proliferating cells. Moreover, these cells contribute both to the optic tectum (TeO) and to the torus semicircularis (TS) as shown in **C** on fourteen-micrometer cross-sections of a brain of a 7-month-old adult zebrafish stained for BrdU (green) 46 days after an initial pulse, HuC/D (neuronal marker, red) and S100 β (radial glia marker, blue). Indeed, adjacent to the PML, BrdU+ cells have moved into the HuC/D+ nuclear areas of the optic tectum and the *torus semicircularis* and into the S100 β + ventricular zone (arrow) of the OT. Adapted from **Grandel et al., 2006**. TeO: optic tectum; TS: *torus semicircularis*; PML: posterior mesencephalic lamina; CCE: *Corpus cerebelli*.

Adult tectal progenitors have been further characterized both in zebrafish (**Ito et al., 2010**) and medaka (**Alunni et al., 2010**). In both species slow-cycling label-retaining cells have been found at the caudal-most tip of the adult tecta. Interestingly, these cells express neural stem cells marker such as Sox2 and Musashi1, but they do not express any radial glia marker such as BLP or GFAP. Together these data highlight the fact that neuroepithelial cells persist until adulthood in teleosts and they actively contribute to neurogenesis in the OT. Slow cycling cells reported in these two works correspond to the dorsal most part of the PML identified by Grandel and colleagues (**Figure 15A; Grandel et al., 2006**). Furthermore, it has been demonstrated, by fluorescent *in situ* hybridization (FISH) experiments, that these cells express three notch receptors (*notch1a/1b/3*; **de Oliveira-Carlos et al., 2013**). Notch signaling might thus be required to keep the progenitor niche as a neuron-free zone (see *Ch1.1 section 1.2.1.2*). It is noteworthy, that Notch signaling and, in particular, the activation of the Notch 3 receptor is required for the quiescence of the radial glial cells in the zebrafish telencephalon (**Chapouton et al., 2010; Alunni et al., 2013**).

Neuroepithelial cells of the OT do not express *her5*. At adulthood, *her5+* cells are located at the junction between the midbrain and the hindbrain barrier. They contact the ventricle ventrally to the torus semicircularis and they contribute to the neurogenesis in the tegmentum (ventral midbrain). They not contribute to the morphogenesis of the tectum. Furthermore, they express radial glia markers (**Figure 16; Chapouton et al., 2006; Chapouton et al., 2011**). Thus, two different progenitor pools contribute to neurogenesis in zebrafish midbrain. One population of radial glial cells contribute to neurogenesis in the ventral part of the midbrain (the tegmentum)

and one population of neuroepithelial cells contribute to the neurogenesis in the OT (**Chapouton et al., 2011; Schmidt et al., 2013**). It is not clear how these two populations arise within the MHB domain during development. One possible scenario is that they share a common origin before segregating. Thus, the original *her5*⁺ cell population (that contributes to tectal morphogenesis during somitogenesis; **see section 2.3**) might split in two subpopulations during development: one dorsally located that retain neuroepithelial characteristics and one ventrally located that starts to express radial glia markers. Alternatively, it is also possible that the two populations are specified separately within the neural tube with the *her5*⁺ population of cells contributing to the early OT morphogenesis.

Further work is needed to characterize the tectal niche of neuroepithelial cells and its embryonic origin. It is in this context that my PhD work has been realized.

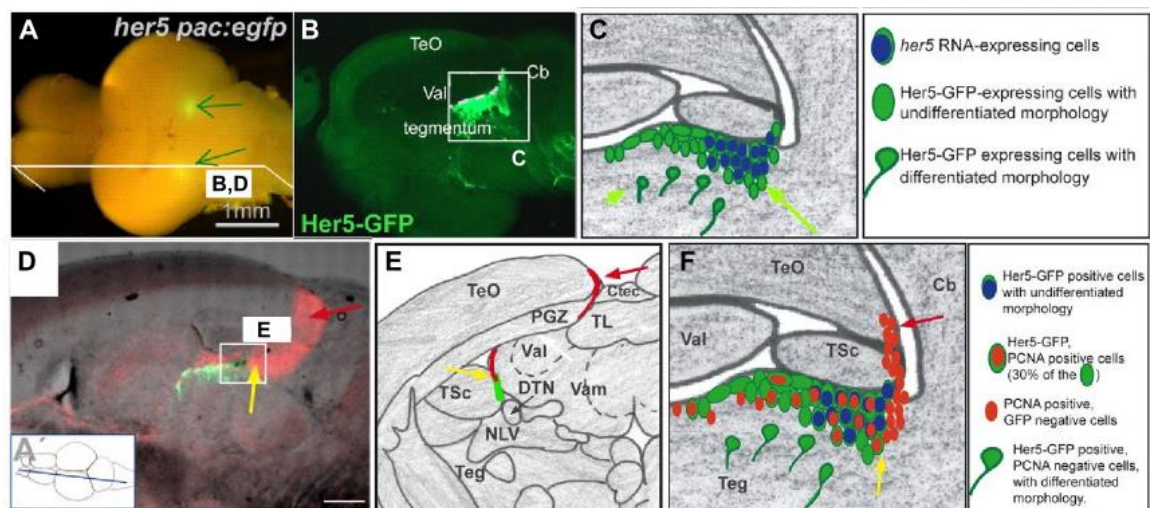


Figure 16. *her5*-positive cells do not contribute to OT formation at adulthood. *her5* expressing cells localize in two clusters at adulthood (**A**) ventrally to the tectum (**B**). Most part of the cells within these clusters display undifferentiated morphology (**C**).GFP-positive cells (i.e. *her5* positive cells) are located in closer proximity to PML described by Grandel and colleagues (**Grandel et al., 2006**; PCNA-positive cells, in red; **D-E**). Only few cells within the *her5*-positive clusters are actively proliferating (**F**). These cells express radial glia markers and they contribute to the formation of the ventral structures of the midbrain (like the tegmentum) rather than contributing to the tectum. Adapted from **Chapouton et al., 2006**.

Cb: cerebellum; Ctec: tectal commissure; DTN: dorsal thalamic nucleus; NLV: *nucleus lateralis valvulae*; PGZ: periventricular grey zone; Teg: tegmentum; TL: *torus longitudinalis*; TeO: optic tectum; TPZ: tectal proliferation zone; TSc: torus semi-circularis; Val: *valvula cerebelli lateralis*; Vam: *valvula cerebelli medialis*.

2.4 THE OT IS A CELLULAR CONVEYOR BELT THAT CAN BE USED AS A PREDICTIVE MODEL TO STUDY GENE FUNCTION.

Because of its radial growth that generates a differentiation gradient from the periphery towards the center of each lobe, the OT can be considered as a cellular conveyor belt (CCB) and can be used to answer cell-cycle related questions. According to the definition “A CCB is an organ, or a part of an organ that has a balanced growth pattern so that, during development, there is no mixing between proliferative cells and cells that exit the cycle. Typically, these are polarized growing organs which bear at one pole (or extremity) a zone of actively dividing progenitors, followed by a zone of cells exiting the cycle, followed by a zone of differentiating cells” (Devès and Bourrat, 2012).

In the OT there is a spatio-temporal correlation between the position of a cell and its differentiation state. Thus, the OT completely fulfills the definition of cellular conveyor belt. Other examples of cellular conveyor belts are represented by the anamniote retina and the mammalian intestinal crypts. (Devès and Bourrat, 2012; Figure 17).

Cells at different steps of the differentiation process will express particular genes (i.e. cells at the periphery of the OT express proliferation markers and cells at the center of the OT express neuronal-specific genes). Moreover, as previously seen the tectum and the retina are functionally and molecularly connected so they share common molecular signatures. They both express many canonical proliferation markers. (Cervený *et al.*, 2012).

All together these features make the OT an excellent predictive model to study gene function. Indeed, an *in situ* hybridization analysis could rapidly tell whether or not a gene is involved in neurogenesis or plays a role during the differentiation process. The predictive capacity of model OT had been tested and validated many times (Candal *et al.*, 2004; Deyts *et al.*, 2005; Candal *et al.*, 2005; Thermes *et al.*, 2007; Brombin *et al.*, 2011; see annex).

As powerful as it might be, teleost OT remains a predictive model. The functional validation of selected candidate genes is, of course, necessary. Thus, functional validations should be provided for every gene studied. To this aim I performed the experiments during my PhD.

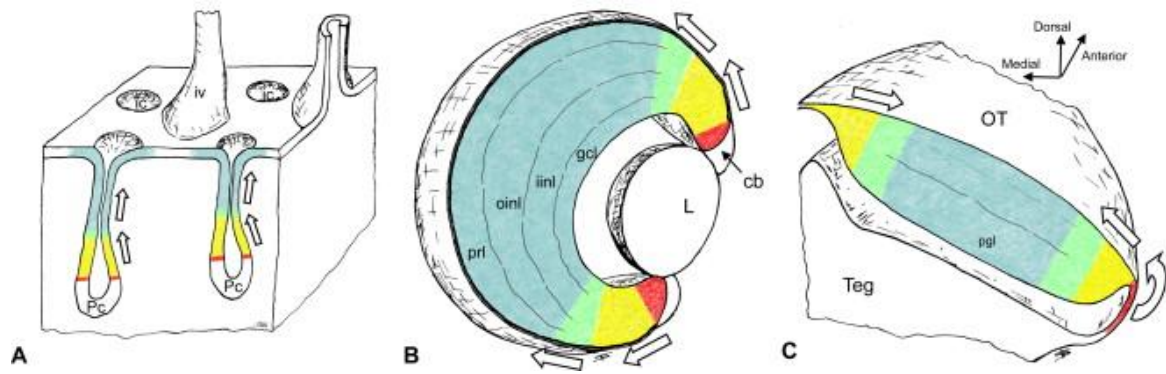


Figure 17. Schematic representations of three examples of cellular conveyor belts. (A) Intestinal crypts of a mammal; **(B)** retina of a teleost fish or a frog; **(C)** Optic tectum of a teleost fish. The stem/ progenitor cell zones are in red, the zones of *actively dividing progenitors* are in yellow, the *cell cycle exit* zones are in green, the zones of *differentiated cells* are in blue. The open arrows indicate the direction of the cellular conveyor belts movements. From **Devès and Bourrat, 2012**.

PART II RIBOSOME BIOGENESIS IS IMPORTANT FOR CELL HOMEOSTASIS

Ribosome biogenesis is a strictly coordinated and highly energetic demanding process which is responsible for the synthesis of the ribosomes. These latter are ribonucleoprotein complexes that translate mRNAs into proteins. They are composed of two subunits (40S and 60S in eukaryotes). In human, 33 ribosomal proteins (RPs) together with the 18S ribosomal RNA (rRNA) constitute the small ribosomal subunit (40S) whereas the large ribosomal subunit (60S) is made of 47 RPs and 3 rRNAs (28S, 5.8S, 5S; **Filipovska and Rackham, 2013**). Their synthesis is fundamental to all life forms and it occurs in a roughly standardized way (see **Fromont-Racine et al., 2003** for review). In eukaryotes, ribosome biogenesis occurs mainly in the nucleolus and it starts with the transcription of the rRNAs. Eukaryotic genomes bear multiple copies of rRNA-coding DNA clusters. In mammals, the 47S rRNA precursors are transcribed in the nucleolus by the RNA polymerase I and then modified to generate the mature rRNAs 18S, 28S and 5.8S. The 5S rRNA is transcribed independently by the RNA polymerase III in the nucleoplasm before being imported into the nucleolus. rRNA precursors are processed while they are still transcribed. They are cleaved and post-transcriptionally modified (pseudouridylated and methylated). During ribosome biogenesis, the almost 80 ribosomal proteins (RPs) are assembled to the rRNAs to form mature ribosomal subunits ribosomes. More than 200 non-ribosomal factors (ribosome biogenesis factors, RBFs) are needed throughout the whole process. They contact temporarily the maturing rRNAs and ribosomes to ensure the final result (**Figure 18**). The biogenesis of ribosomes is a tightly regulated process and it is inextricably linked to other fundamental cellular processes, including growth and cell division (**Thomson et al., 2013**). Moreover, ribosome biogenesis allows cell growth control thereby coupling protein synthesis to nutrient availability via the mTOR pathway (**Mayer and Grummt, 2006**).

Fluctuations in terms of ribosome biogenesis occur during cell cycle progression. Moreover, disrupted ribosome biogenesis leads to cell cycle arrest (and eventually cell death) in normal cells. It is not surprising if ribosome biogenesis is one of the elected targets in cancer therapy. Recent studies have demonstrated that defects in ribosome biogenesis are associated with several hereditary diseases (see **Armistead and Triggs-Raine, 2014**). Furthermore, ribosome biogenesis might indirectly contribute to the translational control of gene expression. Indeed, ribosomes are not simply translation machines but also function as regulatory elements that differentially affect (or filter) the translation of particular mRNAs. Ribosome-driven regulation at the translational level relies on the heterogeneous composition of the ribosome themselves

(Mauro and Edelman, 2007; Xue and Barna, 2012; Filipovska and Rackham, 2013). Surprisingly little is known about the mechanisms generating this diversity. All these ribosome biogenesis-centered mechanisms will be reviewed in this second part of the introduction. At the end, I will focus on the relationship between ribosome biogenesis and stem cells.

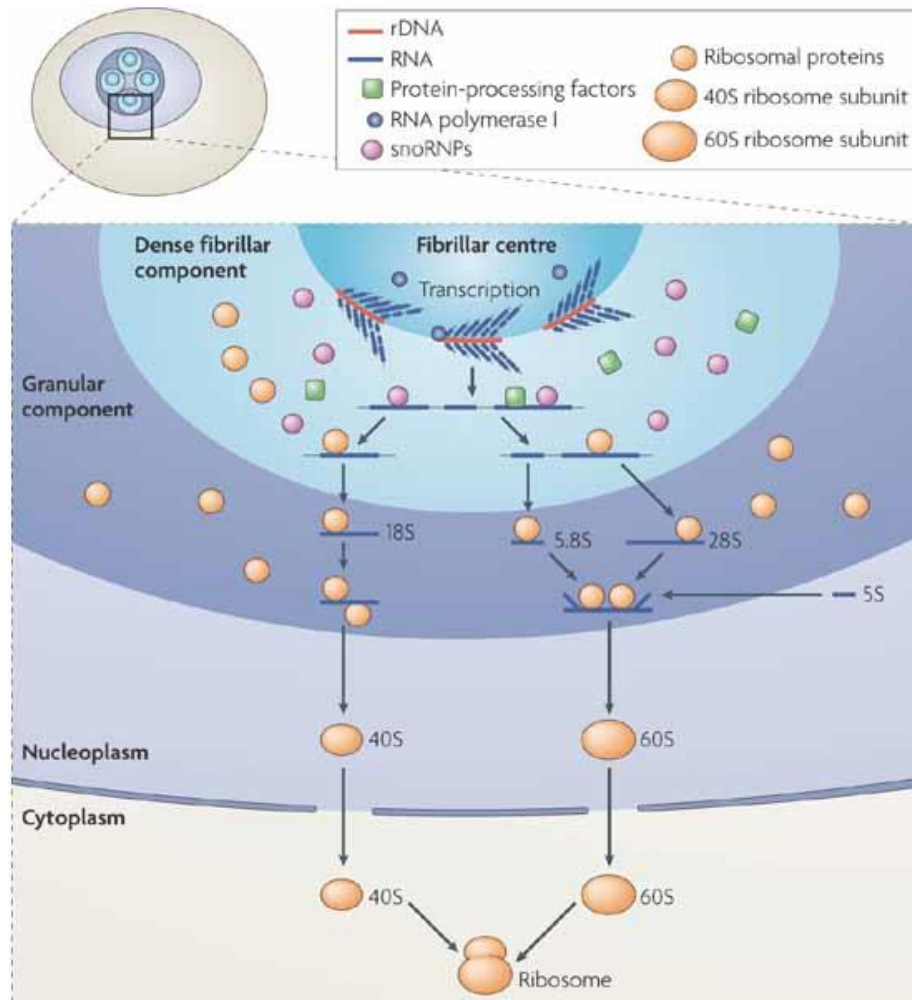


Figure 18. Ribosome biogenesis occurs mainly in the nucleolus. Three zones can be distinguished within the mammalian nucleolus: the fibrillary center, the dense fibrillary component and the granular component. Eukaryotic genomes bear multiple copies of rRNA-coding DNA clusters. In mammals, the 47S rRNA precursors are transcribed in the nucleolus by the RNA polymerase I and then modified to generate the mature rRNAs 18S, 28S and 5.8S. The 5S rRNA is transcribed independently by the RNA polymerase III in the nucleoplasm before being imported in the nucleolus. rRNA transcription occurs at the border between the fibrillary center and the dense fibrillary component. In this compartment, the 47S rRNA precursor is cleaved. It is also methylated by the box C/D snoRNP complexes and pseudouridylated by the box H/ACA snoRNP complexes. Ribosomal proteins are assembled to the maturing rRNAs. Maturation of the pre-ribosomal particles continues in the nucleoplasm and in the cytoplasm after exportation. Mature 40S subunits and 60S subunits will be then assembled to form the functional 80S ribosome. 40S subunit contains the 18S mature rRNA, whereas the 60S contains rRNAs 28S, 5.8S and 5S. From **Boisvert et al., 2007**.

1. RIBOSOME BIOGENESIS AND CELL CYCLE PROGRESSION

Cell cycle progression and ribosome biogenesis are strictly linked processes. A full understanding of this relationship may reveal new ways to induce cell cycle arrest in cancer cell. Moreover, these studies may also provide new insights in the comprehension of the biology of stem and progenitor cells which are, by definition, strictly controlled-cycling cells (**Drygin et al., 2010; James et al., 2014; Marcel et al., 2015**).

There is a mutual regulation between ribosome biogenesis and cell cycle progression that relies on the activity of cyclin-CDK complexes (**Drygin et al., 2010; Volarevic et al., 2000; Derenzini et al., 2005**). Furthermore, feedback-loop mechanisms are activated once ribosome biogenesis is blocked. RBFs, RPs and rRNAs maintain a nucleoplasmic steady-state concentration under normal growth conditions, but assume new functions and act as effectors under nucleolar stress conditions (impaired ribosome biogenesis). Both p53-dependent and p53-independent mechanisms of cell cycle arrest (and eventually apoptosis) can be activated (**James et al., 2014**) and they will be described in the following sections.

1.1 RIBOSOME BIOGENESIS AND CELL CYCLE PROGRESSION ARE MUTUALLY REGULATED

Cyclin-CDK complexes couple the ribosome biogenesis regulation with cell cycle progression.

As previously mentioned ribosome biogenesis starts with the transcription of the rRNA genes by Pol I (**Figure 18**) and Pol III. Many co-factors allow the activation of the polymerases. For example, the active Pol I transcription initiation complex in mouse includes the upstream binding factor UBF, the multi-protein complex TIF-1B (SL-1 in human), TIF-1A, the Pol I complex and many others (**Goodfellow et al., 2013**). The activation of the Pol I is regulated during the cell cycle. In quiescent cells, the hyperphosphorylation of UBF is required to initiate the assembling of the transcriptional complex and the entry of cells in G1 (**Voit et al., 1995**). Then, during cycle, rRNA transcription (and therefore the whole ribosome biogenesis) reaches its maximum during S and G2 phases and decreases during the M phase. This is realized by mean of cyclin-CDK-dependent phosphorylations of both UBF and TIF-1B/SL-1. (**Drygin et al., 2010**) (**Figure 19**). Interestingly, Pol I activity seems to be highly regulated in stem cells (although in a cyclin-CDK-independent manner). Diverse transcription activators and repressors bind either the Pol I or the rDNA loci to regulate rRNA transcription (**Brombin et al., 2015; see Ch1.II section 2.2.4**).

The quantity of ribosomes itself can limit cell cycle progression. It has been shown that the translation of cyclin E is specifically impaired upon ribosomal protein or rRNA haploinsufficiency. Thus, cells lacking a sufficient amount of ribosomal components fail to express cyclin E despite the formation of active cyclin D–CDK4 complexes. The G1/S transition is therefore blocked and cells stop proliferating (Volarevic, 2000; Derenzini *et al.*, 2005).

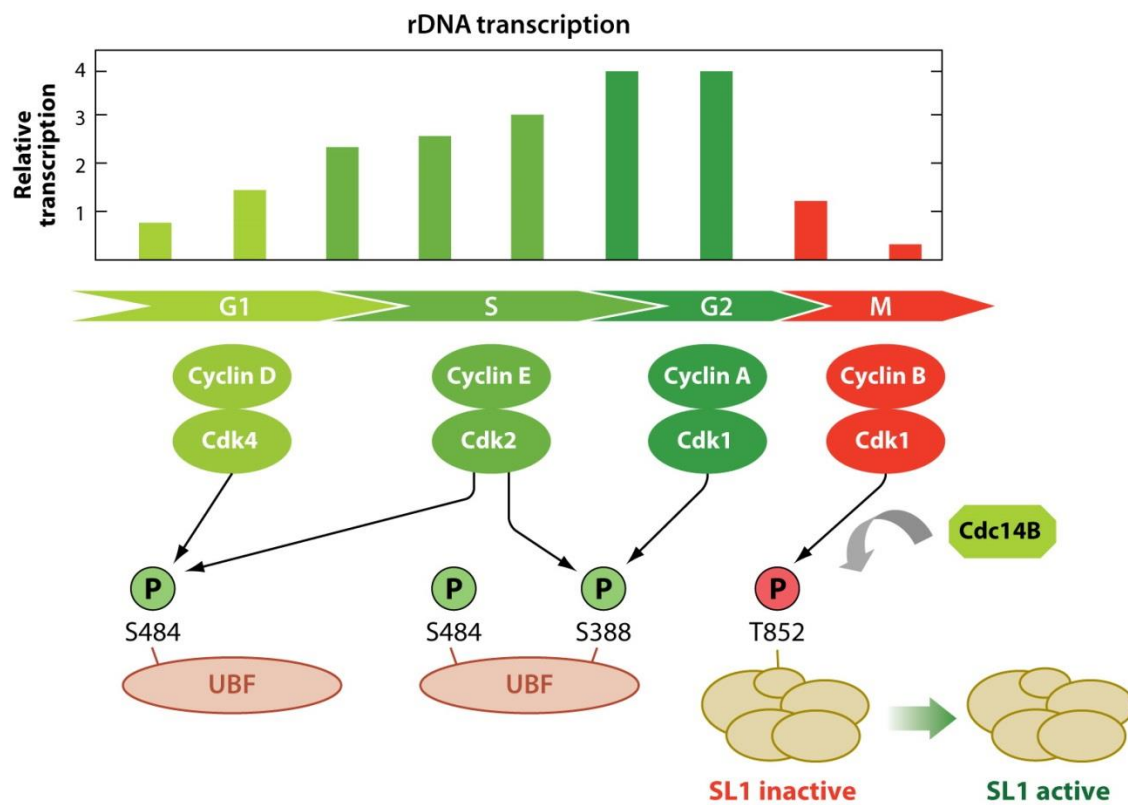


Figure 19. rRNA transcription is regulated during cell cycle progression in a cyclin-CDK-dependent mechanism. UBF is activated during interphase by phosphorylation of serine 484 (S484) by Cdk4/cyclin D and phosphorylation of serine 388 (S388) by Cdk2/cyclin E and A. At the entry into mitosis, phosphorylation of TAF₁₁₀ at threonine 852 (T852) by Cdk1/cyclin B inactivates TIF-IB/SL1. At the exit from mitosis, Cdc14B dephosphorylates T852, leading to recovery of TIF-IB/SL1 activity. All these phosphorylations regulate the activity of the Pol I and the rRNA transcription during cell cycle progression. Activating phosphorylations are marked in green, inhibiting ones in red. From Drygin *et al.*, 2010.

1.2 NUCLEOLAR STRESS AND CELL CYCLE PROGRESSION

1.2.1 p53-dependent mechanisms coupling ribosome biogenesis and cell cycle progression

Tumor protein 53 (Tp53, hereafter p53) is a transcription factor which is able to induce cell cycle arrest and apoptosis by activating the transcription of a plethora of genes and its own

transcription. In normal conditions, p53, is found in the nucleus at a steady-state level under the control of Mouse double minute 2 homolog (Mdm2, HDM2 in human). Mdm2 is an E3-ubiquitin ligase that inhibits p53 activation. In normal conditions, Mdm2 ubiquitylates p53 thereby inducing its degradation in the proteasome (**Figure 20A**). If Mdm2 is inhibited, p53 can be phosphorylated by endogenous kinases and translocate into the nucleus where it activates the transcription of checkpoint genes (such as *p21/waf1/cip1*), DNA repair genes and pro-apoptotic factors (**Figure 20B**). As recently reviewed (**James et al., 2014**), many RBFs can activate p53 via Mdm2 inhibition. Among these factors which are normally segregated in the nucleoli, are the proteins Nucleophosmin (Npm1) and Nucleostemin (NS). The former is a multifunctional protein that acts at many levels of the ribosome biogenesis

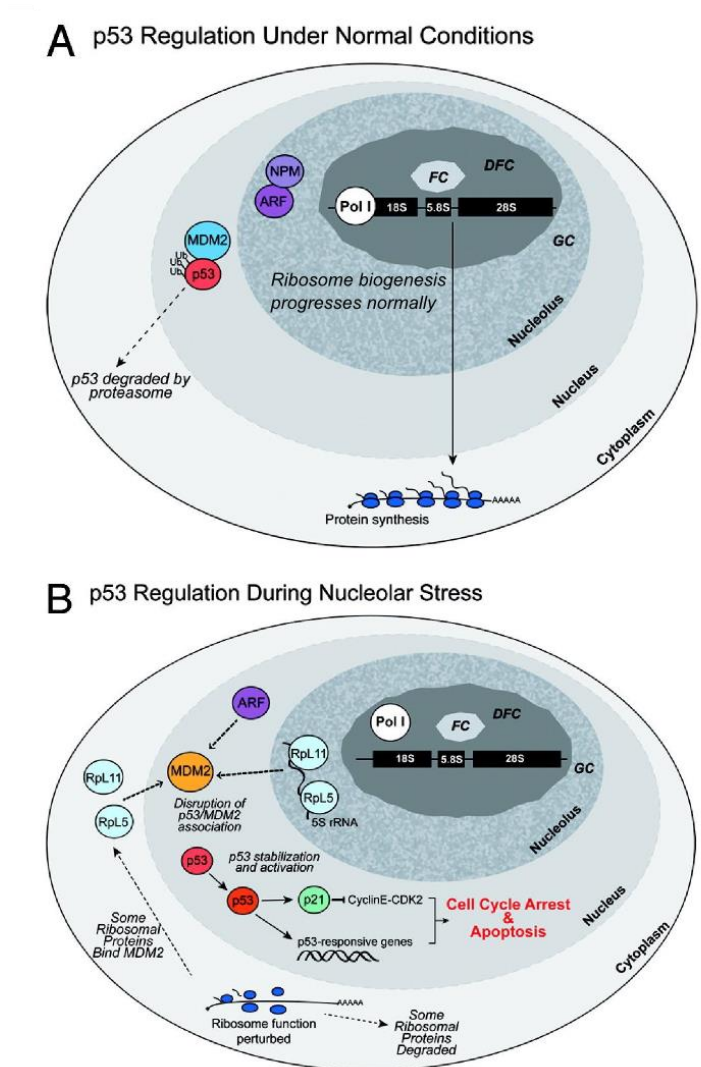


Figure 20. p53 activation upon nucleolar stress. In normal conditions, p53 is ubiquitinated and sent to the proteasome by the action of Mdm2 (**A**). Upon nucleolar stress, free ribosomal proteins (such as Rpl5 and Rpl11) are free to translocate to the nucleoplasm and inhibit Mdm2.

p53 is therefore stabilized and can act as a transcription factor or activate p21 (which in turns inhibit the cyclin E-CDK2 complex). Thus, the cell can be either arrested at the G1/S transition or undergo apoptosis. Many factors that are normally segregated in the nucleolus (Arf) become free to inhibit Mdm2 as well **(B)**. From **James et al., 2014**.

process. It has a pleiotropic function and it can segregate the protein Arf (P14^{ARF} in human, p19^{Arf} in mouse) in the nucleolus **(Figure 21; Bertwistle et al., 2004)**. Upon ribosome biogenesis blockage, Arf is released to the nucleoplasm where it can phosphorylate the acidic domain of Mdm2 thereby preventing it to ubiquitylate p53 **(James et al., 2014)**. When a dominant-negative (constitutively cytoplasmic) form of NPM1 (NPM1c+) is expressed, Arf is translocated to the cytoplasm as well. The subsequent activation of Mdm2 in the nucleoplasm induces the ubiquitylation of p53 and the activation of the proliferation. This has been proposed to be one of the causes of cell expansion in acute myeloid leukemia **(Falini et al., 2009)**. Interestingly, when human NPM1c+ is overexpressed in zebrafish, it leads to the expansion of primitive myeloid cells. Moreover, cell expansion was extended to hematopoietic progenitors in p53-deficient zebrafish suggesting that NPM1 plays a conserved role across evolution and it might be particularly important for progenitor cell homeostasis *in vivo* **(Bolli et al., 2010; see Ch1.II section 2.2.4)**. The role of NS is less straightforward since both its overexpression and its down regulation lead to p53 activation and cell cycle arrest. When it is overexpressed and therefore more abundant in the cytoplasm, NS binds the acidic domain of Mdm2 via its coiled-coil domain. This prevents the ligase activity of Mdm2 leading to the accumulation of p53 **(Dai et al., 2008)**. On the other hand, also the knockdown of NS leads to a p53-dependent cell cycle arrest. This happens as a side effect of NS-dependent ribosome biogenesis disruption that leads to the accumulation of free Rpl5 and Rpl11 both *in vitro* **(Ma and Pederson 2007)** and *in vivo* **(Essers et al., 2014)**.

Besides RBFs, ribosomal proteins can also interact with Mdm2 in order to activate p53. Among others, RPL5, RPL11 and RPL23 appear to be the most important ones. When ribosome biogenesis is impaired (ribosomal stress), these three RPs are prevented from ribosome assembly or released from pre-ribosome to the nucleoplasm where they bind to HDM2 and inhibit HDM2-mediated p53 ubiquitylation and degradation **(Zhou et al., 2015)**. Furthermore, it has been shown that RPL5 and RPL11 can associate with each other via 5S rRNA and this triggers p53 activation after ribosomal stress **(Horn and Vousden, 2008; Donati et al., 2013 ; James et al., 2014)**. Although most of the RPs interact with HDM2 directly, some of them, such as RPS7 **(Zhu et al., 2009)**, RPS15, RPS20, RPL37 **(Daftuar et al., 2013)** and RPS25 **(Zhang et al., 2013b)**

have also been shown to bind HDM2 partners contributing to the stabilization of p53. Interestingly, RPL26 not only interacts with HDM2, but also associates with p53 mRNA and enhances its translation (Takagi *et al.*, 2005).

All together, the mechanisms described in the previous section play important roles in preventing cancer. Thus, they are the target of the newest therapies to treat p53-deficient cancer types representing more than 50% of known cancers.

In this section we saw how ribosome biogenesis regulates cell cycle progression in a p53-dependent manner. The inverse regulation is also important for cell homeostasis. Indeed, p53 can regulate the transcription of RBF-coding genes. Altered RBF-stoichiometry will lead to the synthesis of ribosomes with specific translational activity. Thus, control of cell cycle progression is realized via the translational control of gene expression (see *Ch1.II section 2.1* for details).

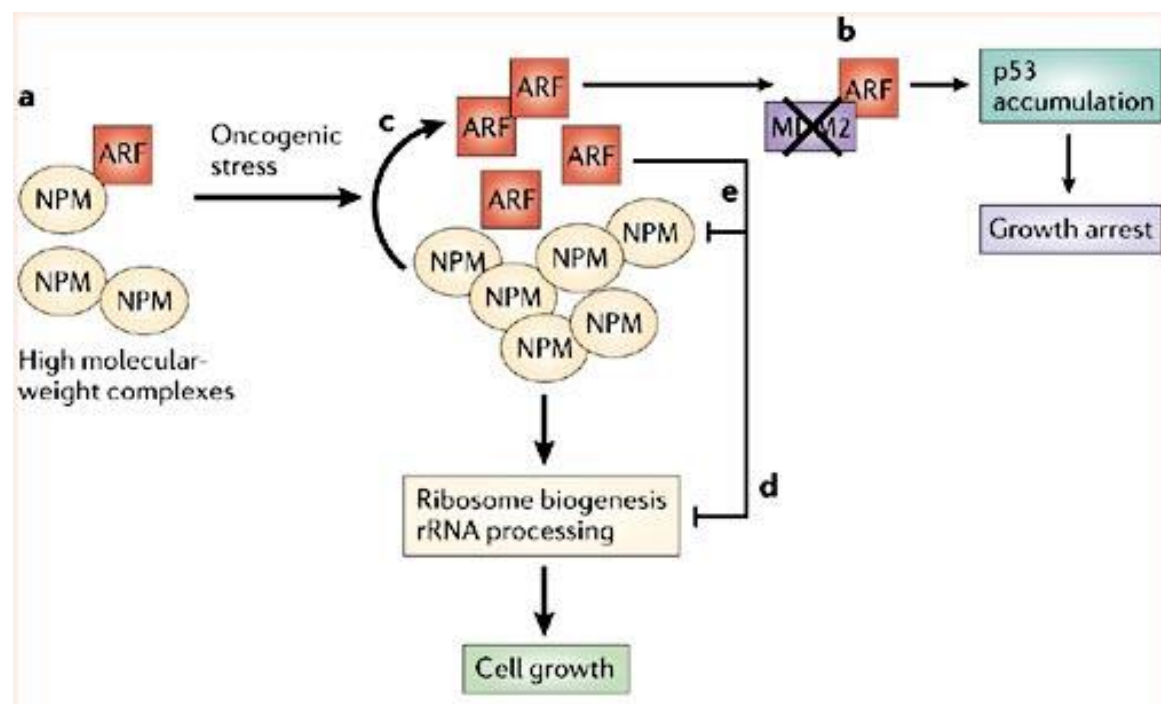


Figure 21. NPM and ARF couple ribosome biogenesis with cell cycle progression. NPM1 is a multifunctional protein that acts at many levels of the ribosome biogenesis process. It has a pleiotropic function and it can segregate the protein ARF in the nucleolus (a). Upon ribosome biogenesis blockage, ARF is released to the nucleoplasm where it can phosphorylate the acidic domain of Mdm2 thereby preventing it to ubiquitylate p53. Thus, NPM1 and couple ribosome biogenesis and cell cycle progression in a p53-dependent manner (b). Elevated levels of NPM lead to the accumulation and the stabilisation of ARF (c) that can negatively regulate ribosome biogenesis by inhibiting rRNA transcription (d) and destabilizing NPM. From Grisendi *et al.*, 2006.

1.2.2 p53-independent mechanisms coupling ribosome biogenesis and cell cycle progression

Although p53 stabilization is the major mechanism that induces cell cycle arrest upon nucleolar stress, recently new mechanisms have been highlighted. Indeed, different mechanisms couple ribosome biogenesis and cell cycle progression in a p53-independent manner. For instance, yeast does express neither p53 nor Mdm2 (**James et al., 2014**) but responds to nucleolar stress. Recently, p53-independent mechanisms have been also reported in mammals, indicating that they might be conserved across evolution. In the following paragraphs, I will give some examples, mostly derived from studies carried out in human cell cultures (**Figure 22**).

Silencing of the catalytic subunit of the POL I (*POLR1A*) leads to p53-dependent cell cycle arrest. Interestingly, p53-deficient cells also stop cycling (at the G1/S transition) after *POLR1A* knock-down and this phenotype could be rescued by pRb silencing (**Donati et al., 2011**). Moreover, these cells displayed low levels of E2F-1. E2F-1 belongs to a family of transcriptional regulators called the E2Fs which control the expression of genes whose products are important for the entry and passage throughout the S phase. In resting cells, hypophosphorylated pRb binds E2F-1, thus it cannot activate its target genes. When the cell enters the cell cycle, phosphorylation of pRb by cyclin-dependent protein kinases let E2F-1 free to activate the target genes involved in the synthesis of DNA. The reduction of E2F-1 expression after the inhibition of rRNA synthesis was observed in all the cell lines examined. This effect did not depend of p53 or pRb function, it was not due to changes in the cell cycle progression, and it was sufficient to decrease proliferation rates. This might be due to the nucleolar stress upon *POLR1A* knock-down. Indeed, free RPL11 binds to HDM2 thereby limiting its association with E2F-1. Thus, E2F-1 becomes unstable and is eventually degraded resulting in cell cycle arrest in G1 (**Figure 22A and 23; Donati et al., 2011**).

Among the proteins that can be released upon nucleolar stress, there is also the serine-threonine kinase PIM1 (**Figure 22B and 23**). This protein is normally associated to the ribosomes via RPS19. When ribosome biogenesis is impaired, PIM1 becomes free and can be degraded via the proteasome. This leads to the stabilization of p27 (which is not anymore phosphorylated and degraded) and to the p53-independent cell cycle arrest before the S phase (**Iadevaia et al., 2010**).

RPs can act as stress-sensors also in a p53-independent manner. This is the case of RpL3 (**Figure 22C and 23**). Upon nucleolar stress RpL3 enters the cell nucleus where it acts as a co-transcription factor. Together with NPM1 it activates the transcription of the p21 gene thereby leading to cell cycle arrest at the G1/S phases transition (**Russo et al., 2013**).

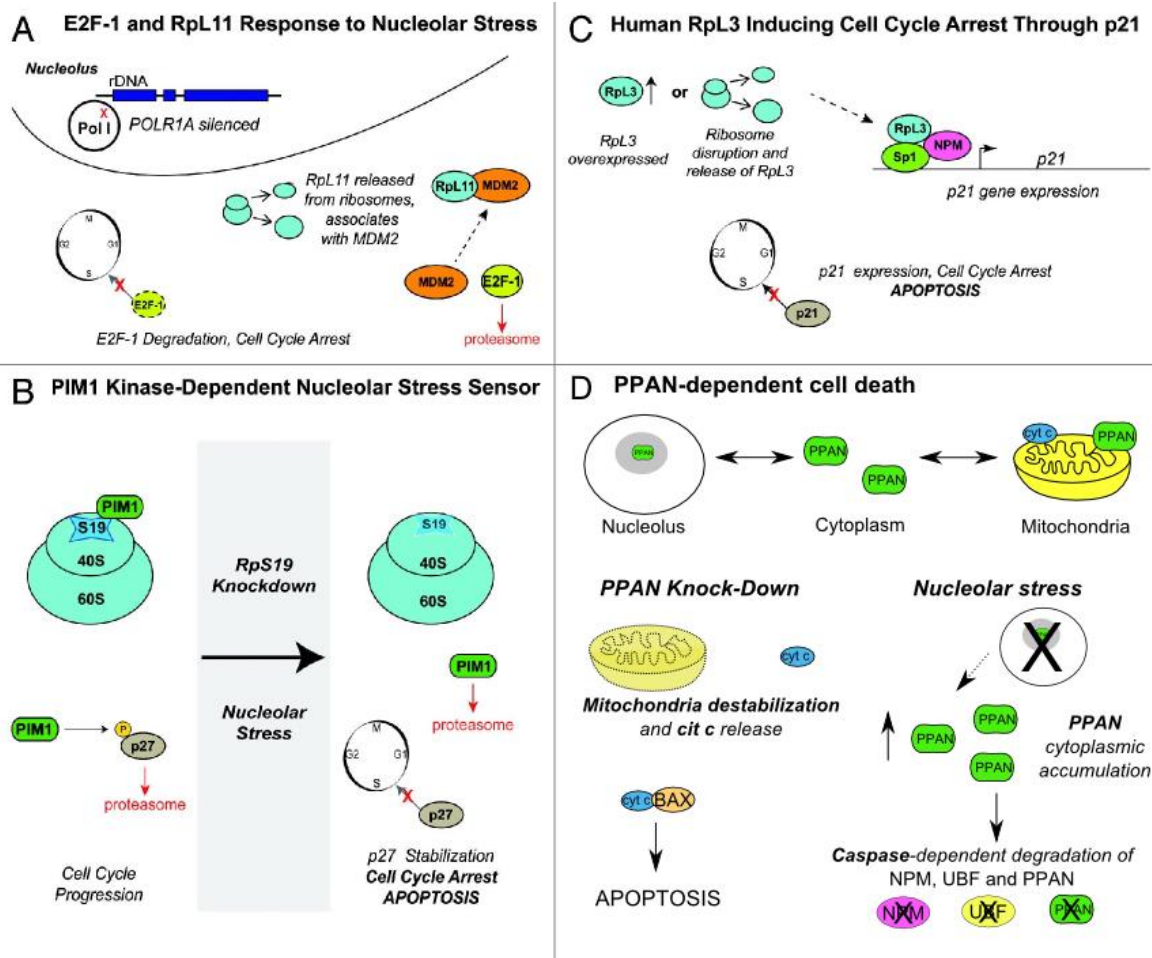


Figure 22. Examples of p53-independent apoptosis and cell cycle arrest mechanisms in metazoans. (A) E2F-1 and Rpl11 response to nucleolar stress. **(B)** Human Rpl3 induces cell cycle arrest through p21. **(C)** PIM 1 kinase-dependent nucleolar stress sensor. **(C)** PPAN-dependent cell death. Adapted from **James *et al.*, 2014**.

Only few other examples of p53-independent cell cycle arrest can be found in literature (see **James *et al.*, 2014** for review and **Figure 22**). I report here the most recently found (**Pfister *et al.*, 2015**). In this case, p53-independent nucleolar stress-response is mediated by a well-known ribosome biogenesis factor called PETER PAN (PPAN) which plays a role for the maturation of the large ribosomal subunit. Interestingly, the transcript for the zebrafish homolog (Ppan) is specifically expressed in neuroepithelial progenitors of the tectum (see *Ch. 2.1*). PPAN shuttles between the nucleolus, cytoplasm and mitochondria as different domains of PPAN are targeted to different cellular compartments. Thus, at a given moment PPAN can be found in all the three subcellular domains. Pfister and colleagues demonstrated that mitochondrial localization of PPAN is important to prevent p53-independent apoptosis. Loss of PPAN induces BAX stabilization, mitochondria depolarization and release of the cytochrome c, demonstrating its

important role as anti-apoptotic factor. Upon chemically induced nucleolar stress, PPAN accumulates in the cytoplasm. This is accompanied by phosphorylation and subsequent cleavage of PPAN by caspases. Moreover, PPAN depletion induces the caspase-independent (or dependent) degradation of NPM and UBF (**Figure 22D**). Thus, PPAN, NPM and BAX are part of a nucleolar stress-response pathway that guarantees cell survival in a p53-independent manner (**Pfister *et al.*, 2015**).

1.2.3 Can the cell cycle be arrested besides the G1/S transition upon nucleolar stress?

Looking at the examples presented in the previous sections it seems that nucleolar stress lead to cell cycle arrest and/or apoptosis prior the S phase. Nevertheless, recent work highlighted that a “general downregulation” of the ribosome biogenesis can lead to cell cycle arrest (and apoptosis) at the G2/M transition (**Figure 23**).

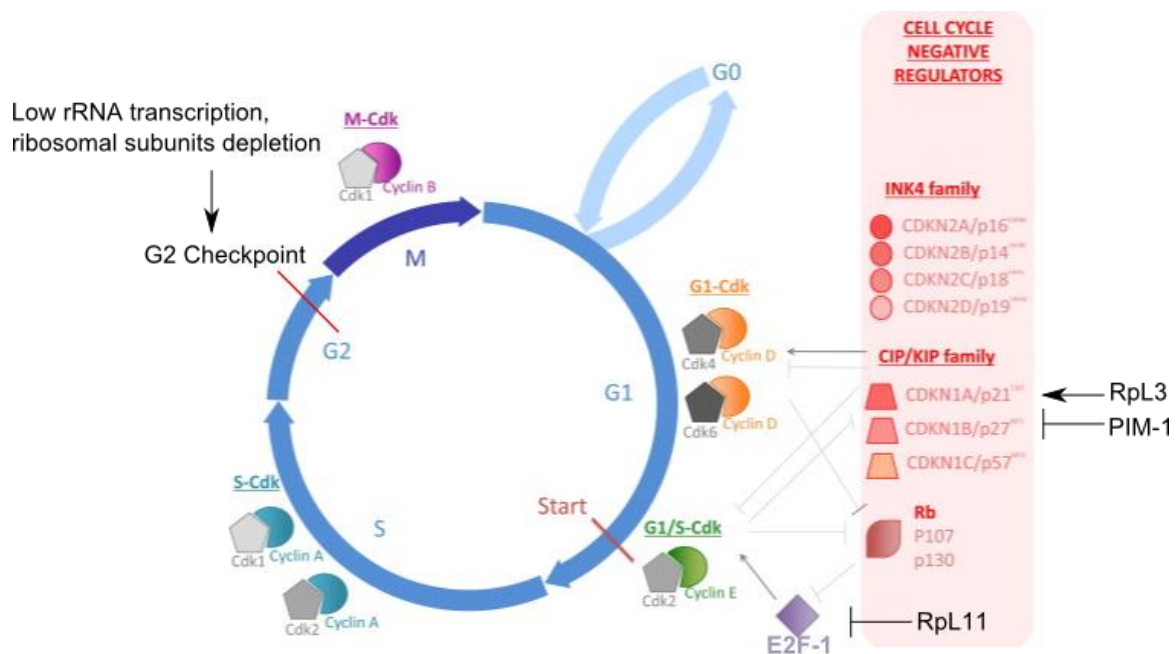


Figure 23. Two different checkpoints can be activated upon ribosome biogenesis impairment. Cell cycle is usually arrested before the S phase either in a p53-dependent or p53-independent manner. Nevertheless, the G2 checkpoint can be activated as well when both ribosomal subunits are depleted or rRNA transcription is downregulated. Adapted from **Devès and Bourrat, 2012**

Fumagalli and colleagues have shown that, the simultaneous knock-down of two RPs (RP6 and RPL7a) induces the overexpression of p53, cell cycle inhibitors and proapoptotic factors and the concomitant translation of RPL11 (from endogenous mRNA). Interestingly, concomitant inhibition of 40S and 60S ribosome biogenesis results in accumulation of cells arrested either in

G1 or in G2/M (**Fumagalli et al., 2012**). In this case, free RPs or RBFs can induce a p53-dependent nucleolar stress response, but their concentration might not be enough elevated to trigger a full apoptotic response in all cells. Thus, some cells are arrested before entering the S phase and others start the duplication of their genome and are blocked before division in a p53-dependent manner. Interestingly, *RPL11* mRNA contains a 5'TOP motif (5'Terminal Oligopyrimidine motif) and can be translated upon depletion of ribosomal subunits (**Fumagalli et al., 2012; Meyuhas and Kahan, 2015**). As previously described, p53 is maintained at low levels in the nucleoplasm by Mdm2/HDM2. Under nucleolar stress, free RPs and RBFs inhibit Mdm2, leading to the activation and stabilization of p53. Among the RPs that can bind Mdm2, is RPL11 (**Chakraborty et al., 2011**). Thus, cells that not undergo apoptosis at the G1/S transition accumulate RPL11 and undergo p53-dependent apoptosis at the G2/M transition.

Similarly, downregulation of the rRNA transcription can induce cell cycle arrest at the G2/M transition and activate the G2 checkpoint (**Negi and Brown, 2015**).

All together these findings highlight the fact that cell cycle arrest might occur at the G2/M transition when the levels of free RPs or RBFs are not enough elevated to trigger a proper nucleolar stress response prior the S phase.

2. DOES RIBOSOME BIOGENESIS PARTICIPATE TO CELL IDENTITY SPECIFICATION?

Ribosomes are not only translational machine but they can control gene expression by selecting the mRNAs to be translated. Indeed, translational capacities of the ribosomes depend on their internal composition and this could be diverse. Moreover, specific ribosomes play specific roles during development, in particular cells or cell subdomains (**Xue and Barna, 2012**). The existence of a “ribosome code” is a new concept in science and there is a great excitement around this topic. Most of the research is focused on understanding how ribosome diversity could participate to the translational control of gene expression (**Xue and Barna, 2012; Buszczak et al., 2014**) or to find specific recognition elements in the mRNA to be transcribed (**Xue et al., 2015**). Nevertheless, virtually nothing is known about the upstream regulatory signals that might produce ribosome heterogeneity in the first place. Neither is known how ribosome biogenesis could contribute to this diversity at a cellular level. It is undeniable that ribosome biogenesis alterations impact cells differently. The tissue-specific phenotypes induced by mutations in RBF-coding genes are relevant examples of this (**Armistead and Triggs-Raine, 2014**).

2.1 SHIFTING RIBOSOME SPECIFICITY TO CHANGE THE CELLULAR PROTEOME

Small nucleolar ribonucleoproteins (snoRNP) are fundamental factors responsible for the site-specific modifications of the newly synthesized ribosomal RNAs (rRNAs). They belong within two classes, the box H/ACA snoRNPs and box C/D snoRNPs, which catalyze site-specific pseudouridylations and 2'-O-methylations of the newly synthesized rRNAs, respectively. In both cases, snoRNPs are part of big RNA-protein complexes where the RNA component (small nucleolar RNA, snoRNA) selects the site to be modified by base pairing with the target site in the rRNA. Moreover, snoRNAs are important for the correct assembly of the snoRNP-complexes since they play both organizing and scaffolding roles (**Watkins and Bohnsack, 2012**). Each snoRNP complex is made of one core protein (i.e. the protein with the catalytic activity) and three associated factors (one involved in snoRNA recognition and binding and the playing structural roles; **Watkins and Bohnsack, 2012**).

Altered levels of the methyltransferase FIBRILLARIN (FBL, core protein of the box C/D RNP complex) have been reported in breast, cervical, lung and prostate cancers, often correlating with poor patient survival (**Marcel et al., 2013; Su et al., 2014**). Interestingly, FBL expression inversely correlates with p53 expression (**Figure 24**). p53 inhibits FBL transcription through direct binding to its first intron. Moreover, in p53-deficient cancer cells, high levels of FBL lead to

increased 2'-O methylation with a concomitant reduction in translation fidelity and stimulation of IRES-dependent translation, notably increasing expression of cancer genes. Thus, through FBL upregulation, the inactivation of p53 specifically stimulates translation of pro-oncogenic, anti-apoptotic and survival proteins whose mRNAs bear IRES sequences (**Figure 24A; Marcel *et al.*, 2013**). Furthermore, an independent study demonstrated that FBL knockdown leads to accumulation of p53 due to protein stabilization and increased IRES-dependent translation (p53 coding sequence bear an IRES element; **Su *et al.*, 2014; Figure 24B**).

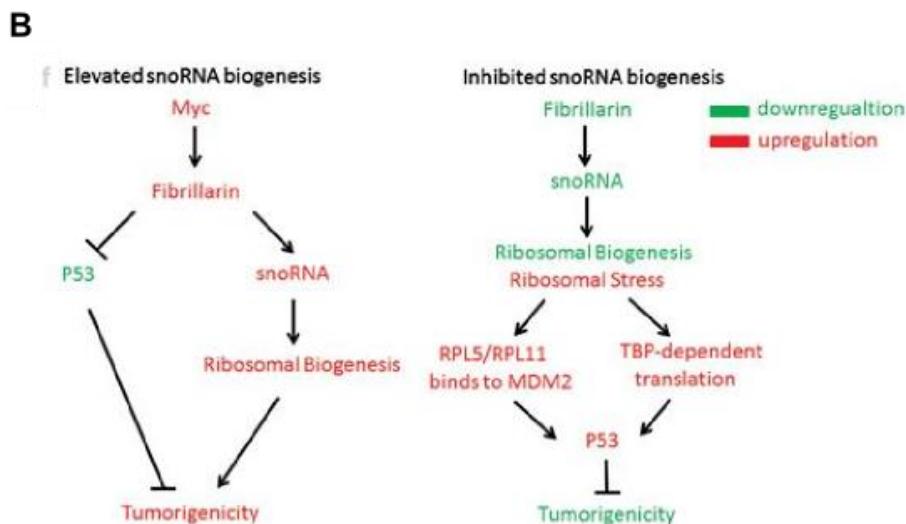
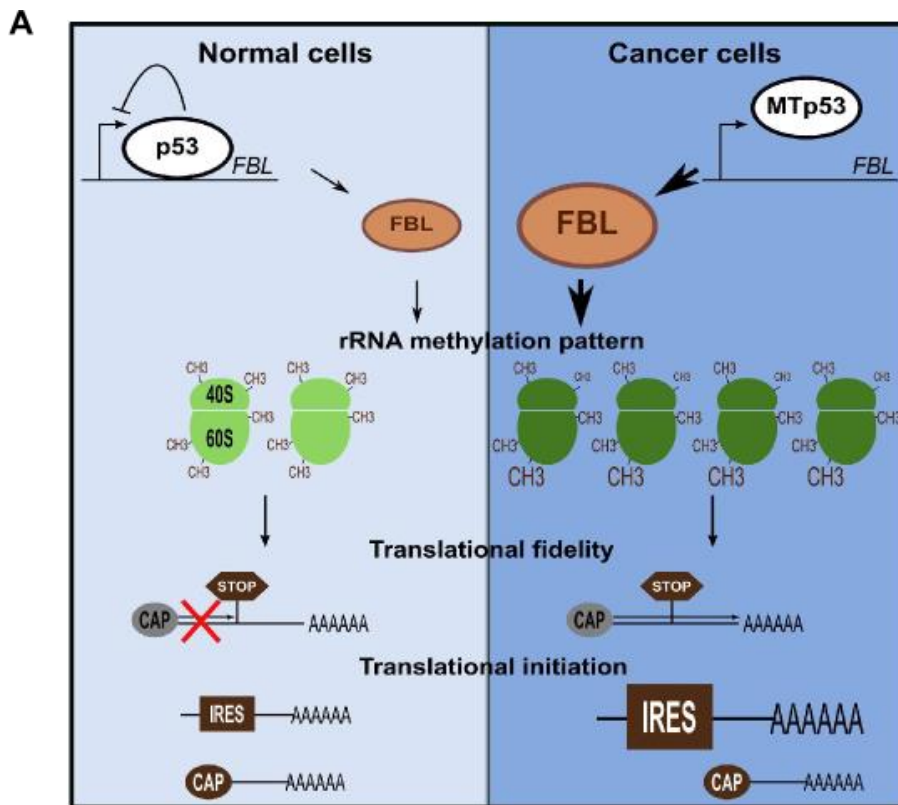


Figure 24. Fbl and p53 levels are mutually and inversely controlled. (A) From Marcel *et al.*, 2013 (B) From Su *et al.*, 2014

IRES-mediated translation can be stimulated also upon decreased pseudouridylation. Indeed, mutations on the *X-Linked Dyskeratosis Congenita-1 (DKC1)* gene are responsible of the decreased transcription of the IRES-bearing tumor suppressor gene p27 and the antiapoptotic XIAP both in mouse and human. DKC1 is the pseudouridine synthase which is the core component of the H/ACA snoRNP complex (**Filipovska and Rackal, 2013; Lafontaine, 2015**).

These findings highlight the fact that changes in the level of expression of ribosome biogenesis factors lead to changes in the translational program of a cell. Thus, snoRNA-mediated rRNA modification is emerging as a major source of ribosome heterogeneity. In this context, it is worth noticing that different types of cell express different amounts and different kinds of snoRNAs (**Lafontaine 2015**). Further investigations will help to determine to which extent this regulation is important at the cellular level and in physiological conditions.

Post-transcriptional modifications of RPs and rRNAs are likely to be the simplest and most common mechanisms to generate ribosome heterogeneity (**Xue and Barna, 2012**). Nevertheless they are not the sole possible mechanisms and other examples will be reported in the next sections.

2.2 DIFFERENT CELLS POSSESS DIFFERENT RIBOSOMES

2.2.1 Different paralogs of the same RP are differently expressed and play different roles

In yeast, different paralogs of the same RP do not have redundant functions. For example, ribosomes containing specific paralogs are required for the translation of localized mRNAs. Integration of different paralogs within ribosomes can confer drug resistance or specify the position of the bud. Thus, already in yeast a “ribosome code” is present and functionally important (**Komili et al., 2007**).

In multicellular eukaryotes, different paralogs of the same ribosomal protein can be expressed in different tissues in the same organism. For example gonads and somatic cells express different RP paralogs both in fly (**Figure 25A**) and human (**Figure 25B**). In human only few other examples can be found, but the list is growing. Among them, the paralog of RPL39, RPL39L, is specifically expressed in embryonic stem cells (**Wong et al., 2014**). Interestingly, this is not the only case in which different RP paralogs play different roles (or are thought to play different roles) between stem cells and differentiated cells. For example, zebrafish *rpl7l1* is specifically expressed in tectal neuroepithelial progenitors (see *Ch. 2.1*). By contrast its paralog *rpl7* has been demonstrated to be strongly and ubiquitously expressed (**zfin.org**). A similar situation might occur in *Drosophila*,

where *RpL7* has been shown to be specifically required in neuroblasts to maintain their proliferation (**Neumüller *et al.*, 2011**) whereas its counterpart (*RpL7-like*) displays ubiquitous expression. Another zebrafish study showed that Rpl22l1 and Rpl22 play essential, distinct and antagonistic roles in hematopoietic stem cells (HSCs; **Zhang *et al.*, 2013b**). Recently, it has been shown that the expression of the ribosomal protein Rpl22 controls ribosome composition by directly repressing expression of its own paralog, Rpl22l1 in mouse (**O’Leary *et al.*, 2013**). Interestingly, the expression of these two paralogs overlaps only partially (**Sugihara *et al.*, 2010**). Differentially expressed RP paralogs in progenitor and differentiated cells might indicate the existence of different ribosome biogenesis in stem/progenitor cells compared to differentiated cells (see *Ch1.II section 2.2.4*).

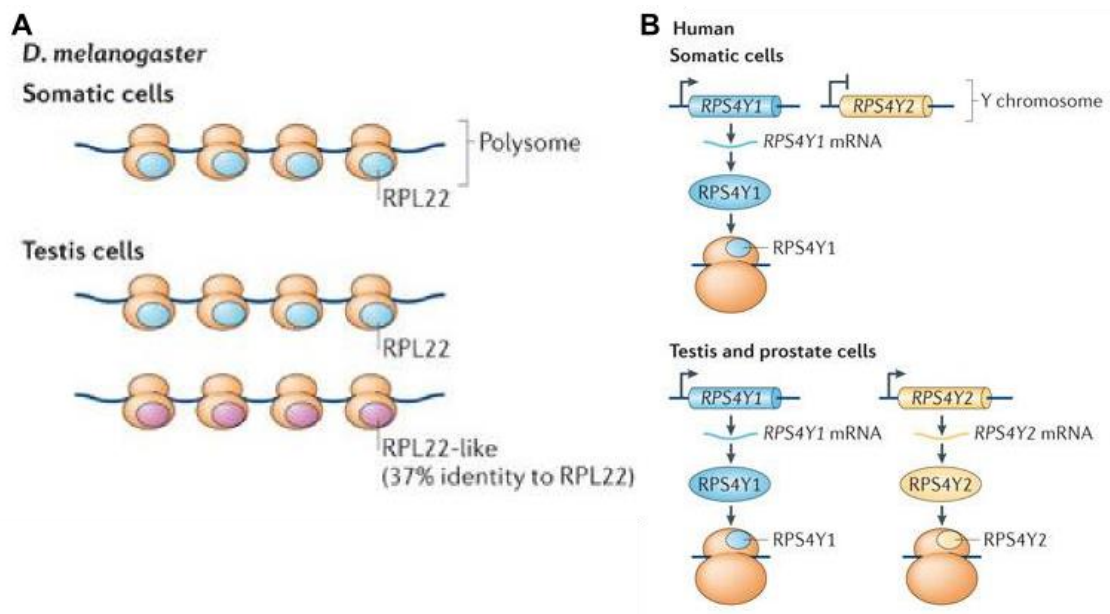


Figure 25. Different paralogs of the same RP are differently expressed. (A) In fly, ribosomal protein paralogs show different expression patterns in the adult testes. For example, RPL22 is expressed ubiquitously, but RPL22-like protein levels are specifically increased in the testes. Both proteins are incorporated into translationally active ribosomes (called the polysomes). Both genes are essential in the fly, which suggests that they are not functionally redundant (**Kearse *et al.*, 2011**). **(B)** In humans, only some ribosomal protein paralogs have been identified; however, notable examples exist. RPS4Y1 is expressed ubiquitously, whereas RPS4Y2 is restricted to the testis and prostate (**Lopes *et al.*, 2010**). Both these examples highlight the fact that a specific translational program might be active gonads of metazoans. Adapted from **Xue and Barna, 2012**.

2.2.2 Different RPs contribute to the translation of specific genes

In an elegant study, Maria Barna’s group showed that Rpl38 is necessary for the translation of some of the *Hox* genes (**Kondrashov *et al.*, 2011**). Mutations in *Rpl38* are responsible for

developmental abnormalities displayed by the tail-short (*Ts/+*) mice, which exhibit skeletal patterning defects, including homeotic transformations and compromised neural tube patterning. Surprisingly *Ts/+* embryos do not exhibit alterations in global translation as compared to wild-type siblings. However, the translation of a subset of mRNAs encoding Hox homeoproteins in embryonic tissues is strongly reduced in *Ts/+* embryos. Interestingly, Rpl38 is enriched in developing tissues including eye, somites, and neural tube where aberrant tissue patterning is observed in *Ts/+* mice. This heterogeneity in the expression of RPs appears to be a general phenomenon during embryonic development, inasmuch as 72 RPs show inter-tissue variation in their expression levels. All together these findings indicate that ribosome composition varies between cells and specialized ribosomes are required to determine cell identity in vertebrates (Kondrashov *et al.*, 2011; Figure 26).

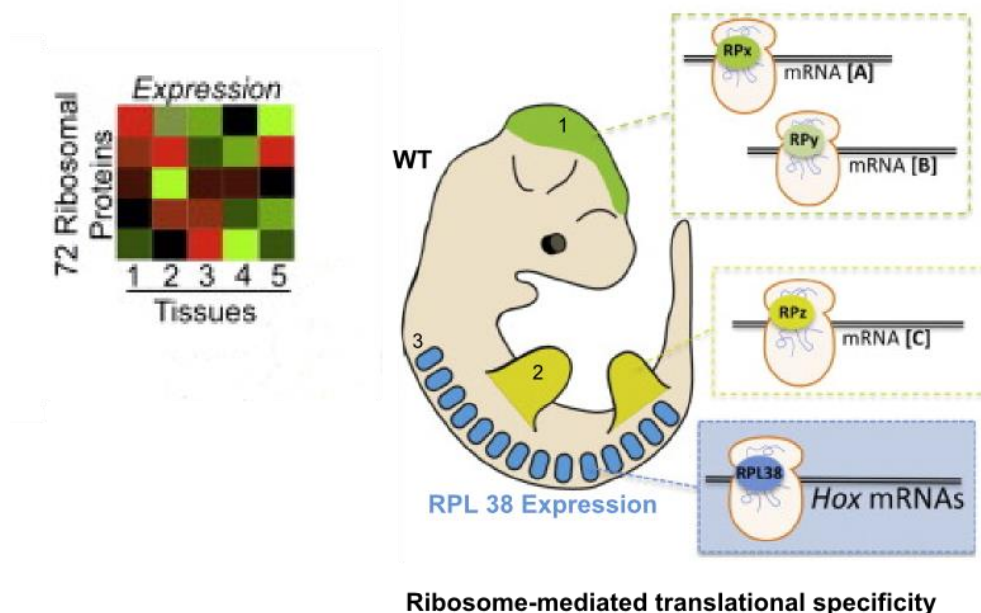


Figure 26. RPL38 is rate-limiting for the translation of HOX mRNAs. The tissue specific phenotypes associated with RPL38 loss of function are explained by the observation that Rpl38 expression is highly regulated during embryonic development. A striking enrichment of Rpl38 transcripts is evident in specific regions of the embryo such as developing somites and within the neural tube. These findings suggest that the increased expression of specific ribosomal proteins may produce heterogeneous ribosomes in distinct cell and tissue types with unique specificities in translating specific classes of mRNAs.

During the last years, the same research group completed the work on Rpl38 and the Hox genes. They discovered the presence of specific RNA regulatory elements within the 5' UTR of the Hox transcripts specifically translated by the Rpl38-containing ribosomes. These structured RNA elements, resemble viral internal ribosome entry sites (IRESs). They facilitate ribosome

recruitment and require the ribosomal protein RPL38 for their activity. This confirms that ribosomes with specific composition can be specific for a subset of mRNAs, thereby adding a new level of complexity at the translational regulation of gene expression (Xue *et al.*, 2015).

2.2.3 Mutations of RP and RBF coding genes lead to tissue-specific phenotypes

The ribosomopathies are a diverse group of disorders which, despite their heterogeneity at a clinical level, affect the same process. They are each caused by mutations in a gene encoding either a ribosomal protein, or a ribosome biogenesis factor. Intuitively, these mutations should affect all tissues and cell types. Surprisingly, there is a tendency toward tissue specificity in ribosomopathies. Although the specific mechanism underlying the ribosomopathies is frequently unclear, the generally accepted etiology is that processing delays or defects in rRNA maturation, resulting in an imbalance of mature ribosomes, lead to reduced rates of protein synthesis and cell proliferation. However, it has become clear that the specificity and activity of the ribosome is regulated, and changes to its composition may begin to explain the heterogeneity among ribosomopathies (see Table 3).

Overall, it is increasingly clear that the ribosomopathies are not simply due to reduced protein synthesis, and are revealing the complex inter-relationships between ribosome biogenesis and its regulatory pathways, the cell cycle, and development of multiple tissues (Armistead and Triggs-Raine, 2014).

Disease	Clinical manifestations	Gene	Function in ribosome biogenesis	Putative mechanism of specificity
Treacher Collins syndrome	Craniofacial abnormalities, occasional microcephaly, mental retardation and psychomotor delay	<i>TCOF1</i> , <i>POLR1D</i> , <i>POLR1C</i>	Transcription of rRNA genes	Treacle strongly expressed in neural crest cells; Treacle interaction with UBF, FBL, NOP56, Plk1
<i>Aplasia cutis congenita</i>	Agenesis of skin, usually on scalp vertex	<i>BMS1</i>	Ribosomal GTPase	Unknown
Shwachman-Diamond syndrome	Exocrine pancreas insufficiency, growth retardation, hematologic defects, skeletal abnormalities, cancer predisposition	<i>SBDS</i>	Removal of eIF6 from 60S in final maturation step, allowing binding of 40S and 60S subunits	SBDS strongly expressed in developing pancreas
Bowen-Conradi syndrome	Severe pre- and postnatal growth	<i>EMG1</i>	Pseudouridine-N1-specific	Unknown

	retardation, psychomotor retardation, microcephaly, micrognathia, joint contractures, rockerbottom feet			methyltransferase	
Cartilage hair hypoplasia	Short stature, sparse hair, immunologic defects, hematological defects, malabsorption, cancer predisposition	<i>RMRP</i>	Pre-rRNA cleavage		Short stature related to rRNA cleavage defect; cancer predisposition putatively caused by defective cyclin B cleavage
Aneuxitic dysplasia	Severe short stature, hypodontia, mental retardation	<i>RMRP</i>	Pre-rRNA cleavage		Short stature related to rRNA cleavage defect; cancer predisposition putatively caused by defective cyclin B cleavage
Alopecia, neurological defects and endocrinopathy syndrome	Hypoplastic hair, microcephaly, mental retardation, progressive motor retardation, adrenal insufficiency	<i>RBM28</i>		Nucleolar component of the spliceosomal small nucleolar ribonucleoprotein, necessary for 60S biogenesis	Unknown
North American Indian childhood cirrhosis	Transient neonatal jaundice progressing to biliary cirrhosis	<i>CIRH1A</i>	Pre-rRNA processing		Cirhin strongly expressed in developing liver
X-linked dyskeratosis congenital and Hoyeraal-Hreidarsson syndrome	Abnormal skin pigmentation, nail dystrophy, leukoplakia, bone marrow failure, cancer predisposition, short stature, microcephaly, immunodeficiency	<i>DKC1</i>	Pseudouridine synthase		Translation of IRES-containing mRNAs including <i>p27</i> , <i>XIAP</i> , <i>Bcl-xL</i>

Table 3. Mutations on RBF-coding genes lead to tissue-specific phenotypes.

2.2.4 Does ribosome biogenesis contribute to stem/progenitor cells homeostasis?

Recent data show that there is a relationship between ribosome biogenesis and stem/progenitor cell homeostasis. This might be intuitive since complex relationships exist between cell cycle progression and ribosome biogenesis (see see *Ch. 1.II section 1*). Nevertheless, it seems that ribosome biogenesis *per se* is important for the homeostasis of the progenitor cells. Thus, I have collected the data published in the last two years which are presented in the following review-type article that has been published by “Current Opinion in Genetics and Development” (Elsevier Publishing Group, The Netherlands).

New tricks for an old dog: ribosome biogenesis contributes to stem cell homeostasis

Alessandro Brombin^{1,2}, Jean-Stéphane Joly^{1,2} and Françoise Jamen^{1,2}



Although considered a 'house-keeping' function, ribosome biogenesis is regulated differently between cells and can be modulated in a cell-type-specific manner. These differences are required to generate specialized ribosomes that contribute to the translational control of gene expression by selecting mRNA subsets to be translated. Thus, differences in ribosome biogenesis between stem and differentiated cells indirectly contribute to determine cell identity. The concept of the existence of stem cell-specific mechanisms of ribosome biogenesis has progressed from an attractive theory to a useful working model with important implications for basic and medical research.

Addresses

¹ CASBAH Group, University Paris-Saclay, University Paris-Sud, UMR CNRS 9197, Neuroscience Paris-Saclay Institute (NeuroPSI), Bât. 32/33, 1 Avenue de la Terrasse, F-91190 Gif-sur-Yvette, France

² INRA, USC 1126, F-91190 Gif-sur-Yvette, France

Corresponding author: Jamen, Françoise (jamen@inaf.cnrs-gif.fr)

Current Opinion in Genetics & Development 2015, 34:61–70

This review comes from a themed issue on **Cell reprogramming, regeneration and repair**

Edited by **Amander T Clark** and **Thomas P Zwaka**

<http://dx.doi.org/10.1016/j.gde.2015.07.006>

0959-4377/© 2015 Elsevier Ltd. All rights reserved.

Introduction

Since the publication of the ribosome filter hypothesis [1], ribosomes are considered as important actors in the translational control of gene expression. Surprisingly, in this context, little attention has been given to the way ribosomes are built. Ribosome biogenesis has always been considered a highly conserved process; therefore, results obtained in yeast were thought to reflect the situation in metazoans (see **Box 1** for a brief overview of the process). However, the repertoire of ribosome biogenesis factors (RBFs) varies considerably among eukaryotes [2]. In particular, the comparison between yeast and human reveals that RBF exclusions and additions characterize the evolution of this ancient pathway [3,4^{**}]. What then is the role of these newly acquired RBFs? Could they play tissue and/or

cell-specific roles thereby finely regulating gene expression at the translational level? In particular, do stem cells and differentiated cells use different ribosome biogenesis pathways? Here, we provide an overview of the most recent literature relevant to ribosome biogenesis in different species, and show that the existence of a stem cell-specific process is no longer simply an attractive speculation, but a useful working model.

To be or not to be (conserved)?

Studies performed in yeast are considered the gold-standard to understand ribosome biogenesis in eukaryotes. Nevertheless, there are several differences between yeast ribosomes and their counterparts in metazoans, suggesting that their respective synthesis pathways are different. Indeed, ribosomes in metazoans contain additional ribosomal proteins (RPs) and longer ribosomal RNAs (rRNAs) compared to yeast [5]. The main differences in ribosome sizes between eukaryotes result primarily from species-specific enlargements in the 25–28S rRNA although the loss or gain of individual proteins is also observed [3]. Additional observations are in favor of a diversity of the ribosome biogenesis pathway in eukaryotes. For instance, mammalian nucleoli have three, rather than two, subcompartments [6]. Moreover, the human nucleolar proteome is bigger than the yeast one [3,7–9]. Recently, bioinformatics analyses performed on yeast genome [2] and a large scale RNAi-based screen on cultured HeLa cells [4^{**}] revealed clear variations in the nucleolar proteome among eukaryotes [7] and the identification of species-specific (or group-specific) RBFs. These factors are completely uncharacterized and may play cell-specific roles.

Independent results showed that known RBF-coding transcripts accumulate in neuroepithelial progenitors in zebrafish [10] and/or appear to be essential for neuroblast survival in fly [11]. The transcriptome of naive human pluripotent stem cells is also enriched in RBFs [12^{*}]. These data raise the hypothesis that both species-specific and evolutionarily conserved RBFs could contribute to the determination of cell identity. In particular, ribosome biogenesis-based control mechanisms of gene expression may exist and contribute to the determination of stem and progenitor cell homeostasis.

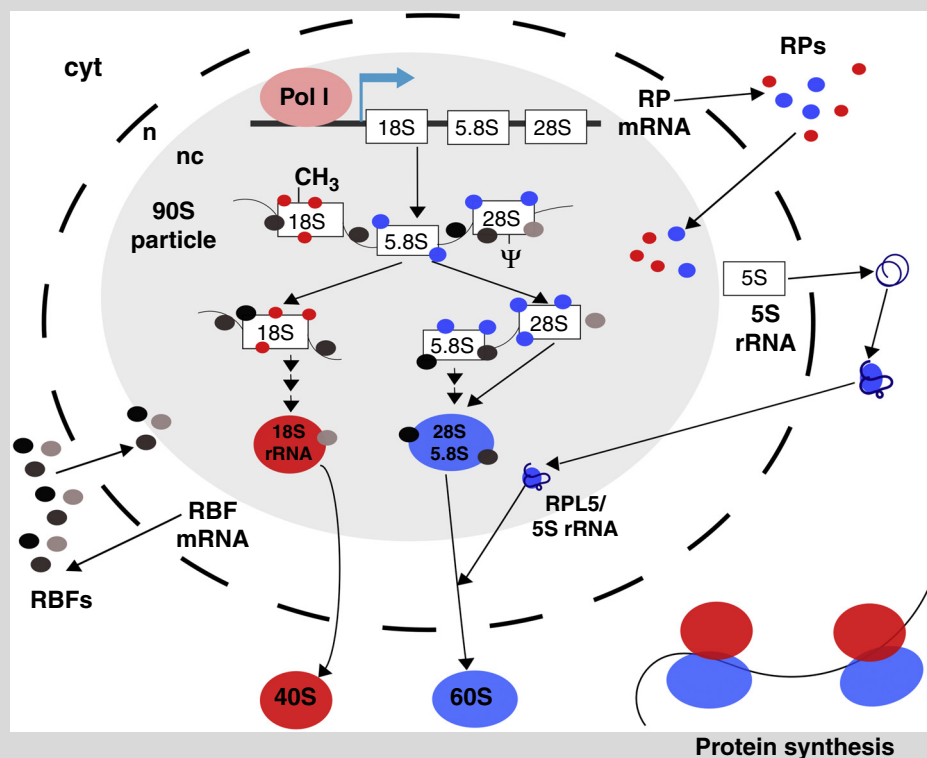
Specificity of ribosome biogenesis in stem cells and progenitors

Recent studies show that different RBFs play specific roles in stem cells and progenitors. Interestingly, this

Box 1 Building the ribosome

Ribosomes are large protein-RNA complexes that translate mRNAs into proteins. They are composed of two subunits. The 60S or large subunit is composed of the 28S (25S in yeast), 5S and 5.8S ribosomal RNAs (rRNAs) and 47 proteins in human; the 40S or small subunit is composed of the 18S rRNA and 33 proteins. Ribosome biogenesis is a highly coordinated, multi-step process that mainly takes place in the nucleolus (nc) but also in the nucleoplasm (n) and cytoplasm (cyt). It requires the activities of the three of RNA polymerases (RNA pol), 75 small nucleolar RNAs (snoRNAs), and more than 250 ribosome biogenesis factors (RBFs). To generate the mature 18S, 28S and 5.8S rRNAs, a precursor 45S rRNA (35S in yeast) is transcribed by RNA pol I as a long polycistronic transcript which is then extensively processed through cleavage and covalent modification events such as 2'-O-methylation (-CH₃) and pseudouridylation (-Ψ). The 5S rRNA is transcribed independently by RNA pol III in the nucleoplasm and undergoes maturation in a separate pathway before being imported to the nucleolus. The ribosomal protein (RP) genes are transcribed by RNA pol II in the nucleoplasm. RBFs include helicases, exo- and endonucleases, methyltransferases and isomerases which modify the nascent rRNA. Other RBFs are required for the nuclear import of RPs and RBFs, maturation and export of ribosomal particles to the cytoplasm and assembly and maturation of the ribosomal subunit particles.

RBFs associate with pre-rRNA to form three types of pre-ribosomal particles: the 90S particle, which is processed into the pre-40S particle and the pre-60S particle. After maturation, the pre-60S and pre-40S ribosomal subunits are exported to the cytoplasm where they undergo final maturation steps to become the mature 60S and 40S subunits, which then associate to form the 80S functional ribosome.



Schematic representation of ribosome biogenesis in human.

applies to many species, which suggests that stem cell-specific regulation exists across the tree of life. Moreover, variations have been evidenced at all steps of the biosynthesis, from rDNA transcription [13,14] to subunit export [15**] (Table 1). Many examples will be presented in the following subsections.

rDNA transcription is differentially regulated in stem cells compared to their differentiated progeny

rDNA transcription is quantitatively regulated in stem cells (Figure 1A) and the rate of rDNA transcription influences cell identity and fate (see the example of

FBL in mESC presented at the end of this subsection and in the 'Lost in translation' section). In general, stem cells display higher rates of rDNA transcription than their daughter cells. During differentiation, rRNA synthesis is down-regulated by phenotype-specific transcription factors (like MyoD in the muscle lineage or Runx2 in the osteoblast lineage) (Figure 1A1, right panel) [16]. Although it is generally believed that the down-regulation of rDNA transcription is simply a consequence of the differentiation process, recent findings show that this event actually triggers differentiation. Furthermore, this mechanism may be evolutionarily conserved, as shown

Table 1

RBFs overexpressed in stem/progenitor cells

Ribosome biogenesis steps	RBF orthologs			Expression in progenitors/stem cells	Functional assays	References	Other functions
	Human	Drosophila	Yeast				
Transcription of rRNAs	TAF1B N.D. POLR1B TCOF1	CG6241 Udd Rpl135 N.D.	Rm7 N.D. RPA135 N.D.	- Drosophila ovarian GSCs - Drosophila ovarian GSCs - Drosophila NBs - Zebrafish midbrain NePs - Mouse NCC and NePs	RNAi reduces GSC proliferation in Drosophila Drosophila mutants display reduced GSC proliferation Mutation induces defects in NCC formation and proliferation.	[14] [15**] [10,56] [57]	- Association with centrosome and kinetochore; Roles in spindle formation and mitotic progression Methyltransferase of histone H2A
Processing of 90S pre-ribosome	FBL	Fib	NOP1	- Zebrafish midbrain NePs - Mouse ESCs	Stable expression in mouse ES cells (cultured without LIF) prolonged their pluripotent state. Knock-down leads to growth inhibition and apoptosis in mESCs. RNAi prevents self-renewal of NBs RNAi induces a premature differentiation of optic lobe NeSCs	[10] [22*] [10,11,36,56]	Methyltransferase of histone H2A
Pseudouridylation of rRNA	NOP56	Nop56	NOP56	- Drosophila NBs - Drosophila optic lobe NeSCs - Zebrafish midbrain NePs - Zebrafish midbrain NePs - Drosophila NBs	RNAi prevents self-renewal of NBs RNAi induces a premature differentiation of optic lobe NeSCs	[10] [11]	Telomere maintenance
Primary assembly steps	DHX37 HEATR1 NOL11 PDCD11 PWP2 TBL3 UTP18	kurz (kz) l(2)k09022 N.D. CG5728 CG12325 CG1671 wcd (wicked)	ECM16 UTP10 N.D. RRP5 PWP2 UTP13 UTP18	- Drosophila NBs - Zebrafish neural progenitors - CNCs in amphibians and mice - Drosophila NBs - Zebrafish midbrain NePs - Drosophila NBs - Drosophila NBs - Drosophila NBs and ovarian GSCs - Drosophila NBs - Zebrafish NCCs	Morpholino KD leads to defects in canalicular and biliary morphology in zebrafish RNAi prevents self-renewal of NBs Mutants display apoptosis in central nervous system. Knock-down in Xenopus RNAi prevents self-renewal of NBs RNAi prevents self-renewal of NBs Mutations induce premature differentiation of GSCs. Zebrafish mutants exhibit defects in NCC derived cartilage development.	[11] [47] [58] [10,56] [11,56] [11,56] [14,30,56] [52] [10,56]	
Secondary assembly steps	WDR43 WDR46 BMS1	CG30349 CG2260 CG7728	UTP5 UTP7 BMS1	- Drosophila NBs - Zebrafish NCCs - Drosophila NBs - Zebrafish midbrain NePs - Drosophila NBs - Zebrafish hepatoblasts	Zebrafish mutants exhibit defects in NCC derived cartilage development.	[52] [10,56] [11] [49]	Telomerase regulation
Tertiary assembly steps	PINX1 IMP4 UTP20	CG11180 CG11920 CG4554	PXR1 IMP4 UTP20	- Drosophila NBs - Zebrafish midbrain NePs - Drosophila NBs	RNAi prevents self-renewal of NBs Zebrafish mutants display reduced hepatoblast proliferation. RNAi prevents self-renewal of NBs RNAi prevents self-renewal of NBs	[11,56] [10] [11,56]	Telomerase regulation

Table 1 (Continued)

Ribosome biogenesis steps	RBF orthologs			Expression in progenitors/stem cells		Functional assays	References	Other functions
	Human		Drosophila	Yeast				
	Human	Drosophila	Drosophila	Yeast	Yeast			
Maturation and export of pre-40S particles (SSU, small subunit)	DDX10		CG5800	HCA4	- Drosophila NBs	RNAi prevents self-renewal of NBs	[11]	
	NAT10		I(1)G0020	KRE33	- Zebrafish midbrain NePs		[10]	
	N.D.		Mbm (mushroom body miniature)	N.D.	- Drosophila NBs	Mutants display impaired NB proliferation.	[23*,56]	
	NOC4L		CG2875	NOC4	- Drosophila NBs		[10,56]	
	NOM1		CG9004	SGD1	- Zebrafish midbrain NePs	Zebrafish mutants exhibit impaired proliferation of pancreatic progenitors.	[51,56]	
	PNO1		I(1)G0004	PNO1	- Drosophila NBs		[10,56]	
	RRP12		CG2691	RRP12	- Zebrafish midbrain NePs		[10,56]	
	RRP36		CG8481	N.D.	- Zebrafish midbrain NePs		[10]	
	TSR1		CG7338	TSR1	- Zebrafish midbrain NePs	RNAi prevents self-renewal of NBs	[11,56]	
	WDR3		CG8064	DIP2	- Drosophila NBs	RNAi prevents self-renewal of NBs	[11,56]	
	BOP1		CG5033	ERB1	- Drosophila NBs	RNAi prevents self-renewal of NBs	[11]	
	Maturation and export of pre-60S particles (LSU, large subunit)	BRIX1		CG11583	BRX1	- Drosophila NBs	RNAi prevents self-renewal of NBs	[11]
CEBPZ			CG7839	MAK21	- Drosophila NBs	RNAi prevents self-renewal of NBs	[11]	
DDX18			pit	HAS1	- Zebrafish midbrain NePs		[10]	
DDX51			Dbp73D	DBP6	- Drosophila NBs	RNAi prevents self-renewal of NBs	[11]	
DDX54			CG32344	DBP10	- Drosophila NBs	RNAi prevents self-renewal of NBs	[11]	
DDX56			hlc	DBP9	- Drosophila NBs	RNAi prevents self-renewal of NBs	[11]	
FTSJ			CG8939	SPB1	- Zebrafish midbrain NePs		[10]	
GLTSCR2			CG1785	NOP53	- Drosophila NBs	RNAi prevents self-renewal of NBs	[11]	
GNL2			ns2	NOG2	- Zebrafish retinal progenitors	Mutant retinal progenitor display a defect in cell cycle exit	[59]	
MKI67IP			CG6937	NOP15	- Zebrafish midbrain NePs		[10]	
NLE1			Nle	RSA4	- Zebrafish midbrain NePs	Conditional knock-out mice exhibit failure to maintain quiescence in HSCs	[10,15**,56]	
NMD3			Nmd3	NMD3	- Zebrafish midbrain NePs		[11,56]	
NOC2L		CG9246	NOC2	- Drosophila NBs	RNAi prevents self-renewal of NBs	[11,56]		
NOC3L		CG1234	NOC3	- Drosophila NBs	RNAi prevents self-renewal of NBs	[10,56]	Promotes replication initiation	
NSA2		Ip259	NSA2	- Drosophila NBs	RNAi prevents self-renewal of NBs	[10]		
PES1		CG4364	NOF7	- Drosophila NBs	Knock-down impairs proliferation of pancreatic progenitors in zebrafish	[10,50,56]		
PPAN		ppan	SSF1	- Drosophila NBs		[10,56]		
RBM28		CG4806	NOP4	- Zebrafish midbrain NePs	RNAi prevents self-renewal of NBs	[11,56]		

RBF	CG	Species	Function	References
RPF2	CG7993	Drosophila NBs	- Drosophila NBs	[10,56]
RRP1	Nnp-1	Zebrafish midbrain NePs	- Zebrafish midbrain NePs	[10,56]
SBDS	CG8549	Drosophila NBs	- Drosophila NBs	[50,56]
SDAD1	Mys45a	Zebrafish pancreatic progenitors	- Zebrafish pancreatic progenitors	[11,56]
WDR12	CG6724	Drosophila NBs	- Drosophila NBs	[10,56]
NPM1	N.D.	Zebrafish midbrain NePs	- Zebrafish midbrain NePs	[10,60,61]

RBFs for which their function in the ribosome biogenesis pathway has not been clearly elucidated

Each RBF has been quoted at the first step in which it is described to be involved. However, many RBFs often acts more than once in the pathway, either at successive steps (and therefore they remain attached to the processome) or at separate steps. CNCs, cranial neural crests; ESCs, embryonic stem cells; GSCs, ovarian germline stem cells; HSCs, hematopoietic stem cells; NBs, neuroblasts; NCCs, neural crest cells; NePs, neuroepithelial progenitors; NeSCs, neuroepithelial stem cells; N.D., not determined.

Knock-down impairs proliferation of pancreatic progenitors in zebrafish
 RNAi prevents self-renewal of NBs

Involved in centrosome duplication, protein chaperoning, histone assembly, cell proliferation, and regulation of p53 and ARF.

Overexpression induces the increase of proliferation and survival upon stress of mouse HSCs *In vitro*.
 Overexpression in mouse ESC results in higher proliferation rates. Downregulation results in reduced proliferation rates.

both in mammalian stem cells (Figure 1A1) [17] and Drosophila germinal stem cells (Figure 1A2) [14]. A high rate of rRNA transcription is a stem cell feature and there is evidence that rRNA synthesis could be regulated by specific factors in embryonic stem cells (ESCs) as it is in differentiating cells. A recent study shows that 17 pluripotency-associated factors bind rDNA loci in mESCs (Figure 1A1, left panel). Moreover, the pluripotency factor OCT4 binds to rDNA in similar patterns in mESCs and hESCs [13]. Moreover, silencing of rDNA genes and down-regulated ribosome biogenesis are associated with stem cell ageing, as shown recently in murine hematopoietic stem cells (HSCs) [18]. It seems that a high rate of rDNA transcription *per se* is necessary for stem cell survival. Indeed, mESCs and induced pluripotent stem cells (iPSCs) treated with low doses of Actinomycin D (rDNA transcription inhibitor) undergo apoptosis [19].

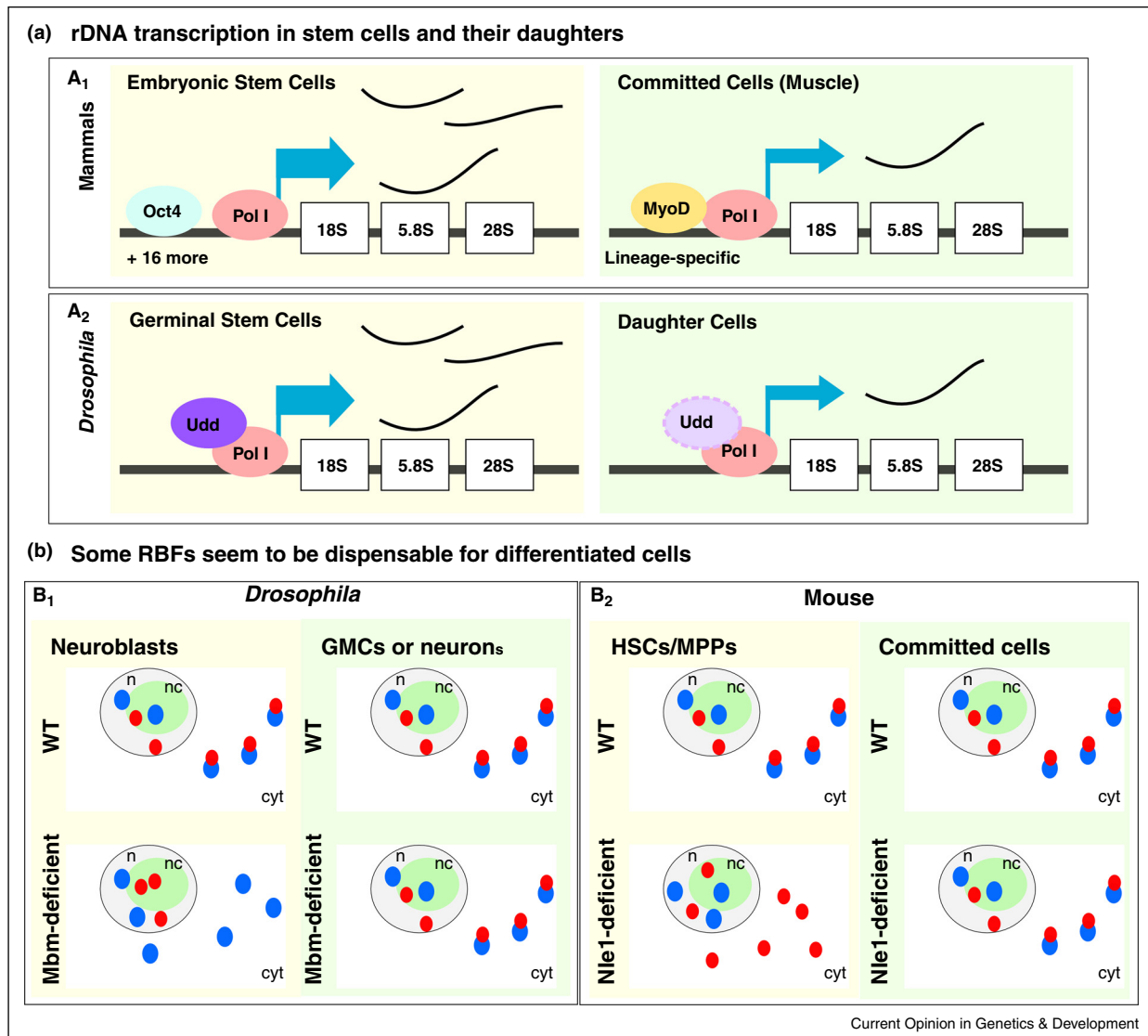
Of note, the methyltransferase FIBRILLARIN (FBL) can methylate both immature rRNAs and histone H2A at rDNA loci. This latter modification serves as a recruitment site for polymerase I only, thereby boosting rDNA transcription and the overall ribosome biogenesis process [20,21]. Interestingly, FBL is overrepresented in the proteome of mESCs [22*] and the zebrafish ortholog of FBL is overexpressed in neuroepithelial-like progenitors of the midbrain [10].

Beyond rDNA transcription: many RBFs at all steps of the process appear to play stem cell-specific roles

Many processing steps (folding, cleavage, chemical modifications) occur while pre-rRNAs are still being transcribed. The activity of many RBFs ensures that ribosome assembly starts at the same time as rRNA transcription. Interestingly, some of these factors act differently in stem cells and in their daughters (Figure 1B). Examples of differentially acting RBFs can be found among metazoans. Here, we limit our discussion to studies performed in fly, zebrafish, mouse and human (see Table 1).

As previously mentioned in the ‘To be or not be (conserved)?’ section, lineage-specific RBFs are found across the tree of life and at least one is stem cell specific. Indeed, analysis of Drosophila mutants showed that the Drosophila-specific factor mushroom body miniature (Mbm) is necessary for the maturation of the small subunit in neuroblasts, but is dispensable in GMCs (Ganglion Mother Cells) and in neurons (neuroblast daughter cells; Figure 1B1) [23*]. Functional analyses of other species-specific factors are currently lacking, nevertheless evolutionarily conserved (and previously characterized) RBFs contribute specifically to stem cell survival and homeostasis as well. For example, disruption of UTP4 (a component of the small subunit processome) causes North American Indian childhood cirrhosis, a

Figure 1



Ribosome biogenesis differs between stem cells and differentiated cells. In general, stem cells display higher rates of rDNA transcription than their daughter cells (A). In mammals, this is controlled at the level of the rDNA chromatin. Histone marks at rDNA loci differ between mESCs and more differentiated cells. Moreover, pluripotency-associated factors bind rDNA in stem cells (both in mouse and human) (A1, left panel). By contrast, lineage-specific factors occupy rDNA loci in committed cells thereby down-regulating rDNA transcription (A1, right panel). Besides the muscle-specific factor (MyoD) represented in the figure, other lineage-specific factors (Myogenin, Runx2, C/EBP β) play similar roles. Interestingly, phenotypic factors interact with UBF-1 which is an activator of the polymerase I, similar to the situation in *Drosophila* germinal stem cells (GSCs) (A2). In this case, the polymerase I co-factor Under-developed (Udd) promotes the transcription of rRNA in GSCs (A2, left panel). The expression level of Udd is lower in daughter cells than in GSCs, resulting in the down-regulation of rDNA transcription. Certain RBFs seem to be dispensable for committed and differentiated cells (B). Loss of the *Drosophila*-specific factor Mbm, for example, leads to the nucleolar accumulation of pre-40S particles in neuroblasts, but not in Ganglion Mother Cells and neurons (B1). Similarly, the loss of Notchless (Nle) leads to the nuclear accumulation of pre-60S particles in HSCs but not in lineage committed-progenitors and differentiated cells (B2). These findings show that ribosome biogenesis is quantitatively and qualitatively different between stem and differentiated cells. cyt (cytoplasm), n (nucleus), nc (nucleolus), GMCs (Ganglion Mother Cells), HSCs (hematopoietic stem cells), MPPs (multipotent progenitors); red dots (pre-40S particles/40S subunits), blue dots (pre-60S particles/60S subunits).

ribosomopathy affecting the biliary system (single tissue phenotype) [24]. Knockdown of Utp4 in zebrafish also leads to specific defects in the biliary system [25], suggesting that the function of this protein in liver progenitors is evolutionary conserved. Similarly, conditional

knock-out of Notchless, a murine ortholog of the yeast 60S subunit maturation factor Rsa4, depletes HSCs and multipotent progenitors, but not mature hematopoietic cells (Figure 1B2) [15**]. Interestingly, the authors of this study suggest that other factors compensate for the lack of

Notchless (Nle1) in differentiated cells and propose that conserved and/or species-specific factors may play this role. Indeed, it is possible that novel ribosome biogenesis-based regulatory mechanisms are also involved in the homeostasis of differentiated cells, although they will not be covered in this review.

Lost in translation: ribosome biogenesis-related mechanisms of gene expression control

Determination and maintenance of stem cell identity are not only a question of rates. Indeed, even if rDNA transcription is generally higher in stem cells than in their progeny (see ‘rDNA transcription is differentially regulated in stem cells compared to their differentiated progeny’ subsection), the rate of global protein synthesis is tightly regulated in mammalian stem cells [26^{**}]. For instance, translation rates are lower in mammalian HSCs than in other cells of the hematopoietic lineage *in vivo*, and this occurs independently of the rate of rDNA transcription [27,28]. On the other hand, the accumulation of Wicked (Wkd) in stem cells might lead to the upregulation of ribosome biogenesis and therefore of the protein synthesis rate. Nevertheless, Wcd may associate with cell type-specific RPs or RBFs performing specialized functions. Indeed, microarray analysis of female GSCs in *Drosophila* showed enrichment in specific isoforms of RPs and regulators of ribosome biogenesis [29,30]. All together, these findings highlight the fact that cell identity might depend upon the types of translated mRNAs and not only upon the global amount of produced proteins.

The choice of mRNAs to be translated is typically modulated by both ribosome-associated factors (acting on mature ribosomes) and ‘specialized’ ribosomes [31,32]. Indeed, ribosomes are not only translational machine but they can control gene expression by selecting the mRNAs to be translated. Translational capacities of the ribosomes depend on their internal composition (in terms of isoforms of RPs, RP post-translational modifications and rRNA post-transcriptional modifications) and this could be diverse [31]. Interestingly, most of the research is focused on understanding how ribosome diversity could participate to the translational control of gene expression [31,26^{**}] or to find specific recognition elements in the mRNA to be transcribed [33]. Virtually nothing is known about the upstream regulatory signals that might produce ribosome heterogeneity in the first place. Neither is known how ribosome biogenesis could contribute to this diversity at a cellular level. Nevertheless, changes in ribosome biogenesis modalities and in RBF amount impact on gene expression and this might be particularly important to determine stem cell identity (Figure 2).

For example, FBL overexpression in P53-deficient cancer cells triggers the hyper-methylation of rRNAs leading

to the synthesis of ribosomes with modified translational specificity such that IRES-containing mRNAs (e.g. cMYC, FGF1, VEGFA) are preferentially translated instead of 5'-capped transcripts [34^{*}]. Interestingly, it was recently shown that FBL is essential for the survival of mESCs. Stable expression of FBL in these cells cultured in differentiating conditions (without LIF) extended their pluripotent state. Moreover, both partial knock-down of FBL and treatment with Actinomycin D induced the expression of differentiation markers and promoted stem cell differentiation into neuronal lineages [22^{*}]. Like FBL, the orthologs of the other components of the same functional complex (NOP58 and NOP56) are also overexpressed in *Drosophila* neuroblasts and in zebrafish neuroepithelial-like progenitors of the mid-brain (Table 1) [10,11,35]. NOP56 ortholog has been described to play a major role in the maintenance of neuroepithelial stem cells of the optic lobe [36] (Figure 2).

Moreover, it has been described that the zebrafish orthologs of these three partners, FBL, NOP56 and NOP58 were up-regulated upon cold exposure induced stress [37]. Studies in *Drosophila*, amphibians and mouse show that stem cells respond better than other cell types to stress [38–40]. Upon stress, IRES-mediated translation is favored over cap-dependent translation [41]. Therefore, it is possible that the capacity of stem cells to survive upon stress is linked to the type of RBFs they express, and thus to the types of mRNAs that are translated.

It is still unclear how differences in ribosome biogenesis contribute to the diversification of proteomes among different cell types. Detailed functional analyses of the newly discovered RBFs are still lacking (see the ‘To be or not to be (conserved)?’ section) and the situation becomes more complicated when the diverse mechanisms of gene expression control are taken in account [26^{**},27]. For example, differentially expressed RBFs could contribute to the generation of the previously mentioned specialized ribosomes. Moreover, it was recently discovered that stem cells and differentiated cells express different subsets of tRNAs [42,43], adding yet another mechanism contributing to the determination of cell identity.

Conclusions and future directions

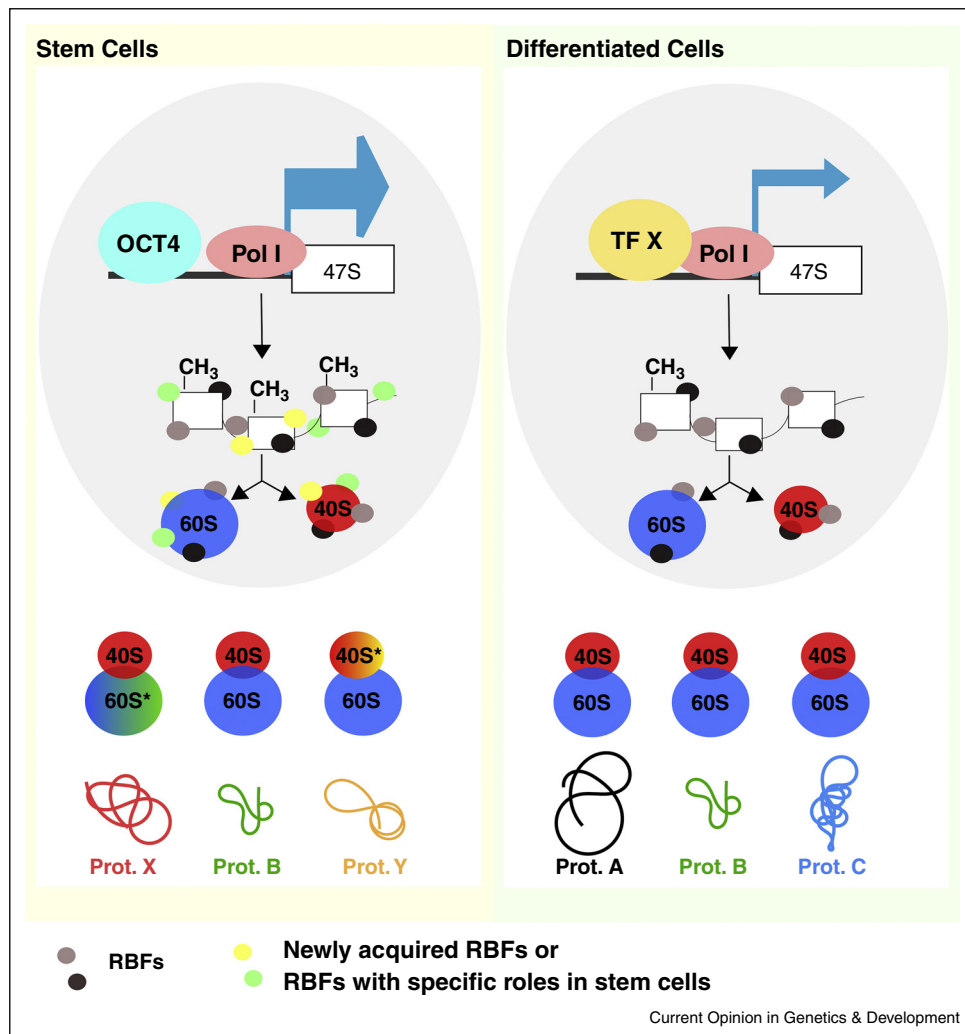
Ribosome biogenesis is fundamental to all life forms, but surprisingly little is known about this pathway in vertebrates. Most of our knowledge derives from studies performed on yeast or mammalian cell cultures. The recent discovery of the diversity of RBF repertoires among eukaryotes opens new avenues of investigation for fundamental research. It is noteworthy that the *Drosophila*-specific RBF Mbm is stem cell-specific [23^{*}] and, besides that, a plethora of previously known RBFs are important for stem cell homeostasis (see Table 1). However, ribosome biogenesis-based mechanisms of gene

expression control may have evolved to regulate differentiation and not to maintain multipotency. Thus, it will be important to compare ribosome biogenesis between stem cells and their daughters at different developmental stages, in different tissues and in different stem cell activation states. Nevertheless, generalizations have to be made carefully since differences among stem cell populations (within the same species) may exist.

Demonstrating that differences in ribosome biogenesis actually exist represents a technical challenge. Indeed, RBF accumulation is not an all-or-nothing asymmetry and mutations in RBF-coding genes are often lethal at early developmental stages. Pescadillo (Pes1), Fibrillarin (Fbl) and Notchless (Nle) disruption, for example, leads to developmental arrest before implantation in murine

embryos [44–46]. Nonetheless, many RBF-coding genes show tissue specific expression in zebrafish and loss of function experiments showed that they play specific roles for the survival of the progenitor cells in the central nervous system [47,48], liver [25,49], pancreas [50,51] and neural crests [52]. Phenotype restriction at late developmental stages in zebrafish is probably a result of the large stock of mature ribosomes provided to the embryo maternally [47]. Given that mammalian development cannot rely on such maternal stocks and that the production of ribosomes is an essential function in all cells, alternative methods to classical knock-out must be considered to investigate the importance of ribosome biogenesis for stem cell survival and homeostasis. In this context, stem cell-specific roles of two RBF-coding genes have been recently demonstrated either using conditional knock-out experiments in mouse

Figure 2



Differences in ribosome biogenesis lead to variations in gene expression. Stem cells display high levels of rDNA transcription. Some RBFs are overexpressed in stem cells and they seem to play important roles in the homeostasis of these cells. This may lead to the synthesis of specialized ribosomes differing from the standard composition both in terms of rRNAs and ribosomal proteins. These ribosomes may have specific target mRNAs. Proteomes of stem and differentiated cells would thereby be different.

[15**] or combinations of overexpression and knock-down in cultured mESCs [22*]. However, few studies have been performed in mammals and a direct correlation between ribosome biogenesis and stem cell homeostasis remains to be demonstrated.

Moreover, ribosome biogenesis-related gene expression control mechanisms merit further investigation because this may open new exciting and so far unexplored routes for fundamental research. Importantly, studies investigating this aspect of translational control *in vivo* may provide insight into tissue-specific clinical phenotypes of ribosomopathies [53–55].

Acknowledgements

We thank Franck Bourrat, Frédéric Catez and Michel Cohen-Tannoudji for critically reviewing and proofreading the manuscript. The present work was supported by the French National Agency for Research (project FINEST: ANR-11-BSV2-0029) and the 'Fondation pour la Recherche Médicale' (FDT20140930792). We apologize to authors whose work could not be cited owing to space constraints.

References and recommended reading

Papers of particular interest, published within the period of review, have been highlighted as:

- of special interest
- of outstanding interest

1. Mauro VP, Edelman GM: **The ribosome filter redux.** *Cell Cycle* 2007, **6**:2246-2251.
2. Ebersberger I, Simm S, Leisegang MS, Schmitzberger P, Mirus O, von Haeseler A, Bohnsack MT, Schleiff E: **The evolution of the ribosome biogenesis pathway from a yeast perspective.** *Nucleic Acids Res* 2014, **42**:1509-1523.
3. Mullineux S-T, Lafontaine DLJ: **Mapping the cleavage sites on mammalian pre-rRNAs: where do we stand?** *Biochimie* 2012, **94**:1521-1532.
4. Tafforeau L, Zorbas C, Langhendries J-L, Mullineux S-T, Stamatoopoulou V, Mullier R, Wacheul L, Lafontaine DLJ: **The complexity of human ribosome biogenesis revealed by systematic nucleolar screening of Pre-rRNA processing factors.** *Mol Cell* 2013, **51**:539-551.
- It is the first comprehensive functional study of the human nucleolar proteome. One of the main outcomes of the study is the discovery of more than 70 RBFs with no yeast ortholog.
5. Melnikov S, Ben-Shem A, Garreau de Loubresse N, Jenner L, Yusupova G, Yusupov M: **One core, two shells: bacterial and eukaryotic ribosomes.** *Nat Struct Mol Biol* 2012, **19**:560-567.
6. Hernandez-Verdun D, Roussel P, Thiry M, Sirri V, Lafontaine DLJ: **The nucleolus: structure/function relationship in RNA metabolism.** *Wiley Interdiscip Rev RNA* 2010, **1**:415-431.
7. Couté Y, Burgess JA, Diaz J-J, Chichester C, Lisacek F, Greco A, Sanchez J-C: **Deciphering the human nucleolar proteome.** *Mass Spectrom Rev* 2006, **25**:215-234.
8. Ahmad Y, Boisvert F-M, Gregor P, Cogley A, Lamond AI: **NOPdb: nucleolar proteome database – 2008 update.** *Nucleic Acids Res* 2009, **37**:D181-D184.
9. Henras AK, Plisson-Chastang C, O'Donohue M-F, Chakraborty A, Gleizes P-E: **An overview of pre-ribosomal RNA processing in eukaryotes.** *Wiley Interdiscip Rev RNA* 2015, **6**:225-242.
10. Recher G, Jouralet J, Brombin A, Heuzé A, Mugniery E, Hermel J-M, Desnoullez S, Savy T, Herbomel P, Bourrat F *et al.*: **Zebrafish midbrain slow-amplifying progenitors exhibit high levels of transcripts for nucleotide and ribosome biogenesis.** *Development* 2013, **140**:4860-4869.

11. Neumüller RA, Richter C, Fischer A, Novatchkova M, Neumüller KG, Knoblich JA: **Genome-wide analysis of self-renewal in Drosophila neural stem cells by transgenic RNAi.** *Cell Stem Cell* 2011, **8**:580-593.
12. Huang K, Maruyama T, Fan G: **The naive state of human pluripotent stem cells: a synthesis of stem cell and preimplantation embryo transcriptome analyses.** *Cell Stem Cell* 2014, **15**:410-415.
- Many datasets, obtained from transcriptomic analysis performed in naive and primed human pluripotent stem cells, have been compared. Naive hPSC transcriptomes share a consensus gene network in RNA processing, ribosome biogenesis, and mitochondrial metabolism.
13. Zentner GE, Balow SA, Scacheri PC: **Genomic characterization of the mouse ribosomal DNA locus.** *G3 (Bethesda)* 2014, **4**:243-254.
14. Zhang Q, Shalaby NA, Buszczak M: **Changes in rRNA transcription influence proliferation and cell fate within a stem cell lineage.** *Science* 2014, **343**:298-301.
15. Le Bouteiller M, Souilhol C, Beck-Cormier S, Stedman A, Burlen-Defranoux O, Vandormael-Pournin S, Bernex F, Cumano A, Cohen-Tannoudji M: **Notchless-dependent ribosome synthesis is required for the maintenance of adult hematopoietic stem cells.** *J Exp Med* 2013, **210**:2351-2369.
- First functional study *in vivo* showing that a RBF (Notchless) is required in hematopoietic stem cells and dispensable in more restricted cells.
16. Ali SA, Zaidi SK, Dacwag CS, Salma N, Young DW, Shakoobi AR, Montecino MA, Lian JB, van Wijnen AJ, Imbalzano AN *et al.*: **Phenotypic transcription factors epigenetically mediate cell growth control.** *Proc Natl Acad Sci U S A* 2008, **105**:6632-6637.
17. Hayashi Y, Kuroda T, Kishimoto H, Wang C, Iwama A, Kimura K: **Downregulation of rRNA transcription triggers cell differentiation.** *PLOS ONE* 2014, **9**:e98586.
18. Flach J, Bakker ST, Mohrin M, Conroy PC, Pietras EM, Reynaud D, Alvarez S, Diolaiti ME, Ugarte F, Forsberg EC *et al.*: **Replication stress is a potent driver of functional decline in ageing haematopoietic stem cells.** *Nature* 2014, **512**:198-202.
19. Morgado-Palacin L, Llanos S, Serrano M: **Ribosomal stress induces L11- and p53-dependent apoptosis in mouse pluripotent stem cells.** *Cell Cycle* 2012, **11**:503-510.
20. Tessarz P, Santos-Rosa H, Robson SC, Sylvestersen KB, Nelson CJ, Nielsen ML, Kouzarides T: **Glutamine methylation in histone H2A is an RNA-polymerase-I-dedicated modification.** *Nature* 2014, **505**:564-568.
21. Lafontaine DLJ: **Noncoding RNAs in eukaryotic ribosome biogenesis and function.** *Nat Struct Mol Biol* 2015, **22**:11-19.
22. Watanabe-Susaki K, Takada H, Enomoto K, Miwata K, Ishimine H, Intoh A, Ohtaka M, Nakanishi M, Sugino H, Asashima M *et al.*: **Biosynthesis of ribosomal RNA in nucleoli regulates pluripotency and differentiation ability of pluripotent stem cells.** *Stem Cells* 2014, **32**:3099-3111.
- The authors demonstrate that Fibrillarin is highly expressed in mouse embryonic stem cells and play a crucial role in regulating their pluripotency.
23. Hovhanyan A, Herter EK, Pfannstiel J, Gallant P, Raabe T: **Drosophila mbm is a nucleolar myc and casein kinase 2 target required for ribosome biogenesis and cell growth of central brain neuroblasts.** *Mol Cell Biol* 2014, **34**:1878-1891.
- This paper describes for the first time a species-specific RBF which is dispensable in GMCs and neurons, but not in neuroblasts.
24. Freed EF, Baserga SJ: **The C-terminus of Utp4, mutated in childhood cirrhosis, is essential for ribosome biogenesis.** *Nucleic Acids Res* 2010, **38**:4798-4806.
25. Wilkins BJ, Lorent K, Matthews RP, Pack M: **p53-mediated biliary defects caused by knockdown of cirh1a, the zebrafish homolog of the gene responsible for North American Indian Childhood Cirrhosis.** *PLOS ONE* 2013, **8**:e77670.
26. Buszczak M, Signer RAJ, Morrison SJ: **Cellular differences in protein synthesis regulate tissue homeostasis.** *Cell* 2014, **159**:242-251.
- This paper reviews current knowledge of the differences in protein synthesis among cells. The heterogeneity of ribosome and tissue-specificity of ribosomopathies are discussed. Protein synthesis control is

critical for the maintenance of tissue homeostasis and mechanisms modifying protein synthesis can promote the development of cancer.

27. Signer RAJ, Magee JA, Salic A, Morrison SJ: **Haematopoietic stem cells require a highly regulated protein synthesis rate.** *Nature* 2014, **509**:49-54.
 28. Barna M, Ruggero D: **Tailor made protein synthesis for HSCs.** *Cell Stem Cell* 2014, **14**:423-424.
 29. Kai T, Williams D, Spradling AC: **The expression profile of purified Drosophila germline stem cells.** *Dev Biol* 2005, **283**:486-502.
 30. Fichelson P, Moch C, Ivanovitch K, Martin C, Sidor CM, Lepesant J-A, Bellaiche Y, Huynh J-R: **Live-imaging of single stem cells within their niche reveals that a U3snoRNP component segregates asymmetrically and is required for self-renewal in Drosophila.** *Nat Cell Biol* 2009, **11**:685-693.
 31. Xue S, Barna M: **Specialized ribosomes: a new frontier in gene regulation and organismal biology.** *Nat Rev Mol Cell Biol* 2012, **13**:355-369.
 32. Filipovska A, Rackham O: **Specialization from synthesis: how ribosome diversity can customize protein function.** *FEBS Lett* 2013, **587**:1189-1197.
 33. Xue S, Tian S, Fujii K, Kladwang W, Das R, Barna M: **RNA regulons in Hox 5' UTRs confer ribosome specificity to gene regulation.** *Nature* 2015, **517**:33-38.
 34. Marcel V, Ghayad SE, Belin S, Therizols G, Morel A-P, Solano-González E, Vendrell JA, Hacot S, Mertani HC, Albaret MA *et al.*: **p53 acts as a safeguard of translational control by regulating fibrillarin and rRNA methylation in cancer.** *Cancer Cell* 2013, **24**:318-330.
- FIBRILLARIN is overexpressed in P53-deficient cancer cells. High levels of FBL are accompanied by modifications of the rRNA methylation pattern, impairment of translational fidelity, and an increase of internal ribosome entry site (IRES)-dependent translation initiation (translational switch).
35. Southall TD, Gold KS, Egger B, Davidson CM, Caygill EE, Marshall OJ, Brand AH: **Cell-type-specific profiling of gene expression and chromatin binding without cell isolation: assaying RNA Pol II occupancy in neural stem cells.** *Dev Cell* 2013, **26**:101-112.
 36. Wang H, Chen X, He T, Zhou Y, Luo H: **Evidence for tissue-specific Jak/STAT target genes in Drosophila optic lobe development.** *Genetics* 2013, **195**:1291-1306.
 37. Long Y, Song G, Yan J, He X, Li Q, Cui Z: **Transcriptomic characterization of cold acclimation in larval zebrafish.** *BMC Genomics* 2013, **14**:612.
 38. McLeod CJ, Wang L, Wong C, Jones DL: **Stem cell dynamics in response to nutrient availability.** *Curr Biol* 2010, **20**:2100-2105.
 39. Yilmaz ÖH, Katajisto P, Lamming DW, Gültekin Y, Bauer-Rowe KE, Sengupta S, Birsoy K, Dursun A, Yilmaz VO, Selig M *et al.*: **mTORC1 in the Paneth cell niche couples intestinal stem-cell function to calorie intake.** *Nature* 2012, **486**:490-495.
 40. Love NK, Keshavan N, Lewis R, Harris WA, Agathocleous M: **A nutrient-sensitive restriction point is active during retinal progenitor cell differentiation.** *Development* 2014, **141**:697-706.
 41. Spriggs KA, Bushell M, Willis AE: **Translational regulation of gene expression during conditions of cell stress.** *Mol Cell* 2010, **40**:228-237.
 42. Gingold H, Tehler D, Christoffersen NR, Nielsen MM, Asmar F, Kooistra SM, Christophersen NS, Christensen LL, Borre M, Sørensen KD *et al.*: **A dual program for translation regulation in cellular proliferation and differentiation.** *Cell* 2014, **158**:1281-1292.
 43. Topisirovic I, Sonenberg N: **Distinctive tRNA repertoires in proliferating versus differentiating cells.** *Cell* 2014, **158**:1238-1239.
 44. Allende ML, Amsterdam A, Becker T, Kawakami K, Gaiano N, Hopkins N: **Insertional mutagenesis in zebrafish identifies two novel genes, pescadillo and dead eye, essential for embryonic development.** *Genes Dev* 1996, **10**:3141-3155.
 45. Newton K, Petfalski E, Tollervey D, Cáceres JF: **Fibrillarin is essential for early development and required for accumulation of an intron-encoded small nucleolar RNA in the mouse.** *Mol Cell Biol* 2003, **23**:8519-8527.
 46. Cormier S, Le Bras S, Souilhol C, Vandormael-Pournin S, Durand B, Babinet C, Baldacci P, Cohen-Tannoudji M: **The murine ortholog of notchless, a direct regulator of the notch pathway in Drosophila melanogaster, is essential for survival of inner cell mass cells.** *Mol Cell Biol* 2006, **26**:3541-3549.
 47. Azuma M, Toyama R, Laver E, Dawid IB: **Perturbation of rRNA synthesis in the bap28 mutation leads to apoptosis mediated by p53 in the zebrafish central nervous system.** *J Biol Chem* 2006, **281**:13309-13316.
 48. Simmons T, Appel B: **Mutation of pescadillo disrupts oligodendrocyte formation in zebrafish.** *PLoS ONE* 2012, **7**:e32317.
 49. Wang Y, Luo Y, Hong Y, Peng J, Lo L: **Ribosome biogenesis factor Bms1-like is essential for liver development in zebrafish.** *J Genet Genom* 2012, **39**:451-462.
 50. Provost E, Wehner KA, Zhong X, Ashar F, Nguyen E, Green R, Parsons MJ, Leach SD: **Ribosomal biogenesis genes play an essential and p53-independent role in zebrafish pancreas development.** *Development* 2012, **139**:3232-3241.
 51. Qin W, Chen Z, Zhang Y, Yan R, Yan G, Li S, Zhong H, Lin S: **Nom1 mediates pancreas development by regulating ribosome biogenesis in zebrafish.** *PLOS ONE* 2014, **9**:e100796.
 52. Zhao C, Andreeva V, Gibert Y, LaBonty M, Lattanzi V, Prabhudesai S, Zhou Y, Zon L, McCann KL, Baserga S *et al.*: **Tissue specific roles for the ribosome biogenesis factor Wdr43 in zebrafish development.** *PLoS Genet* 2014, **10**:e1004074.
 53. Teng T, Thomas G, Mercer CA: **Growth control and ribosomopathies.** *Curr Opin Genet Dev* 2013, **23**:63-71.
 54. Ross AP, Zarbalis KS: **The emerging roles of ribosome biogenesis in craniofacial development.** *Front Physiol* 2014, **5**:26.
 55. Armistead J, Triggs-Raine B: **Diverse diseases from a ubiquitous process: the ribosomopathy paradox.** *FEBS Lett* 2014, **588**:1491-1500.
 56. Berger C, Harzer H, Burkard TR, Steinmann J, van der Horst S, Laurenson A-S, Novatchkova M, Reichert H, Knoblich JA: **FACS purification and transcriptome analysis of drosophila neural stem cells reveals a role for Klumpfuss in self-renewal.** *Cell Rep* 2012, **2**:407-418.
 57. Dixon J, Jones NC, Sandell LL, Jayasinghe SM, Crane J, Rey J-P, Dixon MJ, Trainor PA: **Tcof1/Treacle is required for neural crest cell formation and proliferation deficiencies that cause craniofacial abnormalities.** *Proc Natl Acad Sci U S A* 2006, **103**:13403-13408.
 58. Griffin JN, Sondalle SB, Del Viso F, Baserga SJ, Khokha MK: **The ribosome biogenesis factor Nol11 is required for optimal rDNA transcription and craniofacial development in Xenopus.** *PLoS Genet* 2015, **11**:e1005018.
 59. Matsuo Y, Granneman S, Thoms M, Manikas R-G, Tollervey D, Hurt E: **Coupled GTPase and remodelling ATPase activities form a checkpoint for ribosome export.** *Nature* 2014, **505**:112-116.
 60. Bolli N, Payne EM, Grabher C, Lee J-S, Johnston AB, Falini B, Kanki JP, Look AT: **Expression of the cytoplasmic NPM1 mutant (NPMc+) causes the expansion of hematopoietic cells in zebrafish.** *Blood* 2010, **115**:3329-3340.
 61. Li J, Sejas DP, Rani R, Koretsky T, Bagby GC, Pang Q: **Nucleophosmin regulates cell cycle progression and stress response in hematopoietic stem/progenitor cells.** *J Biol Chem* 2006, **281**:16536-16545.

PART III AIM OF THE PHD

I joined the CASBAH group for my master internship because I was fascinated about the determination of cell fate. In the lab we use the teleost optic tectum to answer cell-cycle related questions.

After an initial work aimed to analyze the whole POU complement in one model organism (**Brombin *et al.*, 2011**; see *annex*), I joined the main topic of the group because I was interested in understanding the molecular cues that contribute to determine the identity of a stem progenitor cell. To this aim, the group was looking for the molecular signature of the neuroepithelial progenitors that support the life-long growth of the teleost OT. First data have been retrieved via an *in situ* hybridization screen aimed to find genes specifically expressed in the proliferation zone of the medaka OT. Interestingly, the expression of some genes appeared to be restricted to a thin layer of cells encompassing the embryonic tectum. What does make these cells so different from the adjacent cells?

To answer this question we switched to zebrafish which is a more widely used and powerful model. We studied the cell behavior and overall the molecular signature of the neuroepithelial cells that wraps the whole tectal periphery, thereby identifying the peripheral midbrain layer (see *Ch. 2.I*). Interestingly, PML cells were characterized by the expression of genes coding for factors involved in nucleotide and ribosome biogenesis factors. Why these general factors are expressed in such a restricted manner? Might they play specific roles in neuroepithelial cell biology?

To this aim I started a functional study to understand the relationship between ribosome biogenesis factor coding genes and PML cells identity. Due to the lack of literature, at the beginning of my PhD, I started to work in the most classical way by studying null mutants (see *Ch 2.II section 1*). Moreover, I started a functional study based on the conditional overexpression of a dominant-negative form of a ribosome biogenesis factor (*nle1*, see *Ch. 2.II section 2*).

At the end of my PhD, many questions remain unanswered, but in the last years, we have assisted to a veritable explosion of papers highlighting the intimate relationship between ribosome biogenesis and progenitor/stem cell biology. Not only ribosome biogenesis contributes to the homeostasis of these cells, but contributes to the determination of their cell identity. All together, these findings allowed me to write a review for Current Opinion in genetics and Development, which is under revision (see *Ch. 1.II section 2.2.4*).

CHAPTER 2

RESULTS

PART I

ZEBRAFISH MIDBRAIN SLOW-AMPLIFYING PROGENITORS EXHIBIT HIGH LEVELS OF TRANSCRIPTS FOR NUCLEOTIDE AND RIBOSOME BIOGENESIS.

Zebrafish is a powerful model for developmental biology and recently became an important model to dissect the mechanisms underlying human pathologies. It is amenable to transgenesis, mutagenesis and *in vivo* imaging.

I used for my thesis project the zebrafish optic tectum (OT) as a model. The OT is a prominent dorsal region of the midbrain that grows in a cellular “conveyor belt” mode (**Devès and Bourrat, 2012**; see *Ch1.I section 2.4*). In this cortical structure there is a spatiotemporal correlation between the differentiation state of a cell and its position in the organ. Concentric cell populations, at a given level of differentiation, are marked by a specific gene expression patterns.

This structure displays a life-long growth sustained by neuroepithelial progenitors forming a thin peripheral layer of cells. It wraps the OT margins both at adulthood (**Ito et al., 2010; Grandel and Brand, 2013**) and at embryonic stages where it takes the name of peripheral midbrain layer (PML*) (**Recher et al., 2013**). Recently, in the lab, PML cells have been shown to be slow-amplifying progenitors (SAPs), which give rise to fast-amplifying progenitors (FAPs) that subsequently differentiate in different tectal cell types. The presence of these SAPs and FAPs in separate domains provided the opportunity to datamine the ZFIN expression pattern database for SAP markers. Surprisingly, PML cell transcriptome is enriched in transcripts coding for nucleotide biosynthesis and ribosome biogenesis associated factors. This suggests that SAPs may function as “storage chambers”, accumulating transcripts useful for the FAPs, as oocytes are “storage chambers” for fast-subsequent blastomere divisions in the early embryo. On the other hand, there are important overlaps between the PML specific gene list and other progenitor/stem cell datasets obtained independently. In particular the PML gene-network dataset display many genes in common with a *Drosophila* neuroblast-specific network or with others related to human pluripotent stem cells or cancer associated gene-networks (**Recher et al., 2013**).

This work allowed us to evidence a first molecular signature of the tectal neuroepithelial cells and served as a basis for the functional studies presented in this manuscript (see *Ch. 2.II*) and underway in the group

* I want to stress the fact that the definition of PML in this chapter (and until the end of the manuscript is different from the definition used by Grandel and colleagues (**Grandel *et al.*, 2006**; see *Ch1.1 section 2.3.2*). Grandel called PML (posterior mesencephalic lamina) a thin layer of cells that starts dorsally at the proliferative tectal margin, continues as non-proliferative lamina and becomes proliferative again as it touches the cerebellar surface. Grandel's PML is most likely the "fusion" between the adult ventral midbrain stem cell niche (Her5+ RGCs) described by Chapouton and colleagues (**Chapouton *et al.*, 2006**; **Chapouton *et al.*, 2011**) and the adult tectal neuroepithelial niche described by Ito and colleagues (**Ito *et al.*, 2010**).

RESEARCH ARTICLE

STEM CELLS AND REGENERATION

Zebrafish midbrain slow-amplifying progenitors exhibit high levels of transcripts for nucleotide and ribosome biogenesis

Gaëlle Recher^{1,2,*}, Julia Jouralet^{1,3,*}, Alessandro Brombin^{1,3}, Aurélie Heuzé^{1,3}, Emilie Mugniery^{1,3}, Jean-Michel Hermel^{1,3}, Sophie Desnoullez^{1,2}, Thierry Savy^{1,2}, Philippe Herbomel^{4,5}, Franck Bourrat^{1,3}, Nadine Peyriéras^{1,2,§}, Françoise Jamen^{1,3,6,‡} and Jean-Stéphane Joly^{1,3,‡,§}

ABSTRACT

Investigating neural stem cell (NSC) behaviour *in vivo*, which is a major area of research, requires NSC models to be developed. We carried out a multilevel characterisation of the zebrafish embryo peripheral midbrain layer (PML) and identified a unique vertebrate progenitor population. Located dorsally in the transparent embryo midbrain, these large slow-amplifying progenitors (SAPs) are accessible for long-term *in vivo* imaging. They form a neuroepithelial layer adjacent to the optic tectum, which has transitory fast-amplifying progenitors (FAPs) at its margin. The presence of these SAPs and FAPs in separate domains provided the opportunity to data mine the ZFIN expression pattern database for SAP markers, which are co-expressed in the retina. Most of them are involved in nucleotide synthesis, or encode nucleolar and ribosomal proteins. A mutant for the *cad* gene, which is strongly expressed in the PML, reveals severe midbrain defects with massive apoptosis and sustained proliferation. We discuss how fish midbrain and retina progenitors might derive from ancient sister cell types and have specific features that are not shared with other SAPs.

KEY WORDS: Neural stem cell, Optic tectum, Retina

INTRODUCTION

In neural stem cells (NSCs) and neural progenitors (NPs), as in other cell types, cell identity is characterised by specific molecular signatures that depend on the environment provided by neighbouring cells (Fuchs et al., 2004). It is therefore important to study NPs *in vivo*. However, few *in vivo* investigations have been performed so far and these have mainly focused on two telencephalic populations in rodents: the subventricular zone (SVZ) and the dentate gyrus of the hippocampus (Zhao et al., 2008; Chojnacki et al., 2009; Kriegstein and Alvarez-Buylla, 2009; Hsieh, 2012). Teleosts and amphibians display an extraordinary capacity for NP activation and maintenance, but also for self-repair and neuronal regeneration in adulthood (Grandel et al., 2006; Zupanc, 2009; Kizil et al., 2011; Zupanc and Sîrbulescu, 2011; Schmidt et al., 2013). They are therefore excellent models for comparative

studies of the NP-based mechanisms underlying neural regeneration and are suitable for studies involving transgenesis and also for live imaging (Rieger et al., 2011; Rinkwitz et al., 2011).

One of the most interesting neurogenic areas, which has been described in both medaka (Alunni et al., 2010) and zebrafish (Grandel et al., 2006; Ito et al., 2010; Grandel and Brand, 2013), is located at the medial, lateral and caudal margins of the adult optic tectum (OT). The OT is a prominent dorsal region of the midbrain that functions as a cellular ‘conveyor belt’ (Devès and Bourrat, 2012). In this cortical structure there is a spatiotemporal correlation between the maturation state of a cell and its position in the OT. Each cell population, at a particular level of differentiation, is marked by concentric gene expression patterns. Similarly, the anamniote retina may be considered a cellular conveyor belt and, as discussed in a recent review (Cervený et al., 2012), tectal cells and retina cells from the ciliary marginal zone (CMZ) share common molecular signatures and express many canonical proliferation markers.

Here we present an integrated study using zebrafish embryos to examine a population of label-retaining multipotent midbrain NPs. This population connects the OT to the torus semicircularis (TS) (a more ventral, but also an alar, midbrain structure) posteriorly and laterally. Medially, it also connects the OT to the cerebellum. Previously described as the ‘caudal wall’ (Palmgren, 1921) and recently as the ‘posterior midbrain lamina’ (Grandel et al., 2006), this structure wraps the embryonic OT both posteriorly and laterally; we therefore find it more appropriate to refer to this structure as the ‘peripheral midbrain layer’ (PML). Three recently published reviews (Cervený et al., 2012; Grandel and Brand, 2013; Schmidt et al., 2013) pointed out the need to know more about the formation and function of this cell layer, which gives rise to different types of tectal cells. It is in close proximity with the *her5*-positive stem cells (SCs) at the midbrain-hindbrain boundary (MHB) and probably derives from this SC population. However, MHB SC and PML progenitors express different markers (glial and neuroepithelial, respectively) (Chapouton et al., 2006) (reviewed by Schmidt et al., 2013).

The zebrafish is a well-established model system for three-dimensional real-time (3D+time) live imaging of morphogenetic events in the eye and nervous system (England et al., 2006; Greiling et al., 2010; Kwan et al., 2012). However, midbrain development remains poorly studied in this organism. The morphogenetic movements that shape the tectum have not been described. Using two-photon laser-scanning microscopy (TPLSM) for imaging neural tissue, and tracking the behaviour of cells in real time, we provide the first comprehensive analysis of the cellular events that shape the OT. We found that the midbrain is formed in a stepwise manner: intense morphogenetic movements shaping the TS (period 1) are followed by continued elongation of the PML and cytological

¹CNRS, UPR3294 Unité Neurobiologie et Développement, F-91198 Gif-sur-Yvette, France. ²MDAM (Multiscale Dynamics in Animal Morphogenesis) group, NED Unit, Institut Fessard, CNRS, F-91198 Gif-sur-Yvette, France. ³INRA, USC1126, F-91198 Gif-sur-Yvette, France. ⁴Institut Pasteur, Macrophages and Development of Immunity, Institut Pasteur, F-75015 Paris, France. ⁵CNRS, URA2578, F-75015 Paris, France. ⁶Université Paris-Sud, F-91400 Orsay, France.

*These authors contributed equally to this work

‡These authors contributed equally to this work

§Authors for correspondence (peyrieras@inaf.cnrs-gif.fr; joly@inaf.cnrs-gif.fr)

Received 14 May 2013; Accepted 25 September 2013

changes without further major morphogenetic movements (period 2). We showed that PML progenitors proliferate slowly by symmetric division. We determined that cells in the PML are slow-amplifying progenitors (SAPs) and turn into fast-amplifying progenitors (FAPs) as they enter into the OT.

Screening expression patterns in the PML allowed us to identify key features of genetic networks that are expressed differentially in progenitors: a network expressed in all proliferating cells (SAP+FAP) and another specific to SAPs. This latter network includes genes involved in ribosome biogenesis and DNA synthesis. We carried out a functional study of the *perplexed* mutant line, which lacks a functional *cad* gene. Our results showed that *cad*, which is strongly expressed only in SAPs, is required more generally for coordinating the cell proliferation and survival of midbrain cells. Therefore, our work leads to the hypothesis that a subset of the ribosome and nucleotide biosynthesis genes, which do not exhibit ubiquitous expression but instead are specific to midbrain SAPs, have a crucial role in proliferating cells during development.

RESULTS

PML morphogenesis occurs in two steps

A histological analysis was carried out on zebrafish embryos from 24 hours post-fertilisation (hpf) to 7 days post-fertilisation (dpf) to study PML morphogenesis. Parasagittal section observations showed that PML can be unambiguously identified in prim-5 stage embryos (24 hpf; end of somitogenesis) (Fig. 1A). At this stage the PML is thick and appears as typical pseudo-stratified neuroepithelium. At 48 hpf (long-pec stage), the PML is a semi-circular layer of cells connecting the OT to more ventral structures originating from the alar neural plate (known as the TS) (Fig. 1C).

There is a similar lateral structure connecting the OT to the TS as seen in transverse sections (not shown). On sagittal sections close to the sagittal plane (Fig. 1D), the medial PML connects the tectum with the medial isthmus proliferation zone, which is itself connected to the cerebellum proliferation zone (CPZ).

The formation of the PML can be divided into two steps: before 48 hpf, the PML undergoes formation as the brain exhibits major morphological changes (period 1); after 48 hpf, the PML structure continues to elongate while the brain grows and the TS and OT become more distant; in addition, PML cells exhibit cytological changes (period 2).

Morphological changes were examined by live imaging of zebrafish embryos expressing nuclear Venus fluorescent protein. Imaging of transverse sections at 26 hpf (during period 1) revealed that, as the tegmentum grows, the TS invaginates and spreads medialwards over the tegmentum from both sides of the embryo (Fig. 1E,F; supplementary material Movie 1). At later stages, proliferation becomes confined to the intermediate zone between the OT and the TS. This lateral proliferation zone becomes marked by slightly more intense staining of the nuclei in the transgenic line. It gradually extends during development and forms the PML between the OT and TS.

We observed no major morphogenetic movements after 48 hpf (period 2); the PML is established and its growth is thereafter coordinated with that of the brain. PML cells undergo prominent cytological changes from a neuroepithelial type (see below) to form a monolayer pavement epithelium. By 7 dpf, these cells are found to be tightly apposed to the posterior side of the OT (Fig. 1A). At this stage, the lateral recesses of the mesencephalic ventricle (located between the tectum and the PML) become invisible (Fig. 1A).

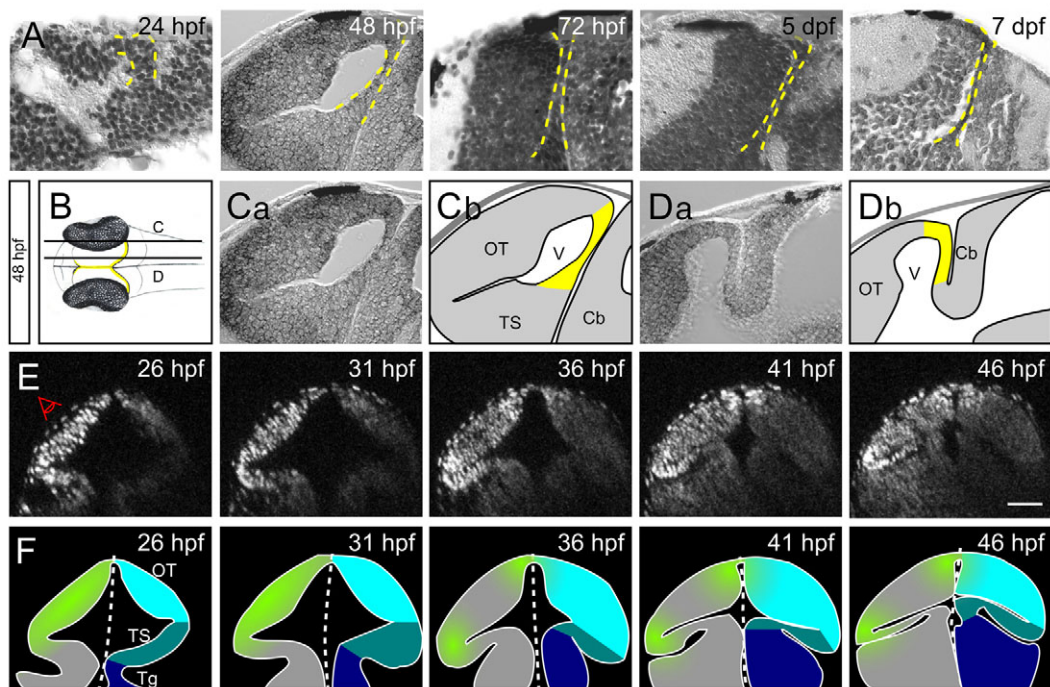


Fig. 1. PML morphogenesis in zebrafish from 1 to 7 dpf. (A) Parasagittal sections of zebrafish from 24 hpf to 7 dpf. As development proceeds, the PML (delineated by a yellow dashed line) becomes thinner and tightly apposed to the OT. (B) Schematic dorsal view of an embryo at 48 hpf. Planes of the sagittal sections in C (more lateral) and D (more medial) are indicated. The PML is found at the margin of the OT (yellow). (C) On lateral sections, the PML connects the OT to the TS. (D) On medial sections, the PML connects the OT to the cerebellum. (E,F) Embryo imaged from its left side (E) and corresponding interpretive schematics (F). Reconstructed midbrain transverse sections were taken at 5-hour intervals. Proliferation (green) becomes restricted to an area between the OT (light blue) and the TS (mid-blue). The tegmentum is in dark blue. Cb, cerebellum; OT, optic tectum; Tg, tegmentum; TS, torus semicircularis; V, ventricle. Scale bar: 50 μ m.

PML cells are large polarised neuroepithelial cells that divide in the planar plane

We examined the localisation of two apical markers in PML cells. At 48 hpf, we found that atypical protein kinase C (aPKC ζ) and Zona occludens protein 1 (ZO-1), which are markers of adherens and tight junctions, respectively, are expressed on the ventricular side (Fig. 2A). We observed that cells of the PML are polarised and have larger nucleoli (Fig. 2B) than those observed in the OT. The chromatin in PML cells appeared decondensed compared with that in OT cells, as shown by electron microscopy (Fig. 2C). Moreover, PML cells exhibited larger and more elongated nuclei, as observed in live imaging (Fig. 2D).

During mitosis, PML cell nuclei transiently swell (Fig. 2E; yellow cells in supplementary material Movie 2) and migrate to the apical side of the layer to divide [interkinetic nuclear migrations (supplementary material Movie 3) (Baye and Link, 2007)]. This is further evidence of the neuroepithelial nature of the PML, as this movement typically occurs during neuroepithelial-like neurogenesis (Götz and Huttnner, 2005). We found that most divisions of PML progenitors are within the plane of the neuroepithelium. Most of the observed mitotic events (94.3%) are planar and only a few (5.7%) are apical-basal (Fig. 2F; supplementary material Movie 2, yellow cells divide in a planar fashion). The mitotic plates rotate and then stabilise in orientation shortly before mitosis to achieve planar divisions (supplementary material Fig. S1); this has been described previously in neuroepithelial cells at earlier stages (Herbomel, 1999; Geldmacher-Voss et al., 2003).

PML cells are SAPs and give rise to FAPs of the OT

To directly examine PML and OT cell cycle lengths, we produced TPLSM 3D+time live imaging datasets of nuclear-labelled transgenic zebrafish (supplementary material Fig. S2). Eight PML nuclei were selected at 30 hpf, digitally tagged with Mov-IT software, and individually tracked (Fig. 3A-C; supplementary material Movie 4). After each mitosis, both daughter cells were followed, resulting in a 15-hour lineage analysis with high spatial and temporal accuracy. We measured an average cell cycle length of $5:51 \pm 1:49$ hours ($n=25$) in the PML and a much shorter interval between two mitoses of $1:35 \pm 1:22$ hours ($n=13$) in the OT (Fig. 3G). This shows that, from 30 hpf to 45 hpf, SAPs are located in the PML, whereas FAPs are in the OT. From this lineage analysis we observed that PML cells initially remain in the PML where they divide approximately twice during the whole imaging session (i.e. from 30 hpf to 45 hpf; Fig. 3; an explicit example is given in Fig. 3D-F and in supplementary material Movie 5). Daughter cells are then located around the midbrain ventricle, and at the end of the movie (45 hpf) are seen in the OT (Fig. 3; supplementary material Movies 4, 5). All trajectories are parallel and in the horizontal plane; most of the progeny of any single PML cell remain confined into a small volume in the tectum, such that clonal dispersion is low.

We observed that the progeny of three PML clones contributed to both the OT and the TS [Fig. 3, red (see also supplementary material Movie 6), orange and dark yellow clones].

The PML displays a specific gene expression profile that is shared with the retina CMZ

We looked for potential genetic signatures in PML cells by data mining the ZFIN gene expression database (www.zfin.org/). To distinguish specifically expressed PML genes from those that are more widely expressed in the midbrain (Fig. 4A) we applied several criteria. At the early prim-15 to prim-25 stages (when most tectal cells are still proliferating), expression of a ‘thinly’ expressed gene

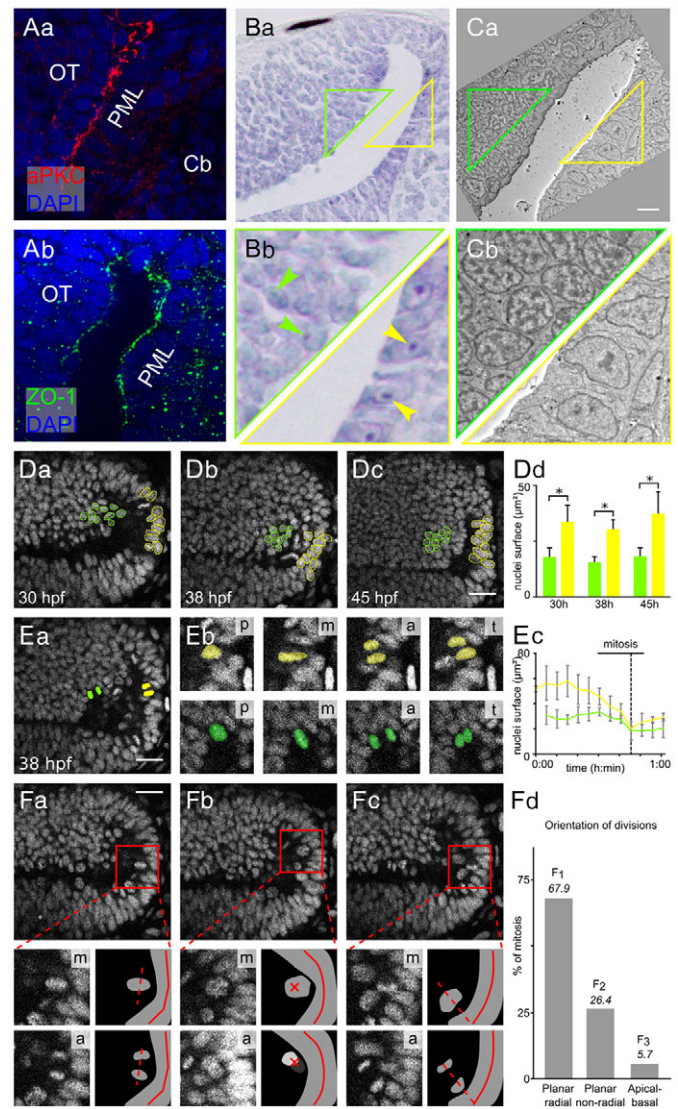


Fig. 2. The PML is a neuroepithelial proliferation zone. (A) Sagittal sections at 48 hpf showing the expression of apical markers in PML cells: aPKC (a) and ZO-1 (b). Nuclei are stained with DAPI. (B) Nissl staining of sagittal sections showing that PML cells (yellow triangle) have larger nuclei with bigger nucleoli than OT cells (green triangle). Arrowheads indicate nucleoli. (C) Electron microscopy image of a sagittal section at 48 hpf showing that PML cells (yellow triangle) have decondensed chromatin, whereas chromatin in OT cells (green triangle) is condensed. (D) Sagittal optical sections of the OT from a *Tg(Xla.Eef1a1:H2B-Venus)* embryo. Interphase nuclei in the PML (yellow) are larger than at the margin of the OT (green). At all stages, the surface areas of the PML and the OT nuclei are significantly different (Mann-Whitney U-test, $*P < 0.001$); error bars indicate s.d. (E) Average PML and OT nucleus size for ten mitoses. (a) Location of tracked nuclei (as detailed in b). p, prophase/prometaphase; m, metaphase; a, anaphase; t, telophase/cytokinesis. (c) M phase is indicated by a dotted line. OT, green; PML, yellow. (F) Mitosis orientations. (a) Planar radial division [30:56 (hours:minutes) hpf]. (b) Planar non-radial division (30:52 hpf). (c) Apicobasal division (31:13 hpf). (Bottom panels) Enlarged metaphase plate (labelled m), subsequent anaphase (labelled a) and corresponding interpretive diagrams. For planar non-radial divisions (b), the two daughter cells are not in the same plane. The anaphase image is the sum of the images centred on the two daughter cells. The red cross indicates the axes of the planar non-radial mitoses. Of 53 mitoses, 36 are planar radial, 14 are planar non-radial and 3 are apicobasal. (d) Non-random predominantly planar radial mitoses according to χ^2 test ($P < 0.001$). Cb, cerebellum; OT, optic tectum; PML, peripheral midbrain layer. Scale bars: 20 μ m.

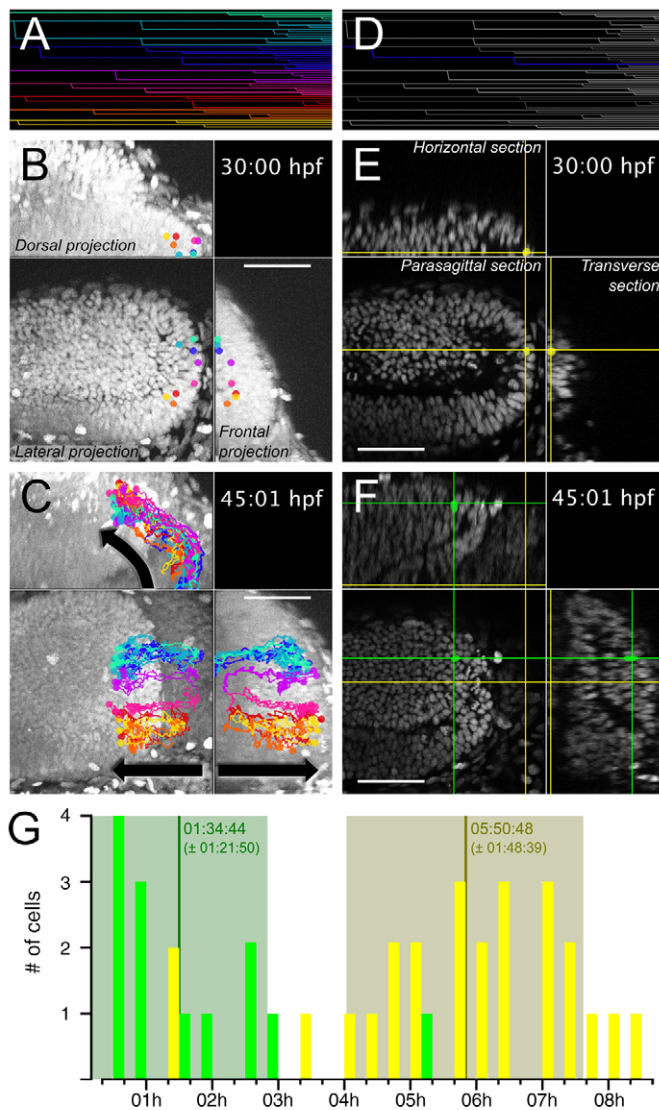


Fig. 3. Slow-amplifying PML cells give rise to tectal FAPs. PML cells were tracked from 30:00 hpf to 45:01 hpf. The complete lineage tree is shown in A. Cells originating from the PML at 30 hpf are found in the external part of the OT 15 hours later (B,C). In B and C, eight clonal cell trajectories, as indicated with different colours, have been overlaid on a volume projection of the left midbrain. The dots indicate the position of the cells at 30 hpf (B) and 45:01 hpf (C) and the lines trace the past trajectory of each clone. For the full movie, see supplementary material Movie 4. (D-F) A clone (represented by the intersection of the cross at the corresponding sagittal, horizontal and transverse planes) is followed from the PML, where it achieved two mitoses (E), to the OT, where two further mitoses occurred (F). For the full movie, see supplementary material Movie 5. (G) Cell cycle durations are separated into two clusters: OT (green) FAP cycles, $1:35 \pm 1:22$ hours ($n=13$); PML (yellow) SAP cycles, $5:51 \pm 1:49$ hours ($n=25$). Scale bars: 50 μ m.

had to be restricted to the peripheral part of the midbrain and not be ubiquitously expressed throughout the whole proliferating midbrain (in the way that proliferation-associated markers are at that stage). At later stages (high-pec to long-pec) the midbrain expression domain had to be thin and restricted to the PML in Nomarski images. Since a striking synexpression in tectum and retina was observed (see below), we also used another criterion: the identification of a ring of retina cells tightly surrounding the lens. More widely expressed genes, associated with all progenitors, are expressed in a wider ring corresponding to proliferative cells of the

CMZ (supplementary material Fig. S3). We found 117 genes associated with proliferation (supplementary material Fig. S3, Table S1). Of these, 68 genes are expressed in a relatively large region of the peripheral OT and of the CMZ, whereas 49 display a very thin expression pattern located at the most peripheral part of the OT and in the most central part of the CMZ (supplementary material Fig. S3). We also added a further two genes to this second category: *ect2* and *nop56* (*nol5a*) (supplementary material Table S1). These were identified from a previous *in situ* hybridisation screening performed on medaka (data not shown) and their specific expression was also confirmed in zebrafish (Fig. 4Ae,f,Cb,c). ZFIN data mining results are presented in supplementary material Fig. S3.

We carried out whole-mount *in situ* hybridisation (WMISH) and histological analysis on a subset of proliferation-associated genes to confirm the data mining results. We identified a group of genes, which included *pcna*, with expression that encompasses both FAPs and SAPs (Fig. 4Aa-c). Other genes, such as *nop56*, display a tight expression pattern that is restricted to PML SAPs (Fig. 4Ad-f). We carefully checked that these PML-associated patterns correlate with expression in SAPs. We found that transcripts of the *pes* gene specifically localise in neuroepithelial cells with large oval nuclei – cells that we called SAPs (Fig. 4B). We also performed WMISH for four genes (*cad*, *ect2*, *nop56* and *pes*; see Fig. 4C) with a very long incubation time (several days) in the staining solution to demonstrate that PML gene expression patterns are really restricted to SAPs.

Two main gene categories are overrepresented in the PML-specific dataset

To define groups of genes with similar functions, we performed several *in silico* analyses. Gene Ontology (GO) term analyses show that, in both of our lists, genes regulating specific cellular functions are overrepresented (Fig. 5; supplementary material Fig. S4). Most genes associated with the proliferation zones of the OT and the PML encode components of the nucleus linked to the global proliferation machinery, more specifically to the machinery regulating cell cycle phases or DNA replication (supplementary material Fig. S4). By contrast, the PML dataset contains mainly genes encoding either nuclear proteins that are active in nucleotide synthesis or nucleolar proteins (Fig. 5A,B). An interaction network analysis using Ingenuity software identified several clusters of PML-specific genes (Fig. 5C), one of which corresponds to a subset of genes encoding proteins involved in rRNA processing (such as *nop56*, *nop58*, *fibrillar*, *pes*, *wdr12* and *nle1*) (Fig. 5C; supplementary material Table S1).

Interestingly, gene networks already identified by a functional RNAi screen as crucial for *Drosophila* neuroblasts are very similar to the PML progenitor-specific networks (supplementary material Fig. S4) (Neumüller et al., 2011). To test the relevance of our dataset with other SC sets, we compared the identified genes with previously assembled mammalian datasets by searching the Molecular Signature Database MSigDB (v3.0) (Subramanian et al., 2005). Our set of PML-specific genes is enriched for genes that are represented in different cancer-associated gene sets (supplementary material Table S2) and, more importantly, in the PluriNet network (Müller et al., 2008) related to human pluripotent stem cells. This study (Müller et al., 2008) indicates that pluripotent cells exhibit a small number of generic molecular signatures, the functions of which are often linked to the maintenance of pluripotency.

The proliferation and survival of tectal progenitors are affected in the *perplexed* mutant

Many genes considered as housekeeping genes exhibit preferential expression in the PML. To test whether these genes play specific

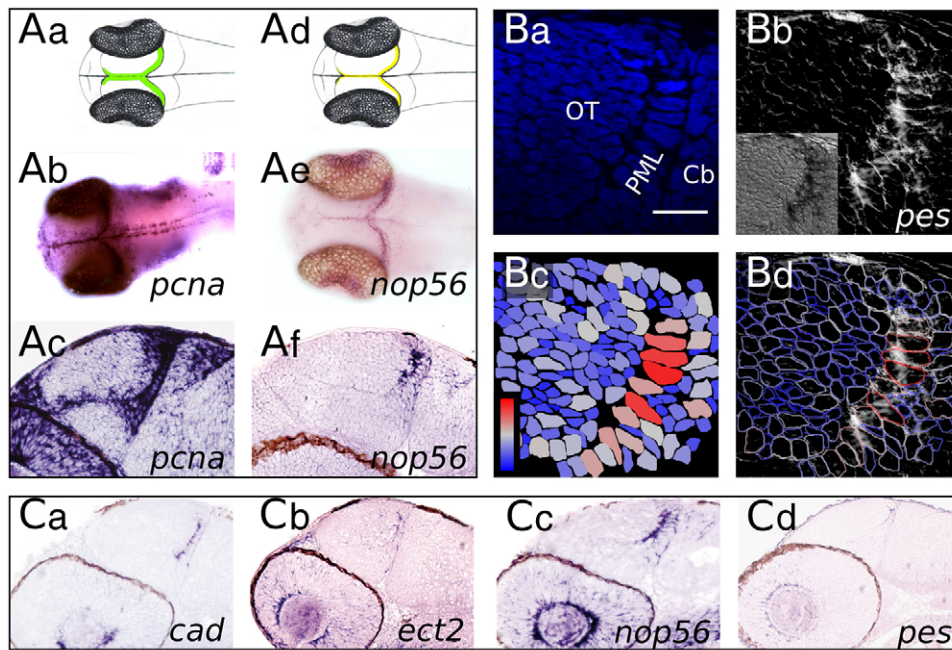


Fig. 4. Transcript distribution in the midbrain: 'large' and 'thin' domains. (A) Whole-mount embryos (b,e) and parasagittal sections (c,f) following *in situ* hybridisation (ISH) with *pcna* (b,c) and *nop56* (e,f) probes. *pcna* is expressed in a 'large' domain containing all proliferating cells. The *nop56* expression domain is 'thin' and restricted to PML SAPs. (B) The *pes* ISH signal colocalises with PML cells (the largest midbrain cells). (a) Nuclear DAPI staining. (b) Inverted colour brightfield image of the same field showing the *pes* ISH signal. Inset shows the real colour brightfield image. (c) Colour-coded nuclei surface. On the blue-red scale, red corresponds to 22 μm^2 and dark blue to 0 μm^2 . (d) Overlay of the inverted brightfield image with the nuclei border colour-coded drawing. Red nuclei exhibit a strong *pes* ISH signal. (C) Sagittal sections of embryos at 2 dpf. ISH long staining time emphasizes PML-specific gene expression. Scale bar: 10 μm .

roles in PML progenitors, we performed an analysis of the *perplexed* mutant, which lacks a functional *cad* (*carbamoyl-phosphate synthetase 2, aspartate transcarbamylase, and dihydroorotase*) gene, which encodes three enzymes involved in *de novo* pyrimidine biosynthesis (Willer et al., 2005). At 48 hpf, we observed that the PML and OT remain recognisable in *perplexed* mutants but their morphologies are strongly affected. The PML appears thicker than in wild-type embryos (Fig. 6A,B). Throughout the midbrain region, the density of cells is low and there are numerous acellular holes. We imaged midbrains of *perplexed* mutants by TPLSM, but apoptosis rates were so high that we were not able to track cells for an entire cell cycle (data not shown). Massive cell death was detected in mutant OT after TUNEL staining (Fig. 6C,D). We monitored proliferation levels by phospho-histone H3 (pH3) immunostaining at 48 hpf. M-phase cells are present in the proliferative areas (FAP areas) of the tectum and of the TS in *perplexed* mutants (Fig. 6E,F). However, more M-phase cells are visible in the central part of the OT in mutants than in wild types. This was confirmed by PcnA immunostaining at later stages (72 and 96 hpf), when proliferation zones become narrower. In wild type, PcnA expression is restricted to the margin of the OT (FAPs) and PML (SAPs), whereas in *perplexed* mutants PcnA-positive cells are found throughout the whole OT and cerebellum (Fig. 6G-J).

DISCUSSION

The PML is formed of neuroepithelial SAPs that give rise to both OT and TS

We have shown in this study that PML cells exhibit the prototypical features of neuroepithelial progenitors. Located in the largest structure of the fish brain (the OT), PML cells are particularly suitable for studies of the functional and structural characteristics of NPs. We provide an extended description of PML progenitors and highlight how the teleost PML can be used as a model for the characterisation of molecular pathways acting in neuroepithelial SAPs.

The large majority of cell divisions occurring in the PML are planar divisions, although we observed a few apicobasal divisions. In the zebrafish telencephalon, radial glial cells predominantly undergo

symmetric gliogenic divisions, which amplify the NSC pool (Rothenaigner et al., 2011). The reason why fish seem to preferentially use this growth mode remains unknown, but it has been shown that a planar orientation of mitoses in neuroepithelia is required for the maintenance of layered structures (Peyre et al., 2011).

We demonstrated that the cell cycle takes about four times longer in the PML than in the OT. To understand the biology of these SAPs, it will be important to identify the factors that induce this relative quiescence in PML cells (see below).

Cells exhibit a major cytological transition when they enter the tectum: from a neuroepithelial phenotype, establishing contacts with the ventricle (apically) and with the pial/basal membrane, to small round cells that sometimes lack contacts with either the pial/basal membrane or the ventricle (data not shown). This transition is apparently correlated with a substantial shift in proliferation rates. It will be interesting to study the factors, positions or cell contacts that trigger this major phenotypic transition. Several well-known signalling molecules are known to induce a fast proliferation mode. For example, sonic hedgehog (Shh) may have a prominent role in the acceleration of cell divisions, as it does in the retina (Locker et al., 2006). The control of progenitor proliferation in the tectum has been shown to be substantially affected in several mutants of the hedgehog pathway (Koudijs et al., 2005).

Our results confirm on live specimens that the OT is a typical cellular conveyor belt (Devès and Bourrat, 2012); it has zones of unmixed FAPs and SAPs at its periphery, a zone of cells exiting the cycle and a central zone of differentiating cells (Cervený et al., 2012) (Fig. 7). Our data show centripetal movements of the progenitors when they enter the tectum. However, we believe that these movements are not due to active migration but rather to passive displacements resulting from intensive cell division. It would be interesting to analyse more globally the major directions of cell displacements that shape the OT, PML and TS (using automated cell tracking and visualisation of kinematic descriptor maps).

None of the tracked cells remains in the PML to replenish the SAPs. One hypothesis is that the bona fide SCs of the PML are localised more medially in the isthmic proliferation zone and

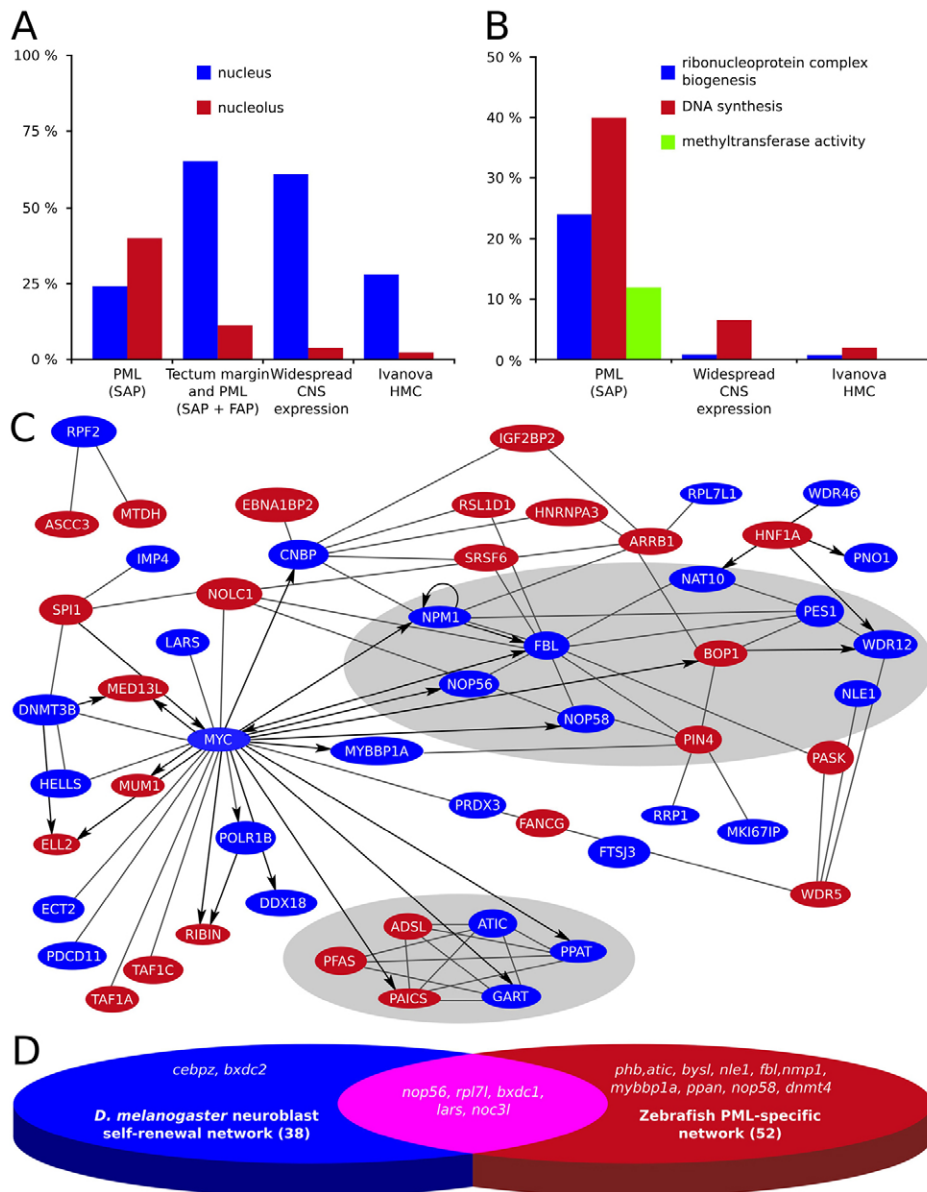


Fig. 5. The PML gene network contains genes encoding nucleotide biosynthesis enzymes, nucleolar components and ribosomal proteins. (A,B) Gene ontology (GO) enrichment analysis of the PML-specific gene list, using the CNS and Ivanova hematopoiesis mature cells (HMC) gene lists as backgrounds. (A) Cellular localisation: genes encoding nucleolar proteins are overrepresented in the PML dataset. (B) Cellular function: in the PML dataset, genes involved in ribosome biogenesis and nucleotide synthesis are overrepresented. (C) Ingenuity pathway analysis of the main gene network for the PML dataset. Two distinct molecular clusters are outlined (grey): nuclear proteins mainly involve purine biosynthesis, and nucleolar proteins involve rRNA and ribosomal processing. PML genes are in blue and genes not included in our study are in red. Arrows starting from *myc* indicate direct Myc target genes or partners. (D) Overlap between fish and *Drosophila* NSC lists.

correspond to the *her5*-positive population described by Chapouton et al. (Chapouton et al., 2006).

We found that the PML contains a subset of progenitors that gives rise to both the OT and TS. It is striking that a single progenitor is able to generate cells belonging to two distinct brain structures. This unusual and unexpected dual contribution seems to be dependent on the location of the tracked progenitor in the PML with respect to the dorsoventral axis. This feature was already proposed by Grandel et al. (Grandel et al., 2006), who noted that the TS has no specific zone of progenitors. However, their study was performed on adults and did not provide any evidence for the location of early TS progenitors. In the mouse embryo, some progenitors have the capacity to populate more than one neural structure; for example, the diencephalon and telencephalon (Mathis and Nicolas, 2006).

PML cells express genes active in stem cells and tumour cells

Pluripotent embryonic SCs have the widest possible capability for gene transcription. As they become more specialised, they refine their transcriptional repertoire (Efroni et al., 2008). In our model of

pluripotent neural cells (the SAP/PML cells), we identified different groups of genes as described below according to the function they fulfil.

One PML cell-specific group contains genes known to play major functions in SCs and tumour cells, where they either contribute to the regulation of DNA methylation (*dnmt4* and *hells*) (Law and Jacobsen, 2010) or inhibit cell apoptosis (*ppan*) (Bugner et al., 2011).

PML cells also express *bystin* transcripts that have been reported to be expressed in type B SCs and in lesioned rat cerebral cortex (Sheng et al., 2004).

Prohibitin (Phb), which is often associated with cancer, is an inhibitor of cell proliferation (Mishra et al., 2006) that could potentially trigger the slowing of progenitor cell divisions. Indeed, genes known to promote definitive cell cycle exit in the differentiating cells of the OT [such as cyclin-dependant kinase inhibitors, *gadd45* or *insm1* (Candal et al., 2004; Candal et al., 2007)] were found not to be expressed in PML progenitors (data not shown). This suggests that the mechanisms inducing quiescence in SCs are distinct from those promoting cell cycle exit during terminal differentiation.

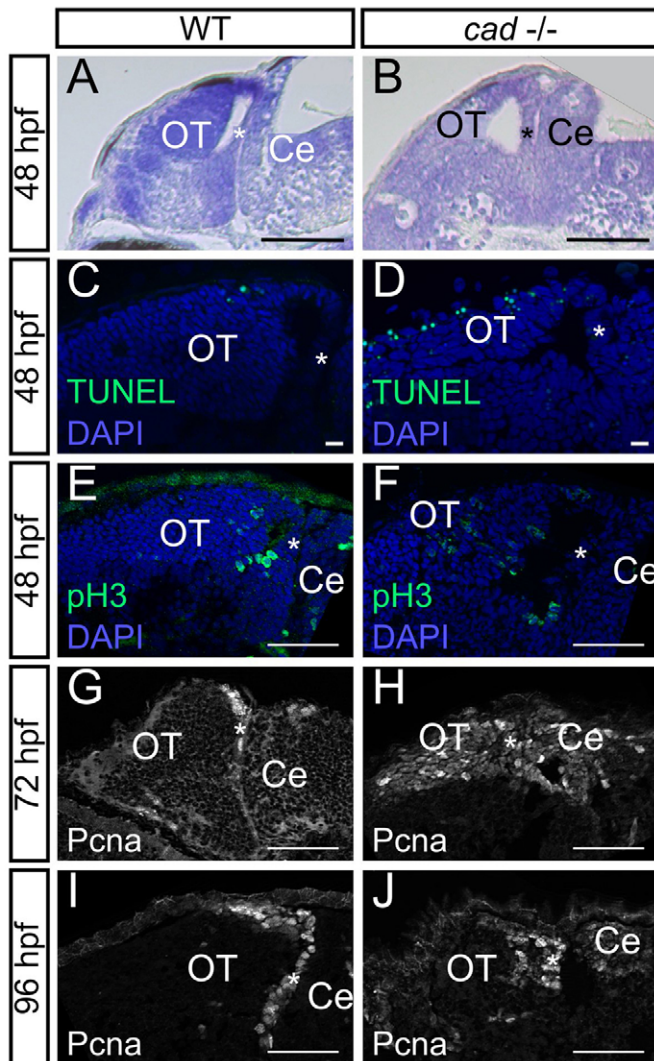


Fig. 6. Absence of *cad* function in homozygous mutant embryos leads to proliferation defects and massive cell death in the midbrain. (A,B) Sagittal sections of wild-type (A) and *perplexed* (B) embryos with Nissl staining at 48 hpf. *perplexed* mutant displays atrophy of the tectum and PML thickening. (C,D) Sagittal sections following TUNEL staining at 48 hpf. More apoptotic cells are observed in *cad*^{-/-} (D) than in wild-type (C) embryos. (E,F) Phospho-histone H3 labelling at 48 hpf showing the presence of proliferative cells not only in the periphery of the tectum but also in the central part in *perplexed* mutants. (G-J) PcnA immunostaining at 72 and 96 hpf showing persistence of wide proliferation zones in the OT of *perplexed* mutants at late larva stages. Anterior is at the left and dorsal at the top of each image. OT, optic tectum, Ce, cerebellum. The asterisk indicates the PML. Scale bars: 100 μ m in A,B; 10 μ m in C,D; 20 μ m in G; 50 μ m in E,F,H-J.

Among the PML cell-specific gene network we identified *c-myc* (*myca* in zebrafish), which is known to be a master regulator of normal cell growth and proliferation (Liu et al., 2008) (Fig. 5D; supplementary material Fig. S3Y2,4) and could play a specific role in SAPs. In *Xenopus*, *c-myc*⁺/*n-myc*⁻ cells were shown to be candidates for a restricted population of retinal SCs found in a subdomain at the tip of the CMZ (Xue and Harris, 2011). Transcripts of several Myc targets are also restricted to the PML (see below; Fig. 5). The gene *mybbp1a* is located at a key node of the established PML network. This gene has been shown to activate *p53* when ribosome biogenesis is suppressed (Tsuchiya et al., 2011) and Mybbp1a might be part of a nucleolar pool of proteins involved in mitotic progression (Perrera et

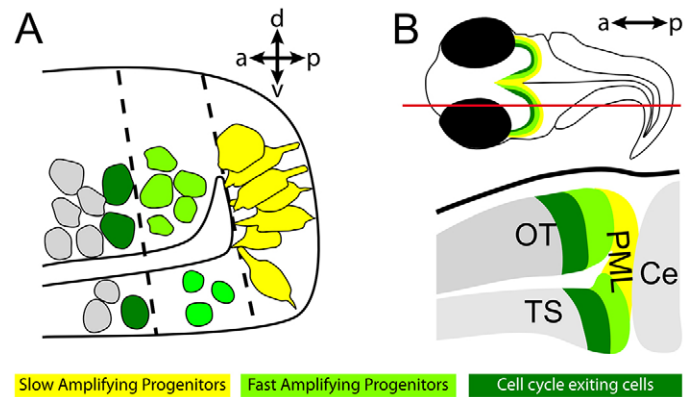


Fig. 7. The PML contributes to the formation of the OT and of the TS. (A) At the periphery of the OT, there are two types of neural progenitors. PML cells (yellow) are SAPs and have big nuclei and contact both apical and basal with membrane extensions. They turn into SAPs (light green) with smaller nuclei when they enter the OT or the TS, then they exit the cell cycle (dark green) and differentiate. (B) Top panel: the previously described differentiation gradient forms a concentric gradation when viewed in horizontal section and correlates with observed gene expression patterns. Red line indicates the parasagittal section shown in the bottom panel. OT, optic tectum; TS, torus semicircularis; Ce, cerebellum; PML, peripheral midbrain layer.

al., 2010). Further studies are needed to clarify the role of Mybbp1a in NSCs and SAPs by focusing on the interplay between its nucleolar and cell cycle-associated functions.

Other genes found to be specifically expressed in the PML encode nucleotide biosynthesis enzymes, nucleolar components and ribosomal proteins.

A large PML-specific gene network encodes nucleolar proteins

Genes encoding nucleolar proteins are present in the PML network. Cancer studies have proposed putative instructive roles for nucleolar proteins in tumorigenesis, highlighting their potential role in the control of cell proliferation (reviewed by Ruggero and Pandolfi, 2003). PML nucleolar genes encode proteins belonging to two main complexes. Nop56, Nop58 and Fibrillarin are small nucleolar ribonucleoproteins (SnoRNPs) that are associated in a complex involved in the processing and modification of rRNA. Transcripts encoding Nop56/58 are signatures of fish PML progenitors (this study), but also of the fish (Fig. 5) and *Xenopus* (Parain et al., 2011) retina. The Wdr12, Pes and Bop1 proteins are associated with PeBoW, a complex crucial for the maturation of the large ribosomal subunits in mammalian cells (Hölzel et al., 2005). *pes* was first identified in zebrafish for promoting proliferation in the CNS (Allende et al., 1996). *nle1* and *wdr12* are involved in the biogenesis of ribosomal pre-60S particles. Interestingly, *nle1* is also required for the maintenance of adult hematopoietic stem cells (HSCs) in mice, as shown by conditional knockouts (Le Boutellier et al., 2013).

The expression of genes coding for ribosomal protein is crucial in SCs and SAPs

Ribosomal genes are thought to be ubiquitously expressed and to have strong and early deleterious effects. It is therefore surprising to observe that PML genes encoding ribosomal proteins have restricted transcription patterns and that some have a mild mutant phenotype. For example, zebrafish *rpl71l* is specifically expressed in PML and CMZ progenitors (supplementary material Fig. S4) and the *rpl71l* mutant apparently has a mild phenotype (source: ZIRC). By contrast,

its paralogue *rpl7* has been demonstrated to be strongly and ubiquitously expressed (Bradford et al., 2011). A similar situation might occur in *Drosophila*, where *RpL7* has been shown to be specifically required in neuroblasts to maintain their proliferation (Neumüller et al., 2011), whereas its counterpart (*RpL7-like*) displays ubiquitous expression. Another zebrafish study shows that *rpl22l1* and *rpl22* play essential, distinct and antagonistic roles in HSCs (Zhang et al., 2013). Since protein synthesis does not seem to be affected in mutants, these two genes might have some extra-ribosomal functions in the regulation of HSCs. Proteins regulating ribosome synthesis seem to be essential for germline stem cell (GSC) maintenance and function in the gonads of *Drosophila* (Fichelson et al., 2009). The accumulation of specific ribosomal proteins in PML cells creates a signature that distinguishes SAPs from FAPs and other cells of the OT. Recent discoveries of ribosome codes in yeast (Komili et al., 2007) and vertebrates (Kondrashov et al., 2011) highlight the importance of such gene expression signatures.

A PML gene network encodes nucleotide biosynthesis enzymes

One PML cluster contains genes involved in pathways of purine synthesis (such as *gart*, *ppat*, *atic*), pyrimidine biosynthesis [such as *cad* (see also below) and *ctps1a*] and nucleotide metabolism (such as *shmt2*, which has been shown to be regulated by *myc*) (Fig. 5; supplementary material Table S1). It is surprising that transcripts encoding nucleotide biosynthesis proteins accumulate only in SAPs and not in all proliferating cells. In cell culture, *cad* activity is strongly upregulated when cells enter the proliferative phase, and then dramatically downregulated as the culture becomes confluent (Sigoillot et al., 2002).

Are PML cells storage chambers?

We chose to analyse the *perplexed* mutant, which lacks a functional *cad* gene, because a previous study carried out in the retina had already highlighted the importance of this gene for NP proliferation and differentiation (Willer et al., 2005). *perplexed* mutants exhibit no lamination of the retina (Link et al., 2001; Willer et al., 2005). Similarly, we observed that they lack a laminated tectum. The presence of a large number of PcnA-positive cells all over the OT indicates that the cell cycle is dysregulated in midbrain progenitors. In time-lapse analysis, cell cycle intervals could not be precisely measured owing to massive apoptosis in mutant OT. Hence, our hypothesis is that, in *perplexed* mutants, because of the absence of *de novo* nucleoside synthesis, tectal cells, as with retinal cells (Willer et al., 2005), do not undergo proper mitoses and remain blocked in M phase and eventually undergo apoptosis. Indeed, in the eye it has been shown that retinoblasts with the *perplexed* mutation require twice as long to complete one cell cycle (Willer et al., 2005). It is known that the *de novo* pathway of pyrimidine synthesis is most active during growth and development, after which the salvage pathway predominates (Anderson and Parkinson, 1997). Since metabolic intermediates along this pathway do not accumulate, the level of uridine monophosphate (UMP) production relies on Cad activity. Thus, we propose that neuroepithelial cells accumulate high levels of Cad enzymes so that OT FAPs can subsequently perform their rapid divisions without *de novo* synthesis of nucleotides. More generally, the accumulation of machineries composed of many different nucleolar/ribosomal proteins or nuclear proteins might point to key roles for these proteins in the biology of these slowly dividing cells, which have high transcriptional and translational activity (Efroni et al., 2008). We speculate that PML cells, which are poised for subsequent rapid divisions, serve as ‘storage chambers’

and thus allow the FAPs to bypass *de novo* synthesis during their intense proliferative activity. This would be similar to the early development strategy whereby maternal components are stored in the huge pluripotent egg cell in readiness for subsequent rapid divisions of the blastomeres.

PML genes are also expressed in the CMZ: evidence of deep homology?

Other PML genes could also have a prominent function in the fish midbrain and eye. Cytological and molecular signatures may help to define cell type homologies from an ‘evo-devo’ perspective (Arendt, 2005). Synexpression of genes in retinal CMZ cells and midbrain progenitors has been noted (Cervený et al., 2012; Ramialison et al., 2012) and the phenotypes of mutants for at least 18 PML-specific genes are illustrated on the ZIRC website (supplementary material Table S3). These mutants share strikingly similar neuroectodermal and ocular defects. Heads and eyes appear smaller and necrosis is often reported in the CNS. Further analyses of these mutants are needed to confirm whether these PML genes affect the midbrain neuroepithelial progenitors, in the way that *cad* does.

At early stages of development, more than one-third of the PML-specific genes (according to the ZFIN database) are expressed in the anterior brain region located between the zona limitans intrathalamica and the MHB. This area is proposed to have derived from that of an ancient bilaterian ancestor (Steinmetz et al., 2011). From an initial situation in urbilateria in which rows of lateral (so-called intermediate) progenitors would have participated in both alar forebrain and midbrain morphogenesis, extent vertebrates now evaginate optic cups and their progenitor zone, called the CMZ, whereas the midbrain progenitors in the PML invaginate as revealed in this study. We therefore suggest that retina and midbrain progenitors might be ‘sister’ cell types with a common evolutionary origin.

Conclusions

We have characterised a population of neuroepithelial midbrain progenitors in zebrafish embryos. Their specific features (long cell cycles, distinctive genetic signatures) emphasize the diversity of NPs in vertebrates. Our work highlights that the PML provides a very useful model with which to study NPs and NSCs. Indeed, we propose that these progenitors have specific metabolic activities and use specific ribosome biogenesis pathways. Future studies should also reinforce interest in this cell type by stressing its role in regenerative processes or in modified nutritional contexts.

MATERIALS AND METHODS

Fish

Zebrafish (*Danio rerio*) wild-type strains (AB and TU) and *perplexed* mutants (*cad^{u52}*) (ZIRC, Eugene, OR, USA) were reared and staged as previously described (Kimmel et al., 1995). For wild-type live imaging, we used a transgenic fish line *Tg(Xla.Eef1a1:H2B-Venus)* to track nuclei. Additionally, we used a double-transgenic fish line resulting from a cross between *Tg(Xla.Eef1a1:H2B-mCherry)* (gift from Georges Lutfalla, Université Montpellier 2, Montpellier, France) and *Tg(Xla.Eef1a1:EGFP-Hsa.HRAS)*.

Two-photon live imaging

To avoid pigmentation zebrafish embryos were treated with 1-phenyl 2-thiourea (0.003%; Sigma), anaesthetised with tricaine (170 µg/ml; Sigma), dechorionated, mounted in 1% standard agarose moulds and covered with 0.5% low melting point agarose. Embryos were imaged laterally and imaging field was focused on the left midbrain. Non-invasiveness was assessed by comparing mitosis between TPLSM and Nomarski imaging (supplementary material Fig. S1). Live imaging was performed using

custom-made two-photon microscopes (BioEmergences). The set-ups are based on a DM6000 and a DM5000 upright microscope (Leica) with 980 nm (Mai Tai, Spectra-Physics/Newport Corporation) and 1030 nm (t-Pulse, Amplitude Systems) excitation wavelengths. Other settings/parameters: objectives, Leica 1.0 NA 20× W (HCX APO) or Olympus 0.95 NA 20× W (XLUMPlanFluo); filters, 525/50 nm (Venus and EGFP), 610/75 nm or 595/45 nm (mCherry); scan speed, 700 Hz; frame average, 3; 512×512 pixels at 0.3 or 0.4 μm wide; a full z-stack was compiled in ~5 minutes. To check that imaging was not deleterious, larvae were allowed to recover in tricaine-free embryo medium until able to feed.

3D+time image analysis

After acquisition, raw images were converted into VTK format and processed with Fiji for rendering and other analysis. We also used the Mov-IT software developed by BioEmergences (Olivier et al., 2010), which enables smooth navigation in orthoslices or in volume rendering acquired at different times, fate map visualisation, and the export of lineage trees with all quantitative information related to cellular dynamics.

Electron microscopy

Zebrafish embryos were anaesthetised at 48 hpf in tricaine (170 μg/ml; Sigma) and rapidly prefixed in fixative A (2.5% paraformaldehyde and 2.5% glutaraldehyde in 0.1 M sodium cacodylate buffer pH 7.2). Embryo heads were dissected and prefixed in fixative A for 12–18 hours at 4°C and then embedded in 1% low melting point agarose and oriented in agarose cubes (<1 mm³). Heads were kept at 4°C and prefixed for a further 12–18 hours. After infiltration in Epon 812 (Electron Microscopy Sciences), blocks were oriented in moulds and left to polymerise for 48 hours at 60°C. Sections (50–60 nm) were cut using a Leica EM UC6 ultramicrotome and a Diatome Histo-Jumbo diamond knife. After intensification in uranyl acetate and lead citrate, the sections were observed using a JEOL 1400 electron microscope (120 kV) and pictures were taken using a SC1000 Orius GATAN camera.

Histology

Whole-mount *in situ* hybridisation (WMISH) was performed as previously described (Xu et al., 1994). Antisense riboprobes and paraffin sections were prepared as previously described (Brombin et al., 2011). Sequences of the DIG riboprobes used for *in situ* hybridisation are given in supplementary material Table S4. Brightfield imaging was performed with a Leica DMRD microscope (Nikon Eclipse E800 camera) or a Nikon AZ100 microscope (Nikon Digital Sight DSRi1). For cryosections, embryos were first protected by incubation in 30% sucrose in phosphate-buffered saline (PBS) for 12–16 hours at 4°C, then embedded in OCT Compound (Sakura), stored at –80°C, and sectioned at 14 μm using a Leica cryostat. Antisera were rabbit anti-phospho-H3 (1:1000; CR10, Millipore), rabbit anti-aPKCζ (1:200; C-20, sc-216, Santa Cruz Biotechnology), mouse anti-ZO-1 (1:100; 1A12, Molecular Probes, Life Technologies) and mouse anti-Pcna (1:200; PC10, DAKO); secondary antibodies were AlexaFluor 488 or AlexaFluor 568 goat anti-mouse or goat anti-rabbit conjugates (1:200; Molecular Probes). Sections were mounted in Prolong Gold Antifade Reagent including DAPI (Invitrogen) and imaged with a Zeiss AxioImager M2 microscope equipped with ApoTome.

TUNEL labelling was performed using the Deadend Fluorometric TUNEL system (Promega) according to manufacturer's instructions. Sections were washed in PBS, counterstained with DAPI (Sigma) and mounted with Vectashield hard-set mounting medium (Vector Laboratories).

Bioinformatic analyses

All homology searches and gene annotations were carried out using the Blast2GO functional analysis suite (<http://www.blast2go.com/b2ghome>; B2G) (Conesa et al., 2005). An InterPro scan was performed to find functional motifs and related GO terms using the specific tool implemented in the Blast2GO software (with the default parameters). We used Fisher's exact test for the statistical analysis of GO term frequency differences between two sets of sequences identified with Enrichment Analysis tools. We used a gene list expressed in whole zebrafish CNS (data mined in ZFIN by Yan Jaszczyszyn, personal communication), together with the Ivanova hematopoiesis mature cells list of genes upregulated in mature blood

cells from adult bone marrow and fetal liver, as backgrounds for enrichment analysis. These lists are available in MSigDB v3.0 (<http://www.broadinstitute.org/gsea/msigdb/index.jsp>).

Ingenuity pathway analysis software (Ingenuity Systems) was used to generate networks based on their connectivity in the bibliography and in microarray experiments.

Acknowledgements

We thank Audrey Colin, Laurent Legendre and Matthieu Simion for excellent fish care; Jean-Yves Tiercelin and Patrick Para for expert technical assistance; Ingrid Colin, Vasily Gurchenkov and Ludovic Leconte for help in molecular biology or microscopy; Maximilian Haeussler and Olivier Mirabeau for help with the *in silico* analysis; Yan Jaszczyszyn for providing a CNS gene list; and Pierre Boudinot for help with the Ingenuity pathway analysis. Bernard and Christine Thisse and the ZFIN members are acknowledged for their excellent *in situ* hybridisation database and for allowing us to publish pictures extracted from ZFIN. The AMAGEN, BioEmergences-IBISA-FBI and IMAGIF platforms are thanked for their excellent services in transgenesis and imaging. We have learned a great deal from all our colleagues and gratefully acknowledge our debt to them, in particular: Guillaume Carita, Karine Badonnel, Sylvia Bruneau, Alberta Palazzo, Frédéric Sohm and Michel Cohen-Tannoudji. We thank Alessandro Alunni, Jakob von Trotha, Georges Lutfalla and Michel Vervoort for reviewing the earlier version of the manuscript.

Competing interests

The authors declare no competing financial interests.

Author contributions

G.R. carried out live imaging and image analysis with the help of N.P. and T.S. who conceived Mov-IT software, and assembled the figures. J.J., A.B., A.H., E.M., F.B. and F.J. performed molecular biology and histology experiments. J.-M.H. performed electron microscopy experiments. S.D. generated the zebrafish fluorescent transgenic lines. P.H. performed the Nomarski movie. J.J. and J.-S.J. performed the datamining and gene network analysis. G.R., J.J., A.B., A.H., E.M., F.J. and J.-S.J. analysed the data and assembled the manuscript. F.J., J.-S.J. and N.P. conceived the study. G.R., F.J. and J.-S.J. wrote the manuscript with contributions from J.J., A.B., A.H., E.M., J.-M.H., F.B. and N.P.

Funding

We acknowledge support from Centre national de la recherche scientifique (CNRS), Institut national de la recherche agronomique (INRA), Institut national de la santé et de la recherche médicale (INSERM), Université Paris Sud, Agence Nationale de la Recherche and the European Commission [STREP Plurigenes, CISSTEM, FP6 NEST program (Embryomics and BioEmergences EC projects) and FP7 Health program (zf-Health project) to N.P.].

Supplementary material

Supplementary material available online at <http://dev.biologists.org/lookup/suppl/doi:10.1242/dev.099010/-/DC1>

References

- Allende, M. L., Amsterdam, A., Becker, T., Kawakami, K., Gaiano, N. and Hopkins, N. (1996). Insertional mutagenesis in zebrafish identifies two novel genes, pescadillo and dead eye, essential for embryonic development. *Genes Dev.* **10**, 3141–3155.
- Alunni, A., Hermel, J. M., Heuzé, A., Bourrat, F., Jamen, F. and Joly, J. S. (2010). Evidence for neural stem cells in the medaka optic tectum proliferation zones. *Dev. Neurobiol.* **70**, 693–713.
- Amsterdam, A., Burgess, S., Golling, G., Chen, W., Sun, Z., Townsend, K., Farrington, S., Haldi, M. and Hopkins, N. (1999). A large-scale insertional mutagenesis screen in zebrafish. *Genes Dev.* **13**, 2713–2724.
- Anderson, C. M. and Parkinson, F. E. (1997). Potential signalling roles for UTP and UDP: sources, regulation and release of uracil nucleotides. *Trends Pharmacol. Sci.* **18**, 387–392.
- Arendt, D. (2005). Genes and homology in nervous system evolution: comparing gene functions, expression patterns, and cell type molecular fingerprints. *Theory Biosci.* **124**, 185–197.
- Baye, L. M. and Link, B. A. (2007). Interkinetic nuclear migration and the selection of neurogenic cell divisions during vertebrate retinogenesis. *J. Neurosci.* **27**, 10143–10152.
- Bradford, Y., Conlin, T., Dunn, N., Fashena, D., Frazer, K., Howe, D. G., Knight, J., Mani, P., Martin, R., Moxon, S. A. et al. (2011). ZFIN: enhancements and updates to the Zebrafish Model Organism Database. *Nucleic Acids Res.* **39**, D822–D829.
- Brombin, A., Grossier, J. P., Heuzé, A., Radev, Z., Bourrat, F., Joly, J. S. and Jamen, F. (2011). Genome-wide analysis of the POU genes in medaka, focusing on expression in the optic tectum. *Dev. Dyn.* **240**, 2354–2363.
- Bugner, V., Tecza, A., Gessert, S. and Kühl, M. (2011). Peter Pan functions independently of its role in ribosome biogenesis during early eye and craniofacial cartilage development in *Xenopus laevis*. *Development* **138**, 2369–2378.

- Candal, E., Thermes, V., Joly, J. S. and Bourrat, F. (2004). Medaka as a model system for the characterisation of cell cycle regulators: a functional analysis of *Oi-Gadd45gamma* during early embryogenesis. *Mech. Dev.* **121**, 945-958.
- Candal, E., Alunni, A., Thermes, V., Jamen, F., Joly, J. S. and Bourrat, F. (2007). *Oi-insm1b*, a SNAG family transcription factor involved in cell cycle arrest during medaka development. *Dev. Biol.* **309**, 1-17.
- Cerveny, K. L., Varga, M. and Wilson, S. W. (2012). Continued growth and circuit building in the anamniote visual system. *Dev. Neurobiol.* **72**, 328-345.
- Chapouton, P., Adolf, B., Leucht, C., Tannhäuser, B., Ryu, S., Driever, W. and Bally-Cuif, L. (2006). *her5* expression reveals a pool of neural stem cells in the adult zebrafish midbrain. *Development* **133**, 4293-4303.
- Chojnacki, A. K., Mak, G. K. and Weiss, S. (2009). Identity crisis for adult periventricular neural stem cells: subventricular zone astrocytes, ependymal cells or both? *Nat. Rev. Neurosci.* **10**, 153-163.
- Conesa, A., Götz, S., Garcia-Gómez, J. M., Terol, J., Talón, M. and Robles, M. (2005). Blast2GO: a universal tool for annotation, visualization and analysis in functional genomics research. *Bioinformatics* **21**, 3674-3676.
- Devès, M. and Bourrat, F. (2012). Transcriptional mechanisms of developmental cell cycle arrest: problems and models. *Semin. Cell Dev. Biol.* **23**, 290-297.
- Efroni, S., Duttagupta, R., Cheng, J., Dehghani, H., Hoepfner, D. J., Dash, C., Bazett-Jones, D. P., Le Grice, S., McKay, R. D., Buetow, K. H. et al. (2008). Global transcription in pluripotent embryonic stem cells. *Cell Stem Cell* **2**, 437-447.
- England, S. J., Blanchard, G. B., Mahadevan, L. and Adams, R. J. (2006). A dynamic fate map of the forebrain shows how vertebrate eyes form and explains two causes of cyclopia. *Development* **133**, 4613-4617.
- Fichelton, P., Moch, C., Ivanovitch, K., Martin, C., Sidor, C. M., Lepesant, J. A., Bellaiche, Y. and Huynh, J. R. (2009). Live-imaging of single stem cells within their niche reveals that a U3snoRNP component segregates asymmetrically and is required for self-renewal in *Drosophila*. *Nat. Cell Biol.* **11**, 685-693.
- Fuchs, E., Tumber, T. and Guschik, G. (2004). Socializing with the neighbors: stem cells and their niche. *Cell* **116**, 769-778.
- Geldmacher-Voss, B., Reugels, A. M., Pauls, S. and Campos-Ortega, J. A. (2003). A 90-degree rotation of the mitotic spindle changes the orientation of mitoses of zebrafish neuroepithelial cells. *Development* **130**, 3767-3780.
- Götz, M. and Huttner, W. B. (2005). The cell biology of neurogenesis. *Nat. Rev. Mol. Cell Biol.* **6**, 777-788.
- Grandel, H. and Brand, M. (2013). Comparative aspects of adult neural stem cell activity in vertebrates. *Dev. Genes Evol.* **223**, 131-147.
- Grandel, H., Kaslin, J., Ganz, J., Wenzel, I. and Brand, M. (2006). Neural stem cells and neurogenesis in the adult zebrafish brain: origin, proliferation dynamics, migration and cell fate. *Dev. Biol.* **295**, 263-277.
- Greiling, T. M., Aose, M. and Clark, J. I. (2010). Cell fate and differentiation of the developing ocular lens. *Invest. Ophthalmol. Vis. Sci.* **51**, 1540-1546.
- Herbomel, P. (1999). Spinning nuclei in the brain of the zebrafish embryo. *Curr. Biol.* **9**, R627-R628.
- Hölzel, M., Rohmoser, M., Schlee, M., Grimm, T., Harasim, T., Malamoussi, A., Gruber-Eber, A., Kremmer, E., Hiddemann, W., Bornkamm, G. W. et al. (2005). Mammalian WDR12 is a novel member of the Pes1-Bop1 complex and is required for ribosome biogenesis and cell proliferation. *J. Cell Biol.* **170**, 367-378.
- Hsieh, J. (2012). Orchestrating transcriptional control of adult neurogenesis. *Genes Dev.* **26**, 1010-1021.
- Ito, Y., Tanaka, H., Okamoto, H. and Ohshima, T. (2010). Characterization of neural stem cells and their progeny in the adult zebrafish optic tectum. *Dev. Biol.* **342**, 26-38.
- Kimmel, C. B., Ballard, W. W., Kimmel, S. R., Ullmann, B. and Schilling, T. F. (1995). Stages of embryonic development of the zebrafish. *Dev. Dyn.* **203**, 253-310.
- Kizil, C., Kaslin, J., Kroehne, V. and Brand, M. (2011). Adult neurogenesis and brain regeneration in zebrafish. *Dev. Neurobiol.* **72**, 429-461.
- Komili, S., Farny, N. G., Roth, F. P. and Silver, P. A. (2007). Functional specificity among ribosomal proteins regulates gene expression. *Cell* **131**, 557-571.
- Kondrashov, N., Pusic, A., Stumpf, C. R., Shimizu, K., Hsieh, A. C., Xue, S., Ishijima, J., Shiroishi, T. and Barna, M. (2011). Ribosome-mediated specificity in Hox mRNA translation and vertebrate tissue patterning. *Cell* **145**, 383-397.
- Koudijs, M. J., den Broeder, M. J., Keijser, A., Wienholds, E., Houwing, S., van Rooijen, E. M., Geisler, R. and van Eeden, F. J. (2005). The zebrafish mutants *dre*, *uki*, and *lep* encode negative regulators of the hedgehog signaling pathway. *PLoS Genet.* **1**, e19.
- Kriegstein, A. and Alvarez-Buylla, A. (2009). The glial nature of embryonic and adult neural stem cells. *Annu. Rev. Neurosci.* **32**, 149-184.
- Kwan, K. M., Otsuna, H., Kidokoro, H., Carney, K. R., Saijoh, Y. and Chien, C. B. (2012). A complex choreography of cell movements shapes the vertebrate eye. *Development* **139**, 359-372.
- Law, J. A. and Jacobsen, S. E. (2010). Establishing, maintaining and modifying DNA methylation patterns in plants and animals. *Nat. Rev. Genet.* **11**, 204-220.
- Le Boutellier M., Souilhol C., Beck-Cormier S., Stedman A., Burlen-Defranco O., Vandormael-Pournin S., Bernex F., Cumano A. and Cohen-Tannoudji M. (2013). Notchless-dependent ribosome synthesis is required for the maintenance of adult hematopoietic stem cells. *J. Exp. Med.* **210**, 2351-2369.
- Link, B. A., Kainz, P. M., Ryo, T. and Dowling, J. E. (2001). The perplexed and confused mutations affect distinct stages during the transition from proliferating to post-mitotic cells within the zebrafish retina. *Dev. Biol.* **236**, 436-453.
- Liu, Y. C., Li, F., Handler, J., Huang, C. R., Xiang, Y., Neretti, N., Sedivy, J. M., Zeller, K. I. and Dang, C. V. (2008). Global regulation of nucleotide biosynthetic genes by c-Myc. *PLoS ONE* **3**, e2722.
- Locker, M., Agathocleous, M., Amato, M. A., Parain, K., Harris, W. A. and Perron, M. (2006). Hedgehog signaling and the retina: insights into the mechanisms controlling the proliferative properties of neural precursors. *Genes Dev.* **20**, 3036-3048.
- Mathis, L. and Nicolas, J. F. (2006). Clonal origin of the mammalian forebrain from widespread oriented mixing of early regionalized neuroepithelium precursors. *Dev. Biol.* **293**, 53-63.
- Mishra, S., Murphy, L. C. and Murphy, L. J. (2006). The Prohibitins: emerging roles in diverse functions. *J. Cell. Mol. Med.* **10**, 353-363.
- Müller, F. J., Laurent, L. C., Kostka, D., Ulitsky, I., Williams, R., Lu, C., Park, I. H., Rao, M. S., Shamir, R., Schwartz, P. H. et al. (2008). Regulatory networks define phenotypic classes of human stem cell lines. *Nature* **455**, 401-405.
- Neumüller, R. A., Richter, C., Fischer, A., Novatchkova, M., Neumüller, K. G. and Knoblich, J. A. (2011). Genome-wide analysis of self-renewal in *Drosophila* neural stem cells by transgenic RNAi. *Cell Stem Cell* **8**, 580-593.
- Olivier, N., Luengo-Oroz, M. A., Duloquin, L., Faure, E., Savy, T., Villeux, I., Solinas, X., Débarre, D., Bourguine, P., Santos, A. et al. (2010). Cell lineage reconstruction of early zebrafish embryos using label-free nonlinear microscopy. *Science* **329**, 967-971.
- Palmgren, A. (1921). Embryological and morphological studies on the mid-brain and cerebellum of vertebrates. *Acta Zoologica* **2**, 1-94.
- Parain, K., Mazurier, N., Bronchain, O., Borday, C., Cabochette, P., Chesneau, A., Colozza, G., El Yakoubi, W., Hamdache, J., Locker, M. et al. (2011). A large scale screen for neural stem cell markers in *Xenopus* retina. *Dev. Neurobiol.* **72**, 491-506.
- Perrera, C., Colombo, R., Valsasina, B., Carpinelli, P., Troiani, S., Modugno, M., Gianellini, L., Cappella, P., Isacchi, A., Moll, J. et al. (2010). Identification of Myb-binding protein 1A (MYBBP1A) as a novel substrate for aurora B kinase. *J. Biol. Chem.* **285**, 11775-11785.
- Peyre, E., Jaouen, F., Saadaoui, M., Haren, L., Merdes, A., Durbec, P. and Morin, X. (2011). A lateral belt of cortical LGN and NuMA guides mitotic spindle movements and planar division in neuroepithelial cells. *J. Cell Biol.* **193**, 141-154.
- Ramialison, M., Reinhardt, R., Henrich, T., Wittbrodt, B., Kellner, T., Lowy, C. M. and Wittbrodt, J. (2012). Cis-regulatory properties of medaka synexpression groups. *Development* **139**, 917-928.
- Rieger, S., Wang, F. and Sagasti, A. (2011). Time-lapse imaging of neural development: zebrafish lead the way into the fourth dimension. *Genesis* **49**, 534-545.
- Rinkwitz, S., Mourrain, P. and Becker, T. S. (2011). Zebrafish: an integrative system for neurogenomics and neurosciences. *Prog. Neurobiol.* **93**, 231-243.
- Rothenaigier, I., Krecsmerik, M., Hayes, J. A., Bahn, B., Lepier, A., Fortin, G., Götz, M., Jagasia, R. and Bally-Cuif, L. (2011). Clonal analysis by distinct viral vectors identifies bona fide neural stem cells in the adult zebrafish telencephalon and characterizes their division properties and fate. *Development* **138**, 1459-1469.
- Ruggero, D. and Pandolfi, P. P. (2003). Does the ribosome translate cancer? *Nat. Rev. Cancer* **3**, 179-192.
- Schmidt, R., Strähle, U. and Scholpp, S. (2013). Neurogenesis in zebrafish - from embryo to adult. *Neural Dev.* **8**, 3.
- Sheng, J., Yang, S., Xu, L., Wu, C., Wu, X., Li, A., Yu, Y., Ni, H., Fukuda, M. and Zhou, J. (2004). Bystin as a novel marker for reactive astrocytes in the adult rat brain following injury. *Eur. J. Neurosci.* **20**, 873-884.
- Sigoillot, F. D., Evans, D. R. and Guy, H. I. (2002). Growth-dependent regulation of mammalian pyrimidine biosynthesis by the protein kinase A and MAPK signaling cascades. *J. Biol. Chem.* **277**, 15745-15751.
- Solnica-Krezel, L., Schier, A. F. and Driever, W. (1994). Efficient recovery of ENU-induced mutations from the zebrafish germline. *Genetics* **136**, 1401-1420.
- Steinmetz, P. R., Kostyuchenko, R. P., Fischer, A. and Arendt, D. (2011). The segmental pattern of *otx*, *gbx*, and *Hox* genes in the annelid *Platynereis dumerilii*. *Dev. Dyn.* **13**, 72-79.
- Subramanian, A., Tamayo, P., Mootha, V. K., Mukherjee, S., Ebert, B. L., Gillette, M. A., Paulovich, A., Pomeroy, S. L., Golub, T. R., Lander, E. S. et al. (2005). Gene set enrichment analysis: a knowledge-based approach for interpreting genome-wide expression profiles. *Proc. Natl. Acad. Sci. USA* **102**, 15545-15550.
- Tsuchiya, M., Katagiri, N., Kuroda, T., Kishimoto, H., Nishimura, K., Kumazawa, T., Iwasaki, N., Kimura, K. and Yanagisawa, J. (2011). Critical role of the nucleolus in activation of the p53-dependent postmitotic checkpoint. *Biochem. Biophys. Res. Commun.* **407**, 378-382.
- Willer, G. B., Lee, V. M., Gregg, R. G. and Link, B. A. (2005). Analysis of the Zebrafish perplexed mutation reveals tissue-specific roles for de novo pyrimidine synthesis during development. *Genetics* **170**, 1827-1837.
- Xu, Q., Holder, N., Patient, R. and Wilson, S. W. (1994). Spatially regulated expression of three receptor tyrosine kinase genes during gastrulation in the zebrafish. *Development* **120**, 287-299.
- Xue, X. Y. and Harris, W. A. (2011). Using myc genes to search for stem cells in the ciliary margin of the *Xenopus* retina. *Dev. Neurobiol.* **72**, 475-490.
- Zhang, Y., Duc, A. C., Rao, S., Sun, X. L., Bilbee, A. N., Rhodes, M., Li, Q., Kappes, D. J., Rhodes, J. and Wiest, D. L. (2013). Control of hematopoietic stem cell emergence by antagonistic functions of ribosomal protein paralogs. *Dev. Cell* **24**, 411-425.
- Zhao, C., Deng, W. and Gage, F. H. (2008). Mechanisms and functional implications of adult neurogenesis. *Cell* **132**, 645-660.
- Zupanc, G. K. (2009). Towards brain repair: Insights from teleost fish. *Semin. Cell Dev. Biol.* **20**, 683-690.
- Zupanc, G. K. and Sirbulescu, R. F. (2011). Adult neurogenesis and neuronal regeneration in the central nervous system of teleost fish. *Eur. J. Neurosci.* **34**, 917-929.

PART II

FUNCTIONAL STUDY OF THE ROLE PLAYED BY NUCLEOLAR PROTEINS IN THE CONTROL OF NEURAL PROGENITOR HOMEOSTASIS USING ZEBRAFISH AS A MODEL

While it is now widely accepted that gene expression can be controlled at the translational level by “specialized ribosomes” (Xue and Barna, 2012; Filipovska and Rackham, 2013) less is known about the mechanisms leading to this diversity. It has long been assumed that ribosome biogenesis is a ubiquitous and fundamental process conserved among eukaryotes. This idea, based on the studies mainly performed in yeast, has been challenged by the most recent literature. Ribosome biogenesis, for instance, is far more complex in humans than previously assumed. Despite the global conservation of ribosome biogenesis factors (RBFs) between ancient and modern eukaryotes, plasticity exists and vertebrates have evolved and adapted different processing strategies, partially based on the components initially present in deeply rooted eukaryotes (Taffoureau *et al.*, 2013; Ebersberger *et al.*, 2014). Recent studies often stress out the fact that RBFs seem to be differentially required during development in *Drosophila* (Wang *et al.*, 2013), zebrafish (Provost *et al.*, 2012; Simmons *et al.*, 2012; Zhao *et al.*, 2014) and mammals (Ross and Zarbalis, 2014). Moreover in these species, many RBFs seem to play specific roles in stem cell biology (see Ch. 1.II section 2.2.4). Little is known about ribosome biogenesis process(es) in vertebrates. Therefore studies about this topic will allow getting insight into gene expression translational control mechanisms and ribosomopathies. Although these latter are caused by defects in ribosome biogenesis, their clinical manifestations are extremely variable and typically display tissue specificity (Armistead and Triggs-Raine; 2014; see Ch. 1.II section 2.2.3).

The main goal of my PhD was to understand how RBFs could specifically participate to progenitor cell biology using zebrafish as a model.

My project focused on the study of a small population of neuroepithelial cells located at the periphery of the optic tectum (OT), in the peripheral midbrain layer (PML). Datamining of the ZFIN gene expression database allowed us to identify around fifty genes preferentially expressed in PML. Interestingly, many “PML genes” code for RBFs. There are important overlaps between the PML specific gene list and other datasets (related to *Drosophila* neuroblasts or human pluripotent stem cells) (Recher *et al.*, 2013; see Ch. 2.II section 1). These data have been

eventually confirmed via transcriptomic analysis (**Dambroise, Simion et al., submitted**). Nevertheless, at the beginning of my PhD the idea that RBF could participate specifically to progenitor cell homeostasis was considered pure “*Avant-guard*”. Thus, when we started to work on the subject we started in the most traditional way and decided to analyse several zebrafish mutants for RBF coding genes. After an initial work on the genes of the PeBoW complex (*pescadillo*, *bop1* and *wdr12*), I started the characterization of mutants for genes coding for members of the box C/D snoRNP complex (*fibrillarin*, *nop56* and *nop58*). This work has been carried out in collaboration with Emilie Dambroise (post-doc in the lab). We found that depletion of these genes leads to p53-dependent cell cycle arrest at the G2/M transition (see *Ch1.I section 1.3*). These unexpected but quite exciting results open new research perspectives. In particular they emphasize the importance of the ribosome biogenesis for the gene expression regulation at the translational level.

Being aware that differences in ribosome biogenesis between progenitor and differentiated cells might not be an “ON/OFF” mechanism, I started the functional study of the PML gene *notchless homolog 1* (*nle1*, the zebrafish ortholog of the mammalian gene *Notchless*), which is required for the maturation of the large ribosomal subunit (60S). It has been shown that the murine *Nle* gene was necessary for the survival of the inner mass cells in preimplantation embryos (**Cormier et al., 2006**). More recently, conditional Knock-Out experiments in mouse showed that *Nle* is required for the maintenance of hematopoietic stem cells, but it is dispensable for differentiated cells (**Le Boutellier et al., 2013**). Likewise, *Nle* is necessary for the survival of the intestinal stem cells (**Stedman et al., 2015**). Does this RBF play the same role in neuroepithelial cells? Our hypothesis is that the PML cells require *Nle1* for the maturation of the 60S subunit, but not neurons which could survive after its deletion. This would demonstrate an important regulatory role played by ribosome biogenesis in SC homeostasis. In order to demonstrate the cell-specific role played by *nle1*, I have generated a Dominant-Negative (DN) form of *nle1* mutating the wild-type (WT) sequence at a hyperconserved site. The efficiency of DN mutation in zebrafish had been tested both in zebrafish cell culture (collaboration with Boudinot’s team, INRA) and *in vivo* via injection of both *nle1-DN* mRNA and *nle1-WT* mRNA in WT zebrafish embryos. The tissue-specific role of *nle1* is currently tested via a transient transgenesis approach. Preliminary results seem to confirm our initial hypothesis (see *Ch. 2.II section 1.3*).

1. LACK OF SNORNP CODING GENES LEADS TO P53-DEPENDENT APOPTOSIS AT THE G2/M TRANSITION IN ZEBRAFISH.

1.1 INTRODUCTION

The box C/D snoRNP complex is responsible for the site-specific 2'-O-methylation of the newly synthesized ribosomal RNAs (rRNAs) during ribosome biogenesis (Watkins and Bohnsack, 2012). Within the complex, the core proteins NHPX (Nhp21a/b in zebrafish), FIBRILLARIN (FBL), NOP56, NOP58 are associated with a box C/D small nucleolar RNA (snoRNA), NHPX being the primary RNA-binding protein. NOP proteins heterodimerize, scaffold the whole complex and are responsible for the correct positioning of FBL (methyltransferase) to the target rRNA (Figure 27) (Watkins and Bohnsack, 2012). Interestingly, box C/D snoRNP coding genes are often overexpressed in p53-deficient cancer cells. FBL and p53 levels are mutually and inversely controlled (Marcel *et al.*, 2013; Su *et al.*, 2014; Cowling *et al.*, 2014; see Ch. 1.II section 2.2.2).

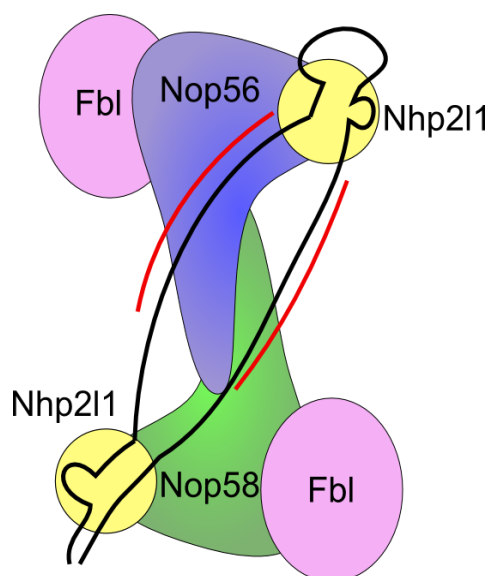


Figure 27. Schematic representation of the box C/D snoRNP complex in eukaryotes. Nhp211 (NHPX in human) is the primary RNA-binding protein. The Nhp211-box C/D snoRNA complex is then recognized by the Nop/Fbl complex. Nop56 and Nop58 heterodimerize (in eukaryotes) via their coiled-coil domains and provide the structural scaffold of the complex thereby positioning the molecules of Fbl (methyltransferase). Adapted from Watkins and Bohnsack, 2012.

Moreover, FBL overexpression in p53-deficient cancer cells leads to the rRNA hyper-methylation of the nascent ribosomes which will display modified translational specificities. IRES-containing mRNAs are therefore preferentially translated and pro-oncogenic, anti-apoptotic and survival proteins are then expressed (Marcel *et al.* 2013). Surprisingly, even the knock-down of *FBL* leads to the IRES-mediated translation of p53 (Su *et al.*, 2014). Interestingly, FBL amount is high in the proteome of mouse embryonic stem cells, where it contributes to maintain the pluripotent state (Watanabe-Susaki, 2014). Like *FBL*, the orthologs of other components of the complex (*NOP58* and *NOP56*) are also strongly expressed in *Drosophila* neuroblasts and in zebrafish neuroepithelial progenitors of the optic tectum (Neumüller *et al.*, 2011; Southall *et al.*, 2013; Recher *et al.*, 2013). *NOP56* ortholog has been described to play a major role in the

maintenance of neuroepithelial stem cells of the optic lobe (Wang *et al.*, 2013). All together, these findings highlight the importance of box C/D snoRNP coding genes in the control of cell survival, probably in a cell-autonomous manner being particularly important for progenitor cells.

The zebrafish optic tectum (OT) is a suitable model to study progenitor cell behavior *in vivo*. Indeed, this large structure of the dorsal midbrain displays life-long oriented growth supported by neuroepithelial cells present at its periphery (in the peripheral midbrain layer, PML; Cervený *et al.*, 2012; Recher *et al.*, 2013). Moreover, neuroepithelial progenitors, fast-amplifying progenitors and post-mitotic cells are found in adjacent domains of the OT, as a consequence of its oriented growth (Devès and Bourrat, 2012). Each cell population is marked by concentric gene expression patterns. Interestingly, a datamining of the ZFIN gene expression database allowed us to identify around 50 genes displaying biased expression in PML cells (neuroepithelial progenitors) (Figure 28). Surprisingly, many “PML genes” code for ribosome biogenesis factors (Recher *et al.*, 2013).

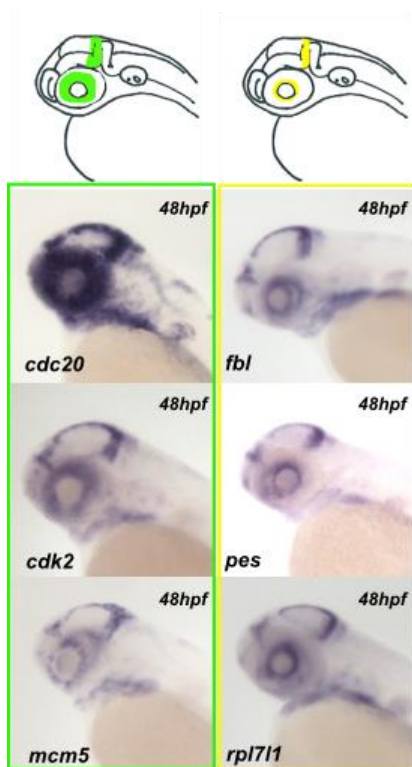


Figure 28. PML cells and retinal stem cells express the same genes. PML cells and retinal stem cells share a common genetic signature. Two kinds of expression patterns can be identified in the proliferation areas of the OT and of the retina (Ciliary Marginal Zone, CMZ) 1) proliferation genes (cyclins, cyclin kinases, etc.). These genes display a large expression pattern encompassing both the transient amplifying progenitors (called FAPs in the OT) and the neuroepithelial stem cells (PML are the progenitor cells of the OT and they are also identified as SAPs) of the two structures (green). 2) Progenitor cell-specific genes with a thin expression pattern (yellow). Many PML specific genes code for ribosome biogenesis factors. Drawings and pictures represent lateral views of 48hpf WT zebrafish embryos (long pec-stage). From zfin.org.

In order to get insight into the role played by RBF-coding genes in neuroepithelial cell homeostasis, we decided to carry out a functional analysis on a subset of them. In this context, we became interested in genes coding for the small nucleolar ribonucleoproteins (snoRNPs) of the box C/D snoRNP complex.

We analyzed zebrafish mutants for *fbl*, *nop56*, *nop58*. All mutants share common phenotypes at the long-pec stage (48hpf) with small eyes and a small head together with midbrain defects.

Mutation of one of the box C/D snoRNP coding genes leads to massive p53-dependent apoptosis, in zebrafish. Surprisingly, mutant cells incorporated thymidine analogs, suggesting that cell cycle was not arrested before the S phase. Thus, we propose that the absence of the box C/D snoRNP coding genes leads to the activation of the G2/M checkpoint in a p53-dependent manner.

1.2 RESULTS

1.2.1 Box C/D snoRNP coding genes are strongly expressed in PML cells

We verified the PML-restricted expression patterns of the box C/D snoRNP coding genes via whole-mount *in situ* hybridization (WMISH) on phenyltiourea treated zebrafish wild-type (WT, AB line) embryos fixed at the long-pec stage (**Figure 29A**). These genes are expressed until adulthood displaying biased expression in all neuroepithelial cells present in the brain (**Dambrose and Simion, personal communication**). Immunohistochemistry analysis on long-pec stage WT embryos revealed that the Fbl protein is clearly present in all cells, labelling the nucleoli, but is more expressed in PML cells (**Figure 29B**). Due to the lack of good antibodies, the expression of the other partners (Nop56, Nop58 and Nhp2l1) has not been assessed.

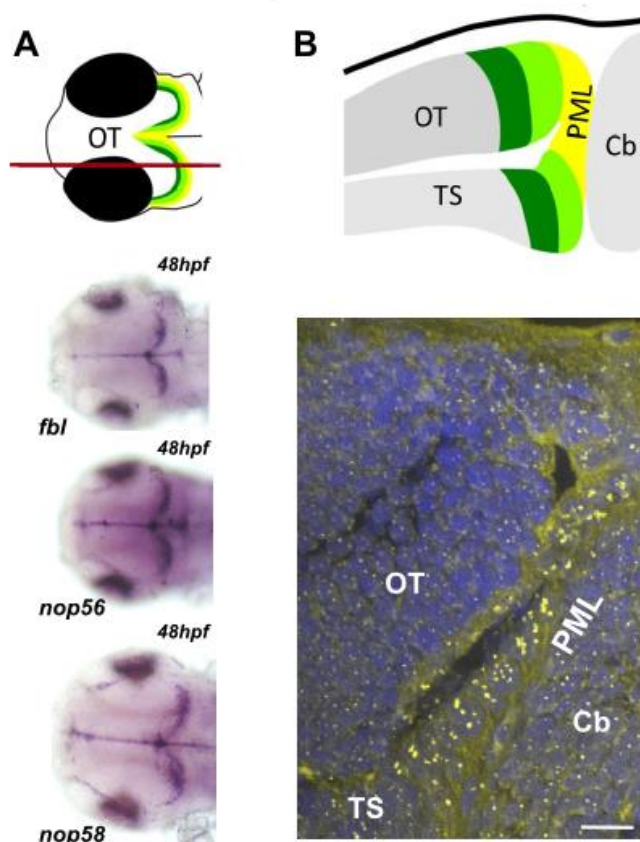


Figure 29. Box C/D snoRNP coding genes are strongly expressed in the PML. (A) Expression patterns of the SnoRNPs coding genes were verified in the lab. 48hpf WT zebrafish embryos (dorsal view). *nop56* expression pattern is not implemented in zfin.org. All three genes analyzed display the same expression pattern restricted to PML and CMZ cells. (B) Immunohistochemistry for the Fbl protein on 12µm parasagittal cryosections, 48hpf WT zebrafish embryo. Section plane of the B picture is indicated in A (upper panel) with a red line. Fbl is also accumulated in PML cells. Blue: DAPI, Yellow: Fbl. Scale bar: 25µm

Cb: cerebellum; PML: peripheral midbrain Layer; OT: optic tectum; TS: torus semicircularis

1.2.2 Box C/D snoRNP mutants display common phenotypes

We used mutants generated by retroviral insertion (**Amsterdam *et al.* 2004**). In all cases presented, retroviral elements are located in the 5' portion of the gene of interest. In particular, a 6kb retroviral sequence was found in the 5'UTR (position -30) of the *fbl* gene and sequences of similar length were found in the first intron of *nop56* and *nop58* transcribed regions (**Figure 30A**). RT-PCR analysis confirmed that all mutants used in this study are null mutants. Mutation of either *fbl* or *nop56* has no effect on the expression of the other snoRNP coding genes. However, their expression is affected in *nop58*^{hi3118} embryos (**Figure 30B**). Mutants analyzed share common phenotypes. At the long-pec stage (48hpf) they display smaller heads and smaller eyes than their siblings. Moreover, box C/D snoRNP mutants present cardiac edemas. Their yolk is bigger and round shaped and they display a tiny yolk extension (**Figure 30C**). Histological analyses revealed that mutants have smaller tecta than their WT siblings. Acellular holes can be detected in the tectum of every mutant analyzed; nevertheless PMLs are formed but thicker than PML of stage-matched WT embryos (data not shown). Morphological defects start to be visible at 30hpf and mutant embryos die within 6 days of development (data not shown).

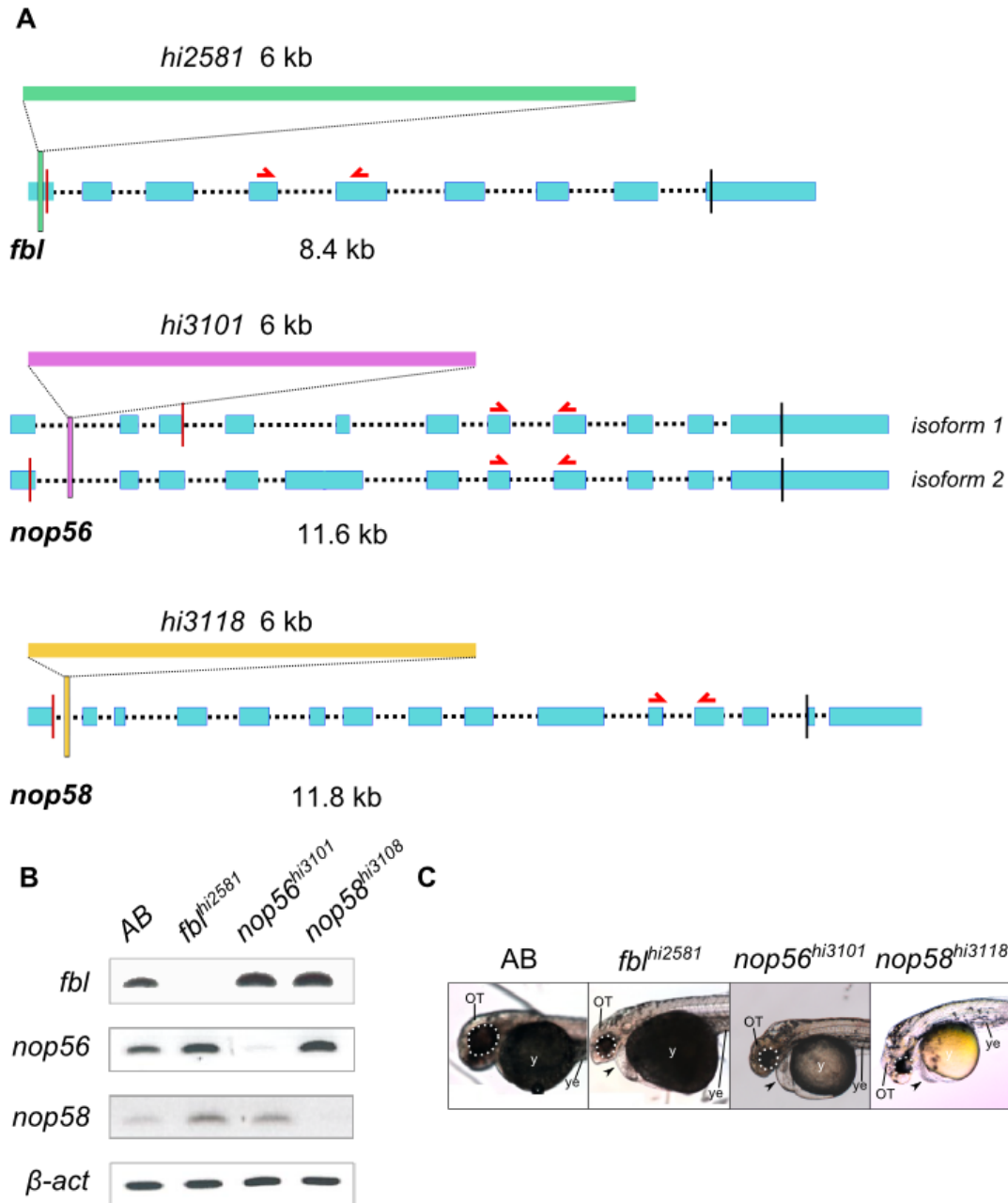


Figure 30. The insertional mutants for the SnoRNP coding genes are null and generate similar phenotypes. (A) Mutants for the SnoRNP coding genes had been generated via retroviral mutagenesis. The position of each retroviral insertion is depicted on the diagram of the mutated gene. Each light blue bar represents an exon; red vertical bars indicate the position of the START codon; black vertical bars indicate the position of the STOP codon. Red signs above exons indicate the position of the primers used for the RT-PCR in **B**. **(B)** Insertional mutagenesis generates null-mutants as demonstrated via RT-PCR. Interestingly, the knock-out of one of the SnoRNP coding genes does not impact the expression of the others for all the analyzed genes but *nop58*. **(C)** All SnoRNP mutants share the same phenotype at 48hpf. They are smaller than

control embryos and they have smaller eyes (dotted circles) and tecta. Mutants can be easily recognized because they have a pericardial edema (arrowhead) and smaller yolk extensions. They all die within 6 days of development.

OT: optic tectum; y: yolk; ye: yolk extension.

1.2.3 Midbrain structures seem to be most affected in box C/D snoRNP mutants

In order to check whether brain territories were properly specified during development, we performed WMISH on WT and mutant embryos. To this aim we used the *elavl3* riboprobe to assess whether cells were specified towards neuronal fate. Moreover, the expression *eomes* and *otx2* allowed us to check the specification of the anterior territories of the developing brain. *eomes* is specifically expressed in the developing forebrain. *otx2* is a general marker for anterior brain in the neural tube whose expression is limited posteriorly by the activity of the Isthmic organizer. *otx2* expression becomes restricted to the developing midbrain thanks to the signaling activity of the *zona limitans intrathalamica* (Vieira *et al.*, 2010; Cavodeassi and Houart, 2012).

The expression pattern of *elavl3* showed that dorsally located cells did not acquire neuronal identity in mutants at 48hpf (Figure 31A-D). *elavl3* expression was weak in the ventral parts of the nervous system in *fb^{hi2581}* (Figure 31B) and *nop56^{hi3101}* (Figure 31B) embryos. In contrast, *nop58^{hi3118}* embryos displayed strong *elavl3* expression in the forebrain (telencephalon) and in ventral midbrain and hindbrain but not tectal cells (Figure 31D). The absence of *elavl3* expression in mutant tecta indicates that these cells fail to acquire neuronal identity in all the analyzed mutants.

eomes expression was maintained in all snoRNP mutants (Figure 31E-H) indicating that lack of snoRNP coding genes did not affect forebrain development. Interestingly, *otx2* expression was affected in all cases (Figure 31I-L). The ventral-most and anterior-most expression of *otx2* was maintained at least at low levels in *fb^{hi2581}* (Figure 31I) and *nop58^{hi3118}* (Figure 31L) embryos. In *nop56^{hi3101}* embryos *otx2* extended ectopically and encompass the hindbrain indicating that the MHB territory was misspecified.

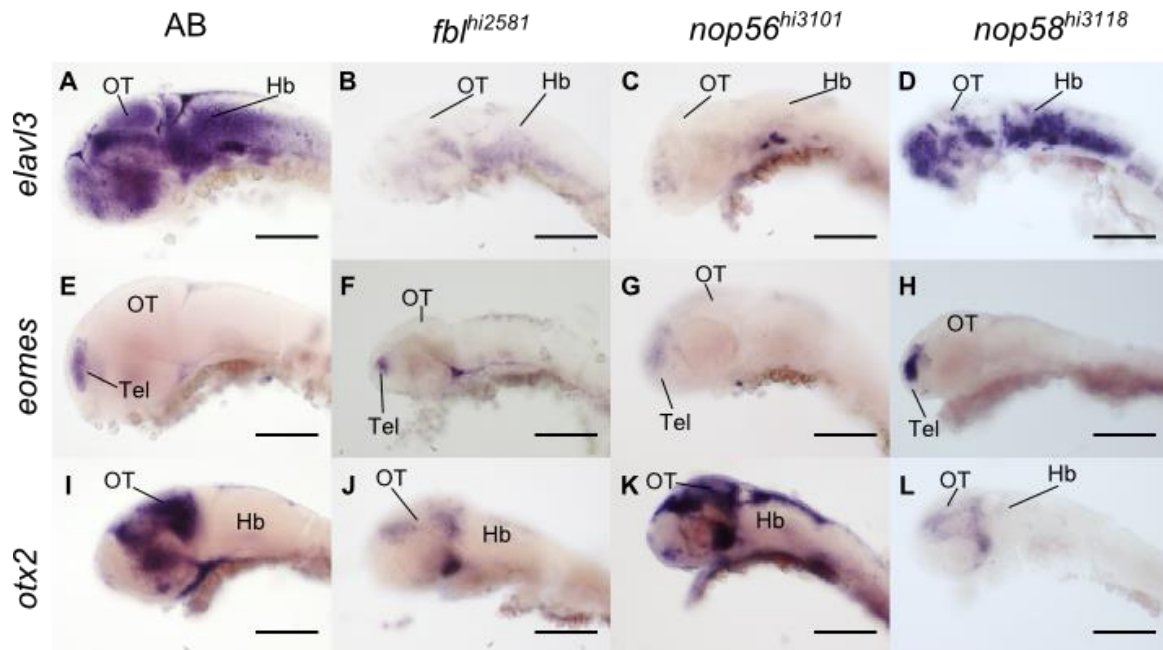


Figure 31. Differentiation markers are affected in SnoRNP mutants. Expression analysis performed on WT, *fbl*^{hi2581}, *nop56*^{hi3101} and *nop58*^{hi3118} embryos (column from left to right) at 48hpf. Ribobrobes used are indicated on the left. *elavl3* label cells committed towards neuronal fate, *eomes* is a forebrain identity marker and *otx2* is a midbrain marker. Scale bar: 100µm

Hb: hindbrain, OT: optic tectum, Tel: telencephalon.

1.2.4 Cells in mutants undergo massive apoptosis

TUNEL staining of WT and mutant embryos revealed massive cell death in mutant tecta (**Figure 32**). A huge number of pyknotic nuclei could be found all over the tectum, but never in the PML as shown both with TUNEL staining on mutant cryosections (**Figure 32A**) and with whole-mount imaging of *fbl* mutants (**Figure 32B**). Cell death could be p53-dependent as suggested by the strong activation of this latter gene monitored via RT-PCR (**Figure 32C**). Interestingly, p53 transcript levels are already up-regulated at 24hpf in *fbl* mutants (**Figure 32D**).

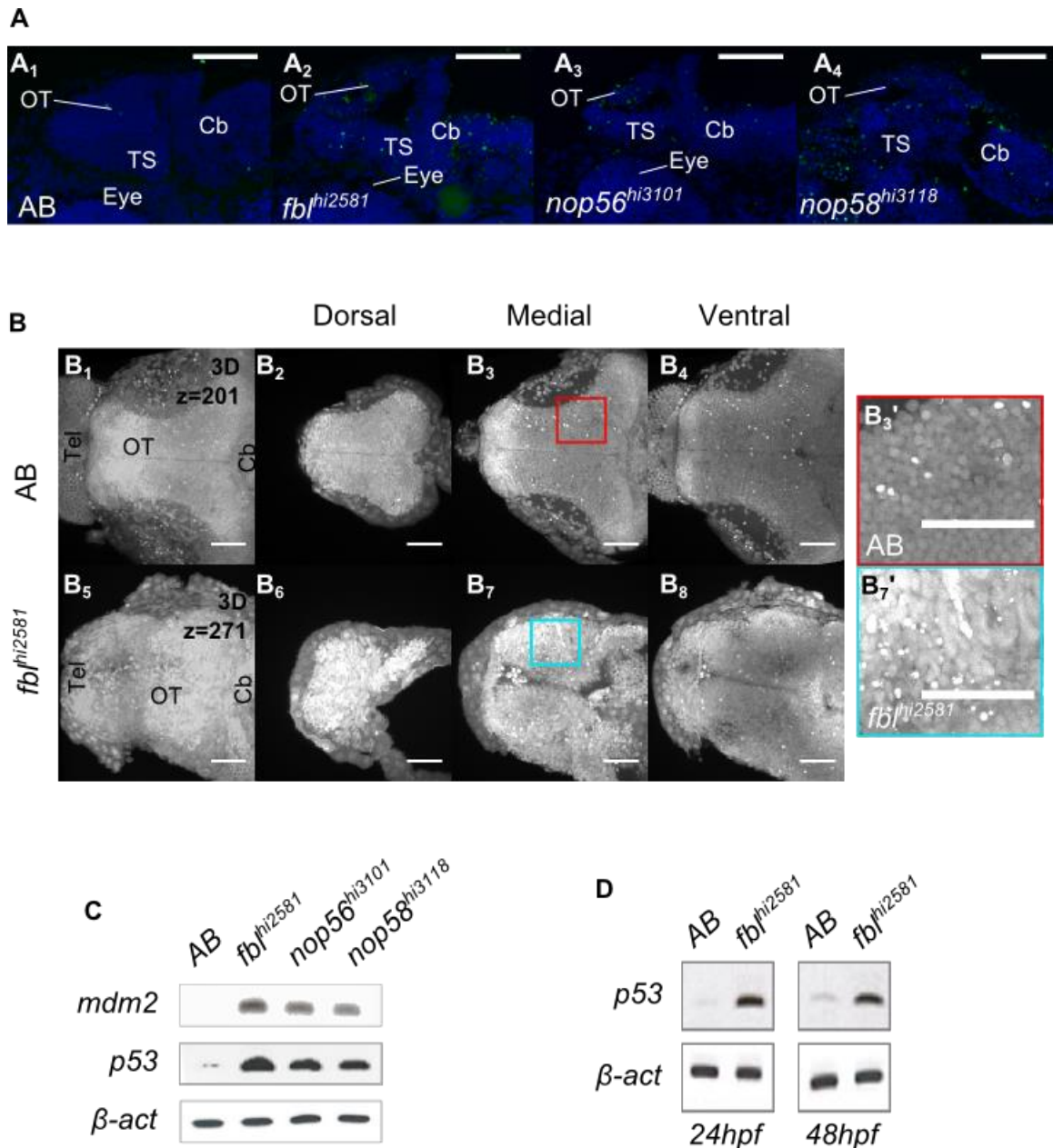


Figure 32. SnoRNP mutants display p53-mediated apoptosis. (A) TUNEL analysis on parasagittal cryosections of 48hpf embryos. Sections are 12 μ m thick. TUNEL positive cells can be detected in all samples, but their number is higher in mutants. Green: TUNEL; Blue: DAPI. Scale bar 50 μ m. **(B)** WT (**B**₁-**B**₄) and *fbl*^{hi2581} (**B**₅-**B**₈) brains from 72hpf embryos stained with DAPI and imaged dorsally. *fbl*^{hi2581} brain (**B**₅) is visibly smaller than the brain of control embryos (**B**₁). In *fbl*^{hi2581} brain (**B**₆-**B**₈) a huge number of pyknotic nuclei can be seen compared to control embryos (**B**₂-**B**₄). **B**₁: 3D projection of the brain of a WT embryo; **B**₂-**B**₄: Maximum projections of 30 optical sections of a WT embryo brain; dorsal region (**B**₂), medial (**B**₃) and ventral region (**B**₄); **B**₅: 3D projection of a *fbl*^{hi2581} embryo brain; **B**₆-**B**₈: Maximum projections of 30 optical sections of a WT embryo brain; dorsally (**B**₆), medially (**B**₇) and ventrally (**B**₈). Z-step: 0.62 μ m. Scale bar: 50 μ m **(C)** Mutants display high levels of *p53* and *mdm2* transcripts and this indicates that mutant cells die in a p53-dependent manner.

Cb: hindbrain, OT: optic tectum, Tel: telencephalon.

1.2.5 Cell cycle is affected in snoRNP mutants

Apoptosis and cell proliferation are usually regulated in opposite way. Thus, we performed a proliferation analysis by means of incorporation of a thymidine analog (EdU). Surprisingly, ectopic DNA replication could be observed in the tectum in all mutants at the long-pec stage (48hpf) after a 2h pulse (**Figure 33A**) indicating that these cells massively enter the S phase of the cell cycle. In order to check whether this phenotype was related or not to a general developmental delay, the experiment had been performed at later stages and gave similar results (data not shown).

Interestingly, box C/D snoRNP mutants displayed significantly larger nuclei and nucleoli than WT embryos, as shown in **Figure 33B-D** in the OT of the *fbl* mutant.

To better understand the mutant phenotypes, we crossed the *fbl* mutant line with the zebrafish Fucci line (zFucci) (**Sugiyama et al., 2009**). In “Fucci” fish, cell nuclei are labelled in G1 and S/G2/M phases with different colors. Hence, G1-nuclei are labeled by the expression of monomeric Kusabira Orange2 (mKO2) fused to G1-specific factor Cdt1 and S/G2/M nuclei are labeled by the expression of monomeric Azami Green protein (mAG) fused to Geminin (**Sugiyama et al., 2009**). Unexpectedly, in *fbl*^{hi2581} embryos, nuclei appeared mostly orange in retina and in the whole OT at 30hpf. This pattern highly differs from WT pattern in which retinal and tectal nuclei are mostly labeled by green fluorescence at the same stage (**Figure 33E**). This result indicates that mutant cells express *cdt1* while WT cells express Geminin, marker of S, G2 and M phases. Moreover, by WMISH, we found that mutant embryos expressed *ccnd1* (that codes for the G1-specific cyclin, cyclin D). Nonetheless, contrary to WT embryos, they do not express *cdkn1c* (that codes for an inhibitor of the cyclin E/Cdk2 complex which is necessary for the G1/S transition, **Figure 33F**). These data suggest that the cell cycle regulation is strongly altered in mutant embryos.

1.3 DISCUSSION

In order to get insight into the role of the box C/D snoRNP coding genes in cell homeostasis, we analyzed three mutants. Results show that cells lacking the snoRNP genes display deregulated cell cycle that eventually triggers apoptosis, probably after activation of p53.

1.3.1 Do box C/D snoRNP mutants display specific phenotypes?

RBF coding genes show strong expression in neuroepithelial cells of the retina and of the PML (**Recher et al., 2013**). Whether these genes play specific roles for the homeostasis of neuroepithelial cells is still matter of debate and investigation. As demonstrated via Fbl

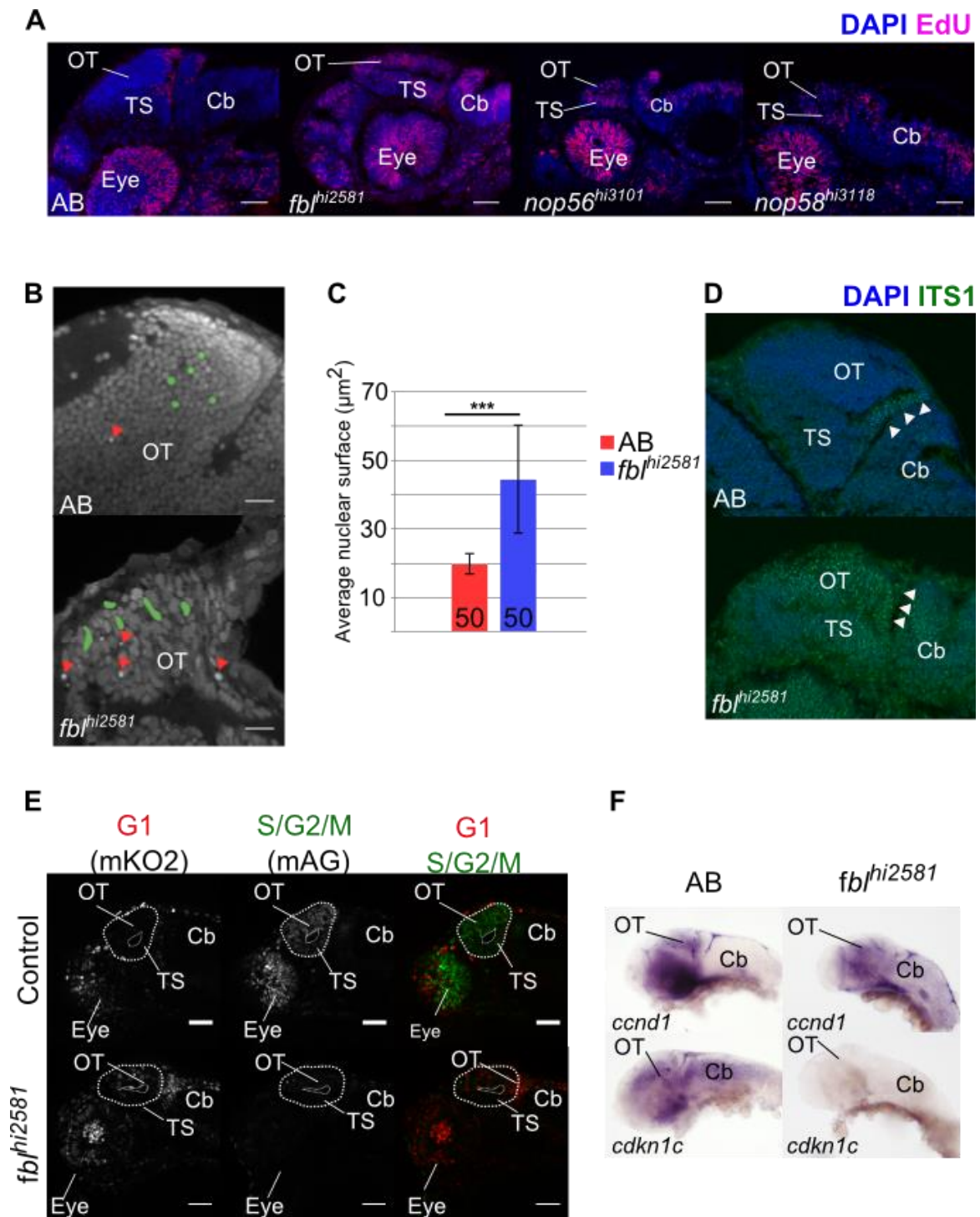


Figure 33. Lack of the snoRNP coding genes leads to cell cycle arrest at both G1/S and G2/M transitions. (A) Proliferation analysis on WT (AB line), *fbl*^{hi2581}, *nop56*^{hi3101} and *nop58*^{hi3118} embryos (from left to right). Embryos were injected with EdU at 48hpf. A two hour pulse was then applied. EdU+ cells are restricted to the PML and to the proliferative regions of the OT and of the *torus semicircularis* (TS) (the other brain structure originating from PML cells) in WT embryos. Staining is wider in mutant embryos indicating that the proliferation in the adjacent tissue is stimulated. Scale bar: 50 µm **(B)** *fbl*^{hi2581} embryos display bigger nuclei than WT embryos. WT (upper panel) and *fbl*^{hi2581} (lower panel) brains from 72hpf embryos stained with DAPI and imaged dorsally. Pictures shows one optical section extracted from the whole right

tectal lobe. Some nuclei have been highlighted in green. Red arrowheads point pyknotic nuclei. Scale bar: 20 μm . **(C)** Average nuclear surface of the nuclei in WT and *fb1*^{hi2581}. Measurements were made on random nuclei on random optical sections of the photos taken as described in **B**. ***: P<0.001. **(D)** *fb1* mutants display larger nucleoli than WT embryos. 12 μm -parasagittal cryosections were made from 48hpf WT (AB line, upper panel) and mutant embryos (lower panel) and stained with DAPI and ITS1 RNA-FISH probe coupled with Alexa Fluor 488. (see *Ch. 2.11 section 2.2.4*). White arrowheads highlight the position of the PML. **(E)** *fb1*^{hi2581/+} adults were crossed with zFucci adults (*Tg(EF1 α :mKO2-zCdt1(1/190))^{rw0405b,d} x *Tg(EF1 α :mAG-zGem(1/100))^{rw0410h}*) to get *fb1*^{hi2581/+}; zFucci double transgenics. Adult were then incrossed to obtain *fb1*^{hi2581}; zFucci embryos. Mutant embryos were imaged at 30hpf (lower panels) and stage matched zFucci embryos were used as controls (upper panel). Cells in the *fb1* mutants massively express mKO2 (red) indicating that cells are either blocked in G1 phase or overexpress Cdt1. Scale bar 50 μm **(F)** Expression analysis performed on WT, *fb1*^{hi2581} embryos (columns, from left to right) at 48hpf. Riboprobes used are *ccnd1* and *cdkn1* (lines, downward). *ccnd1* (cyclin D) is expressed during G1 phase, *cdkn1c* encode for an inhibitor of the G1/S transition (cdkn1c, p57) and is absent in mutant embryos. Scale bar: 100 μm*

Cb: cerebellum, OT: optic tectum, Tel: telencephalon.

immunodetection (**Figure 29B**), RBF expression is not an all-or-nothing asymmetry in PML cells compared to more differentiated cells of the tectum. Indeed, Fbl is expressed in all cells but at different levels. Mutations in RBF-coding genes are often lethal at early developmental stages in mammals (**Allende et al., 1996; Newton et al., 2003; Cormier et al., 2005**). Nonetheless many RBF-coding genes display tissue specific expression in zebrafish and loss of function experiments show that they play tissue-restricted roles for the survival of progenitor cells in the central nervous system (**Azuma et al., 2006; Simmons et al., 2012**), liver (**Wilkins et al., 2013; Wang et al., 2013**), pancreas (**Provost et al., 2012; Qin et al., 2014**) and neural crests (**Zhao et al., 2014**). The appearance of the mutant phenotype after gastrulation, during organogenesis (rather than an early lethality) is probably a result of the large maternal stock of mature ribosomes and RBFs in the zebrafish oocyte (**Azuma et al., 2006**).

Another possible explanation for the restricted phenotypes might be related to the kinetics of early development. Indeed, not all cells of the neural tube are recruited for neurogenesis at the same time (see *Ch. 1.1 section 1.2.1.3*; **Vieira et al., 2010; Cavodeassi and Houart, 2012**). PML is located at the midbrain/hindbrain boundary which is a known secondary neuroepithelial organizer (see *Ch. 1.1 section 2.2.3*). Thus, cells of the forebrain and cells of the midbrain would differentiate at different time points and therefore they could be differently affected by the lack

of box C/D snoRNP coding genes (**Figure 31**). However, to our knowledge, neither the ribosomal maternal stock nor its transmission kinetics to daughter cells has been investigated so far.

Nonetheless, some ribosome biogenesis factors might play specific roles in progenitor cells. This would explain the tissue-specific phenotypes of ribosomopathies due to RBF or RP loss-of-function (see *Ch. 1.II section 2.2.3*). Moreover, it has been shown that many RBF coding genes are necessary for the survival of different kinds of progenitor cells (see *Ch. 1.II section 2.2.4*). In particular, Fbl has been recently shown to be essential for the survival of murine embryonic stem cells. Stable expression of Fbl in these cells cultured in differentiating conditions (without LIF) extended their pluripotent state. Furthermore, both partial knock-down of FBL and treatment with Actinomycin D (inhibitor of the rRNA transcription) induced the expression of differentiation markers and promoted stem cell differentiation into neuronal lineages (**Watanabe-Susaki et al., 2014**). These findings indicate that ribosome biogenesis-related control of progenitor cell homeostasis cannot be an “ON/OFF” mechanism. Further work is thus needed to fully understand the origin of the observed tissue-specific effects.

1.3.2 At which point of the cell cycle do mutant cells undergo apoptosis?

When ribosome biogenesis is impaired, cell cycle is typically arrested at the G1/S transition. Indeed, free RBFs or RPs can activate cell cycle inhibitors (e.g. p21, p27, etc.) that negatively interact with cyclin E-CDK2 complex at the G1/S checkpoint (**James et al., 2014**). Analysis of *fb^{hi2581}*;zFucci embryos showed that most of the cells express G1-specific factor Cdt1, suggesting a cell cycle arrest at the G1/S transition (**Figure 33E**). However, other experimental evidences suggested that mutant cells progress in the cell cycle at least until the S phase. In particular, mutant cells incorporated thymidine analogs (EdU; **Figure 33A**) and displayed large nuclei (**Figure 33B**) that were significantly bigger than in WT cells (**Figure 33C**) suggesting a possible endoreplication (**Davoli and de Lange, 2011**). This hypothesis is further supported by the finding that most mutant cells expressed Cdt1. Indeed, this protein is responsible for the replication origin licensing of the DNA during G1 phase. If Cdt1 is not degraded, DNA can duplicate more than once. All these results indicate that mutant cells could have bypassed the G1/S checkpoint.

Mutant phenotypes could be also explained by considering the cells of the tectum as a heterogeneous population. Thus, some cells would undergo apoptosis before entering the S phase and others before mitosis.

Cell cycle arrest and apoptosis at the G2/M transition, upon ribosome biogenesis impairment, was seen only few other times in metazoans: upon depletion (with siRNA) of both ribosomal subunits in mammalian cell cultures (**Fumagalli et al., 2012**) and upon down-regulation of rRNA

transcription in leukemia cells (**Negi and Brown, 2015**). Thus, cell cycle arrest at the G2/M transition occurs upon a “general downregulation” of the ribosome biogenesis. Interestingly, in both cases, it was shown that a nucleolar stress response was activated to arrest cells prior entering the S phase. Hence, cells could die either before the G1/S transition or at the G2/M transition. This was explained with the fact that not all cells reached the threshold level to start a full apoptotic response at the G1/S transition (**Fumagalli et al., 2012**). Thus, it could be possible that cells in snoRNP mutants undergo apoptosis after the activation of the two different checkpoints.

It is noteworthy that FBL is a multifunctional protein (**Rodriguez-Corona et al., 2015**). One of its functions is to methylate the Q104 on the histone H2A in rDNA loci. This modification induces the recruitment of the RNA-polymerase I and thus boosts the whole rRNA transcription (**Tessarz et al., 2014**). Interestingly it has been recently shown that an overall rRNA transcription downregulation induced apoptosis and cell cycle arrest in G2 phase, supporting the hypothesis an arrest at the G2/M transition in snoRNP mutants (**Negi and Brown, 2015**).

Su and colleagues made the hypothesis that *FBL* knockdown in cancer cell leads to cell cycle arrest at the G1/S transition. Indeed, P21 protein was overexpressed in a RPL5/RPL11-dependent manner (**Su et al., 2014**). Nevertheless, the activation of the ATM/ATR-ChK1/ChK2-dependent pathway (at the G2/M transition) was not checked. Interestingly, *RPL11* mRNA contains a 5'TOP (5' terminal oligopyrimidine) motif and can be translated upon depletion of ribosomal subunits (**Fumagalli et al., 2012; Meyuhas and Kahan, 2015**). p53 is maintained at low levels in the nucleoplasm by Mdm2/HDM2. Upon nucleolar stress, free RPs and RBFs inhibit Mdm2, leading to the activation and stabilization of p53. Among the RPs that can bind Mdm2, is RPL11 (**Chakraborty et al., 2011**). Thus, cells that do not undergo apoptosis at the G1/S transition accumulate RPL11 and undergo p53-dependent apoptosis at the G2/M transition (**Fumagalli et al., 2012**).

IRES elements from *p53* and *GADD45* (inhibitor of the cell cycle progression) were responsive to *FBL* knock-down (**Su et al., 2014**). Interestingly, p21 (also overexpressed upon *FBL* knock-down) interacts with *GADD45* to arrest cell cycle progression at the G1/S transition but *GADD45* contributes to the cell cycle arrest at the G2/M transition as well (see **Tamura et al., 2012** for review). Thus, many and diverse mechanisms could contribute to the arrest at the G2/M transition in snoRNP mutants.

Further analyses are required to determine whether *fb1* depletion (and that of *nop56* and *nop58*) leads to apoptosis at the G2/M transition only or alternatively at the G1/S and G2/M transitions.

It would be informative to analyse the expression (by RT-PCR) of several proapoptotic p53 target genes (including *puma*, *noxa* and *bax*). To observe the activation of the G2/M checkpoint, the analysis by Western blot of the expression of RbL11, p21 p53 and its phosphorylated form will be performed. Finally the measure of the DNA content of mutant cells by flow cytometry will allow validate or invalidate the different presented hypotheses.

2. FUNCTIONAL STUDY OF *nle1*

2.1 Introduction

Notchless (*Nle*) encodes a WD40 repeat-containing protein which was initially studied in *Drosophila* as an inhibitor of the Notch signaling pathway (Royet *et al.*, 1998). It is necessary for the survival of the blastomeres of the inner cell mass in murine pre-implantation embryos (Cormier *et al.*, 2006). Interestingly, *Notchless* is conserved across eukaryotes. *Notchless* ortholog can be found in yeast (called *Rsa4*) and plants, which lack the Notch signaling pathway (de la Cruz *et al.*, 2005; Chantha *et al.*, 2006). It has been demonstrated in many contexts that *Notchless* gene plays a conserved role in ribosome biogenesis. In particular, it is important for the export of the large ribosomal subunit (60S) in yeast (Ulbrich *et al.*, 2009; Bassler *et al.*, 2010; Kressler *et al.*, 2012; Bassler *et al.*, 2014), plants (Chantha *et al.*, 2006; Chantha *et al.*, 2007) and mouse (LeBoutellier *et al.*, 2013; Stedman *et al.*, 2015).

Murine *Nle1* is necessary for the survival and the homeostasis of both hematopoietic stem cells (LeBoutellier *et al.*, 2013) and intestinal stem/progenitor cells (Stedman *et al.*, 2015), but not for the survival of their differentiated progenies. Interestingly, the defective ribosome biogenesis (i. e. defective 60S subunit exportation) leads to p53-mediated removal of stem cells and progenitors in both cases. p53-independent mechanisms seem to be active as well (Stedman *et al.*, 2015).

The zebrafish optic tectum (OT) is a prominent dorsal region of the midbrain. Life-long growth of the OT is supported by neuroepithelial cells located at the periphery of the structure itself (Devès and Bourrat, 2012). Neuroepithelial cells constitute the so-called peripheral midbrain layer (PML) and exhibit high levels of transcripts for nucleotide and ribosome biogenesis (Recher *et al.*, 2013).

Among the genes that display biased expression in PML cells is the zebrafish ortholog of *Nle* (*notchless homolog 1*, *nle1*) (Recher *et al.*, 2013). Thus, we wondered whether this gene could be necessary for the survival of the neuroepithelial cells and dispensable in differentiated cells. To this aim, we have generated a Dominant-Negative (DN) form of *nle1*. Thus, we mutated the *nle1* ORF in order to get an aspartate in position 76 to reproduce the yeast DN mutation (Bassler *et al.*, 2010) (see Figure 34A for details). DN construction was had been tested both *in vivo* and *in vitro*. Both the DN and WT form of *nle1* was sub-cloned in order to be expressed in different areas of the zebrafish brain (by using specific *cis*-regulatory sequences) (Figure 34B). Survival of the neuroepithelial progenitors overexpressing the DN negative form of *nle1* is strongly affected.

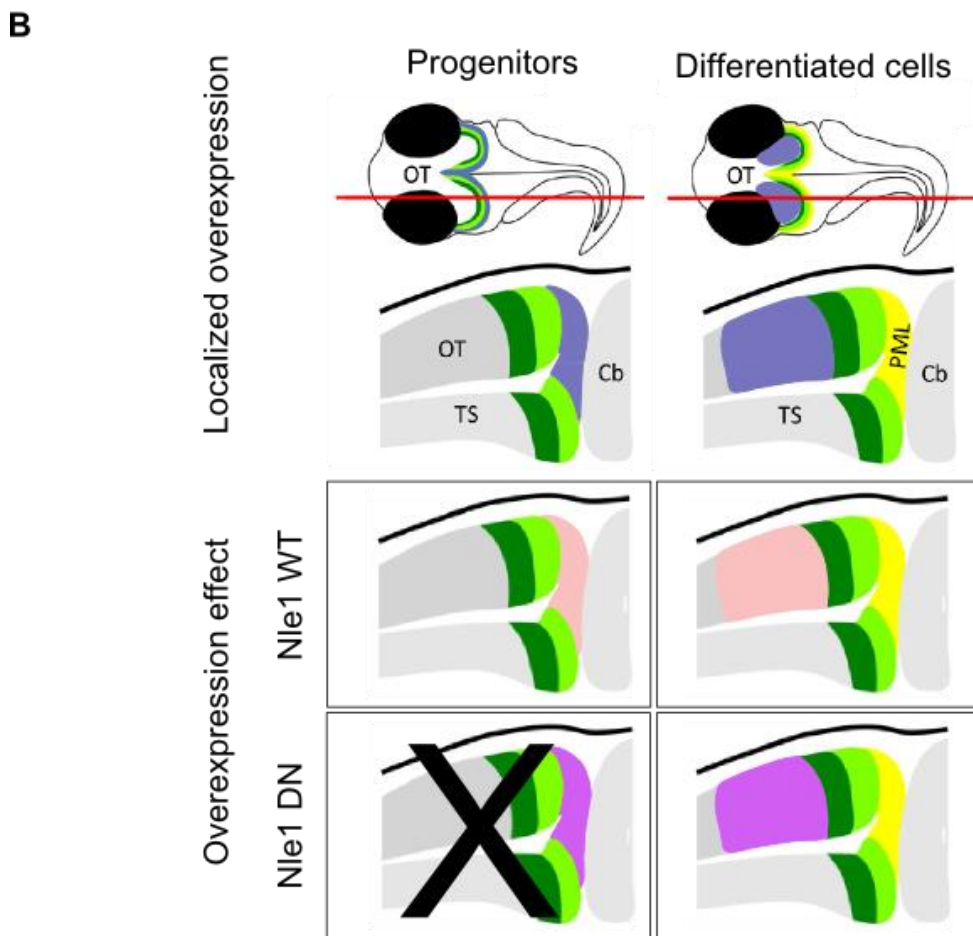
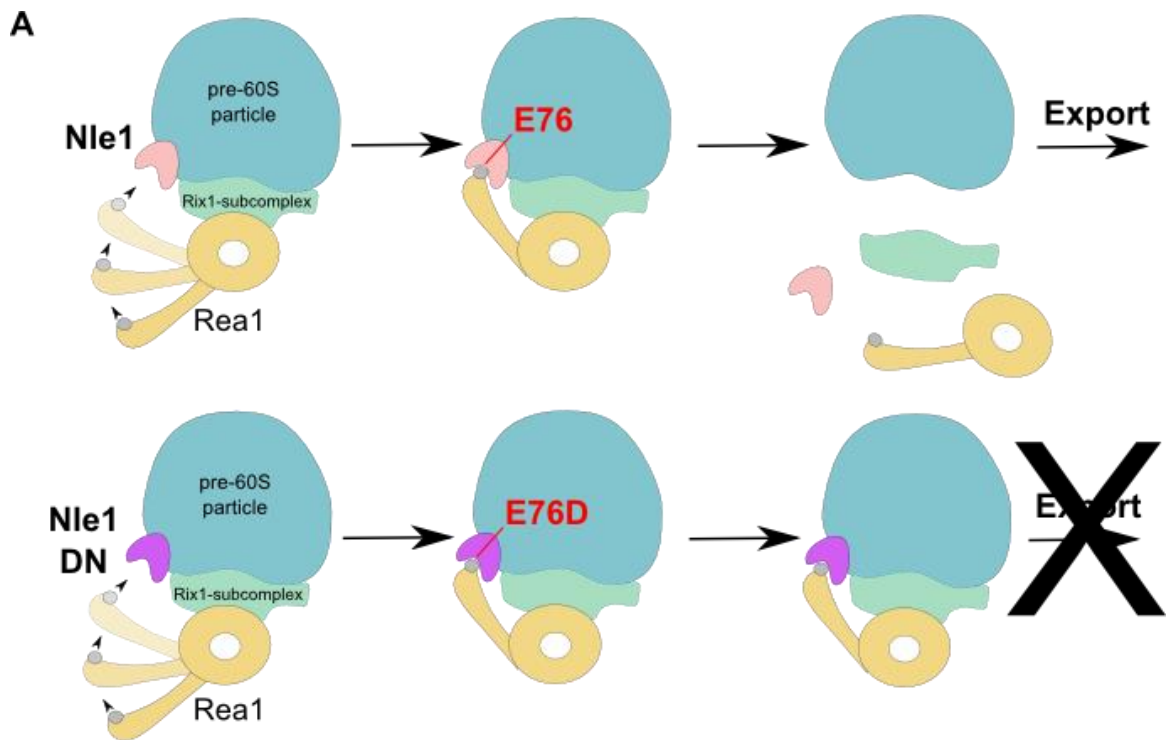


Figure 34. Targeted expression of a DN form of Nle1. According to the model proposed by Ulbrich and colleagues (Ulbrich *et al.*, 2009), Rea1 (composed of a hexameric AAA ATPase ring and a protruding tail) and Rsa4 (with a MIDAS binding site) interact during ribosome biogenesis.

Rsa4 (yeast ortholog of Nle1), Rea1 and the Rix1-subcomplex are released in an ATP-dependent manner. The tip of the flexible Rea1 tail harbours the MIDAS domain, which coordinates the MIDAS ion (Mg²⁺). The AAA ring of Rea1 is attached via an adaptor structure (Rix1-subcomplex) to the 60S moiety, but the MIDAS tail can move up and contact the pre-60S particle at a distant site where Rsa4 (yeast ortholog of Nle1) is located. In a hypothetical pre-60S intermediate, the MIDAS is docked to Rsa4 and hence tensile force generated by ATP hydrolysis in the Rea1 AAA domain can be used to pull off Rsa4, the Rix1-subcomplex and Rea1 from the pre-60S particle. Thus, the MIDAS-Rsa4 interaction is essential for ATP-dependent dissociation of a group of non-ribosomal factors from the pre-60S particle and allows the following exportation from the nucleus of the pre-60S particle. This model was generated in yeast after electron microscopy direct observation. This model is depicted in **A (upper panel)** and transposed to zebrafish. Thus, the position of Nle1 is indicated. It has been demonstrated that glutamate to aspartate substitution (E114D) in the Notchless domain of yeast Rsa4 leads to the generation of a DN phenotype (**Bassler et al., 2010**). Thus, Rsa4 cannot act anymore as a tension generator for the detachment of Rea1 and the Rix1-complex. Nuclear exportation of the pre-60S ribosomal particle is therefore prevented. E114 of yeast Rsa4 corresponds to the E76 of the zebrafish Nle1 (**A, lower panel**). Thus, we mutated the *nle1* ORF in order to get an aspartate in position 76 (to generate *nle1DN*) and we aimed to target its overexpression in both PML cells (using *enh101* driver) and differentiated cells of the OT (using the *brn3a* promoter). According to our model, the overexpression in differentiated cells of both *nle1WT* and *nle1DN* should not lead to any defect (**B, right column**). On the contrary the overexpression of *nle1DN* (but not *nle1WT*) in PML cells should lead to the disruption of the midbrain structures (black cross in **B, left column**).

Cb: cerebellum; OT: optic tectum; PML: peripheral midbrain layer; TS: *torus semicircularis*.

2.2 Results

2.2.1 *nle1* transcripts are accumulated in PML cells

nle1 expression was assessed via whole mount *in situ* hybridization (WMISH) at different developmental stages (**Figure 35A**). *nle1* expression pattern mimicked the expression of other PML genes (**Recher et al. 2013**). It is widely expressed after somitogenesis (24hpf) in many proliferative tissues (**Figure 35A₁**). As seen on parasagittal sections, *nle1* expression was already restricted to the ventricular cells of the midbrain (**Figure 35A₄, 35A_{4'}**). These cells are actively proliferating since, at this stage, the midbrain is expanding and the proliferation zones are not yet restricted to the periphery of the tectum (**Recher et al. 2013**). *nle1* expression became more and more restricted during development. At long-pec stage (48hpf) (**Figure 35A₂**), *nle1* was expressed in both PML and ciliary marginal zone (CMZ). Interestingly it was also expressed in the hindbrain where some cells retain neuroepithelial characteristics until adulthood and in other highly proliferative areas such as the gut and branchial arches. Moreover, *nle1* positive cells were detected in the adenohypophysis. Parasagittal sections showed that *nle1* was expressed by

few cells in the PML. Moreover, transcripts accumulate at the ventricular (apical) side of the cells (**Figure 35A₅** and **35A_{5'}**). At later stages (72hpf), *nle1* is restricted to the PML and the CMZ (**Figure 35A₃**; **35A₆**; **35A_{6'}**). Staining could still be detected in the gut. *nle1* expression could not be detected in adult neuroepithelial cells of the tectum (data not shown) and this was confirmed by transcriptomic analyses on juveniles (**Emilie Dambroise, personal communication**).

Surprisingly, the Nle1 protein is not accumulated in PML cells, but it can be detected in all cells of an AB embryo at 72hpf (**Figure 35B**).

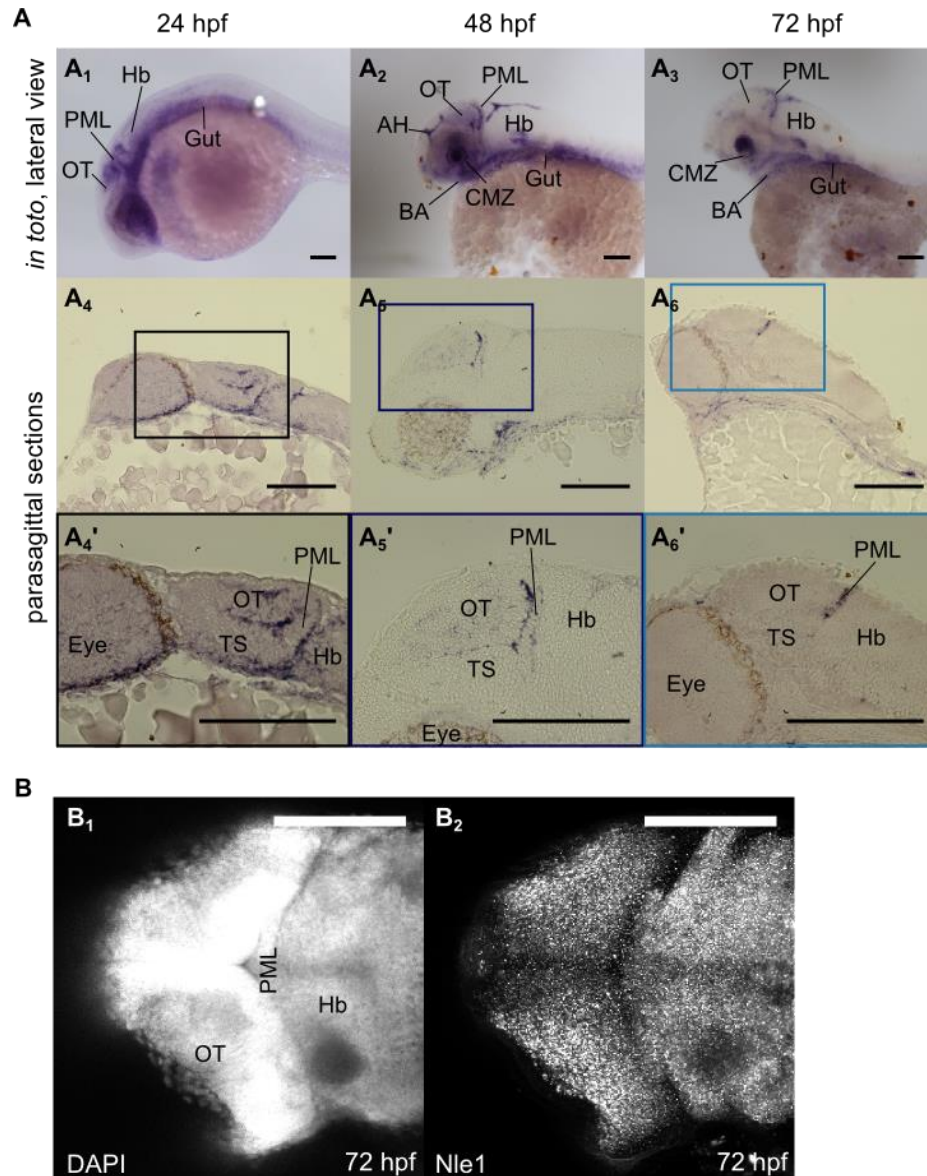


Figure 35. *nle1* transcript is over-represented in PML cells and proliferative tissues, but Nle1 protein does not show biased expression. (A) *nle1* expression analysis by *in situ* hybridization at prim 5 stage (24hpf; **A₁**, **A₄**, **A_{4'}**), long pec stage (48hpf; **A₂**, **A₅**, **A_{5'}**) and protruding mouth stage (72hpf; **A₃**, **A₆**, **A_{6'}**) performed on WT embryos (AB line). Pictures in **A₄**, **A₅** and **A₆** are taken from paraffin parasagittal sections of the embryos imaged *in toto* laterally in **A₁**, **A₂** and **A₃** respectively. Colored boxes in **A₄**, **A₅**, **A₆** define the magnified area in **A_{4'}**, **A_{5'}**, **A_{6'}** respectively. Scale bar: 200µm. **(B)** Results of the immunohistochemistry for Nle1 on WT embryos at protruding mouth

stage (72hpf). Embryos were imaged dorsally and pictures are referred to maximum projection of 60 optical sections taken medially to the tectum. In **B₁** nuclei are stained with DAPI and in **B₂** anti-Nle1 staining is reported. Merge is not represented. Voxel 0.87x0.87x0.87 $\mu\text{m}/\text{pixel}$. Scale bar: 100 μm .

AH: adenohypophysis; BA: branchial arches; CMZ: ciliary marginal zone; Hb; hindbrain; OT: optic tectum; PML: peripheral midbrain layer; TS: *torus semicircularis*.

2.2.2 Reverse genetics approaches to study *nle1* function

In order to study *nle1* function, two reverse genetics approaches were performed. First, a morpholino-based approach was undertaken. Morphant embryos displayed slight developmental delays and were less affected than embryos injected with the control morpholino (data not shown).

In order to invalidate *nle1* gene we started the generation of a knock-out via TALEN-mediated mutagenesis (**in collaboration with the AMAGEN platform**). We aimed to inactivate the *nle1* gene by targeting two different sites: one at the junction exon 1 / intron 1 and the other at the junction intron 1 / exon 2 (**Figure 36A**). We chose the first target sequence (junction exon 1 / intron 1) in order to disrupt the splice donor site at the beginning of intron 1. Successful disruption of this site should result in retention of intron 1 (19515 bp) in the processed mRNA. The second target sequence (junction intron 1 / exon 2) was chosen to induce mutations in the splice acceptor site at the end of intron 1 leading to the skipping of exon 2 (218 bp) and consequently frameshift in the open reading frame of the mRNA. Nle1 functional domain is located in the exon 2.

At present, two different mutations were isolated (**Figure 36B and 36C**). Heterozygous animals did not display any developmental defects (data not shown). F2 adults are ready to be incrossed.

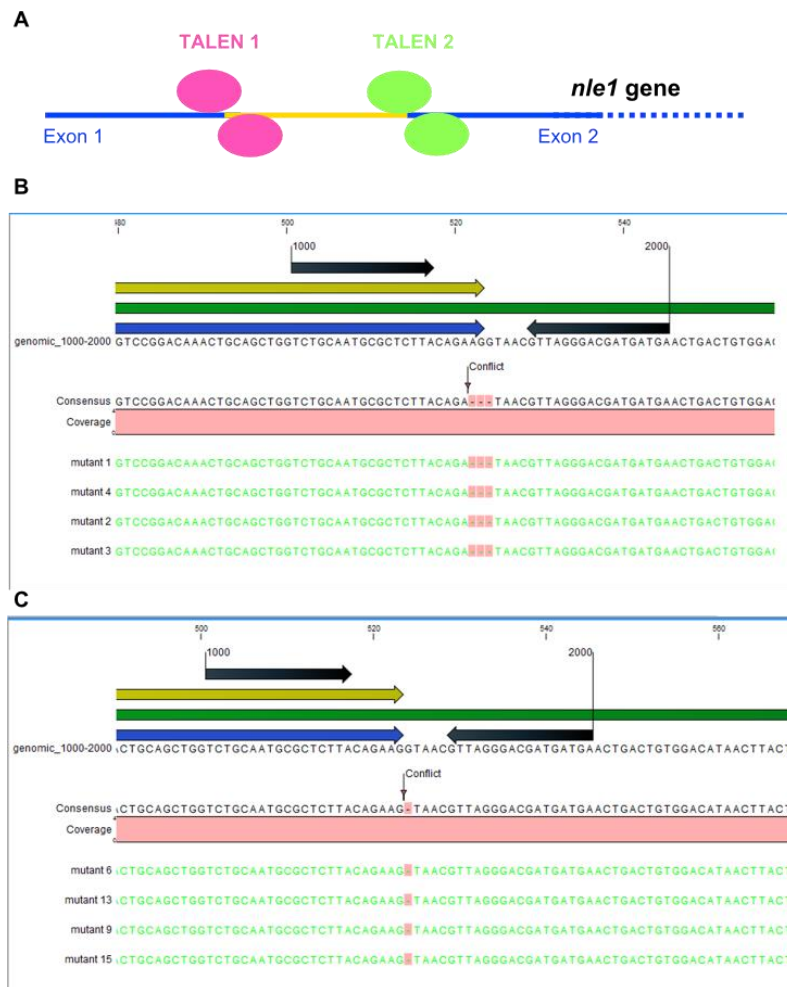


Figure 36. TALEN mediated mutagenesis of the *nle1* locus in zebrafish. (A) We designed and purchased from Collectis two TALENs in order edit the *nle1* locus in zebrafish. TALEN 1 was designed to target the junction exon 1/intron 1 (TALEN 1, pink) and the other at the junction intron 1/exon 2 (TALEN 2, green). Two mutations had been generated using TALEN 1. Thus, F1 carriers bear either a 3bp deletion (Mutation 1931.1; **B**) or a 1bp deletion at the exon 1/intron 1 junction (Mutation 1931.2; **C**). The possible outcomes of the two mutations are not known yet. Mutation 1931.1 (**B**) is expected to trigger an ORF frameshift, an exon skipping or an intron-retaining phenomena. Mutation 1931.2 (**C**) is expected to generate an ORF frameshift. Alignments in **B** and **C** had been generated with the CLC main workbench 7 software. Genomes of the F1 carriers of the mutation are indicated as mutant + number. Blue arrows: exon 1 position in the *nle1* locus; yellow arrows: CDS within the *nle1* locus; green line: part of the *nle1* locus sequenced in order to compare WT and possible mutant genomes (300bp long, cropped in figure); black arrows: TALEN 1 binding sites. Zebrafish *nle1* locus ID: NM_001020582.

2.2.3 *nle1* DN overexpression leads to developmental delays and embryonic death

A Dominant-Negative form of *nle1* had previously been generated in yeast. Hence, it had been demonstrated that the amino acid glutamate at position 114 of the yeast protein Rsa4 (ortholog of Nle1) was necessary for its function (**Bassler et al., 2010**). Moreover, the replacement of this amino-acid with an aspartate residue generated a dominant negative phenotype causing the arrest of the exportation of the 60S subunit. This glutamate residue is ultraconserved and

corresponds to the glutamate 76 of the Nle1 zebrafish protein (**Figure 37A**). The *nle1* ORF was mutated in order to code for a mutant protein with an aspartate in position (**Figure 37B**).

The injection of the *nle1-DN* mRNA in zebrafish embryos produced a broad range of phenotypes. Almost 50% of the injected embryos died within the first 48 hours of development and the ones that survived showed strong developmental delays. Interestingly, 10% of the survivors were acephalic. In contrast, the overexpression of the WT form of *nle1* did not affect embryonic development. The coinjection of both *nle1-DN* mRNA and a double dose of *nle1-WT* mRNA rescued the DN phenotypes. 48 hours after the injection, less than 20% of the embryos died (normal percentage seen after zygotic injection) and all the survivors displayed a wild type-like morphology (**Figure 38A**).

Following the initial observation that a high number of embryos died within the first two days, we examined earlier phenotypes. The overexpression of the DN form of *nle1* led to a massive block of epiboly. At later stages, when normal embryos completed epiboly, epiboly eventually started to occur in *nle1DN* injected embryos but often very abnormally (**Figure 38B**).

A

```

P25382_Rsa4_S.c. 1 MSTLIPPPSKKQKKEAQLPREVAIIPKDLPNVSIKQALDGTGDNVGGALRVEGAISEKQL 60
O74855_Rsa4_S.p 1 MATLLPFPKSKRQKESLNPTT-IEIPEKFLVNVQFRASDDSNEL-ASLLVFGNSSVRQL 58
F1QDT3_Nle1_D.r. 1 -----MSADVERVLIQLQ-DEAGEVLGSPFDVLDISPDKL 35
B2GV82_Nle1_R.n. 1 MAAAVE-----VSDEAAASDVQRLLVQFQ-DEGGQLLGSPFDVVDITPDQL 46
Q8VEJ4_Nle1_M.m. 1 --MAAA-----VVEEAAAAGDVQRLLVQFQ-DEGGQLLGSPFDVVDITPDKL 44
Q58D20_Nle1_B.t. 1 -MAAAA-----AADEAATRVDQRLLVQFQ-DEGGQLLGSPFDVVDITPDKL 45
Q9NVX2_Nle1_H.s. 1 --MAAA-----VPDEAVARVDQRLLVQFQ-DEGGQLLGSPFDVVDITPDRL 44
Q9FLX9_Nle1_A.t. 1 ----MT-----M---MDTDEGKTVMCLLT-DPEGTHLGSAMYIPEQKAGPLQL 39
          .   :   :   .   :   :   *   :   *
-----
P25382_Rsa4_S.c. 61EELLNQLNGTSDDPVPEYTESCTIQGKKASDPVKTIDITDNLVSSLIKPGYNSTEDQITLL 120
O74855_Rsa4_S.p 59EALLNQLLENSDDPVYPYFALHHE-----DETIEIQDNIYTSVFHNGLMKTEDHITLL 111
F1QDT3_Nle1_D.r. 36QLVCNALLQK-EEPVFLEFVKDAEL-----VSSLG-SCIQTGLGLETEQVLPVV 82
B2GV82_Nle1_R.n. 47QLVCNALLAQ-DEPLPLAFYVHDAEI-----VSSLG-KTLESQSVETEKIVDII 93
Q8VEJ4_Nle1_M.m. 45QLVCNALLAQ-EEPLPLAFYVHDAEI-----VSSLG-KTLESQSVETEKIVDII 91
Q58D20_Nle1_B.t. 46QLVCNALLAQ-EDPLPLAFYVHDAEI-----VSSLG-RTLESQAVETEKVLDII 92
Q9NVX2_Nle1_H.s. 45QLVCNALLAQ-EDPLPLAFYVHDAEI-----VSSLG-KTLESQAVETEKVLDII 91
Q9FLX9_Nle1_A.t. 40TQLVNRFLDN-EEMLPYSEFVVSDEEL-----LVPVG-TYLEKNKVSVEKVLITIV 86
          : * :   : : * *   :   :   : *   :   :
-----
P25382_Rsa4_S.c. 121YTPRAVEFKVPVTRSSSAIAGHGSTILCSAFAPHTSSRMVTGAGDNTARLWDCDTQTPMH 180
O74855_Rsa4_S.p 112YTPOAVERVRAVTRCTASMNGHDGTIIISAQFSPSTSSRLVTGSGDFTARLWDCDTQTPIA 171
F1QDT3_Nle1_D.r. 83YQPOAVERVRAVARCTSSLEGHTEAVISVAFSPTG-KYLASGSGDITVRFWDLSTETPHH 141
B2GV82_Nle1_R.n. 94YQPOAVERVRAVTRCTSSLEGHSEAVISVAFSPTG-KYLASGSGDITVRFWDLSTETPHF 152
Q8VEJ4_Nle1_M.m. 92YQPOAVERVRAVTRCTSSLEGHSEAVISVAFSPTG-KYLASGSGDITVRFWDLSTETPHF 150
Q58D20_Nle1_B.t. 93YQPOAIFRVRAVTRCTSSLEGHSEAVISVAFSPTG-KYLASGSGDITVRFWDLSTETPHF 151
Q9NVX2_Nle1_H.s. 92YQPOAIFRVRAVTRCTSSLEGHSEAVISVAFSPTG-KYLASGSGDITVRFWDLSTETPHF 150
Q9FLX9_Nle1_A.t. 87YQQOAVFIRIRPVNRCSTIAGHAEAVLCSFSPDQ-KQLASGSGDITVRLWDLTYTETPLF 145
          *   : * : : * * : : * * : : . : : * * * * * * * * * * * *

```

B

```

          200          220          240
nle1WT  WT base
Translation ORF TGCATTTCAGACATTGGGTCTGGAGACGGAGCAGGTGCTACCGGTGGTGTATCA
                  C I Q T L G L E T E Q V L P V V Y Q
nle1DN  DN mutation (G->T)
Translation ORF TGCATTTCAGACATTGGGTCTGGAGACGGATCAGGTGCTACCGGTGGTGTATCA
                  C I Q T L G L E T D Q V L P V V Y Q

```

Figure 37. The E114 residue in Rsa4 yeast protein is ultraconserved. Rsa4 is the yeast ortholog of Nle1. The glutamate in position 114 is ultraconserved across evolution and corresponds to the glutamate in position 76 of zebrafish Nle1. To obtain the alignment shown in **A**, the yeast protein Rsa4 was aligned with seven orthologs. For clarity, only the first 180 residues of the alignment are shown. The ultraconserved glutamate residue has been highlighted in red. The black bar above the alignment indicates the position of the Notchless functional domain in the yeast Rsa4 protein (called MIDO domain in yeast). The alignment had been generated using the clustal O algorithm in the UniProt website. Protein sequences aligned: P25382 (*S.c.*: *Saccharomyces cerevisiae*, budding yeast), OP74855 (*S.p.*: *Schizosaccharomyces pombe*, fission yeast), F1QDT3 (*D.r.*: *Danio rerio*, zebrafish), B2GV82 (*R.n.*: *Rattus norvegicus*, rat), Q8VEJ4 (*M.m.*: *Mus musculus*, mouse), Q58D20 (*B.t.*: *Bos taurus*, bovin), Q9NVX2 (*H.s.*: *Homo sapiens*, human), Q9FLX9 (*A.t.*: *Arabidopsis thaliana*). We mutated the zebrafish *nle1* ORF (ENSEMBL ID: ENSDARG0000057105:ENSDART00000148333) in order to get an aspartate at the position 76 via site-directed mutagenesis. **B** shows the alignment of the sequences of the zebrafish *nle1* ORFs (*nle1WT* and *nle1DN*) after the site-directed mutagenesis (sequence had been verified via direct sequencing). Beneath the sequences, the translated protein sequence is presented. Alignment generated with the CLC Main Workbench software.

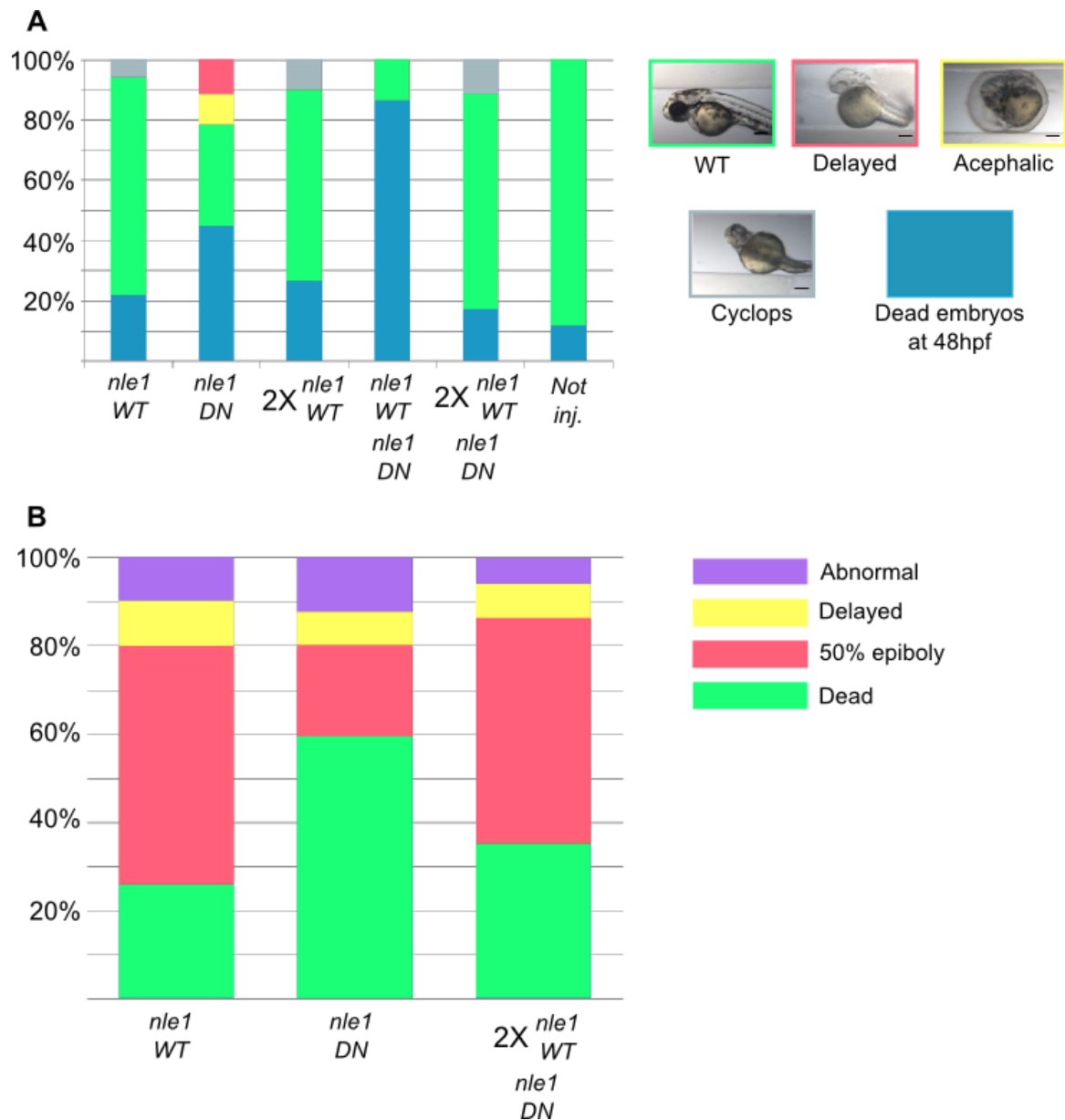


Figure 38. *nle1* DN overexpression leads to developmental delays and embryonic death. (A) The injection of *nle1*-DN mRNA in zebrafish embryos produced a broad range of phenotypes (shown on the right). Almost 50% of the injected embryos died within the first 48 hours of development and the ones that survived showed strong developmental delays. The co-injection of both *nle1*-DN mRNA and the ones that survived showed strong developmental delays. The co-injection of both *nle1*-DN mRNA and a double dose of *nle1*-WT mRNA rescued the DN phenotypes. Embryos injected: *nle1*WT (n=50), *nle1*DN (n=107), 2X *nle1*WT (n=68), *nle1*WT/*nle1*DN (n=82), 2X *nle1*WT/*nle1*DN (n=105), Not injected (n=312), total (n=724). Scale bar: 200 μ m. **(B)** The overexpression of the DN form of *nle1* led to massive embryonic death before the onset of the gastrulation. Embryos injected: *nle1*WT (n=85), *nle1*DN (n=141), 2X *nle1*WT/*nle1*DN (n=154), total (n=380). In both experiments, zebrafish WT embryos were injected at one cell stage with the following mixes of mRNA: *nle1*WT (200pg of *nle1*WT mRNA), *nle1*DN (200pg of *nle1*DN mRNA), 2X *nle1*WT (400pg of *nle1*WT mRNA), *nle1*WT/*nle1*DN (200pg of *nle1*WT mRNA + 200pg of *nle1*DN mRNA), 2X *nle1*WT/*nle1*DN(400pg of *nle1*WT mRNA + 200pg of *nle1*DN mRNA). In cases 50pg of *eGFP* mRNA were injected as control of the injection.

2.2.4 60S subunit export is not modified upon *nle1DN* overexpression

Imaging-based techniques were used to determine whether 60S subunit export was blocked in PML cells, as expected. In particular, we wanted to directly visualize the relative localizations of the two ribosomal subunits and their immature precursors. This could be achieved by assessing the localization of the ribosomal proteins (RP) within a cell by direct immune-labeling (RP-IF), or alternatively by monitoring rRNA maturation via *in situ* hybridization (RNA-FISH). This latter protocol was developed recently by Pierre-Emanuel Gleizes group (O'Donohue *et al.* 2010). **Figure 39** illustrates both the techniques and the expected phenotypes of cells. Protocols to assess cell-specific ribosome biogenesis were first tested on zebrafish cultured cells (ZFTU line).

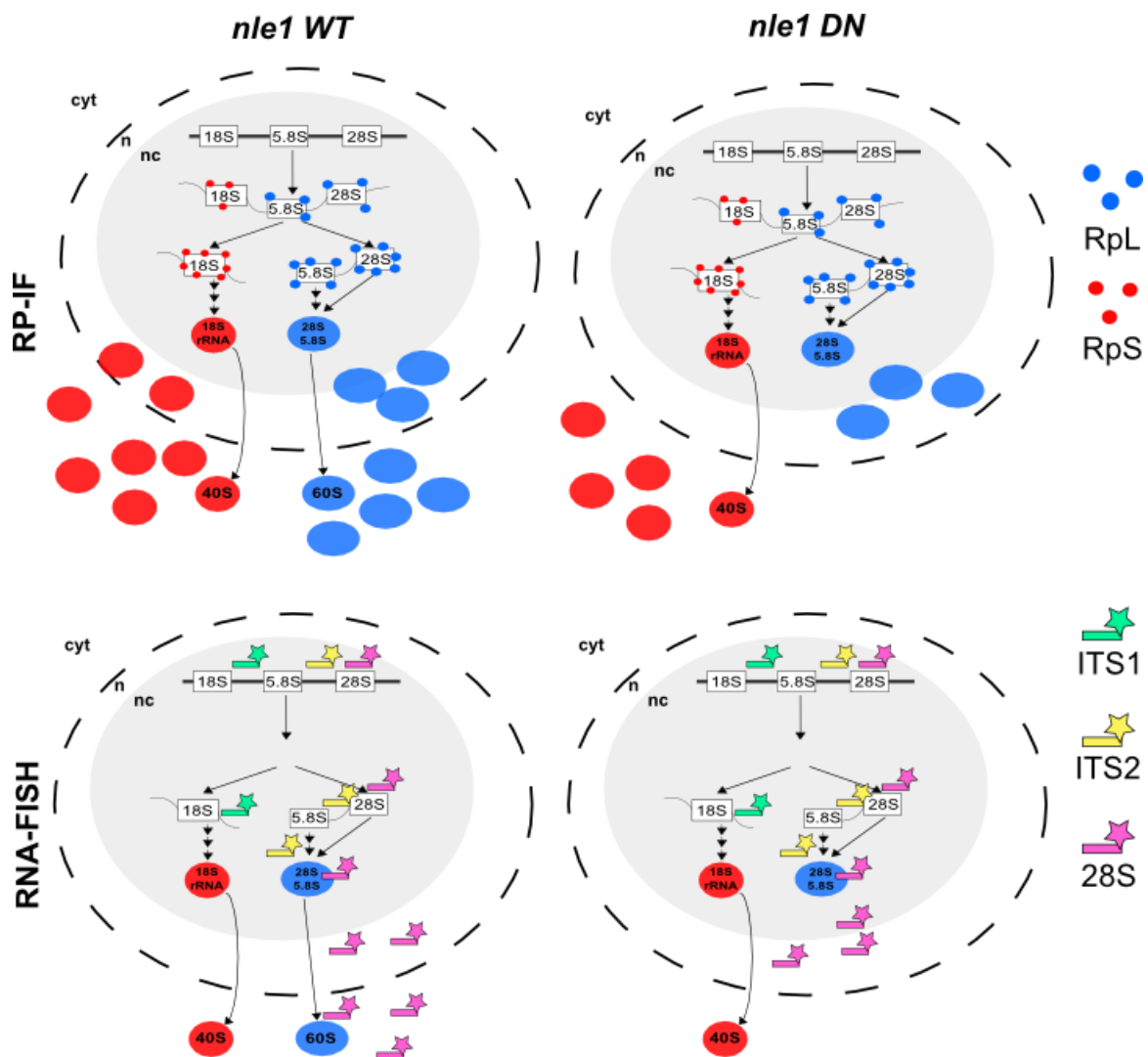
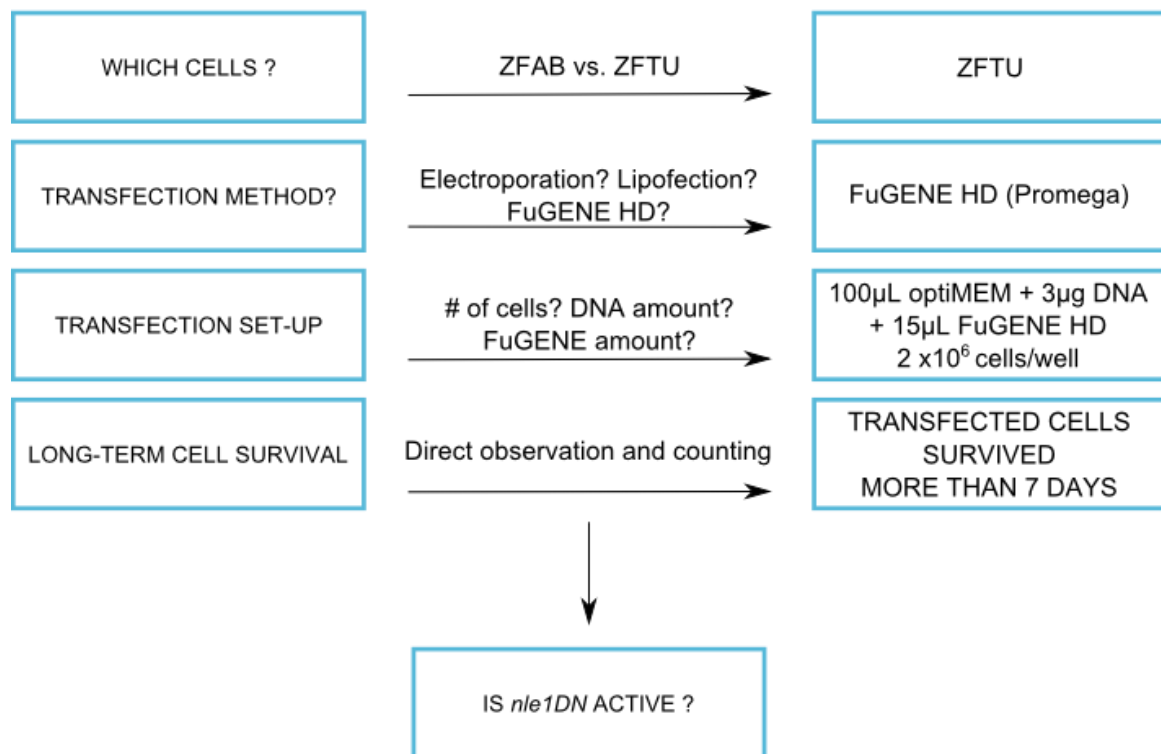


Figure 39. Assessment of the ribosome biogenesis at the cellular level. Ribosome biogenesis progression can be assessed by direct staining of either the ribosomal proteins (RP-IF) or the mature/immature rRNAs (RNA-FISH). We expect the blockage of the 60S subunit exportation. Thus, upon overexpression of *nle1DN* we expect to not find anymore rpl proteins nor the 28S_rRNA probe in the cytoplasm. ITS2 probe should accumulate in the nucleolus.

Both WT and DN *nle1* ORFs expressed under the control of a CMV promoter were transfected in ZFTU cells. eGFP under the control of the same promoter was used as a positive control for the transfection and as negative control for subsequent phenotyping of the transfected cells. **Figure 40A** illustrates all the steps needed to set-up the transfection protocol. 48 hours post transfection, cells were fixed and ribosome biogenesis was assessed (**Figure 40B**). No construction was deleterious for cell survival and no difference in terms of ribosome biogenesis was highlighted between cells transfected with the different constructions (**Figure 40B**).

A



B

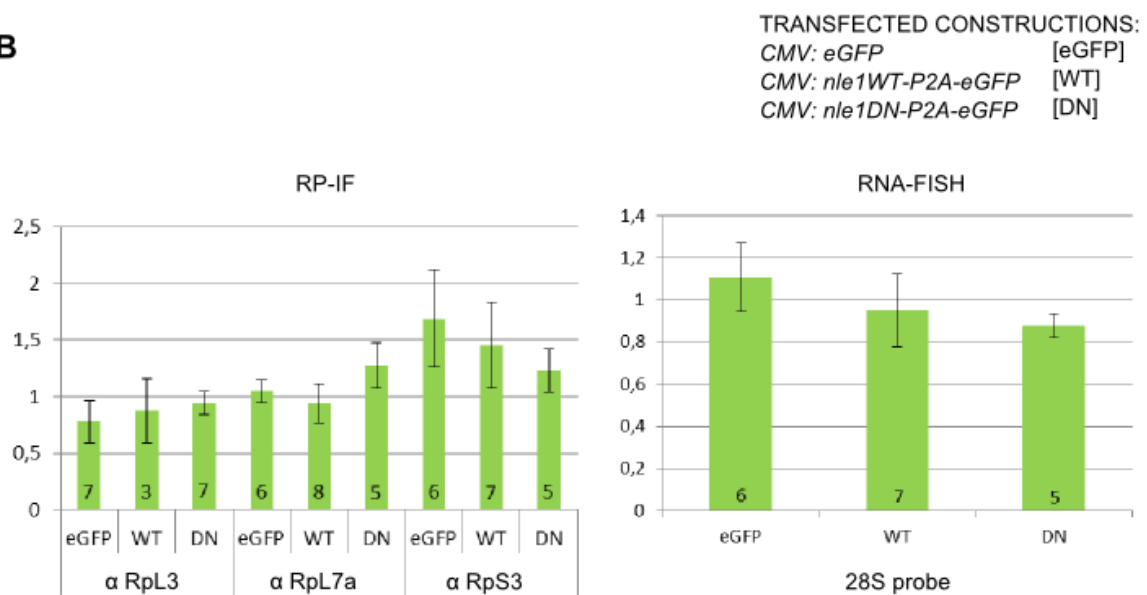


Figure 40. 60S subunit export is not modified upon *nle1DN* overexpression. In order to assess whether the exportation of the 60S subunit was impaired upon overexpression of the DN form of *nle1*, we undertook a series of *in vitro* experiments using the ZFTU cell line (unpublished). **A** illustrates all the passages that had been necessary in order to achieve a proper transfection of the cultured cells. Once transfection was set up (**B**), we transfected the cells with three constructions listed above the plots. Cells were fixed 48 hours post transfection and ribosome biogenesis was assessed by RP-IF (**left plot**) and RNA-FISH (**right plot**). In both cases a fluorescent staining was realized: RPs were directly detected with specific antibodies (α -RpL3 and α -RpL7a for the 60S).

Zebrafish constructs were also transfected in murine ES cells. No construction was deleterious for cell survival and no stable transfection was achieved (Michel Cohen-Tannoudji, Pasteur Institute, personal communication).

In order to overcome the cell culture-related issues, I moved towards a novel approach thereby mixing *in vivo* and *in vitro* techniques. To this aim, I injected both *nle1WT* and *nle1DN* mRNAs in *enh101-hsp70: GFP* line (101 line; **Aurélie Heuzé, unpublished**) and performed RNA-FISH with ITS2 probe on dissociated cells 48 hours after injection. Thus, PML cells could be identified in any moment since they are GFP positive. No 60S subunit exportation defects were highlighted in GFP positive cells (data not shown)

2.2.5 PML-specific *nle1DN* overexpression triggers cell death in the tectum

A transgenesis-based approach was then used in order to study whether *nle1* plays a specific role in PML cells. To this aim *nle1WT* and *DN* coding sequences (CDSs) were subcloned in expression vectors suitable for transgenesis in fish. Vectors used have been designed by the AMAGEN platform (Gif-sur-Yvette, France). They allowed the expression under the control of specific *cis*-regulatory elements (either promoters or enhancers). Moreover they bear recognition sequences both for ISce1 (**Thermes et al., 2002; Soroldoni et al., 2009**) for transitory expression and *Tol2* (**Kawakami, 2007; Suster et al., 2009**) for genomic integration of the transgene in zebrafish. Cells bearing the transgene could be easily detected thanks to the coexpression of eGFP linked to Nle1 via a self-cleavable P2A viral peptide (**Provost et al., 2007**) (see **Figure 41** for details).

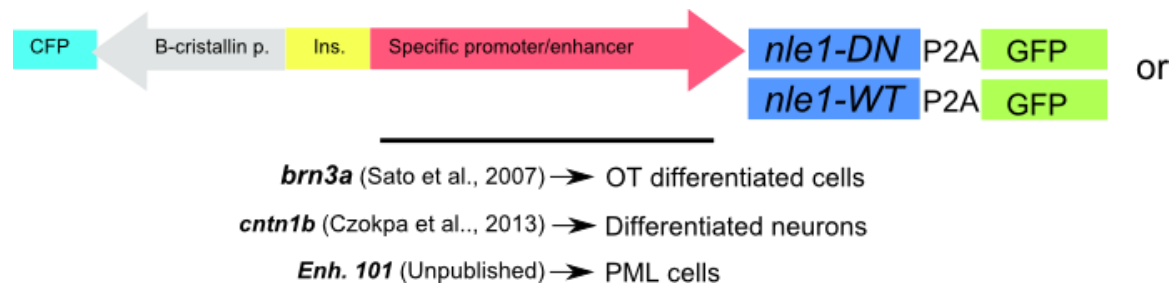


Figure 41. Transgenesis strategy. In order to target the overexpression of the *nle1* ORFs in the OT, different promoters were tested. Promoters for differentiated cells (*brn3a* and *cntn1b*) failed to drive the expression of the transgenesis constructions (*nle1WT-P2A-eGFP* and *nle1DN-P2A-eGFP*), but not the driver for PML cells (*Enh. 101*, isolated within our group) which was used for this work. Genomic insertion could be verified thanks to the expression of CFP (driven by the β -cristallin promoter) in the lens of the injected embryos.

While no one of the tested promoters was able to drive expression of the *nle1* ORF in differentiated cells of the tectum, the enhancer 101 efficiently drove expression of all the transgenes in PML cells

In order to get insight about the effects of the targeted overexpression of *nle1* (WT or DN), we imaged (at different developmental stages: 48hpf, 72hpf and 96hpf) *ef1a:H2B-mcherry* embryos injected either with *enh101-hsp70:nle1WT-P2A-eGFP* or *enh101-hsp70:nle1DN-P2A-eGFP* construction (**Figure 42 A**).

Embryos injected with *enh101-hsp70: nle1WT-P2A-eGFP* developed normally with WT-like tecta. On the contrary, embryos injected with *enh101-hsp70: nle1DN-P2A-eGFP* displayed delayed tectal formation. Green healthy-looking cell clones can be detected over time in the central part of the tectum of embryos injected with WT construction. Embryos injected with *enh101-hsp70: nle1DN-P2A-eGFP* displayed low embryonic survival after injection and living embryos displayed huge clusters of bright-green dead cells located ventrally to the tectum. (**Figure 42B**).

These data indicate that *nle1* might be necessary for the survival of the neuroepithelial cells of the tectum.

2.3 Discussion

With this work we wanted to demonstrate that *nle1* is necessary in neuroepithelial cells and dispensable in differentiated cells. To this aim, we generated a DN form of *nle1* whose expression had to be targeted in different areas of the zebrafish brain.

Although the DN form of *nle1* seems to be active *in vivo*, we failed to demonstrate a DN-dependent impairment of the ribosome biogenesis. Moreover, due to the lack of efficient drivers, the targeted overexpression of *nle1DN* in differentiated cells could not be achieved so

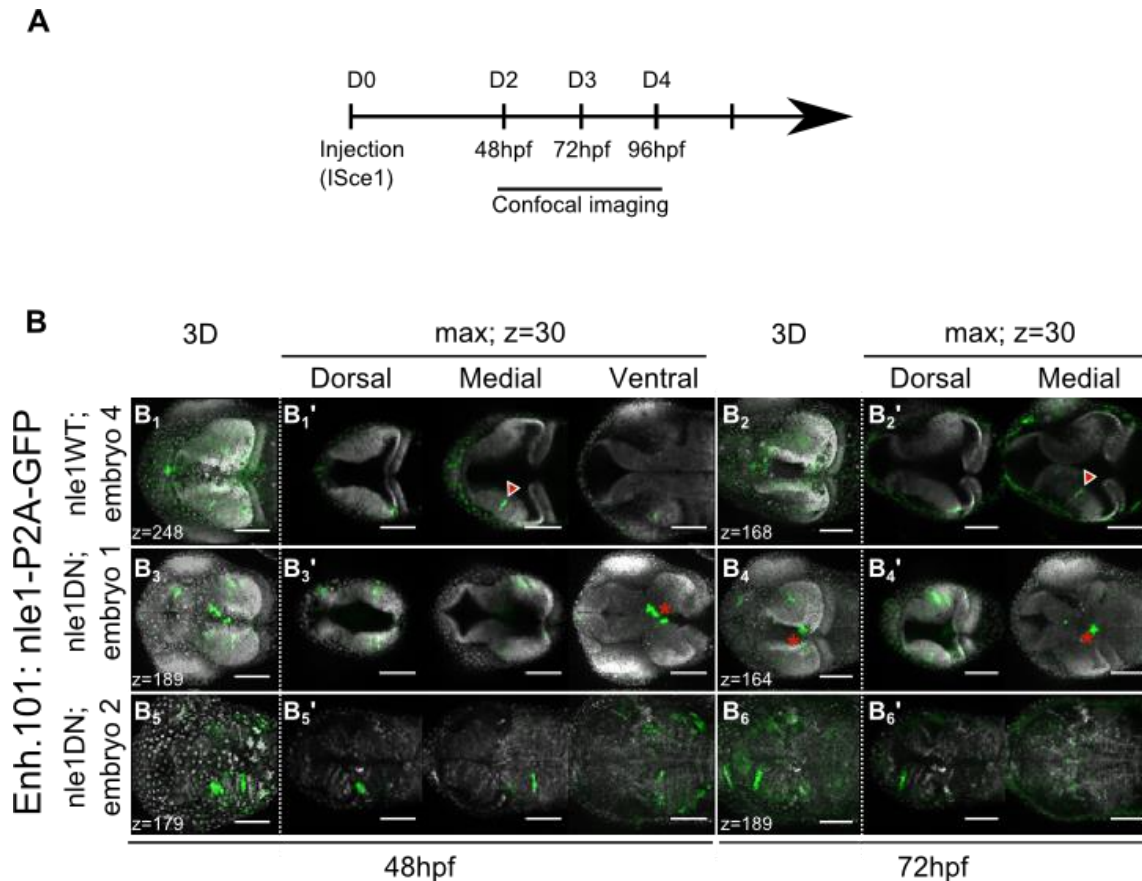


Figure 42. PML-specific *nle1DN* overexpression triggers cell death in the tectum. In order to get insight about the effects of the targeted overexpression of *nle1* (WT or DN), we imaged (at different developmental stages: 48hpf, 72hpf and 96hpf) *ef1a:H2B-mcherry* embryos injected either with *enh101-hsp70:nle1WT-P2A-eGFP* or *enh101-hsp70:nle1DN-P2A-eGFP* construction. **A** shows the experiment timeline. Embryos injected with *enh101-hsp70: nle1WT-P2A-eGFP* developed normally with WT-like tecta (**B₁-B₂**). On the contrary, embryos injected with *enh101-hsp70: nle1DN-P2A-eGFP* displayed delayed tectal formation (**B₃-B₆**). Green healthy-looking cell clones can be detected over time in the central part of the tectum of the embryos injected with the WT construction (red arrowhead in **B₁'** and **B₂'**). The central position of these clones might be due to the early activation of the enhancer 101. Embryos injected with *enh101-hsp70: nle1DN-P2A-eGFP* displayed low embryonic survival after injection and living embryos displayed huge clusters of bright-green dead cells located ventrally to the tectum (red asterisks in **B₃'** and **B₄'**). Injections were performed in *ef1a:H2B-mcherry* embryos. Green: eGFP; White: mCherry. Embryos were imaged dorsally. Every line contains pictures taken from the same embryos over time. Within the same line, 3D projections of the whole brain are presented (**B₁, B₂, B₃, B₄, B₅, B₆**) and maximum projection of 30 optical sections taken at different z-levels (**B₁', B₂', B₃', B₄', B₅', B₆'**). Voxel 48hpf: 0.79x0.79x0.79 μ m. Voxel 72hpf: 0.86x0.86x0.86 μ m. Scale Bar: 100 μ m.

far. Thus, demonstrating that *nle1* play a specific role in PML cells homeostasis appeared to be a technical challenge. Further analyses will be therefore needed. In particular, we will look at earlier stages if ribosome biogenesis is blocked in epiboly blocked embryos. Indeed, the activity of the *nle1* mRNAs is likely to be stronger at this stage.

2.3.1 Finding the good way to assess ribosome biogenesis in zebrafish

Among the protocols which are currently used in yeast, the polysome profiling has been successfully used also in zebrafish (**Pereboom *et al.*, 2011; Essers *et al.*, 2014**). Northern blots using probes for immature and mature species of the rRNAs are used to assess ribosome biogenesis impairments in zebrafish as well (**Azuma *et al.*, 2006**). Finally, ribosome biogenesis could be assessed by measuring the relative amounts of 18S and 28S rRNAs after total RNA extraction (**Qin *et al.*, 2014**). Although efficient, these approaches cannot detect ribosome biogenesis defects at the cellular levels, but they could be used on whole embryos. The original hypothesis of my project was that PML cells specifically require *nle1* and not the differentiated cells of the tectum. For this, a DN form of *nle1* had to be specifically expressed in the two cell populations (see **Figure 34**). Thus, ribosome biogenesis was expected to be differentially impaired in two juxtaposed cell populations thereby excluding the possible use of whole mount approaches. Nevertheless, these approaches could have been used to assess ribosome biogenesis after mRNA injection on embryos at early stages in order to have a clear picture of the action of the DN negative form of Nle1. On the short term, measurements of the relative amounts of 18S and 28S rRNAs will be performed to allow the publication of the present work. Nonetheless, this control must be performed carefully since ribosome biogenesis might trigger the loss of one of the two rRNA species (28S in the present work). The evaluation of the 28S/18S should be done on the total RNA extracted from an equivalent number of cells rather than on equivalent amount of total RNA extracted from injected embryos (**LeBoutellier *et al.*, 2013**).

We chose to assess ribosome biogenesis at the cellular level by directly visualizing ribosomal proteins or mature and immature rRNA species (see **Figure 39**). These approaches were hard to set up since they are fixation-dependent and so far they failed to work on tissue, so we are currently performing these experiments on early stages, when penetration of probe might be less hard to achieve. Thus, they appeared to be inefficient to detect cell-specific defects. An efficient positive control with impaired ribosome biogenesis is currently missing. Testing these protocols on ribosome biogenesis mutants (such as the the box C/D snoRNP mutants,) will allow to verify their efficiency.

2.3.2 Is the DN mutation active in zebrafish?

At present, nothing demonstrates that the zebrafish DN form of *nle1* is not active. Transitory overexpression via mRNA injection proves that phenotypes seen are *nle1DN*-specific (**Figure 38**). Moreover targeted expression of Nle1DN in PML cells disrupted tectum development (**Figure 42B**). All together, these findings tell us that the DN mutation has got an effect in zebrafish. Nevertheless, ribosome biogenesis defects could not be documented. For this, many explanations might exist. For instance, it could be possible that the phenotyping methods used were not well suited. Moreover, ZFTU cell line had been established from whole zebrafish larvae and they display a fibroblast-like phenotype. No 60S subunit exportation defect has been seen. This might be an indirect proof that Nle1 is dispensable in certain cell types. *nle1* expression is higher in a restrict number of tissues (**Figure 35**). This would explain the lack of ribosome biogenesis-related phenotypes in ZFTU cells. Moreover, no zebrafish construct was deleterious for cell survival and no stable transfection was achieved upon transfection in murine embryonic stem cells. This might be due differences between the zebrafish and mouse protein. Indeed, there is only 75% identity on the whole protein sequence and only 68% identity on the N-terminal part where the DN aminoacidic substitution is located.

Finally, nothing is known about the stability of either *nle1* mRNA or Nle1 protein. Thus, ribosome biogenesis assessment 48 hours after mRNA injection might be too late in time. The cell-dissociation of embryos injected with the transgenesis constructions might help to get insight into the question since, in this case, consistent levels of the exogenous *nle1* (WT or DN) will be maintained over time. Moreover, ribosome biogenesis could be assessed on mRNA-injected embryos before 48hpf. Nonetheless, in the absence of more evidence for perturbation of ribosome biogenesis, it must be taken in account the fact that Nle1-DN might act in a ribosome biogenesis independent-manner.

2.3.3 Does *nle1* play a specific role in progenitor cells?

Since we never managed to target *nle1* overexpression in differentiated cells of the tectum, the demonstration that Nle1 is dispensable in these cells is still lacking in zebrafish. Among the many promoters that have been tested, are the *brn3a* promoter (**Sato et al., 2007**) and the *cntn1b* promoter (**Czopka et al., 2013**). Although able to drive the expression of simple fluorescent proteins, these promoters failed to drive the expression of bigger constructions (*nle1-P2A-eGFP*). Indeed, no GFP positive cells could be detected after injection. Whether they were not capable to drive the expression of the whole polycistronic sequence or just eGFP is not known. Nevertheless, a direct Nle1-eGFP fusion might not allow the correct positioning of Nle1 within

the immature 60S subunit. In order to overcome this problem, we are currently cloning other possible drivers.

Until recently, conditional knock-out could not be performed in zebrafish (**Ablain et al. 2015**) and driver-independent strategies had been discarded at the beginning of this work. For example, in order to achieve the targeted overexpression of *Nle1*, we evaluated the possibility to follow a strategy based on photo-activated genetic recombination. For this, *nle1* ORFs had to be subcloned in Mosiman's *ubi:switch* construction (*ubi:loxP-EGFP-loxP-mCherry*) (**Mosimann et al., 2011**) by substituting the *mCherry* ORF *nle1-P2A-mCherry* ORF. Transgenic lines (WT and DN) should have been generated. After crossing these lines with the *Tg(-3.5ubi:cre^{ERT2};cmlc2-EGFP)*, overexpression of the *nle1WT* or *nle1DN* ORF would have been induced upon tamoxifen-driven Cre/Lox recombination. Search for cell-specific promoters would have been avoided by using caged 4-hydroxy-tamoxifen and light to uncage the tamoxifen (**Sinha et al., 2010**). Alternatively, photomorpholinos could have been used to specifically knock-down *nle1* either in PML cells or in differentiated cells of the tectum (**Tallafuss et al., 2012**). Although promising, both methods had been avoided since light controlled overexpression could have been performed only at early developmental stages. Indeed, ubiquitin-driven *cre^{ERT2}* expression decreases during development. Similarly, photo-morpholino concentration decreases over time (since photo-morpholinos are not genetically encoded). Novel CRISPR-based techniques will allow the precise knock-in of *nle1* ORFs under the control of tissue specific promoters thereby allowing targeted overexpression (**Hisano et al., 2015**).

CHAPTER 3

FINAL REMARKS

1. THE TELEOST PML AS MODEL TO STUDY NEUROEPITHELIAL CELLS

The optic tectum is a life-long growing structure of the teleost midbrain. This feature got a lot of attention in the teleost community. On one side, the continued growth of the teleost visual system has got some exciting functional applications. Indeed, novel connections must be generated on a daily basis in order to continuously maintain the Cartesian map of the surrounding visual space (**Cervený et al., 2012**). Thus, the teleost optic tectum has become an important model to study synaptic plasticity. Moreover, continued proliferation must be tightly controlled over time and this makes the OT a good model to answer cell cycle related questions. In this context, the study of the neuroepithelial progenitors of the peripheral midbrain layer (PML) gains importance. We demonstrated that PML cells contribute both to the OT and to the *torus semicircularis*. Nevertheless, many questions remain unanswered.

The PML originates in the territory of the midbrain/hindbrain boundary probably under the influence of the isthmic organizer. In this area some cells start to express *her5* and contribute to the formation of both midbrain and hindbrain structures during somitogenesis (**Talafuss and Bally-Cuif, 2003**). These cells do not contribute to the formation of the OT at adulthood (**Chapouton et al., 2006**). Thus, the progeny of the *her5+* cells might contribute only to the initial expansion of the OT, then PML cells become responsible for the radial growth of the OT (**Recher et al., 2013**). Mechanisms and timing of PML specification within the midbrain/hindbrain territory are not known. Nevertheless, a single marker to identify univocally PML cell (and neuroepithelial cells) is missing (**Table 1**) and the knowledge of the early specification of the PML cells is far to be achieved.

Our 4D-imaging experiments highlighted that PML cells continuously divide (**Recher et al., 2013**). This feature persists until adulthood, as demonstrated both in medaka (**Alunni et al., 2010**) and zebrafish (**Ito et al., 2010**), but self-renewal of these cells has never been demonstrated. Neuroepithelial cells of the neural tube divide symmetrically first and asymmetrically later (**Götz and Huttner, 2005**). The first kind of division is non-neurogenic (two neuroepithelial cells originates from a neuroepithelial progenitor) whereas the second is neurogenic. Neurogenic asymmetric divisions occur at the apical (ventricular) surface with the cell committed towards neuronal fate localized more apically (**Alexandre et al., 2010**). We found that most divisions of PML progenitors are within the plane of the neuroepithelium. Most of the observed mitotic events (94.3%) are planar and only a few (5.7%) are apical-basal (**Recher et al., 2013**). It would be logical to assume that the planar divisions are responsible for the expansion of the PML progenitor pool and the second kind responsible for the expansion of the tectum. Nevertheless, our cell-tracking never highlighted that daughter cells remain confined in the PML region. For

this reason, at the time of the publication, we never used the term “stem cell” to define PML progenitors. Thus, it would be interesting to get insight about the division mode of PML cells by using techniques involving mosaic labeling of the PML cells (see **Alexandre et al., 2010**, for comparison). This will allow checking for PML cells self-renewal. Nevertheless, the possibility that PML cells might actually be of intermediated progenitors cannot be excluded.

2. THE TELEOST PML IS CHARACTERIZED BY A SPECIFIC MOLECULAR SIGNATURE

One of the most interesting features of PML cells is represented by their genetic signature. Gene ontology analysis demonstrated that the transcriptome of PML cells is enriched in mRNAs coding for nucleotide and ribosome biogenesis (**Recher et al., 2013**). This was confirmed by a transcriptomic analysis on 1 month old medaka brains (**Dambroise, Simion et al., submitted**). In this experiment the transcriptome of PML cells was compared to the transcriptome of differentiated cells of the tectum. These transcripts were enriched by 2 or 3 folds in PML cells compared to other cells in tectum. It is not known whether these transcripts play a functional role or whether they are stored in order to supply fundamental transcripts for the adjacent fast amplifying progenitors. Nonetheless, in recent years, a wealth of papers was published highlighting a functional relationship between ribosome biogenesis and stem/progenitor cell homeostasis. Interestingly, transcriptomic analysis highlighted that neuroepithelial cells of the tectum also express genes that have been involved in human microcephalies: *mcp1* (*microcephalin*), *casc5* (*cancer susceptibility candidate 5*), *aspm* (*abnormal spindle like microcephaly-associated protein*), *cenpj* (*centromere protein j*) and *phc1* (*polyhomeotic-like protein 1*) (**Dambroise, personal communication**).

3. APOPTOSIS AT THE G2/M TRANSITION

During my PhD, I performed a study of the functional relationship between ribosome biogenesis and PML cell homeostasis. Since ribosome biogenesis is fundamental for all cells, its study at the cellular level represents a technical challenge. Thus, traditional knock-out should be avoided. At first sight, snoRNP mutants displayed severe phenotypes affecting the neuroepithelial-derived structures (i.e. tectum and retina). After a more careful analysis all cells seemed to be affected by the depletion of the components of the box C/D snoRNP complex. Moreover, we demonstrated that the *fb1* depletion might lead to arrest of the cell cycle at the G2/M transition.

Of note, Fbl is a multifunctional protein and this versatility is due to its interaction with many partners (**Rodriguez-Corona et al., 2015**). The typical Fibrillarin interacting partners are Nop56 and Nop58 which interact with the methyltransferase only for the methylation of the nascent rRNAs. The depletion of the genes coding for Nop56 and Nop58 in zebrafish leads to phenotypes which are similar to the phenotypes seen in *fbl* mutants. Data from *nop56* and *nop58* are more fragmented than the data obtained with *fbl* mutant, but the commonalities among the three phenotypes suggest that the mutant phenotype is linked to the impaired methylation of the newly synthesized rRNAs.

With our experiments we cannot say that components of box C/D snoRNP complex are specifically necessary for the survival of the neuroepithelial cells of the PML. Indeed, snoRNP mutants displayed correctly shaped PMLs, with little or no apoptosis. Other cell types, instead, seem to undergo massive apoptosis at the G2/M transition. Interestingly a relatively high portion of the PML cells seems to be arrested in G2/M (**Dambroise, personal communication**). Moreover, PML cells cycle at significantly lower rates than the adjacent fast-amplifying progenitors (**Recher et al., 2013**). All together these findings suggest that PML cells might be longer protected from death because their survival relies on the maternal stocks of ribosomes or on the stocks of ribosomes correctly methylated by the maternally-provided components of the box C/D snoRNP complex. Nevertheless, this might just be temporary since mutant embryos die within the first six days of development.

Understanding what happens outside the PML is even trickier. We highlighted that mutant cells can be arrested at the G2/M transition. Cells might endoreplicate before being arrested at the G2/M in transition in a p53-dependent manner. Understanding the mechanisms leading to this phenotype might get insight into the process of tumorigenesis. Other “canonical mechanisms” are for sure involved. FBL methylates the Q104 of the human H2A histone and this modification is necessary for the recruitment of the RNA polymerase I on the rDNA loci (**Tessarz et al., 2014**). Thus, the total rRNA transcription might decrease upon Fbl depletion and this would free ribosomal components that could contribute to cell cycle arrest in a p53-dependent or independent manner (**James et al., 2014**). The depletion of genes coding for the components of the box C/D snoRNP complex would lead to the synthesis of ribosomes with hypomethylated rRNAs. Thus, ribosomes are functional and probably the free ribosomal components are not enough to start a proper nucleolar stress response at the G1/S transition, but enough to start the stabilization of p53 and increase its nuclear levels. p53 acts as transcription factor and its stabilization leads to the expression of cell cycle arrest genes and pro-apoptotic factors. p53 can also interact with many partner via protein-protein interactions (**Vaughan et al., 2014**). Thus,

cell death might be delayed at the G2/M transition in some cells. To conclude, further investigations are required to fully understand the phenotypes of the snoRNP mutants at the molecular level.

4. FUNCTIONAL STUDY OF *nle1*

nle1 display higher expression in PML cells compared to adjacent cells and we wondered whether it might play a specific roles for the maintenance of these cells. To this aim, I generated a putative DN form of *nle1* to be overexpressed either in PML cells or in differentiated cells of the tectum.

This project encountered several technical difficulties. I could not find a good driver to target the overexpression of *nle1* ORFs in differentiated cells of the tectum. Indeed, both *brn3a* promoter (**Sato et al., 2007**) and *cntn1b* promoter (**Czopka et al., 2013**) failed to express big constructions in differentiated neurons. In order to overcome this problem, I started to test putative enhancer sequences. For this I looked for conserved regions in the intergenic spaces in the genomes of medaka and zebrafish. In particular, I focused my attention on two enhancer identified in medaka by Laurence Ettwiller's group (**Mongin et al., 2011**). The enhancer of the medaka genes *foxb1a* and *ebf3* were able to drive the expression of a fluorescent protein in the center of the tectum in medaka. Nonetheless, the corresponding regions in the zebrafish genome that I have cloned failed to drive the expression of *nle1* ORFs in zebrafish tectum. Probably an enhancer screen, performed at the beginning of my PhD would have overcome this problem. Other elements are currently being tested (**collaboration with BMGif platform**) and I hope to be able to target the overexpression of *nle1* ORFs to the center of the tectum. This will allow me to confirm that *nle1* is necessary in neuroepithelial cells and dispensable in differentiated cells of the tectum.

Transient overexpression of *nle1DN* is deleterious for embryonic development in zebrafish (**Figure 37**) and its targeted overexpression in neuroepithelial cells leads to cell death in the tectum (**Figure 41**) suggesting the *nle1DN* is active in zebrafish. Obviously these findings do not verify our initial hypothesis, but they do not exclude the possibility that the *nle1* is necessary for the survival of the neuroepithelial cells in zebrafish. Other experiments, at early developmental stages are currently underway to confirm our hypothesis. Nevertheless, I could not verify that the exportation of the 60S subunit was blocked upon *nle1DN* overexpression. Reasons for this have been extensively discussed in the results section. Also in this case, other experiments are

currently undertaken, and, the possibility that *nle1DN* might act in a ribosome-biogenesis independent manner cannot be excluded.

Nle1 is necessary for the survival of both hematopoietic stem cells (**Le Boutellier *et al.*, 2013**) and intestinal stem cells (**Stedman *et al.*, 2015**). Hence, the demonstration of the essential role of Nle1 in zebrafish neuroepithelial cells would highlight a conserved role of this protein between different progenitor cell types and across evolution.

CHAPTER 4
EXPERIMENTAL PROTOCOLS
AND REAGENTS

EXPERIMENTAL PROTOCOLS AND REAGENTS

1 GENERAL METHODS

1.1 Fish lines and husbandry

For this work the following zebrafish lines were used: wild-type, strain AB; “snoRNP” mutants, *fb^{hi2581}*, *nop56^{hi3101}*, *nop58^{hi2581}* (ZIRC, Eugene, OR, USA); zFucci, *Tg(EF1α:mKO2-zCdt1(1/190))^{rw0405b,d}* × *Tg(EF1α:mAG-zGem(1/100))^{rw0410h}* (Riken Brain Science Institute, Yokohama, Japan); *Tg(Xla.Eef1a1:H2B-mCherry)* (gift from Georges Lutfalla, Université Montpellier 2, Montpellier, France); *nle1* mutants: 90.1931 (Amagen, Gif sur Yvette, France, unpublished); *enh101-hsp70:GFP* (Aurélié Heuzé, Gif sur Yvette, France, unpublished).

All fish were reared according to standard procedures and staged as previously described (Kimmel *et al.*, 1995). The creation and maintenance of *nle1* mutant lines and *enh101-hsp70:GFP* line were approved by the local ethics committee.

1.2 Microinjection of zebrafish embryos

Embryos at the one-cell stage were placed in an agarose mold adapted to maintain them immobile; embryos were oriented and the cell was placed at the top of the embryo. Glass capillaries with one sharp end were prepared and filled with the injection solution containing the mRNA (at the desired concentration) or the transgenesis mix (15ng/μl transgenesis construction + 7.5U ISce1 meganuclease or 8ng/μl *tol2* mRNA) to inject. The injected volume was adjusted by varying the injection pressure and time on a PicoSpritzer injector and measuring the size of the injected droplet on a graduated glass overlaid with mineral oil. 1nl of the solution was injected in the cell of each fish embryo.

48hpf embryos were prepared similarly for injection and injected in the yolk.

1.3 Histology

Paraffin sections: PFA-fixed embryos were dehydrated in ethanol solutions of increasing concentrations (80%, 95%, 100%) and were then incubated in butanol before embedding in paraffin. Serial sections (8 μm) were prepared with a Leica rotary microtome and mounted according to standard procedures.

Cryosections: PFA-fixed embryos were first protected by incubation in 30% sucrose/phosphate-buffered saline (PBS) for 12-16 hours at 4°C, then embedded in OCT Compound (Sakura), stored at -80°C, and sectioned at 14 μm using a Leica cryostat. Embryos used for immunohistochemistry on cryosections were treated overnight with ethanol (70%) at 4°C before sucrose cryoprotection.

1.4 Imaging

Brightfield imaging was performed with a Nikon Eclipse E800 microscope (Camera: Nikon Digital Camera DXM1200; Objectives: PlanFluor 10X/0.3 DIC L, PlanFluor 20X/0.5 DIC M, PlanFluor 40X/0.75 DIC M) or a Nikon AZ100 microscope (Camera: Nikon Digital Sight DSRi1; Objectives: AZ PlanApo 1X/0.1; AZ PlanApo 4X/0.4). Stained cryosections were imaged with a Zeiss AxioImager M2 microscope equipped with ApoTome (Camera: AxioCam Mrm; Objectives: FLUAR 5X/0.25, FLUAR 20X/0.75, ACHROPLAN 40X/0.80 W, Plan-NEOFLUAR 40X/1.3 Oil DIC, Plan-APOCHROMAT 63X/1.4 Oil DIC). *In toto* imaging and imaging of cells were performed using a Confocal Laser Scanning microscope (Leica SP8) with internal PhotoMultiplier Tubes (Airy: 1; Objectives: Fluotar VISIR 25x/0.95 WATER; Plan-APOCHROMAT 40x/1.10 WATER).

2 GENOTYPING

Note. Genotyping was carried out on adult fish (at each generation) to identify carriers of the mutant alleles. Many genotyping rounds were carried out on cohorts of putative mutant embryos in order to allow the visual identification of the mutant embryos without any mistake.

2.1 Lysis of embryos and fin clips

48hpf putative-mutant and WT embryos were euthanized with a lethal dose of tricaine MS222 (Sigma) buffered with sodium bicarbonate, placed individually in 50µl of lysis buffer (10mM Tris-HCl pH 8.0, 50mM KCl, 0.3% Tween 20, 0.3% Igepal CA-630 [Sigma], 4mM EDTA) supplemented with proteinase K to 250ng/µl just before use. Lysis was performed for 16 h at 55°C and proteinase K was subsequently inactivated by incubation for 10 min at 95°C.

For fin clip lysates, adult fish were anesthetized with 0.5mg/ml tricaine MS222 (Sigma-Aldrich) buffered with sodium bicarbonate and biopsies from the caudal fin removed with a sharp blade. Fin clip biopsies were lysed in the same manner as embryos.

2.2 Genotyping of the *fbl*^{hi2581}, *nop56*^{hi3101}, *nop58*^{hi2581} lines

Genotyping was performed with a double PCR. Forward primer was designed on the genomic region upstream to the retroviral insertion. Two different reverse primers were designed either on the retroviral insertion or on its downstream region (see **Table 4**). This system allowed the detection of all three possible allelic combinations. PCRs were performed using the GoTaq Flexi DNA polymerase (Promega) in standard 50µl reactions with 1µl lysate per reaction as template. Specificity and concentration of the PCR product were verified on an agarose gel in 0.5x TBE SYBRsafe-DNA gel staining (Life technologies).

2.3 Genotyping of the *nle1* mutants

Genotyping was performed with a single PCR (primers are shown in **Table 4**) followed by heteroduplex mobility assay (HMA) and direct sequencing (GATC Biotech). Sequences of mutant alleles were obtained by deconvolution (PolyPeak Parser) from electrophoregrams containing double peaks from the site of the insertion/deletion.

3 GENE/PROTEIN EXPRESSION ANALYSES

3.1 Whole-mount *in situ* hybridization

Riboprobes were synthesized as follow: cDNA (PCR amplified with specific primers, see **Table 5**) was inserted into a pCR II-TOPO vector (Molecular probes). Sequences and orientation of the inserts were checked by direct sequencing (GATC Biotech). The products of PCR amplification of the inserts with generic SP6-T7 primers were used to synthesize the antisense riboprobes, with the T7 or SP6 polymerase (Promega) (chosen on the basis of the sequencing results). Digoxigenin (DIG)-conjugated probes were synthesized with the UTP-DIG nucleotide mix (Roche) and purified then with the RNA clean up kit (Macherey-Nagel). Information about DIG riboprobes used for *in situ* hybridization is indicated in **Table 5**.

Whole-mount *in situ* hybridization was performed on manually dechorionated PTU-treated (**zfin.org**) embryos fixed in 4% paraformaldehyde (PFA)/phosphate buffered saline (PBS) at a particular Kimmel stage (**Kimmel *et al.*, 1995**) and stored in methanol at -20°C. Briefly, methanol-stored embryos were rehydrated in a methanol/PBS series, permeabilized with proteinase K (10 mg/ml), pre-hybridized, and then hybridized overnight at 65°C in hybridization mixture (HM: 50% formamide, 5X standard saline citrate [SSC], 0.1% Tween 20, 100 mg/ml heparin, 100 mg/ml tRNA in water). After a series of washes in 50% SSC/formamide and SSC/PBST, embryos were incubated in blocking solution (0.2% Tween 20, 0.2% Triton X-100, 2% sheep serum in PBST) and incubated overnight at 4°C with AP-conjugated anti-DIG antibodies (Roche) diluted 1:4000 in blocking solution. Embryos were then washed in PBST, soaked in staining buffer (TMN: 100mM NaCl, 100 mM Tris-HCl, pH 9.5, 0.1% Tween 20 in water) and then incubated in NBT/BCIP (nitroblue tetrazolium/5-bromo-4-chloro-3-indolyl phosphate) solution (Roche).

3.2 RT-PCR

Total RNA was extracted from 48hpf embryos using TRIzol reagent according to the manufacturer's protocol (Life technologies). Double-stranded cDNA was synthesized using M-MLV reverse transcriptase (Promega). Primers and RT-PCR conditions are listed in **Table 6**. PCRs were performed on the same amount of template cDNA. Each amplification reaction was verified on an agarose gel in 0.5x TBE SYBRSafe-DNA gel staining (Life technologies).

3.3 Immunohistochemistry (IHC)

IHC on cryosections: sections were rehydrated with PBS, permeabilized with 0.5% triton-X/PBS, blocked with blocking solution (10% normal goat serum [NGS], 0.1% triton in PBS), incubated overnight at 4°C with primary antibody diluted in blocking solution, washed with PBS and incubated with secondary antibody in PBS during 1 hour at room temperature. Sections were then counterstained with DAPI (Sigma) and mounted with Vectashield hard-set mounting medium (Vector Laboratories).

Whole mount IHC was performed exactly as previously described (**Inoue and Wittbrodt, 2011**).

Antisera used: human anti-FBL (1:1000, autoimmune serum, gift from Danièle Hernandez-Verdun, Jacques Monod Institute, Paris France) and rabbit anti-Nle1 (1:3000). Rabbit anti-Nle1 was custom generated via rabbit-immunization (peptide used for immunization: SADVERVLIQLQDEAGEVLG) and purified by affinity purification (Proteogenix SAS, Oberhausbergen, France)

Secondary antibodies were AlexaFluor 633 or AlexaFluor 568 goat anti-human or goat anti-rabbit conjugates (1:200; Molecular Probes, Life technologies).

4 CELL PROLIFERATION AND CELL DEATH ANALYSES

4.1 EdU incorporation and revelation

2nl of 5-ethynyl-2'-deoxyuridine (EdU; Molecular probe, life technologies) solution (10mM) were injected in the yolk of 48hpf WT or mutant embryos. After 2 hours incorporation embryos were fixed and cryosectioned as previously described.

EdU revelation was performed on cryosections with the Click-iT EdU Alexa Fluor 647 Imaging Kit (Molecular probes, Life technologies) according to the manufacturer's protocol. Sections were then counterstained with DAPI (Sigma) and mounted with Vectashield hard-set mounting medium (Vector Laboratories).

4.2 TUNEL staining

TUNEL labelling was performed using the Deadend Fluorometric TUNEL system (Promega) according to manufacturer's instructions. Sections were washed in PBS, counterstained with DAPI (Sigma) and mounted with Vectashield hard-set mounting medium (Vector Laboratories).

5 OVEREXPRESSION OF THE *nle1* CDS

5.1 *nle1* CDS subcloning and site-directed mutagenesis

nle1 coding sequence (ENSDARG00000057105:ENSDART00000148333) was synthesized *in vitro* (GenScript, U.S.A.) and cloned in a pUC57 vector. *nle1* CDS was then subcloned into the pSPE3-Rfa vector to obtain pT3-*nle1*WT (Roure *et al.*, 2007) in order to allow mRNA *in vitro* transcription from the T3 promoter. Subcloning was performed using Gateway Cloning Technology (Life technologies). Primers used are indicated in **Table 7**.

Site-directed mutagenesis was performed on pT3-*nle1*WT (previously generated) in order to perform a single base substitution (G->T) to get a single aminoacid substitution (E76D). Primers for the site directed mutagenesis were designed using QuickChange Primer Design software (Agilent technologies) and are indicated in **Table 7**. Site-directed mutagenesis was performed with GeneART site-directed mutagenesis system (Life technologies) following manufacturer's instruction. Sequences of the inserts were checked, at each passage, by direct sequencing (GATC Biotech). Plasmid obtained pT3-*nle1*DN

5.2 *In vitro* transcription and injection

pT3-*nle1WT* and pT3-*nle1DN* were linearized with KpnI endonuclease (New England Biolabs) and used for the *in vitro* synthesis of mRNAs by the mMESSAGE mMACHINE T3 Transcription Kit (Life Technologies).

nle1WT and *nle1DN* mRNAs were injected in one-cell stage WT (AB line) embryos and phenotypes were analyzed. .

5.3 Constructions for transient transgenesis

pDEST AMA plasmids were designed for transgenesis in fish (Amagen platform, Gif sur Yvette, France). They bear recognition sequences either for the meganuclease ISceI (**Thermes et al., 2007**) or *Tol2* transposase (**Suster et al., 2009**) to allow genomic integration. Moreover, they bear a transgenesis marker (AMA). Thanks to this, CFP is expressed in the fish lens upon genomic integration. Enhancers and promoters can be inserted using Gateway Cloning Technology (Life technologies) and the desired transgene can be entered in the vector via restriction/ligation.

I used the pDEST AMA12H-hsp70:*Ntr-P2A-KR* as a basis to generate my transgenesis constructions.

A fusion PCR (**Shevchuk et al., 2004**) was performed to generate *nle1WT-P2A-eGFP* and *nle1DN-P2A-eGFP*. *nle1WT* and *nle1DN* CDSs were amplified from pSPE3-*nle1WT* and pSPE3-*nle1DN* respectively, *P2A* (sequence for a viral self-cleavable peptide; **Kim et al., 2011**) was amplified from pDEST AMA12H-hsp70:*Ntr-P2A-KR* (Aur lie Heuz , unpublished) and *eGFP* was amplified from pDEST AMA12H-eGFP (gift from AMAGEN platform). *P2A* fragment was fused with *eGFP* and the resulting *P2A-eGFP* fragment was fused either with *nle1WT* or with *nle1DN* fragments to generate *nle1WT-P2A-eGFP* and *nle1DN-P2A-eGFP*. In order to perform fusion PCRs, chimeric primers were designed using the 3' end of one fragment and the 5' end of the following fragment. Primers for fusion PCRs are listed in **Table 7**. In order to clone the fused fragments into the vector suitable for transgenesis, I added restriction sites (XhoI and NheI at the 5' end and NotI at the 3' end) to *nle1WT-P2A-eGFP* and *nle1DN-P2A-eGFP*. Each fusion was cloned by restriction/ligation in pDEST AMA12H-hsp70:*Ntr-P2A-KR* replacing either hsp70:*Ntr-P2A-KR* or *Ntr-P2A-KR*. Indeed, transgene expression is assured by the presence of the hsp70 minimal promoter. Similar plasmids were also generated without hsp70 minimal promoter to allow the expression of the transgenesis constructs by a specific promoter.

Expression of the *nle1* fusions was targeted to PML cells thanks to the *enhancer 101* (*enh101*; Aur lie Heuz ), whereas published promoters (*brn3a*, **Sato et al., 2007**; *cntn1b*, **Czopka et al., 2013**) were used to drive their expression in differentiated cells of the tectum. Primers used for cloning are indicated in **Table 7**.

Two additional sequences were tested in order to overexpress *nle1* fusions in differentiated cells of the tectum. The putative enhancer *foxb1a* and *ebf3* were cloned from zebrafish genomic DNA and inserted in the transgenesis vectors described above. Primers used for cloning are indicated in **Table 7**. Sequences of the inserts were checked, at each passage, by direct sequencing (GATC Biotech).

6 CELL CULTURE METHODS

6.1 ZFTU line

ZFTU cell line was generated and maintained by Pierre Boudinot's group (INRA, Jouy-en Josas, France).

6.2 Transfection plasmids

nle1 fusions (described above) were subcloned in the pCMV:eGFP (Clontech) by replacing the eGFP coding sequence. Primers used for cloning are indicated in **Table 7**. Sequences of the inserts were checked by direct sequencing (GATC Biotech).

6.3 Transfection

Different transfection methods were tested: electroporation (AMAXA Nucleofactor System, Lonza; according manufacturer's protocol), lipofectamins (according to standard protocols), and FuGENE HD transfection system (Promega). This latter was chosen for its low toxicity.

Cells were plated on poly-D-lysine coated coverslips and transfected the following day using FuGENE HD reagent (transfection conditions: 100µl optiMEM [Gibco, Life technologies] + 3µg plasmid + 15µl FuGENE HD reagent/ 2×10^6 cells/coverslips; transfected plasmids pCMV: *nle1WT-P2A-eGFP*; pCMV: *nle1DN-P2A-eGFP*; pCMV: *eGFP*). Cells were fixed after 48hpf.

6.4 Cell dissociation after mRNA injection

100pg *nle1WT* or *nle1DN* mRNAs were injected at the one-cell stage embryos of *enh101-hsp70:GFP* line prior cell dissociation at 48hpf.

Cell dissociation was performed according to standard protocols (**zfin.org**). Dissociated cells were plated on poly-D-lysine coated coverslips (25 embryos/coverslips) and fixed 5 hours after plating. Between plating and fixation cells were in culture medium (10% SVF, 10% tryptose, 10% glutamine, 100 U/mL penicillin, 100µg/mL streptomycin) supplemented with 0.8 mM CaCl_2 at 28°C

6.5 Assessment of the exportation of the 60S ribosomal subunit

Cells for RP-IF were fixed in ice cold methanol and stored in methanol overnight, cells for RNA-FISH were fixed during 30min with 4% PFA at 4°C and permeabilized with 70% ethanol overnight at 4°C.

6.51 RP-IF

Methanol-stored cells were rehydrated in a methanol/PBS series, permeabilized with 0.1% triton-X/PBS, blocked with blocking solution (10% normal goat serum [NGS], 0.1% triton in PBS), incubated during 1h with primary antibody diluted in blocking solution at room temperature, washed with PBS and incubated with secondary antibody during 1 hour at room temperature. Sections were then counterstained with DAPI (Sigma) and mounted with Vectashield hard-set mounting medium (Vector Laboratories).

Antisera used: chicken anti-GFP (1:500, Aves Labs), rabbit anti-RpL3 (1:1000, Genetex), rabbit anti-RpL7a (1:1000, Genetex), rabbit anti-RpS3 (1:1000, Genetex).

Secondary antibodies were AlexaFluor 488 goat anti-chicken or AlexaFluor 555 goat anti-rabbit conjugates (1:200; Molecular Probes, Life technologies).

6.5.1 RNA-FISH

Cells were washed twice in PBS and permeabilized for 18 h in 70% ethanol at 4°C. After two washes in 2× SSC containing 10% formamide, the following steps were performed in the dark: hybridization at 37°C for ≥5 h in a buffer containing 10% formamide, 2.1× SSC, 0.5 µg/ml tRNA, 10% dextran sulfate, 250 µg/ml BSA, 10mM ribonucleoside vanadyl complexes, and 0.5 ng/µl of each probe. After two washes at 37°C with 2× SSC containing 10% formamide, the cells were rinsed in PBS, counterstained with DAPI (Sigma) and mounted with Vectashield hard-set mounting medium (Vector Laboratories) (O'Donohue *et al.*, 2010). This protocol has been adapted for cryosections adding a further permeabilization treatment before pre-hybridization (10µg/ml proteinase K during 8 minutes)

Probe used: 28S_AF633: 5' AGAGGAGGACCCTCGCGGTCCCCG 3', ITS1_AF488 5'CGCCAGGTTACCGTTTTCCGAGAAGGGC3', ITS2_Cy5 GCGCAGACCGTCACGCCACCGTC 3' (Eurogentec)

Mutant line	Fwd Primer (5' -> 3')	Rev Primers (5' -> 3')
<i>fb1</i> ^{hi2581}	GAGGAAAAGCGGGTCTGAG	R _{WT} AGTGCCTGGCTAACTCATCC R _{MUT} GAAGCCTATAGAGTACGAGCCATAG
<i>nop56</i> ^{hi3101}	GTGATCCGAAGAAACGCAAC	R _{WT} AGAAGCATGCCAATCTCCTC R _{MUT} CCAGCTGAAGCCTATAGAGTACG
<i>nop58</i> ^{hi2581}	GTGGAGAGAGCGACTCCTTG	R _{WT} GCGTCTCAAACCTCCTCCAC R _{MUT} CGGGGGTCTTTCATAACAG
<i>nle1</i>	ACTTGTTTCGAGTTTCGTG	CAACGGCATTAAACATTTTGATTAG

Table 4. Primers used for genotyping.

Riboprobe/targeted transcript	ENSEMBL ID	Primers (5' -> 3')
<i>ccnd1</i>	ENSDARG00000035750	Fwd GACTCGAGCTCCAGCTTTC Rev AGGAAGTTGGTGAGGTTCTG
<i>cdkn1c</i>	ENSDARG00000010878	Fwd AAACAAACGTCGGCTCAC Rev GAGGACTGAAGAACGAGCTG
<i>fbf1</i>	ENSDARG00000053912	Fwd TGGTAAGGAGGATGCTCTGG Rev TATGGCTCCAGTGTGAGCTG
<i>nle1</i>	ENSDARG00000057105	Fwd CTGCGTACAGGAGCATTGA Rev GCTTCTAGACGCCTGATTGG
<i>nop56</i>	ENSDARG0000001282	Fwd TGGTCAAACGAGTGCCTTC Rev ACCAATGAGAGCTGCGAGAT
<i>nop58</i>	ENSDARG00000104353	Fwd AGCCTGTGGAAGGAGTTGA Rev TTGTTCTTGGCTGTGGTCTG
<i>otx2</i>	ENSDARG0000001123	Fwd ACTCCTCGAAAGCAGAGACG Rev GAGGCACCGTAACCTTGTGT

Table 5. Riboprobes used for WMISH. *elavl3* and *eomes* riboprobes were a kind gift of Maryline Blin (NeuroPSI, Gif sur Yvette, France).

Gene	Primers (5' -> 3')	Number of cycles
<i>fbl</i>	Fwd GAGGATGCTCTGGTCACAAAG Rev CTGAAAGGATTCCACGCTCT	30
<i>nop56</i>	Fwd ATCTCTCACGCTGGCAGTTT Rev CTTAGGCGTGTTTCCTCTGG	30
<i>nop58</i>	Fwd CATCAGTGGTTCAGGCAAAG Rev GGGAGTGTTGAGTCACCAGA	30
<i>p53</i>	Fwd TAAGAAGTCCGAGCATGTGG Rev GATTGCCCTCCACTCTTATCA	30
<i>mdm2</i>	Fwd TCGCTCATCTACCTCACAACA Rev AGAACGCAGGAAGAGGCATA	30
<i>β-actin</i>	Fwd GCCAACAGGGAAAAGATGAC Rev GACACCATCACCAGAGTCCA	25

Table 6. Primers and RT-PCR conditions

nle1 CDS subcloning

nle1_Fwd *ggggacaagtttgtaaaaaagcaggcttcctcgagacc*ATGAGCGCGGATGTGGAGCG

nle1_Rev *ggggaccactttgtacaagaagctgggtcccggg*TACTTCCTCCATATCCTTA

Site-directed mutagenesis

nle1_E76D_Fwd GTCTGGAGACGGATCAGGTGCTACCGG

nle1_E76D_Rev CCGGTAGCACCTGATCCGTCTCCAGAC

Fusion PCR

XhoI_NheI_nle1_Fwd *cagatcctcgaacagatcgctagcacc*ATGAGCGCGGATGTGGAG

GFP_NotI_Rev *cagatcgggccgc*TACTTGTACAGCTCGTCCA

P2A_GFP_Fwd GAGGAGAATCCTGGCCCAATGGTGTAGCAAGGGCGA

P2A_GFP_Rev TCGCCCTTGCTCACCATTGGGCCAGGATTCTCCTC

nle1_P2A_FwdAAAATGTTTAAGGATATGGAGGAAGGGCAGTGGAGAGGGCAGAG

nle1_P2A_Rev CTCTGCCCTCTCCACTGCCCTCCTCCATATCCTTAAACATTT

Promoters/Enhancers

brn3a_attB1_START_Fwd *ggggacaagtttgtaaaaaagcaggcttc*CGTATTACGCCATGCATTAG

brn3a_attB2_END_Rev *ggggaccactttgtacaagaagctgggtctt*GTACCGTGGACTGCAGCA

contactin1b_5kb_attB1_Fwd *ggggacaagtttgtaaaaaagcaggcttc*CTGATCATTTGAGTCCAAGCG

contactin1b_5kb_attB2_Rev *ggggaccactttgtacaagaaagctgggtctt*GATCCAGCAGTCCAAAAACC
B1-Clal-ebf3_enh_START_Fwd *ggggacaagttgtacaaaaagcaggctt*catcgatCGCTGTTATTCGGTTTGTTC
B2-XhoI-ebf3_enh_END_Rev *ggggaccactttgtacaagaaagctgggtctt*ctcgagCCATCTACTGTTTAAGCTGGGC
B1-Clal-foxb1a_enh_START_Fw *ggggacaagttgtacaaaaagcaggctt*catcgatTCAGCATCTCTCCAGCTCG
B2-XhoI-foxb1a_enh_END_Rev *ggggaccactttgtacaagaaagctgggtctt*ctcgagAGCTCGGTAATGAATCTCAACAG

Table 7. Primers used for *nle1WT* and *nle1DN* overexpression. Italic: Gateway cassette, Underlined: restriction site, Bold: Kozak sequence

REFERENCES

A

Ablain J, Durand EM, Yang S, Zhou Y, Zon LI: **A CRISPR/Cas9 Vector System for Tissue-Specific Gene Disruption in Zebrafish.** *Developmental Cell* 2015, **32**:756–764.

Abujarour R, Efe J, Ding S: **Genome-wide gain-of-function screen identifies novel regulators of pluripotency.** *Stem Cells* 2010, **28**:1487–1497.

Alexandre P, Reugels AM, Barker D, Blanc E, Clarke JDW: **Neurons derive from the more apical daughter in asymmetric divisions in the zebrafish neural tube.** *Nat. Neurosci.* 2010, **13**:673–679.

Allende ML, Amsterdam A, Becker T, Kawakami K, Gaiano N, Hopkins N: **Insertional mutagenesis in zebrafish identifies two novel genes, pescadillo and dead eye, essential for embryonic development.** *Genes Dev.* 1996, **10**:3141–3155.

Alunni A, Hermel J-M, Heuzé A, Bourrat F, Jamen F, Joly J-S: **Evidence for neural stem cells in the medaka optic tectum proliferation zones.** *Dev Neurobiol* 2010, **70**:693–713.

Alunni A, Krecsmarik M, Bosco A, Galant S, Pan L, Moens CB, Bally-Cuif L: **Notch3 signaling gates cell cycle entry and limits neural stem cell amplification in the adult pallium.** *Development* 2013, **140**:3335–3347.

Amsterdam A, Nissen RM, Sun Z, Swindell EC, Farrington S, Hopkins N: **Identification of 315 genes essential for early zebrafish development.** *Proc. Natl. Acad. Sci. U.S.A.* 2004, **101**:12792–12797.

Andoniadou CL, Martinez-Barbera JP: **Developmental mechanisms directing early anterior forebrain specification in vertebrates.** *Cell. Mol. Life Sci.* 2013, **70**:3739–3752.

Armistead J, Triggs-Raine B: **Diverse diseases from a ubiquitous process: the ribosomopathy paradox.** *FEBS Lett.* 2014, **588**:1491–1500.

Azuma M, Toyama R, Laver E, Dawid IB: **Perturbation of rRNA synthesis in the *bap28* mutation leads to apoptosis mediated by p53 in the zebrafish central nervous system.** *J. Biol. Chem.* 2006, **281**:13309–13316.

Azuma M, Toyama R, Laver E, Dawid IB: **Perturbation of rRNA synthesis in the *bap28* mutation leads to apoptosis mediated by p53 in the zebrafish central nervous system.** *J. Biol. Chem.* 2006, **281**:13309–13316.

B

Bae Y-K, Shimizu T, Hibi M: **Patterning of proneuronal and inter-proneuronal domains by hairy- and enhancer of split-related genes in zebrafish neuroectoderm.** *Development* 2005, **132**:1375–1385.

Baier H: **Synaptic laminae in the visual system: molecular mechanisms forming layers of perception.** *Annu. Rev. Cell Dev. Biol.* 2013, **29**:385–416.

Bassler J, Kallas M, Pertschy B, Ulbrich C, Thoms M, Hurt E: **The AAA-ATPase *Rea1* drives removal of biogenesis factors during multiple stages of 60S ribosome assembly.** *Mol. Cell* 2010, **38**:712–721.

Bassler J, Paternoga H, Holdermann I, Thoms M, Granneman S, Barrio-Garcia C, Nyarko A, Stier G, Clark SA, Schraivogel D, et al.: **A network of assembly factors is involved in remodeling rRNA elements during preribosome maturation.** *J. Cell Biol.* 2014, **207**:481–498.

Beck-Cormier S, Escande M, Souilhol C, Vandormael-Pournin S, Sourice S, Pilet P, Babinet C, Cohen-Tannoudji M: **Notchless is required for axial skeleton formation in mice.** *PLoS ONE* 2014, **9**:e98507.

Belin S, Beghin A, Solano-González E, Bezin L, Brunet-Manquat S, Textoris J, Prats A-C, Mertani HC, Dumontet C, Diaz J-J: **Dysregulation of ribosome biogenesis and translational capacity is associated with tumor progression of human breast cancer cells.** *PLoS ONE* 2009, **4**:e7147.

Bertwistle D, Sugimoto M, Sherr CJ: **Physical and functional interactions of the Arf tumor suppressor protein with nucleophosmin/B23.** *Mol. Cell. Biol.* 2004, **24**:985–996.

Blow JJ, Dutta A: **Preventing re-replication of chromosomal DNA.** *Nat. Rev. Mol. Cell Biol.* 2005, **6**:476–486.

Boisvert F-M, van Koningsbruggen S, Navascués J, Lamond AI: **The multifunctional nucleolus.** *Nature Reviews Molecular Cell Biology* 2007, **8**:574–585.

Bolli N, Payne EM, Grabher C, Lee J-S, Johnston AB, Falini B, Kanki JP, Look AT: **Expression of the cytoplasmic NPM1 mutant (NPMc+) causes the expansion of hematopoietic cells in zebrafish.** *Blood* 2010, **115**:3329–3340.

Brombin A, Grossier J-P, Heuzé A, Radev Z, Bourrat F, Joly J-S, Jamen F: **Genome-wide analysis of the POU genes in medaka, focusing on expression in the optic tectum.** *Dev. Dyn.* 2011, **240**:2354–2363.

Brombin A, Joly J-S, Jamen F: **New tricks for an old dog: ribosome biogenesis contributes to stem cell homeostasis.** *Curr. Opin. Genet. Dev.* 2015, **34**:61–70.

Buszczak M, Signer RAJ, Morrison SJ: **Cellular differences in protein synthesis regulate tissue homeostasis.** *Cell* 2014, **159**:242–251.

C

Candal E, Nguyen V, Joly J-S, Bourrat F: **Expression domains suggest cell-cycle independent roles of growth-arrest molecules in the adult brain of the medaka, *Oryzias latipes*.** *Brain Res. Bull.* 2005, **66**:426–430.

Candal E, Thermes V, Joly J-S, Bourrat F: **Medaka as a model system for the characterisation of cell cycle regulators: a functional analysis of Ol-Gadd45gamma during early embryogenesis.** *Mech. Dev.* 2004, **121**:945–958.

Cavodeassi F, Houart C: **Brain regionalization: of signaling centers and boundaries.** *Dev Neurobiol* 2012, **72**:218–233.

Celesia GG: **Hearing disorders in brainstem lesions.** *Handb Clin Neurol* 2015, **129**:509–536.

Cervený KL, Varga M, Wilson SW: **Continued growth and circuit building in the anamniote visual system.** *Dev Neurobiol* 2012, **72**:328–345.

Cervený KL, Varga M, Wilson SW: **Continued growth and circuit building in the anamniote visual system.** *Dev Neurobiol* 2012, **72**:328–345.

Chakraborty A, Uechi T, Kenmochi N: **Guarding the “translation apparatus”: defective ribosome biogenesis and the p53 signaling pathway.** *Wiley Interdisciplinary Reviews: RNA* 2011, **2**:507–522.

Chantha S-C, Emerald BS, Matton DP: **Characterization of the plant Notchless homolog, a WD repeat protein involved in seed development.** *Plant Mol. Biol.* 2006, **62**:897–912.

Chantha S-C, Tebbji F, Matton DP: **From the notch signaling pathway to ribosome biogenesis.** *Plant Signal Behav* 2007, **2**:168–170.

Chapouton P, Adolf B, Leucht C, Tannhäuser B, Ryu S, Driever W, Bally-Cuif L: **her5 expression reveals a pool of neural stem cells in the adult zebrafish midbrain.** *Development* 2006, **133**:4293–4303.

Chapouton P, Skupien P, Hesl B, Coolen M, Moore JC, Madelaine R, Kremmer E, Faus-Kessler T, Blader P, Lawson ND, et al.: **Notch activity levels control the balance between quiescence and recruitment of adult neural stem cells.** *J. Neurosci.* 2010, **30**:7961–7974.

Chapouton P, Webb KJ, Stigloher C, Alunni A, Adolf B, Hesl B, Topp S, Kremmer E, Bally-Cuif L: **Expression of hairy/enhancer of split genes in neural progenitors and neurogenesis domains of the adult zebrafish brain.** *J. Comp. Neurol.* 2011, **519**:1748–1769.

Cormier S, Le Bras S, Souilhol C, Vandormael-Pournin S, Durand B, Babinet C, Baldacci P, Cohen-Tannoudji M: **The Murine Ortholog of Notchless, a Direct Regulator of the Notch Pathway in *Drosophila melanogaster*, Is Essential for Survival of Inner Cell Mass Cells.** *Molecular and Cellular Biology* 2006, **26**:3541–3549.

Cowling VH, Turner SA, Cole MD: **Burkitt’s lymphoma-associated c-Myc mutations converge on a dramatically altered target gene response and implicate Nol5a/Nop56 in oncogenesis.** *Oncogene* 2014, **33**:3519–3527.

Czopka T, Ffrench-Constant C, Lyons DA: **Individual oligodendrocytes have only a few hours in which to generate new myelin sheaths in vivo.** *Dev. Cell* 2013, **25**:599–609.

D

Daftuar L, Zhu Y, Jacq X, Prives C: **Ribosomal Proteins RPL37, RPS15 and RPS20 Regulate the Mdm2-p53-MdmX Network.** *PLoS ONE* 2013, **8**:e68667.

Dai M-S, Sun X-X, Lu H: **Aberrant expression of nucleostemin activates p53 and induces cell cycle arrest via inhibition of MDM2.** *Mol. Cell. Biol.* 2008, **28**:4365–4376.

Davoli T, de Lange T: **The causes and consequences of polyploidy in normal development and cancer.** *Annu. Rev. Cell Dev. Biol.* 2011, **27**:585–610.

De la Cruz J, Sanz-Martínez E, Remacha M: **The essential WD-repeat protein Rsa4p is required for rRNA processing and intra-nuclear transport of 60S ribosomal subunits.** *Nucleic Acids Res.* 2005, **33**:5728–5739.

Del Bene F, Wehman AM, Link BA, Baier H: **Regulation of neurogenesis by interkinetic nuclear migration through an apical-basal notch gradient.** *Cell* 2008, **134**:1055–1065.

Del Bene F: **Interkinetic nuclear migration: cell cycle on the move.** *EMBO J.* 2011, **30**:1676–1677.

De Oliveira-Carlos V, Ganz J, Hans S, Kaslin J, Brand M: **Notch receptor expression in neurogenic regions of the adult zebrafish brain.** *PLoS ONE* 2013, **8**:e73384.

Derenzini M, Montanaro L, Chillà A, Tosti E, Vici M, Barbieri S, Govoni M, Mazzini G, Treré D: **Key role of the achievement of an appropriate ribosomal RNA complement for G1-S phase transition in H4-II-E-C3 rat hepatoma cells.** *J. Cell. Physiol.* 2005, **202**:483–491.

Devès M, Bourrat F: **Transcriptional mechanisms of developmental cell cycle arrest: problems and models.** *Semin. Cell Dev. Biol.* 2012, **23**:290–297.

Deyts C, Candal E, Joly J-S, Bourrat F: **An automated in situ hybridization screen in the Medaka to identify unknown neural genes.** *Dev. Dyn.* 2005, **234**:698–708.

Dirian L, Galant S, Coolen M, Chen W, Bedu S, Houart C, Bally-Cuif L, Foucher I: **Spatial regionalization and heterochrony in the formation of adult pallial neural stem cells.** *Dev. Cell* 2014, **30**:123–136.

Donati G, Brighenti E, Vici M, Mazzini G, Trere D, Montanaro L, Derenzini M: **Selective inhibition of rRNA transcription downregulates E2F-1: a new p53-independent mechanism linking cell growth to cell proliferation.** *Journal of Cell Science* 2011, **124**:3017–3028.

Donati G, Peddigari S, Mercer CA, Thomas G: **5S Ribosomal RNA Is an Essential Component of a Nascent Ribosomal Precursor Complex that Regulates the Hdm2-p53 Checkpoint.** *Cell Reports* 2013, **4**:87–98.

Dong Z, Yang N, Yeo S-Y, Chitnis A, Guo S: **Intralineage directional Notch signaling regulates self-renewal and differentiation of asymmetrically dividing radial glia.** *Neuron* 2012, **74**:65–78.

Drygin D, Rice WG, Grummt I: **The RNA polymerase I transcription machinery: an emerging target for the treatment of cancer.** *Annu. Rev. Pharmacol. Toxicol.* 2010, **50**:131–156.

E

Ebersberger I, Simm S, Leisegang MS, Schmitzberger P, Mirus O, Haeseler A von, Bohnsack MT, Schleiff E: **The evolution of the ribosome biogenesis pathway from a yeast perspective.** *Nucleic Acids Res.* 2014, **42**:1509–1523.

Eifert C, Farnworth M, Schulz-Mirbach T, Riesch R, Bierbach D, Klaus S, Wurster A, Tobler M, Streit B, Indy JR, et al.: **Brain size variation in extremophile fish: local adaptation versus phenotypic plasticity: Brain size variation in extremophile fish.** *Journal of Zoology* 2015, **295**:143–153.

Eivers E, Demagny H, De Robertis EM: **Integration of BMP and Wnt signaling via vertebrate Smad1/5/8 and Drosophila Mad.** *Cytokine Growth Factor Rev.* 2009, **20**:357–365.

Essers PB, Pereboom TC, Goos YJ, Paridaen JT, Macinnes AW: **A comparative study of nucleostemin family members in zebrafish reveals specific roles in ribosome biogenesis.** *Dev. Biol.* 2014, **385**:304–315.

F

Falini B, Bolli N, Liso A, Martelli MP, Mannucci R, Pileri S, Nicoletti I: **Altered nucleophosmin transport in acute myeloid leukaemia with mutated NPM1: molecular basis and clinical implications.** *Leukemia* 2009, **23**:1731–1743.

Filipovska A, Rackham O: **Specialization from synthesis: How ribosome diversity can customize protein function.** *FEBS Letters* 2013, **587**:1189–1197.

Fischer AJ, Bosse JL, El-Hodiri HM: **The ciliary marginal zone (CMZ) in development and regeneration of the vertebrate eye.** *Exp. Eye Res.* 2013, **116**:199–204.

Fromont-Racine M, Senger B, Saveanu C, Fasiolo F: **Ribosome assembly in eukaryotes.** *Gene* 2003, **313**:17–42.

Fumagalli S, Ivanenkov VV, Teng T, Thomas G: **Suprainduction of p53 by disruption of 40S and 60S ribosome biogenesis leads to the activation of a novel G2/M checkpoint.** *Genes Dev.* 2012, **26**:1028–1040.

G

Gadisieux JF, Evrard P: **Glial-neuronal relationship in the developing central nervous system. A histochemical-electron microscope study of radial glial cell particulate glycogen in normal and reeler mice and the human fetus.** *Dev. Neurosci.* 1985, **7**:12–32.

Geling A: **bHLH transcription factor Her5 links patterning to regional inhibition of neurogenesis at the midbrain-hindbrain boundary.** *Development* 2003, **130**:1591–1604.

Geling A, Plessy C, Rastegar S, Strähle U, Bally-Cuif L: **Her5 acts as a prepattern factor that blocks neurogenin1 and coe2 expression upstream of Notch to inhibit neurogenesis at the midbrain-hindbrain boundary.** *Development* 2004, **131**:1993–2006.

Gerety SS, Breau MA, Sasai N, Xu Q, Briscoe J, Wilkinson DG: **An inducible transgene expression system for zebrafish and chick.** *Development* 2013, **140**:2235–2243.

Gilbert SF: *Developmental biology.* Sinauer Associates; 2010.

Gómez-Skarmeta JL, Modolell J: **Iroquois genes: genomic organization and function in vertebrate neural development.** *Curr. Opin. Genet. Dev.* 2002, **12**:403–408.

Goodfellow SJ, Zomerdijk JCBM: **Basic mechanisms in RNA polymerase I transcription of the ribosomal RNA genes.** *Subcell. Biochem.* 2013, **61**:211–236.

Göritz C, Dias DO, Tomilin N, Barbacid M, Shupliakov O, Frisén J: **A pericyte origin of spinal cord scar tissue.** *Science* 2011, **333**:238–242.

Götz M, Huttner WB: **The cell biology of neurogenesis.** *Nat. Rev. Mol. Cell Biol.* 2005, **6**:777–788.

Götz M, Sirko S, Beckers J, Irmeler M: **Reactive astrocytes as neural stem or progenitor cells: In vivo lineage, In vitro potential, and Genome-wide expression analysis: Hallmarks of Neural Stem Cells In Vivo and In Vitro.** *Glia* 2015, **63**:1452–1468.

Grandel H, Brand M: **Comparative aspects of adult neural stem cell activity in vertebrates.** *Dev. Genes Evol.* 2013, **223**:131–147.

Grandel H, Kaslin J, Ganz J, Wenzel I, Brand M: **Neural stem cells and neurogenesis in the adult zebrafish brain: Origin, proliferation dynamics, migration and cell fate.** *Developmental Biology* 2006, **295**:263–277.

Grisendi S, Mecucci C, Falini B, Pandolfi PP: **Nucleophosmin and cancer.** *Nature Reviews Cancer* 2006, **6**:493–505.

Guérout N, Li X, Barnabé-Heider F: **Cell fate control in the developing central nervous system.** *Exp. Cell Res.* 2014, **321**:77–83.

H

Hans S, Scheer N, Riedl I, Weizsäcker E v, Blader P, Campos-Ortega JA: **her3, a zebrafish member of the hairy-E(spl) family, is repressed by Notch signalling.** *Development* 2004, **131**:2957–2969.

Hartenstein V, Stollewerk A: **The evolution of early neurogenesis.** *Dev. Cell* 2015, **32**:390–407.

Hernandez-Verdun D, Roussel P, Thiry M, Sirri V, Lafontaine DLJ: **The nucleolus: structure/function relationship in RNA metabolism.** *Wiley Interdiscip Rev RNA* 2010, **1**:415–431.

Hisano Y, Sakuma T, Nakade S, Ohga R, Ota S, Okamoto H, Yamamoto T, Kawahara A: **Precise in-frame integration of exogenous DNA mediated by CRISPR/Cas9 system in zebrafish.** *Scientific Reports* 2015, **5**:8841.

Holliday DL, Speirs V: **Choosing the right cell line for breast cancer research.** *Breast Cancer Res.* 2011, **13**:215.

Horn HF, Vousden KH: **Cooperation between the ribosomal proteins L5 and L11 in the p53 pathway.** *Oncogene* 2008, **27**:5774–5784.

Hovhanyan A, Herter EK, Pfannstiel J, Gallant P, Raabe T: **Drosophila mbm is a nucleolar myc and casein kinase 2 target required for ribosome biogenesis and cell growth of central brain neuroblasts.** *Mol. Cell. Biol.* 2014, **34**:1878–1891.

Hu WF, Chahrour MH, Walsh CA: **The diverse genetic landscape of neurodevelopmental disorders.** *Annu Rev Genomics Hum Genet* 2014, **15**:195–213.

Huang C, Chan JA, Schuurmans C: **Proneural bHLH genes in development and disease.** *Curr. Top. Dev. Biol.* 2014, **110**:75–127.

I

Iadevaia V, Caldarola S, Biondini L, Gismondi A, Karlsson S, Dianzani I, Loreni F: **PIM1 kinase is destabilized by ribosomal stress causing inhibition of cell cycle progression.** *Oncogene* 2010, **29**:5490–5499.

Inoue D, Wittbrodt J: **One for all--a highly efficient and versatile method for fluorescent immunostaining in fish embryos.** *PLoS ONE* 2011, **6**:e19713.

Ito H, Ishikawa Y, Yoshimoto M, Yamamoto N: **Diversity of brain morphology in teleosts: brain and ecological niche.** *Brain Behav. Evol.* 2007, **69**:76–86.

Ito Y, Tanaka H, Okamoto H, Ohshima T: **Characterization of neural stem cells and their progeny in the adult zebrafish optic tectum.** *Developmental Biology* 2010, **342**:26–38.

Itoh M, Kim C-H, Palardy G, Oda T, Jiang Y-J, Maust D, Yeo S-Y, Lorick K, Wright GJ, Ariza-McNaughton L, et al.: **Mind bomb is a ubiquitin ligase that is essential for efficient activation of Notch signaling by Delta.** *Dev. Cell* 2003, **4**:67–82.

J

Jackson RJ: **The Current Status of Vertebrate Cellular mRNA IRESs.** *Cold Spring Harbor Perspectives in Biology* 2013, **5**:a011569–a011569.

James A, Wang Y, Raje H, Rosby R, DiMario P: **Nucleolar stress with and without p53.** *Nucleus* 2014, **5**:402–426.

Janssen SF, Gorgels TGMF, Bossers K, Brink JB Ten, Essing AHW, Nagtegaal M, van der Spek PJ, Jansonius NM, Bergen AAB: **Gene expression and functional annotation of the human ciliary body epithelia.** *PLoS ONE* 2012, **7**:e44973.

K

Kageyama R, Ohtsuka T, Kobayashi T: **Roles of Hes genes in neural development.** *Dev. Growth Differ.* 2008, **50 Suppl 1**:S97–103.

Kageyama R, Shimojo H, Imayoshi I: **Dynamic expression and roles of Hes factors in neural development.** *Cell Tissue Res.* 2015, **359**:125–133.

Kaslin J, Ganz J, Geffarth M, Grandel H, Hans S, Brand M: **Stem cells in the adult zebrafish cerebellum: initiation and maintenance of a novel stem cell niche.** *J. Neurosci.* 2009, **29**:6142–6153.

Kawakami K: **Tol2: a versatile gene transfer vector in vertebrates.** *Genome Biology* 2007, **8**:S7.

Kearse MG, Chen AS, Ware VC: **Expression of ribosomal protein L22e family members in *Drosophila melanogaster*: rpL22-like is differentially expressed and alternatively spliced.** *Nucleic Acids Res.* 2011, **39**:2701–2716.

Kim JH, Lee S-R, Li L-H, Park H-J, Park J-H, Lee KY, Kim M-K, Shin BA, Choi S-Y: **High Cleavage Efficiency of a 2A Peptide Derived from Porcine Teschovirus-1 in Human Cell Lines, Zebrafish and Mice.** *PLoS ONE* 2011, **6**:e18556.

Kimmel CB, Ballard WW, Kimmel SR, Ullmann B, Schilling TF: **Stages of embryonic development of the zebrafish.** *Dev. Dyn.* 1995, **203**:253–310.

Kizil C, Kaslin J, Kroehne V, Brand M: **Adult neurogenesis and brain regeneration in zebrafish.** *Developmental Neurobiology* 2012, **72**:429–461.

Koh CM, Iwata T, Zheng Q, Bethel C, Yegnasubramanian S, De Marzo AM: **Myc enforces overexpression of EZH2 in early prostatic neoplasia via transcriptional and post-transcriptional mechanisms.** *Oncotarget* 2011, **2**:669–683.

Komili S, Farny NG, Roth FP, Silver PA: **Functional specificity among ribosomal proteins regulates gene expression.** *Cell* 2007, **131**:557–571.

Kondrashov N, Pusic A, Stumpf CR, Shimizu K, Hsieh AC, Xue S, Ishijima J, Shiroishi T, Barna M: **Ribosome-mediated specificity in Hox mRNA translation and vertebrate tissue patterning.** *Cell* 2011, **145**:383–397.

Korčeková D, Gombitová A, Raška I, Cmarko D, Lanctôt C: **Nucleologenesis in the *Caenorhabditis elegans* embryo.** *PLoS ONE* 2012, **7**:e40290.

Krauzlis RJ, Lovejoy LP, Zénon A: **Superior colliculus and visual spatial attention.** *Annu. Rev. Neurosci.* 2013, **36**:165–182.

Kressler D, Hurt E, Bassler J: **Driving ribosome assembly.** *Biochim. Biophys. Acta* 2010, **1803**:673–683.

Kressler D, Hurt E, Bergler H, Bassler J: **The power of AAA-ATPases on the road of pre-60S ribosome maturation--molecular machines that strip pre-ribosomal particles.** *Biochim. Biophys. Acta* 2012, **1823**:92–100.

Kriegstein A, Alvarez-Buylla A: **The glial nature of embryonic and adult neural stem cells.** *Annu. Rev. Neurosci.* 2009, **32**:149–184.

Kudoh T, Dawid IB: **Role of the iroquois3 homeobox gene in organizer formation.** *Proc. Natl. Acad. Sci. U.S.A.* 2001, **98**:7852–7857.

L

Lafontaine DLJ: **Noncoding RNAs in eukaryotic ribosome biogenesis and function.** *Nat. Struct. Mol. Biol.* 2015, **22**:11–19.

Le Bouteiller M, Souilhol C, Beck-Cormier S, Stedman A, Burlen-Defranoux O, Vandormael-Pournin S, Bernex F, Cumano A, Cohen-Tannoudji M: **Notchless-dependent ribosome synthesis is required for the maintenance of adult hematopoietic stem cells.** *J. Exp. Med.* 2013, **210**:2351–2369.

Lee H-K, Lee H-S, Moody SA: **Neural transcription factors: from embryos to neural stem cells.** *Mol. Cells* 2014, **37**:705–712.

Lenkowski JR, Raymond PA: **Müller glia: Stem cells for generation and regeneration of retinal neurons in teleost fish.** *Prog Retin Eye Res* 2014, **40**:94–123.

Li A, Blow JJ: **Cdt1 downregulation by proteolysis and geminin inhibition prevents DNA re-replication in Xenopus.** *EMBO J.* 2005, **24**:395–404.

Lin R, Iacovitti L: **Classic and novel stem cell niches in brain homeostasis and repair.** *Brain Res.* 2015, doi:10.1016/j.brainres.2015.04.029.

Lindsey BW, Darabie A, Tropepe V: **The cellular composition of neurogenic periventricular zones in the adult zebrafish forebrain.** *J. Comp. Neurol.* 2012, **520**:2275–2316.

Lopes AM, Miguel RN, Sargent CA, Ellis PJ, Amorim A, Affara NA: **The human RPS4 paralogue on Yq11.223 encodes a structurally conserved ribosomal protein and is preferentially expressed during spermatogenesis.** *BMC Mol. Biol.* 2010, **11**:33.

Lossie AC, Lo C-L, Baumgarner KM, Cramer MJ, Garner JP, Justice MJ: **ENU mutagenesis reveals that Notchless homolog 1 (Drosophila) affects Cdkn1a and several members of the Wnt pathway during murine pre-implantation development.** *BMC Genetics* 2012, **13**:106.

M

Ma H, Pederson T: **Depletion of the nucleolar protein nucleostemin causes G1 cell cycle arrest via the p53 pathway.** *Mol. Biol. Cell* 2007, **18**:2630–2635.

Mansour-Robaey S, Pinganaud G: **Quantitative and morphological study of cell proliferation during morphogenesis in the trout visual system.** *J Hirnforsch* 1990, **31**:495–504.

- Marcel V, Catez F, Diaz J-J: **p53, a translational regulator: contribution to its tumour-suppressor activity.** *Oncogene* 2015, doi:10.1038/onc.2015.25.
- Marcel V, Ghayad SE, Belin S, Therizols G, Morel A-P, Solano-González E, Vendrell JA, Hacot S, Mertani HC, Albaret MA, et al.: **p53 acts as a safeguard of translational control by regulating fibrillar and rRNA methylation in cancer.** *Cancer Cell* 2013, **24**:318–330.
- Marcus RC, Delaney CL, Easter SS: **Neurogenesis in the visual system of embryonic and adult zebrafish (*Danio rerio*).** *off. Vis. Neurosci.* 1999, **16**:417–424.
- Mauro VP, Edelman GM: **The ribosome filter redux.** *Cell Cycle* 2007, **6**:2246–2251.
- Mayer C, Grummt I: **Ribosome biogenesis and cell growth: mTOR coordinates transcription by all three classes of nuclear RNA polymerases.** *Oncogene* 2006, **25**:6384–6391.
- Meletis K, Barnabé-Heider F, Carlén M, Evergren E, Tomilin N, Shupliakov O, Frisén J: **Spinal cord injury reveals multilineage differentiation of ependymal cells.** *PLoS Biol.* 2008, **6**:e182.
- Melixetian M, Ballabeni A, Masiero L, Gasparini P, Zamponi R, Bartek J, Lukas J, Helin K: **Loss of Geminin induces rereplication in the presence of functional p53.** *J. Cell Biol.* 2004, **165**:473–482.
- Meyuhas O, Kahan T: **The race to decipher the top secrets of TOP mRNAs.** *Biochim. Biophys. Acta* 2015, **1849**:801–811.
- Mihaylov IS, Kondo T, Jones L, Ryzhikov S, Tanaka J, Zheng J, Higa LA, Minamino N, Cooley L, Zhang H: **Control of DNA replication and chromosome ploidy by geminin and cyclin A.** *Mol. Cell Biol.* 2002, **22**:1868–1880.
- Miller DM, Thomas SD, Islam A, Muench D, Sedoris K: **c-Myc and cancer metabolism.** *Clin. Cancer Res.* 2012, **18**:5546–5553.
- Mizuseki K, Kishi M, Matsui M, Nakanishi S, Sasai Y: **Xenopus Zic-related-1 and Sox-2, two factors induced by chordin, have distinct activities in the initiation of neural induction.** *Development* 1998, **125**:579–587.
- Mizuseki K, Kishi M, Shiota K, Nakanishi S, Sasai Y: **SoxD: an essential mediator of induction of anterior neural tissues in Xenopus embryos.** *Neuron* 1998, **21**:77–85.
- Mokrejs M, Masek T, Vopalensky V, Hlubucek P, Delbos P, Pospisek M: **IRESite--a tool for the examination of viral and cellular internal ribosome entry sites.** *Nucleic Acids Research* 2010, **38**:D131–D136.
- Mongin E, Auer TO, Bourrat F, Gruhl F, Dewar K, Blanchette M, Wittbrodt J, Ettwiller L: **Combining computational prediction of cis-regulatory elements with a new enhancer assay to efficiently label neuronal structures in the medaka fish.** *PLoS ONE* 2011, **6**:e19747.
- Mosimann C, Kaufman CK, Li P, Pugach EK, Tamplin OJ, Zon LI: **Ubiquitous transgene expression and Cre-based recombination driven by the ubiquitin promoter in zebrafish.** *Development* 2011, **138**:169–177.
- Müller M, Weiszäcker E von, Campos-Ortega JA: **Transcription of a zebrafish gene of the hairy-Enhancer of split family delineates the midbrain anlage in the neural plate.** *Dev. Genes Evol.* 1996, **206**:153–160.

N

Negi SS, Brown P: **rRNA synthesis inhibitor, CX-5461, activates ATM/ATR pathway in acute lymphoblastic leukemia, arrests cells in G2 phase and induces apoptosis.** *Oncotarget* 2015, [no volume].

Neumüller RA, Richter C, Fischer A, Novatchkova M, Neumüller KG, Knoblich JA: **Genome-wide analysis of self-renewal in Drosophila neural stem cells by transgenic RNAi.** *Cell Stem Cell* 2011, **8**:580–593.

Newton K, Petfalski E, Tollervey D, Cáceres JF: **Fibrillarin is essential for early development and required for accumulation of an intron-encoded small nucleolar RNA in the mouse.** *Mol. Cell. Biol.* 2003, **23**:8519–8527.

Nguyen V, Deschet K, Henrich T, Godet E, Joly JS, Wittbrodt J, Chourrout D, Bourrat F: **Morphogenesis of the optic tectum in the medaka (*Oryzias latipes*): a morphological and molecular study, with special emphasis on cell proliferation.** *J. Comp. Neurol.* 1999, **413**:385–404.

Niehrs C: **On growth and form: a Cartesian coordinate system of Wnt and BMP signaling specifies bilaterian body axes.** *Development* 2010, **137**:845–857.

Ninkovic J, Götz M: **A time and place for understanding neural stem cell specification.** *Dev. Cell* 2014, **30**:114–115.

O

O'Connell LA: **Evolutionary development of neural systems in vertebrates and beyond.** *J. Neurogenet.* 2013, **27**:69–85.

O'Donohue M-F, Choismel V, Faubladiet M, Fichant G, Gleizes P-E: **Functional dichotomy of ribosomal proteins during the synthesis of mammalian 40S ribosomal subunits.** *J. Cell Biol.* 2010, **190**:853–866.

Ohata S, Aoki R, Kinoshita S, Yamaguchi M, Tsuruoka-Kinoshita S, Tanaka H, Wada H, Watabe S, Tsuboi T, Masai I, et al.: **Dual roles of Notch in regulation of apically restricted mitosis and apicobasal polarity of neuroepithelial cells.** *Neuron* 2011, **69**:215–230.

O'Leary MN, Schreiber KH, Zhang Y, Duc A-CE, Rao S, Hale JS, Academia EC, Shah SR, Morton JF, Holstein CA, et al.: **The Ribosomal Protein Rpl22 Controls Ribosome Composition by Directly Repressing Expression of Its Own Paralog, Rpl22i1.** *PLoS Genetics* 2013, **9**:e1003708.

Osumi N, Shinohara H, Numayama-Tsuruta K, Maekawa M: **Concise review: Pax6 transcription factor contributes to both embryonic and adult neurogenesis as a multifunctional regulator.** *Stem Cells* 2008, **26**:1663–1672.

Ozair MZ, Kintner C, Brivanlou AH: **Neural induction and early patterning in vertebrates.** *Wiley Interdiscip Rev Dev Biol* 2013, **2**:479–498.

P

Paridaen JTML, Huttner WB: **Neurogenesis during development of the vertebrate central nervous system.** *EMBO Rep.* 2014, **15**:351–364.

Passemard S, Ghouzzi V El, Nasser H, Verney C, Vodjdani G, Lacaud A, Lebon S, Laburthe M, Robberecht P, Nardelli J, et al.: **VIP blockade leads to microcephaly in mice via disruption of Mcph1-Chk1 signaling.** *J. Clin. Invest.* 2011, **121**:3071–3087.

Pera EM, Acosta H, Gougnard N, Climent M, Arregi I: **Active signals, gradient formation and regional specificity in neural induction.** *Exp. Cell Res.* 2014, **321**:25–31.

Pereboom TC, van Weele LJ, Bondt A, MacInnes AW: **A zebrafish model of dyskeratosis congenita reveals hematopoietic stem cell formation failure resulting from ribosomal protein-mediated p53 stabilization.** *Blood* 2011, **118**:5458–5465.

Perron M, Harris WA: **Retinal stem cells in vertebrates.** *Bioessays* 2000, **22**:685–688.

Pfister AS, Keil M, Kühl M: **The Wnt Target Protein Peter Pan Defines a Novel p53-independent Nucleolar Stress-Response Pathway.** *J. Biol. Chem.* 2015, **290**:10905–10918.

Pierfelice T, Alberi L, Gaiano N: **Notch in the vertebrate nervous system: an old dog with new tricks.** *Neuron* 2011, **69**:840–855.

Provost E, Rhee J, Leach SD: **Viral 2A peptides allow expression of multiple proteins from a single ORF in transgenic zebrafish embryos.** *Genesis* 2007, **45**:625–629.

Provost E, Wehner KA, Zhong X, Ashar F, Nguyen E, Green R, Parsons MJ, Leach SD: **Ribosomal biogenesis genes play an essential and p53-independent role in zebrafish pancreas development.** *Development* 2012, **139**:3232–3241.

Q

Qin W, Chen Z, Zhang Y, Yan R, Yan G, Li S, Zhong H, Lin S: **Nom1 mediates pancreas development by regulating ribosome biogenesis in zebrafish.** *PLoS ONE* 2014, **9**:e100796.

R

Raymond PA, Easter SS: **Postembryonic growth of the optic tectum in goldfish. I. Location of germinal cells and numbers of neurons produced.** *J. Neurosci.* 1983, **3**:1077–1091.

Recher G, Jouralet J, Brombin A, Heuzé A, Mugniery E, Hermel J-M, Desnoullez S, Savy T, Herbomel P, Bourrat F, et al.: **Zebrafish midbrain slow-amplifying progenitors exhibit high levels of transcripts for nucleotide and ribosome biogenesis.** *Development* 2013, **140**:4860–4869.

Remus D, Diffley JF: **Eukaryotic DNA replication control: Lock and load, then fire.** *Current Opinion in Cell Biology* 2009, **21**:771–777.

Rodriguez-Corona U, Sobol M, Rodriguez-Zapata LC, Hozak P, Castano E: **Fibrillarlin from Archaea to human.** *Biol. Cell* 2015, **107**:159–174.

Ross AP, Zarbalis KS: **The emerging roles of ribosome biogenesis in craniofacial development.** *Front Physiol* 2014, **5**:26.

Roure A, Rothbacher U, Robin F, Kalmar E, Ferone G, Lamy C, Missero C, Mueller F, Lemaire P: **A multicassette Gateway vector set for high throughput and comparative analyses in ciona and vertebrate embryos.** *PLoS ONE* 2007, **2**:e916.

Royet J: **Notchless encodes a novel WD40-repeat-containing protein that modulates Notch signaling activity.** *The EMBO Journal* 1998, **17**:7351–7360.

Russo A, Esposito D, Catillo M, Pietropaolo C, Crescenzi E, Russo G: **Human rpl3 induces G₁/S arrest or apoptosis by modulating p21 (waf1/cip1) levels in a p53-independent manner.** *Cell Cycle* 2013, **12**:76–87.

S

Sabelström H, Stenudd M, Réu P, Dias DO, Elfineh M, Zdunek S, Damberg P, Göritz C, Frisé J: **Resident neural stem cells restrict tissue damage and neuronal loss after spinal cord injury in mice.** *Science* 2013, **342**:637–640.

Sato T, Hamaoka T, Aizawa H, Hosoya T, Okamoto H: **Genetic single-cell mosaic analysis implicates ephrinB2 reverse signaling in projections from the posterior tectum to the hindbrain in zebrafish.** *J. Neurosci.* 2007, **27**:5271–5279.

Sauer FC: **Mitosis in the neural tube.** *The Journal of Comparative Neurology* 1935, **62**:377–405.

Schmidt R, Strähle U, Scholpp S: **Neurogenesis in zebrafish - from embryo to adult.** *Neural Dev* 2013, **8**:3.

Shevchuk NA: **Construction of long DNA molecules using long PCR-based fusion of several fragments simultaneously.** *Nucleic Acids Research* 2004, **32**:19e–19.

Shimojo H, Ohtsuka T, Kageyama R: **Dynamic expression of notch signaling genes in neural stem/progenitor cells.** *Front Neurosci* 2011, **5**:78.

Simmons T, Appel B: **Mutation of pescadillo disrupts oligodendrocyte formation in zebrafish.** *PLoS ONE* 2012, **7**:e32317.

Sinha DK, Neveu P, Gagey N, Aujard I, Benbrahim-Bouzidi C, Le Saux T, Rampon C, Gauron C, Goetz B, Dubruille S, et al.: **Photocontrol of protein activity in cultured cells and zebrafish with one- and two-photon illumination.** *Chembiochem* 2010, **11**:653–663.

Soroldoni D, Hogan BM, Oates AC: **Simple and efficient transgenesis with meganuclease constructs in zebrafish.** *Methods Mol. Biol.* 2009, **546**:117–130.

Southall TD, Gold KS, Egger B, Davidson CM, Caygill EE, Marshall OJ, Brand AH: **Cell-type-specific profiling of gene expression and chromatin binding without cell isolation: assaying RNA Pol II occupancy in neural stem cells.** *Dev. Cell* 2013, **26**:101–112.

Stedman A, Beck-Cormier S, Le Bouteiller M, Raveux A, Vandormael-Pournin S, Coqueran S, Lejour V, Jarzebowski L, Toledo F, Robine S, et al.: **Ribosome biogenesis dysfunction leads to p53-mediated apoptosis and goblet cell differentiation of mouse intestinal stem/progenitor cells.** *Cell Death Differ.* 2015, doi:10.1038/cdd.2015.57.

Stigloher C, Chapouton P, Adolf B, Bally-Cuif L: **Identification of neural progenitor pools by E(Spl) factors in the embryonic and adult brain.** *Brain Res. Bull.* 2008, **75**:266–273.

Su H, Xu T, Ganapathy S, Shadfan M, Long M, Huang TH-M, Thompson I, Yuan Z-M: **Elevated snoRNA biogenesis is essential in breast cancer.** *Oncogene* 2014, **33**:1348–1358.

Sugihara Y, Honda H, Iida T, Morinaga T, Hino S, Okajima T, Matsuda T, Nadano D: **Proteomic analysis of rodent ribosomes revealed heterogeneity including ribosomal proteins L10-like, L22-like 1, and L39-like.** *J. Proteome Res.* 2010, **9**:1351–1366.

Sugiyama M, Sakaue-Sawano A, Iimura T, Fukami K, Kitaguchi T, Kawakami K, Okamoto H, Higashijima S -i., Miyawaki A: **Illuminating cell-cycle progression in the developing zebrafish embryo.** *Proceedings of the National Academy of Sciences* 2009, **106**:20812–20817.

Suster ML, Kikuta H, Urasaki A, Asakawa K, Kawakami K: **Transgenesis in zebrafish with the tol2 transposon system.** *Methods Mol. Biol.* 2009, **561**:41–63.

T

Tafforeau L, Zorbas C, Langhendries J-L, Mullineux S-T, Stamatopoulou V, Mullier R, Wacheul L, Lafontaine DLJ: **The complexity of human ribosome biogenesis revealed by systematic nucleolar screening of Pre-rRNA processing factors.** *Mol. Cell* 2013, **51**:539–551.

Takagi M, Absalon MJ, McLure KG, Kastan MB: **Regulation of p53 Translation and Induction after DNA Damage by Ribosomal Protein L26 and Nucleolin.** *Cell* 2005, **123**:49–63.

Tallafuss A, Bally-Cuif L: **Tracing of her5 progeny in zebrafish transgenics reveals the dynamics of midbrain-hindbrain neurogenesis and maintenance.** *Development* 2003, **130**:4307–4323.

Tallafuss A, Gibson D, Morcos P, Li Y, Seredick S, Eisen J, Washbourne P: **Turning gene function ON and OFF using sense and antisense photo-morpholinos in zebrafish.** *Development* 2012, **139**:1691–1699.

Tamura RE, de Vasconcellos JF, Sarkar D, Libermann TA, Fisher PB, Zerbini LF: **GADD45 proteins: central players in tumorigenesis.** *Curr. Mol. Med.* 2012, **12**:634–651.

Temple S: **The development of neural stem cells.** *Nature* 2001, **414**:112–117.

Tessarz P, Santos-Rosa H, Robson SC, Sylvestersen KB, Nelson CJ, Nielsen ML, Kouzarides T: **Glutamine methylation in histone H2A is an RNA-polymerase-I-dedicated modification.** *Nature* 2014, **505**:564–568.

Than-Trong E, Bally-Cuif L: **Radial glia and neural progenitors in the adult zebrafish central nervous system.** *Glia* 2015, doi:10.1002/glia.22856.

Thermes V, Candal E, Alunni A, Serin G, Bourrat F, Joly J-S: **Medaka simplet (FAM53B) belongs to a family of novel vertebrate genes controlling cell proliferation.** *Development* 2006, **133**:1881–1890.

Thermes V, Grabher C, Ristoratore F, Bourrat F, Choulika A, Wittbrodt J, Joly J-S: **I-SceI meganuclease mediates highly efficient transgenesis in fish.** *Mech. Dev.* 2002, **118**:91–98.

U

Ulbrich C, Diepholz M, Bassler J, Kressler D, Pertschy B, Galani K, Böttcher B, Hurt E: **Mechanochemical removal of ribosome biogenesis factors from nascent 60S ribosomal subunits.** *Cell* 2009, **138**:911–922.

V

Vaughan C, Pearsall I, Yeudall A, Deb SP, Deb S: **p53: its mutations and their impact on transcription.** *Subcell. Biochem.* 2014, **85**:71–90.

Vaziri C, Saxena S, Jeon Y, Lee C, Murata K, Machida Y, Wagle N, Hwang DS, Dutta A: **A p53-dependent checkpoint pathway prevents rereplication.** *Mol. Cell* 2003, **11**:997–1008.

Vieira C, Pombero A, García-Lopez R, Gimeno L, Echevarria D, Martínez S: **Molecular mechanisms controlling brain development: an overview of neuroepithelial secondary organizers.** *Int. J. Dev. Biol.* 2010, **54**:7–20.

Voit R, Kuhn A, Sander EE, Grummt I: **Activation of mammalian ribosomal gene transcription requires phosphorylation of the nucleolar transcription factor UBF.** *Nucleic Acids Res.* 1995, **23**:2593–2599.

Volarevic S, Stewart MJ, Ledermann B, Zilberman F, Terracciano L, Montini E, Grompe M, Kozma SC, Thomas G: **Proliferation, but not growth, blocked by conditional deletion of 40S ribosomal protein S6.** *Science* 2000, **288**:2045–2047.

Voutev R, Killian DJ, Ahn JH, Hubbard EJA: **Alterations in ribosome biogenesis cause specific defects in C. elegans hermaphrodite gonadogenesis.** *Dev. Biol.* 2006, **298**:45–58.

W

Wang H, Chen X, He T, Zhou Y, Luo H: **Evidence for tissue-specific Jak/STAT target genes in Drosophila optic lobe development.** *Genetics* 2013, **195**:1291–1306.

Watanabe-Susaki K, Takada H, Enomoto K, Miwata K, Ishimine H, Intoh A, Ohtaka M, Nakanishi M, Sugino H, Asashima M, et al.: **Biosynthesis of ribosomal RNA in nucleoli regulates pluripotency and differentiation ability of pluripotent stem cells.** *Stem Cells* 2014, **32**:3099–3111.

Watkins NJ, Bohnsack MT: **The box C/D and H/ACA snoRNPs: key players in the modification, processing and the dynamic folding of ribosomal RNA.** *Wiley Interdiscip Rev RNA* 2012, **3**:397–414.

Wilkins BJ, Pack M: **Zebrafish models of human liver development and disease.** *Compr Physiol* 2013, **3**:1213–1230.

Willardsen MI, Link BA: **Cell biological regulation of division fate in vertebrate neuroepithelial cells.** *Dev. Dyn.* 2011, **240**:1865–1879.

Wong QW-L, Li J, Ng SR, Lim SG, Yang H, Vardy LA: **RPL39L is an example of a recently evolved ribosomal protein paralog that shows highly specific tissue expression patterns and is upregulated in ESCs and HCC tumors.** *RNA Biol* 2014, **11**:33–41.

Wurst W, Bally-Cuif L: **Neural plate patterning: upstream and downstream of the isthmic organizer.** *Nat. Rev. Neurosci.* 2001, **2**:99–108.

X

Xue S, Barna M: **Specialized ribosomes: a new frontier in gene regulation and organismal biology.** *Nat. Rev. Mol. Cell Biol.* 2012, **13**:355–369.

Xue S, Tian S, Fujii K, Kladwang W, Das R, Barna M: **RNA regulons in Hox 5' UTRs confer ribosome specificity to gene regulation.** *Nature* 2015, **517**:33–38.

Z

Zénon A, Krauzlis R: **[Superior colliculus as a subcortical center for visual selection]**. *Med Sci (Paris)* 2014, **30**:637–643.

Zhang X, Wang W, Wang H, Wang M-H, Xu W, Zhang R: **Identification of ribosomal protein S25 (RPS25)–MDM2–p53 regulatory feedback loop**. *Oncogene* 2013, **32**:2782–2791.

Zhang Y, Duc A-CE, Rao S, Sun X-L, Bilbee AN, Rhodes M, Li Q, Kappes DJ, Rhodes J, Wiest DL: **Control of Hematopoietic Stem Cell Emergence by Antagonistic Functions of Ribosomal Protein Paralogs**. *Developmental Cell* 2013, **24**:411–425.

Zhao C, Andreeva V, Gibert Y, LaBonty M, Lattanzi V, Prabhudesai S, Zhou Y, Zon L, McCann KL, Baserga S, et al.: **Tissue specific roles for the ribosome biogenesis factor Wdr43 in zebrafish development**. *PLoS Genet.* 2014, **10**:e1004074.

Zhou X, Liao W-J, Liao J-M, Liao P, Lu H: **Ribosomal proteins: functions beyond the ribosome**. *Journal of Molecular Cell Biology* 2015, **7**:92–104.

Zhu W, Chen Y, Dutta A: **Rereplication by depletion of geminin is seen regardless of p53 status and activates a G2/M checkpoint**. *Mol. Cell. Biol.* 2004, **24**:7140–7150.

Zhu Y, Poyurovsky MV, Li Y, Biderman L, Stahl J, Jacq X, Prives C: **Ribosomal Protein S7 Is Both a Regulator and a Substrate of MDM2**. *Molecular Cell* 2009, **35**:316–326.

Zupanc GKH, Hinsch K, Gage FH: **Proliferation, migration, neuronal differentiation, and long-term survival of new cells in the adult zebrafish brain**. *The Journal of Comparative Neurology* 2005, **488**:290–319.

ANNEX

